ULRR

Thermal treatment technologies for low moisture and dehydrated manure feedstock

Item Type	Thesis
Authors	Taupe, Natalie
Download date	2026-01-17 22:02:05
Item License	https://creativecommons.org/licenses/by-nc-sa/1.0/
Link to Item	https://hdl.handle.net/10344/7113

Thermal treatment technologies for low moisture and dehydrated manure feedstock

UNIVERSITY of LIMERICK

OLLSCOIL LUIMNIGH

Thesis presented for the award of Doctor of Philosophy

By Natalie Taupe

Department of Chemical and Environmental Sciences

University of Limerick

Supervisors:

Prof. Dr. James J. Leahy

Dr. Witold Kwapinski

Submitted to the University of Limerick

November 2016

Declaration

The work presented in this thesis is the original work of the author, conducted under the supervision of Prof. Dr. J.J. Leahy and Dr. Witold Kwapinski. Due reference has been made, where necessary, to the work of others. No part of this thesis has been previously submitted to this or any other university.

Natalie Taupe Date

Acknowledgement

I would like to thank my supervisors Prof. James J. Leahy, Dr. Witold Kwapinski and co-supervisor Dr. Marzena Kwapinska for their kind and firm support and guidance throughout this research. Furthermore, I would like to thank Prof. Michael H.B. Hayes, Dr. Achim Schmalenberger, Cristiano Dela Piccolla, Dr. Paulo Trazzi, Israel Ikoyi, Dr. Daya Shankar Pandey, Alberto Garcia, Ray McInerney, Dr. Lydia Fryda and Dr. Iria Regueiro for their scientific contribution to the work.

I would like to thank the principal coordinator of the ReUseWaste project, Prof. Lars Stoumann Jensen, Dr. Myles Oelofse and all ReUseWaste partners and fellows. The project meetings, training activities and collaborations were truly inspiring, motivating, and fun. Being part of ReUseWaste was a life changing experience and opened doors for my future career.

During the course of this work I had the opportunity to undertake a secondment abroad at the 'Centro de Edafología y Biología Aplicada del Segura (CEBAS)' belonging to the 'Consejo Superior de Investigaciones Científicas (CSIC)', the Spanish National Research Council, in Murcia, Spain, under the guidance of Prof. M. Pilar Bernal and the assistance of my friend and colleague Dr. André Santos. I would like to thank the entire department for making my time in Murcia so enjoyable.

I would like to thank Prof. Carlo Grignani, my friend and colleague Dr. Raghunath Subedi, and the other members of the University of Torino, Italy, for the great collaborations together. I would like to thank the technical staff of the Chemical and Environmental Science department, all members of the Carbolea Research Group and friends in UL for their help, advice and friendship.

To my friends inside and outside UL, thank you so much for supporting me in the last four years and making my stay in Ireland so enjoyable.

Last, but certainly not least, I would like to express my deepest gratitude to my family and boyfriend for their love and support. I could not have done this without you.

I would like to acknowledge the financial support from the People Programme (Marie Curie Actions) of the European Union's Seventh Framework Programme FP7/2007-2013/ under REA grant agreement n° [289887].

Abstract

The research carried out throughout this project has helped to further advance the area of producing biochar from animal manure feedstocks, as well as producing biochar from virgin wood for its application in manure management systems. On-farm auto-thermal updraft gasification of poultry litter (PL) was carried out to yield a low calorific value product gas (3.39 MJ m^{-3}_{N} LHV), along with a tar and char residue. The ash melting point of 639 °C of PL made low temperature operation necessary, resulting in a low cold gas efficiency (GCE = 0.26). The same PL feedstock, dehydrated cow manure, and pre-digested swine manure were subject to slow pyrolysis to produce nutrient rich biochars and to recycle them back to agricultural land. All biochars exceeded the set thresholds of Zn and Cu (400 g t^{-1} and 100 g t^{-1} respectively) for European biochar certification. Recoveries in biochars were high (~90 wt.%) for all nutrients except for N and S (28-62 wt.%) and some heavy metals, e.g. Pb and Ni (21-31 wt.%). Biochars produced at 400 °C resulted in a significantly higher nutrient uptake to lettuce (*Lactuca sativa*) than biochars produced at 600 °C, and slow pyrolysis biochars significantly increased N uptake as opposed to the gasification char.

Sitka spruce biochar was produced using a uniquely designed Kon-Tiki kiln. The biochar along with sulfuric acid were used as cow slurry additives to evaluate their impact on NH_3, CH_4 and H_2S emissions. Biochar alone had no significant effect on NH_3 and H_2S, but biochar might be able to reduce CH_4 emissions. Sulfuric acid reduced cumulative NH_3 by about 50 % and cumulative CH_4 by about 80 %, but increased H_2S emissions. Pre-acidification of biochar might be promising and needs further investigation. The same Sitka spruce biochar was amended with cow slurry to see the effect on nitrate leaching, nitrogen uptake to grass (*Lolium perenne*) and changes in nitrification and denitrification capabilities in soil by determining the abundances of bacterial and archaeal *amoA* and *nosZ* genes. Biochar alone had no significant effect on either of the investigated parameters; however, in combination with slurry biochar decreased the abundance of archaeal *amoA* at the slurry application zone and increased the abundance at lower soil depth. This might be attributed to adsorption of dissolved organic carbon to biochar, and an increase in ammonium leaching. The results of this study reveal that biochar affects soil-N dynamics differently when in combination with slurry than in its un-amended state.

List of references

Peer-reviewed articles

Paper I: Taupe, N.C., Lynch, D., Wnetrzak, R., Kwapinska, M., Kwapinski, W., Leahy, J.J., 2016. Updraft gasification of poultry litter at farm-scale – A case study. Waste Manag. 50, 324-333.

Paper II: Subedi, R., Taupe, N., Ikoyi, I., Bertora, C., Zavattaro, L., Schmalenberger, A., Leahy, J.J., Grignani, C., 2016. Chemically and biologically-mediated fertilising value of manure-derived biochar. Sci. Total Env. 550, 924–933.

Paper III: Subedi, R., Taupe, N., Pelissetti, S., Petruzzelli, L., Bertora, C., Leahy, J.J., Grignani, C., 2016. Greenhouse gas emissions and soil properties following amendment with manure-derived biochars: Influence of pyrolysis temperature and feedstock type. J. Environmental Management. 166, 73-83.

Paper IV: Subedi, R., Kammann, C., Pelissetti, S., Taupe, N., Bertora, C., Monaco, S., Grignani, C., 2015. Does soil amended with biochar and hydrochar reduce ammonia emissions following the application of pig slurry? European Journal of Soil Science. 66 (6), 1044-1053.

Presentations

Oral: "Updraft gasification of poultry litter", ManuResource 2013, Brugge, Belgium.

Poster: "Characterization of poultry litter chars produced by slow pyrolysis and gasification", ManuResource 2013, Brugge, Belgium.

Poster: "Thermal treatment of animal manure", BCD2013 (Biochars, Composts, and Digestates), Bari, Italy.

*Poster: "*Influence of biochar volatile matter on plant growth", Engineering, Informatics and Science Research Day 2013, Galway, Ireland.

Poster: "Thermal treatment technologies for low moisture and dehydrated manure feedstock", Biochar Summer School 2013, Geneva, Switzerland.

Poster: "Gasification and pyrolysis of poultry litter: An opportunity to produce bioenergy and recover nutrients". LIT 'Energy Efficiency Benefits for Industry' Seminar 2015 & University of Limerick Open Days 2014 and 2015.

Table of Contents

List of tables

List of figures

Nomenclature

Symbol	Description	Unit
A	absorption	Abs
A_m	cross sectional area of adsorbed gas for N_2	0.162 nm^2
C	effective heat capacity	J K^{-1}
c	concentration	mol L^{-1}
C_a	constant relating to the free energy of adsorption	
d	path length	cm
ε	molar absorptivity co-efficient	M^{-1} cm^{-1}
m	mass	g
n_m	number of molecules adsorbed	
N	Avogadro's constant	6.023 x 10^{23} mol^{-1}
Q_g	higher heating value at constant volume	J g^{-1}
Q_i	contribution from the ignition wire	J
$q_{v,ba}$	certified higher heating value of benzoic acid	J g^{-1}
p	partial vapour pressure of adsorbate gas	Pa
p_0	saturation pressure	Pa
V_m	volume of gas adsorbed unit mass of adsorbent	ml
V_{mol}	molar volume of adsorbate at STP	22.4 l mol^{-1}
ΔT	corrected temperature rise	° K
λ	wavelength	nm

Abbreviations

AD	Anaerobic digestion
A_{actual}	Actual Air to Fuel Ratio
A_{stoich}	Stoichiometric Air
AEC	Anion Exchange Capacity
Amo	Ammonia monooxygenase
AOA	Ammonia Oxidising Archaea
AOB	Ammonia Oxidising Bacteria
ar	As-received (weight of fresh samples)
BAT	Best Available Technology
BET	Brunauer-Emmett-Teller
BJH	Barrett-Joyner-Halenda
BM	Bedding Material
CCE	Carbon Conversion Efficiency
CGE	Cold Gas Efficiency
CEBAS	Centro de Edafología y Biología Aplicada del Segura
CEC	Cation Exchange Capacity
CPMAS ^{13}C-NMR	Cross-Polarization and Magic Angle Spinning Nuclear Magnetic Resonance Spectroscopy
CSIC	Consejo Superior de Investigaciones Científicas
CH_4	Methane
CLRTP	Long-range Transboundary Air Pollution
CO_2	Carbon dioxide
CO	Carbon monoxide
daf	Dry ash-free basis (weight after ashing at 550 °C)
db	Dry-basis (weight after drying at 105 °C)
DI	De-Ionised water
DL	Detection limit
DM	Dry Matter
DNA	Deoxyribonucleic Acid
DOC	Dissolved organic carbon
DTA	Differential Thermal Analysis

EBC	European Biochar Certificate
ECN	Energy research Centre of the Netherlands
ER	Equivalence Ratio
EU	European Union
FA-AAS	Flame Assisted – Atomic Absorption Spectroscopy
FAO	Food and Agriculture Organisation
FBC	Fluidised Bed Combustor
FC	Fixed Carbon
FSAI	Food Safety Authority of Ireland
FTIR	Fourier transform infrared spectroscopy
GC-MS	Gas Chromatography and Mass Spectrometry
GHG	Green House Gas(es)
H_2	Hydrogen
H_2S	Hydrogen sulphide
HHV	Higher Heating Value
HM	Heavy Metals
ICP-OES	Inductively Coupled Plasma - Optical Emission Spectrometry
IPCC	Intergovernmental Panel on Climate Change
IPPC	Integrated Pollution Prevention Control
LHV	Lower Heating Value
LSU	Livestock units
MC	Moisture content
m/z	Mass to charge ratio
N_2O	Nitrous oxide
ND	Not determined
nosZ	Nitrous oxide reductase
NH_3	Ammonia
NH_4^+	Ammonium
NO_3^-	Nitrate
OM	Organic Matter
PAH	Polycyclic Aromatic Hydrocarbons

PCB	Polychlorinated biphenyl
PCDD/PCDF	Polychlorinated dibenzo-ρ-dioxins and dibenzofurans
PCM	Pyrogenic carbonaceous material
PCR	Polymerase Chain Reaction
PL	Poultry Litter
PM	Particulate Matter
PO_4^{3-}	Phosphate
RNA	Ribonucleic Acid
SEAI	Sustainable Energy Authority of Ireland
SEM-EDS	Scanning Electron Microscopy - Energy Dispersive Spectroscopy
SSA	Specific Surface Area
SSD	Sewage sludge directive
TAN	Total ammoniacal nitrogen
TC	Total Carbon
TCD	Thermal Conductivity Detector
TGA	Thermal Gravimetric Analysis
TN	Total Nitrogen
TOC	Total Organic Carbon
UE	Uptake efficiency
UL	University of Limerick
UN	United Nations
UTO	University of Torino
VM	Volatile Matter
VOC	Volatile organic compounds
WHC	Water Holding Capacity
WP	Work Package

Samples

Chapter 4

BC400	Biochars: slow pyrolysis, maximum temperature 400 °C
BC600	Biochars: slow pyrolysis, maximum temperature 600 °C
CM	Cow manure
CM400	CM biochar: slow pyrolysis, maximum temperature 400 °C
CM600	CM biochar: slow pyrolysis, maximum temperature 600 °C
CM_{BC}	CM biochars
PL	Poultry litter
PL400	PL biochar: slow pyrolysis, maximum temperature 400 °C
PL600	PL biochar: slow pyrolysis, maximum temperature 600 °C
PLgas	PL biochar: auto-thermal updraft gasification at < 700 °C
PL_{BC}	PL biochars
SM	Swine manure
SM400	SM biochar: slow pyrolysis, maximum temperature 400 °C
SM600	SM biochar: slow pyrolysis, maximum temperature 600 °C
SM_{BC}	SM biochars

Chapter 5

S	Slurry
SB	Slurry amended with biochar (3.5 $wt.\%_{ar}$)
SpH	Acidified slurry (pH 5.5)
SpHB	Acidified slurry amended with biochar (pH 5.5; 3.5 $wt.\%_{ar}$)

Chapter 6

C	Control soil
B	Biochar amended soil (10 $t\ ha^{-1}_{ar}$)
S	Slurry amended soil (170 kg N ha^{-1})
SB	Biochar amended slurry

1. Introduction

In this chapter the topic of animal manure recycling is introduced to provide the reader with the necessary background information in order to fully recognise the importance of this research area. The scope of the ReUseWaste project is described followed by an outline of the individual scientific studies conducted at the University of Limerick as well as collaborations between other ReUseWaste partners.

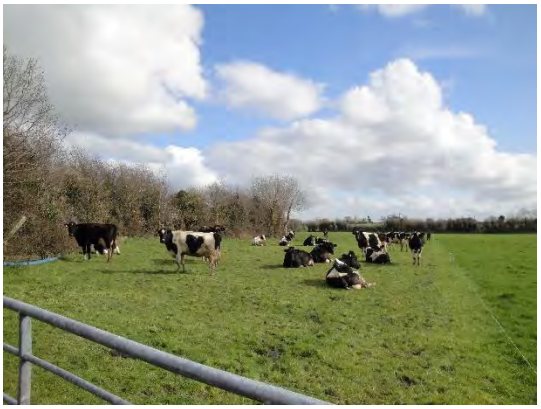

1.1 Animal Manure Recycling

1.1.1 Livestock production in the EU and Ireland

Livestock production is one of the fastest growing sectors of the agricultural economy (FAO, 2016) driven by a growing world population (UN, 2015) and the simultaneous demand for animal protein. In 2013, the total livestock population in the European Union (EU) made up to 130.6 million livestock units (LSU), of which cattle represented 48.3%, pigs 26.1%, and poultry 15.3% (Eurostat, 2015). Figure 1-1 displays the distribution of livestock densities of the EU member states and averaged 0.77 LSU per hectare of utilised agricultural in 2010. Livestock density in the Republic of Ireland is above average at 1.16 LSU per hectare (Eurostat, 2012).

In Ireland, the agri-food industry is the most important indigenous sector and provides primary employment for 170,000 people. About 64% (4.5 million hectares) of the total land area of Ireland (6.9 million hectares) is used for agriculture, of which 81% is devoted to pasture, hay and grass silage, 11% to rough grazing, and 8% to crops, fruit and horticulture production (European Commission, 2016). Grazing cattle are particularly dominant in Ireland, at 76.2% of the total livestock population in 2013 (Eurostat, 2015). Grazing animals, such as dairy cows, cattle and sheep, are common in regions with large areas of grassland, temperate weather, and a relatively high degree of rainfall.

The agriculture sector is responsible for the greatest share of greenhouse gas (GHG) emissions of any individual sector across the economy (Gilbert, 2012) and Ireland is far above the EU emissions average (EPA, 2015). Systematic changes in manure management are necessary for Ireland's emissions abatement. Pig and poultry enterprises generally keep animals indoors all year round, hence the collection and storage of manure to subsequently spread onto agricultural land is easy. However, recycling manure in livestock systems with a high proportion of grazing cattle and disposing most of the manure in the pastures for most of the year, may greatly influence the possibilities for collecting and processing manures.

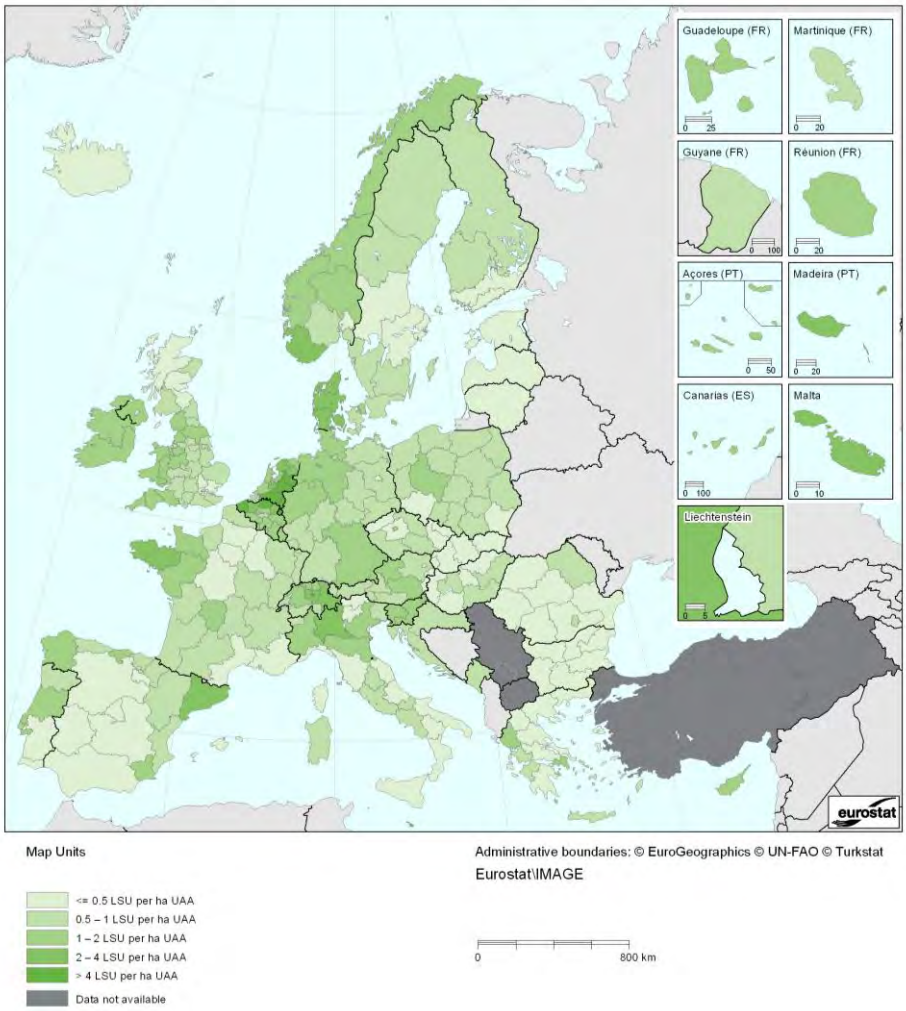

Figure 1-1: Livestock density - livestock units (LU) per hectare of utilised agricultural area (Eurostat, 2012)

1.1.2 Manure management

Manure management is one component of livestock farming that is becoming increasingly challenging as environmental and health consequences of commercial farming become more apparent (EurActiv, 2012). Traditional farming practices in mixed livestock and crop production have moved towards large, specialised and geographically concentrated production units (Sommer, 2013). A direct consequence of these structural changes is that far more animal waste is produced in specific areas than can be managed by land disposal. This has given rise to a number of environmental concerns, such as pathogen contamination, water eutrophication, bad odours, volatilisation of NH_3 and emissions of GHGs (De Vries *et al*., 2012, Kelleher *et al*., 2002).

Emissions to the atmosphere and water bodies occur throughout the whole manure management chain (Figure 1-2). Petersen *et al.* (2007) highlight the importance of a whole-farm perspective taking into account side-effects and on-farm interactions to assess strategies to mitigate pollution during all stages. These stages generally involve the collection of manure in animal houses or beef feedlots; manure storage; treatment of manure; transport; application and crop production (Sommer and Christensen, 2013). Also the production of animal feed can lead to excessive consumption of energy and water, especially when grains are used to feed the animals, as these are often grown in monocultures and require chemical fertilisers, pesticides, herbicides and water to grow, resulting in water pollution and pesticide resistant insects (Altieri, 1998). Furthermore, the import of nutrients through animal feed further increases the nutrient imbalance and the overload in agricultural areas.

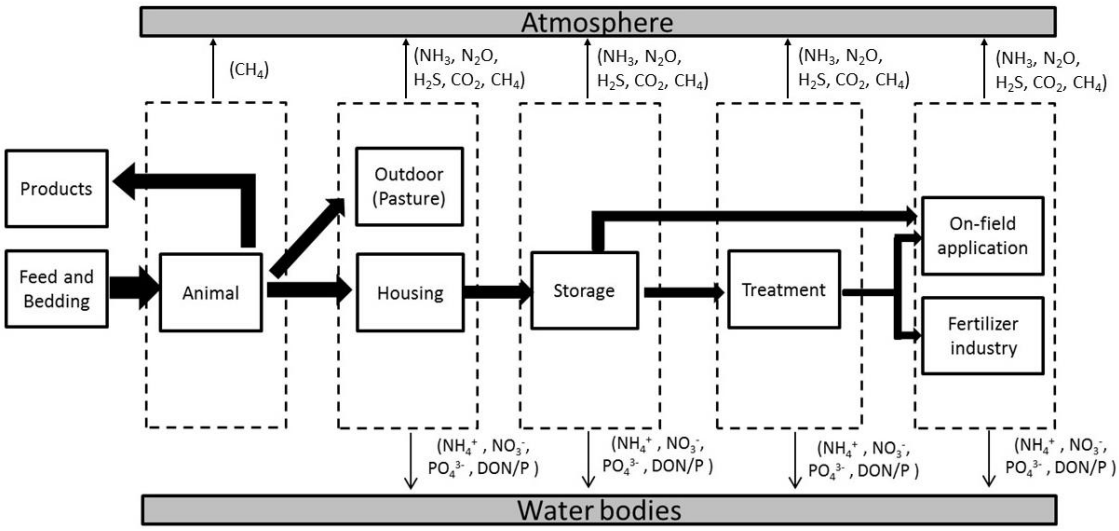

Figure 1-2: Manure management chain with interlinked stages. At each stage there is a risk of nutrient loss to the environment causing environmental pollution. DON/P (Dissolved organic nitrogen/phosphorus) (Yong Hou, Wageningen University and Research Centre)

European Union members now have to adapt to a policy context requiring manure management to improve its environmental performance and mitigate its impact on climate change. The most significant pieces of legislation are the Water Framework Directive (2000/60/EC), which aims for good status for all water bodies, and the Nitrates Directive (91/676/EEC), which aims to protect waters against pollution from nitrates, which can derive from, for example, manure and animal waste.

Animal manure is a mixture of faeces and urine, bedding material, spilt feed and drinking water, and water used for washing (Lynch *et al*., 2013). The composition varies depending on e.g. feed, animal type, husbandry practices, and manure removal technologies. Animal slurries contain less than 12% dry matter (DM) content, while deep litter is comprised of manure mixed with large amounts of bedding material and hence has a relatively high DM content (Christensen and Sommer, 2013). Each manure category is composed of water, organic matter, nutrients and other inorganic elements, and depending on its composition can be valuable to ameliorate soil, be used as an energy carrier (Lynch, *et al.,* 2013; Taupe *et al*., 2016 - *paper I*), or in the fertilising industry (Thygesen and Johnsen, 2012).

Waste was traditionally viewed as a simple residue of linear processes, however is now seen as part of a dynamic material cycle with potential end uses (Tanto and Magette, 2008). The Waste Framework Directive (2008/98/EC) sets the basic concepts and definitions related to waste management, such as definitions of waste, recycling and recovery. The Directive requires that all EU member states adopt waste management plans and waste prevention programmes according to the outlined waste management hierarchy: prevent → re-use → recycle → recover → dispose. At an EU level re-use and recycling over disposal of animal waste is supported, where prevention and minimisation cannot be achieved. In general, processed animal manure, with characteristics suitable for fertilisation or soil amendment, reaches the end-of-waste status and is considered a by-product and not a waste (Ehlert and Schoumans, 2015). Incineration of manure in its natural state still makes animal manure a waste, unless processed on-farm, in which case manure is considered an animal by-product (Commission Regulations (EU) No 592/2014) (see chapter 3).

Very often re-use and recycling of manure, e.g. in form of pelletising, feed additives, soil remediation, are not effective in solving environmental issues satisfactorily and manure treatment in form of nutrient and energy recovery using advanced technologies are required (Henihan, 2006). The choice of treatment technology depends on several factors, e.g. the manure's properties and availability, the desired end products and their economic value. Manure properties and availability can vary from year to year and within years, which can lead to challenges for manure processing and during product development.

1.1.3 Manure treatment technologies

The aim of developing novel manure treatment technologies is to sustainably utilise manure for the production of bioenergy and green bio-fertilisers and to improve soil, air and water quality. As already mentioned in section 1.1.2, progress can only be achieved by carefully managing the entire chain, from feeding of the animals, housing, storage and treatment to field application (Jensen, 2013a; Petersen *et al.,* 2007). This requires structural optimisation and a shift from linear process chains to process networks. Network optimisation can be achieved by interacting with different partners, increasing efficiency and innovative material and energy flow management (Narodoslawsky, 2013; Ingram, 2015). The choice of technology has a strong influence on energy, nutrient and GHG balances (De Vries *et al*., 2012; Prapaspongsa *et al*., 2010), and the risk of pollution swapping should be considered carefully (De Vries *et al*., 2015). A schematic of the different treatment technologies used during animal manure recycling is illustrated in Figure 1-3.

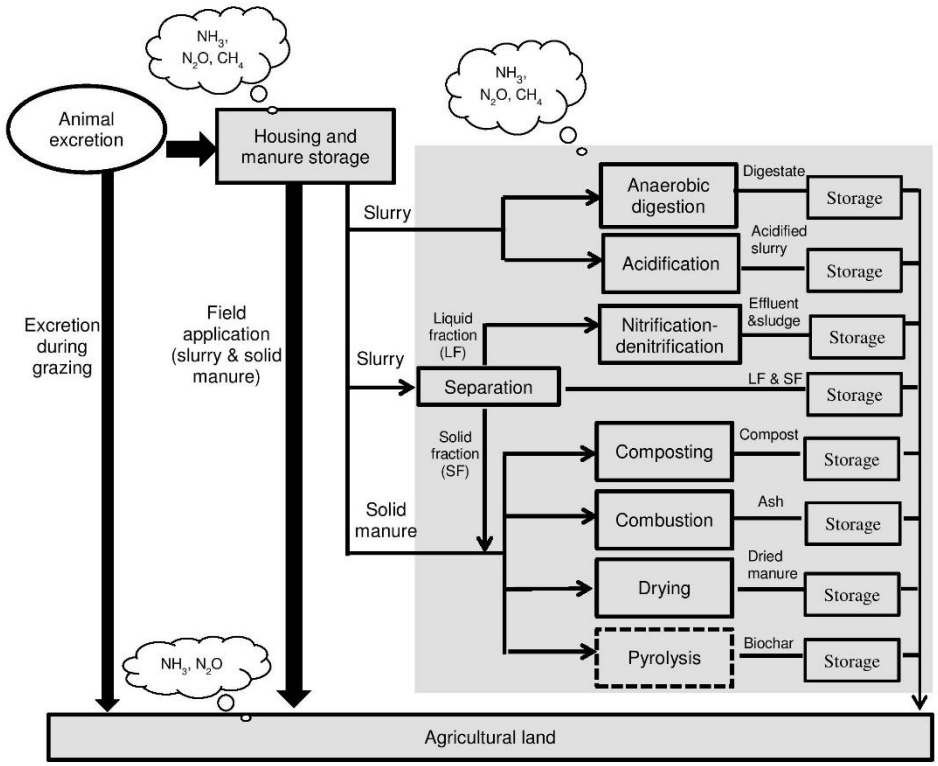

Figure 1-3: Stages of animal manure recycling, with integration of different treatment technologies. The diagram and depicts some harmful emissions deriving from housing and manure storage, field application and manure treatment. (Yong Hou, Wageningen University and Research Centre)

Anaerobic digestion (AD) takes place in the presence of a biodegradable material, such as animal slurry (Pessuto *et al.,* 2016; Jurado *et al*., 2016; Li *et al*., 2015), in an anaerobic environment. A biogas is produces through microbial fermentation of OM, which is primarily transformed to CO_2 and CH_4 and some H_2. The gases can be used directly for energy, or can be upgraded to transportation fuels and chemicals. The remaining residue (digestate) is sterile, rich in nutrients, and emits less odour compounds compared to the original manure (Sommer *et al*., 2013c, Li *et al*., 2011).

Emissions of NH_3 and GHGs can occur during all stages of manure management (Chadwick *et al*., 2011; Kupper *et al*., 2015). Ammonia emissions are affected by several factors, such as the concentration of total ammoniacal nitrogen (TAN = NH_4^+ + NH_3), pH, temperature, surface area and turbulences in manure and air (see section 5.2; Sommer and Feilberg, 2013). Greenhouse gases, including CO_2, CH_4, N_2O, are produced by microorganisms, and these are affected by the oxygen status, climate, the nature of the OM and chemical compounds in the manure. Aeration of slurry can effectively reduce NH_3, odorants and other undesirable compounds as a result of microbial oxidation. Reduction of GHG can be achieved by management and technologies that induce an environment that is unfavourable for the microorganisms (Sommer *et al*., 2013a). Other ways of NH_3 and GHG reduction is by diet manipulation and slurry additives, including salts and acids can alter the pH and hence gas emissions significantly (Feilberg and Sommer, 2013; Sommer *et al*., 2013b). For more detailed information on slurry additives and acidification see chapter 5.

Animal slurry can also be separated into a solid and liquid fraction (Hjorth *et al*., 2010). The aim is to obtain a DM and nutrient rich solid fraction, which can be exported to agricultural areas with a demand of nutrients, while the liquid fraction is intended to be used directly on the farm (Christensen *et al*., 2013). Hereby the transportation costs of the liquid fraction are reduced. In addition, separation may also decrease odour emissions and the solid fraction may be used for energy production and other thermochemical conversion processes, such as pyrolysis (see chapter 4).

Composting involves the microbial transformation, mineralisation and stabilisation of OM of solid manure in an aerobic environment (Oudart *et al*., 2015). The main aim of composting is to improve the fertility of an organic biomass and soil quality after application. Compost is easier to handle and apply as it is more concentrated and

uniform than manure. In addition, composting eliminates pathogens and reduces the risk of odour and gaseous emissions. However, composting results in high cost of installation and management, gaseous losses, and limited recovery of energy. (Jensen, 2013b)

1.1.4 Manure fertiliser value

Animal manure contains a number of plant macro- and micronutrients, but also undesirable compounds, such as heavy metals and pathogens (Mostofa Amin *et al.,* 2013; Nicholson *et al.*, 1999). The quality of manure with respect to its use as a soil amendment and crop nutrient supply depends on its chemical, biological and physical nature and its interactions with soil. These interactions can be complex. More than 50 factors affect crop growth and yield, including climate impact, soil properties and crop requirements (Havlin *et al*., 1999). Certain soil properties are vital to crop growth, such as soil minerology and texture (proportions of sand, silt and clay), soil OM content, soil porosity, cation exchange capacity (CEC), base saturation, slope and topography, and soil temperature and depth. Crop requirements are influenced by crop species, planting date, seeding rate and quality, water availability, nutrition, pests, and harvest efficiency (Jensen, 2013c; Havlin *et al*., 1999).

Some mineral elements are essential for the plants' metabolic functions and having an impact on the plants' life cycle. These mineral elements include macronutrients (N, P, K, S, Ca, and Mg) and micronutrients (Fe, Zn, Mn, Cu, B, Cl, and Mo) and are required in different amounts (0.1 g kg^{-1}-1.0 g kg^{-1}) (Jensen, 2013c). The quantity of minerals supplied can either be deficient, sufficient or excessive and toxic to plants (Havlin *et al*., 1999). When nutrient deficiency is corrected the plant grows rapidly. This rapid growth dilutes the nutrient concentration in the plant tissue, as growth increases more rapidly than nutrient uptake (Steenberg effect). On the other hand, excessive quantities reduce plant yields by toxicity and by reducing the concentrations of other nutrients. In general, crop yield is determined by Leibig's law of the minimum and is proportional to the amount of the most limiting nutrient. Even though all nutrients are equally important for plant growth, usually N, P, and K are the most limiting (Ågren *et al*., 2012). N and S are more important with microbial processes, while mineral surface exchange reactions are more important for K, Ca and Mg. Furthermore, nutrient concentration does not reflect the nutrient availability. The nutrient supply to

plant roots is a dynamic process and involves ion exchange in soil, movements of ions from soil to roots and ion absorption by plants. (Jensen, 2013c; Havlin *et al*., 1999)

Manure is introduced to soil in organic and inorganic form and can be a valuable source of OM and nutrients, in particular N, P and K, but also several micronutrients (Fe, Mn, B, Zn, Cu) (Chen *et al*., 2003). The chemical composition of manures depends on the entire chain from which it is produced (crop – feed – excreta – storage – field application). Depending on the manure and soil conditions, immobilisation of inorganic to organic nutrient forms or mineralisation of organically bound nutrients will occur. Nitrogen is in most cases the plant nutrient that has the largest influence on crop DM production (Burns, 1992), hence the nitrogen cycle plays a significant role for manure fertility. A schematic of the nitrogen cycle is illustrated in Figure 1-4. Nitrogen released as microbial biomass occurs in the form of NH_4^+ which may be nitrified to NO_3^-. Both NH_4^+ and NO_3^- can be taken up by plants, lost by leaching (NO_3^-) (chapter 6) or lost as gaseous form due to denitrification and volatilisation (NH_3, N_2O, N_2). (Jensen, 2013c)

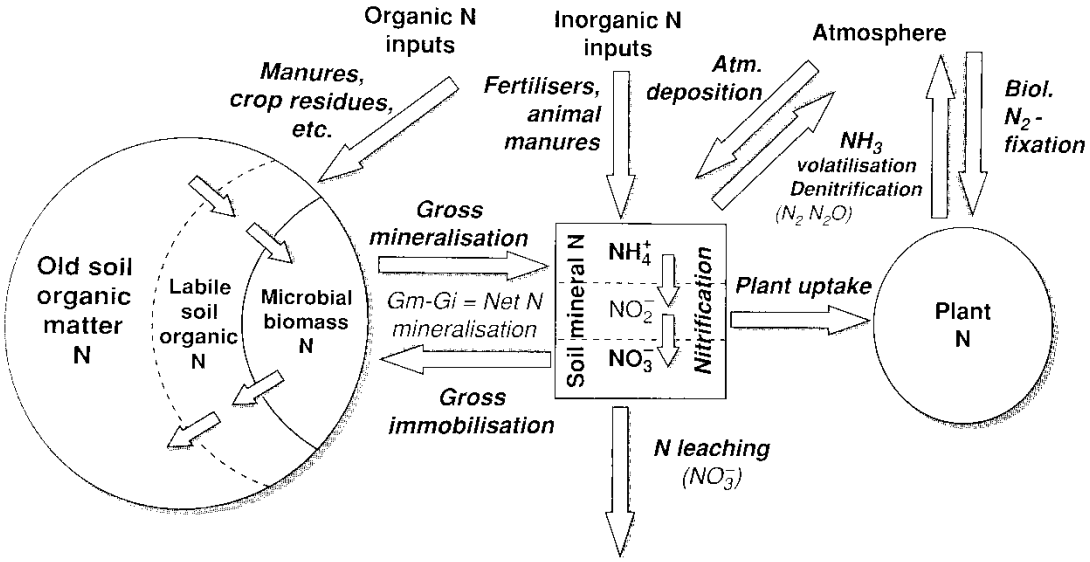

Figure 1-4: Nitrogen cycle in the soil - plant - atmosphere system (Jensen, 2013c)

Nutrient speciation is important for assessing the manure's benefits to plant growth (Uchimiya, 2014). Nitrogen species vary greatly between different manure types from a very high proportion of NH_4^+ (70-90%) in liquid manure to very low proportion in deep litter. Phosphorus is predominantly (80-90%) and K exclusively in inorganic form. Micronutrients may be chelated or complexed by organic compound, partly

soluble and partly particle bound (Jensen, 2013a). Manure application may indirectly influence their availability through the action of dissolved manure OM or by altering soil pH (Soti *et al*., 2015). Furthermore, manure application to soil might also affect soil biology positively through stimulation of microbial and faunal activity and hence mineralisation and turnover of organically bound nutrients (Masunga *et al*., 2016).

1.2 Thermochemical treatment technologies

Energy conversion technologies have the advantage of converting biomass into value added products for their use as biofuels, chemicals and fertilisers, while at the same time generating heat and electricity (Cantrell *et al*., 2007). Energy recovery is significant for countries like Ireland, as Ireland imports 86% of its fuels making it the most import dependent country in the EU (SEI, 2015). Furthermore, developments in biomass to energy conversion technologies would provide a valuable source of employment in rural areas. While wet wastes such as cattle manure and pig manure are suitable for bio-chemical conversion, such as AD (Pessuto *et al.,* 2016; Jurado *et al*., 2016; Li *et al*., 2015), or hydrothermal carbonisation (Yin *et al*., 2010; Xiu *et al.*, 2010; Ye *et al*., 2012), low moisture wastes such as PL can be subject to thermal treatment, such as combustion, gasification and pyrolysis. (McKendry, 2002a; Yoder *et al*., 2011; Lynch *et al*., 2013).

1.2.1 Combustion

Combustion is the oldest, the most developed, and therefore most frequently used thermochemical conversion technology (Basu, 2010a). Through oxidation of carbon and hydrogen present in the biomass CO_2 and H_2O are formed. The heat released from this exothermic reaction currently represents the largest source of energy for human consumption. Combustion units exist at a small scale for cooking and heating or at district or industrial scale using steam generated in biomass-fired boilers. The ash residue can be used in the fertilising industry and as a component in building materials (Pels *et al*., 2005). Combustion takes place in three steps (Basu, 2010a; Loo and Koppejan, 2008):

1) Heating and drying of the fuel: Evaporation of moisture requires energy and lowers the temperature in the combustion unit, therefore the efficiency of combustion is dependent on the fuel's moisture content.

2) Devolatilisation and combustion of volatiles: Devolatilisation, or pyrolysis, is a process where gaseous hydrocarbons are released as a result of thermal decomposition of the fuel. Volatiles are subsequently combusted in the gas phase.

3) Char combustion: Oxygen undergoes a heterogeneous oxidation reaction with carbon at the surface of the char particle to produce CO and CO_2. Char burns much slower than volatiles and is hence the rate determining step.

The two main combustion systems that exist today are fixed bed and fluidised bed combustion (Basu, 2010a). In fixed bed combustion systems primary air is fed into the combustion unit through the bed for subsequent drying, devolatilisation and combustion of the fuel. The combustible gases are burned by feeding secondary air into the combustion zone above the bed. Fixed bed combustion systems often use grate furnaces and underfeed stokers. Their design aims to distribute the fuel and the char uniformly over the entire surface, and to evenly supply air to all areas. Inhomogeneous air supply may result in ash agglomeration, slagging of the furnace, or increased oxygen requirements, and this leads to heat losses and inefficient combustion (Loo and Koppejan, 2008). Incomplete combustion may lead to the formation of gaseous pollutants such as SO_x, NO_x, CO, volatile organic compounds (VOC), polycyclic aromatic hydrocarbons (PAHs) and chlorinated hydrocarbons such as polychlorinated dibenzo-ρ-dioxins and dibenzofurans (PCDD/PCDF) dioxin (Bowen *et al*., 2010; Wang *et al*., 2016). Deposit formation and corrosion are particularly a concern with fuels containing high Cl and K, such as biomass (Yin *et al*., 2008).

For fluidised bed combustion, a wide range of fuels of different sizes, shapes, moisture contents and heating values can be used, as a result of the high level of contact between gases and solids, which increases efficiency (Werther *et al*., 2000). Fluidisation occurs when air is passed through a bed material, usually silica sand, which begins to behave like a liquid due to reduction of internal friction forces and cohesion. The fluidising air velocity determines the configuration of the unit, e.g. bubbling, turbulent, or circulating (Williams, 2005). A more detailed description of these configurations is provided in the following section (1.2.2).

1.2.2 Gasification

Biomass gasification transforms the solid fuel into a gaseous energy carrier called "product gas" or "producer gas" under sub stoichiometric oxygen conditions (Arena, 2012). This means that the oxygen supplied to the reaction zone in the gasifier is below the amount of oxygen required for complete stoichiometric combustion. The product gas consists of gases which are not completely oxidised and vary in composition depending on the feedstock (Sarkar *et al*., 2014, Thanapal *et al*., 2012), process type (Couto *et al*., 2013) and process parameters (Xue *et al*., 2014; Pandey *et al*., 2016). Generally, gasification produces a mixture of CO, H_2, CH_4, CO_2, H_2O, N_2 and contaminants, such as particulates, tar, H_2S, HCl, NH_3, HCN, COS (McKendry, 2002b). The low to medium calorific value gas (4 and 6 MJ Nm^{-3}) can either be burned directly or used as a fuel for gas engines and turbines after the necessary gas cleaning steps (Arena, 2012). The main components CO and H_2, also called "syngas", allow the production of chemicals (e.g. methanol) and fuels (Fisher Tropsch synthesis) (Isaksson *et al*., 2013; Selvatico *et al*., 2016).

Gasification includes a sequence of endothermic and exothermic steps, similar to the ones described in section 1.2.1 (Basu, 2010b):

1) Heating and drying of the biomass (< 160 °C): in an auto-thermal gasification system, part of the vapours and char formed during pyrolysis are combusted to supply heat for drying the feedstock, for maintaining the process temperature, and for the endothermic gasification reactions. For allo-thermal gasification an external heat supply is used.

2) Pyrolysis (devolatilisation) (< 700 °C): the biomass is converted to light permanent gases (non-condensable gases), primary tar (condensable gases), and char due to the thermal decomposition in an oxygen free environment. The composition of the volatiles depends on the original feedstock, temperature, pressure, atmosphere and heating rate. The condensed primary tar is also called bio-oil and is composed of oxygenated hydrocarbons (levoglucosan, acetic acid and alcohols). Primary tar is further cracked to permanent gases and secondary tar. The secondary tars are comprised of a mixture of phenols, cresol, benzene and methyl- and hydroxyl-derivates. Cracking of secondary to ternary tars produce methyl-derivates of aromatic components (toluene and xylene) and polycyclic components like naphthalene.

3) Gasification (700 °C – 900 °C): during gasification endothermic reactions between gas-gas and solid-gas phases take place in a reducing environment. Table 1-1 lists the most important gas forming reactions. The endothermic gasification reactions are all equilibrium reactions. The final gas composition is determined by the reaction rates and catalytic effects. For example, the pyrolysis process is several orders of magnitude faster than char gasification with CO_2 and H_2O. This is relevant for biomasses with a high moisture and volatile matter (VM) content, as oxygen prefers to react with the volatile gases before gasifying the char with CO_2 and H_2O. The reactivity of the char particles may also play a role kinetically and depends on the composition of the original feedstock. For example, elements in the biomass ash, such as alkaline (K, Na), alkaline earth (Ca, Mg) and transition (Fe) metals, can act as catalysts to promote carbon reaction.

Table 1-1: Typical gasification reactions at 25 °C (Basu, 2010b)

Carbon reactions		
R1 (Boudouard)	$C + CO_2 \leftrightarrow 2CO$	$+ 172$ kJ mol^{-1}
R2 (Water-gas or steam)	$C + H_2O \leftrightarrow CO + H_2$	$+ 131$ kJ mol^{-1}
R3 (Hydrogasification)	$C + 2\ H_2 \leftrightarrow CH_4$	$- 74.8$ kJ mol^{-1}
R4	$C + 0.5\ O_2 \rightarrow CO$	$- 111$ kJ mol^{-1}
Oxidation reactions		
R5	$C + O_2 \rightarrow CO_2$	$- 394$ kJ mol^{-1}
R6	$CO + 0.5\ O_2 \rightarrow CO_2$	$- 284$ kJ mol^{-1}
R7	$CH_4 + 2\ O_2 \leftrightarrow CO_2 + 2\ H_2O$	$- 803$ kJ mol^{-1}
R8	$H_2 + 0.5\ O_2 \rightarrow H_2O$	$- 242$ kJ mol^{-1}
Water-gas shift reaction		
R9	$CO + H_2O \leftrightarrow CO_2 + H_2$	$- 41.2$ kJ mol^{-1}
Methanation reactions		
R10	$2\ CO + 2H_2 \rightarrow CH_4 + CO_2$	$- 247$ kJ mol^{-1}
R11	$CO + 3\ H_2 \leftrightarrow CH_4 + H_2O$	$- 206$ kJ mol^{-1}
R14	$CO_2 + 4\ H_2 \rightarrow CH_4 + 2\ H_2O$	$- 165$ kJ mol^{-1}
Steam-Reforming Reactions		
R12	$CH_4 + H_2O \leftrightarrow CO + 3\ H_2$	$+ 206$ kJ mol^{-1}
R13	$CH_4 + 0.5\ O_2 \rightarrow CO + 2\ H_2$	$- 36$ kJ mol^{-1}

The type of gasification system is defined based on the heat supply (direct/indirect), pressure (atmospheric/pressurised), gasification agent (air, oxygen, steam, plasma), reactor design (fixed bed, fluidised bed, entrained flow), temperature (low/high), bottom ash status (dry/vitrified) and energy recovery (heat/power) (McKendry, 2002b). Air is the most commonly used gasifying agent, since it is inexpensive; however, the calorific value of the gas is significantly lower than oxygen or steam gasification due to dilution with N_2, and this also increases the size of downstream gas cleaning equipment (Arena, 2012).

A biomass gasification plant consists of consecutive parts, including biomass handling and feeding system, gasifier reactor, gas clean-up system and ash or solid residue removal system. For each type of gasifier there is an appropriate range of application. Fixed (or moving) bed gasifiers can be built inexpensively at small scale (10 kW_{th} to 10 MW_{th}). Fluidised bed gasifyers are appropriate for intermediate units (5 MW_{th} to 100 MW_{th}) and entrained flow gasifyers are used as large capacity units (> 50 MW_{th}). (Basu, 2010c). To select an appropriate gasifier some considerations have to be made first, such as feedstock, capital, operating and maintenance costs, transport, and feedstock preparation, such as drying, separation, size reduction, and pelletising (McKendry, 2002b; Siedlecki *et al*., 2011). For waste biomasses the feedstock costs are often negligible; however, additional operational costs might be involved. Waste treatment plants at large scale are very often not accepted by local communities. Small scale plants are more sympathetic, since the perception is that small scale plants encourage waste recycling. Small scale gasifiers can be implemented in developing countries supplying communities with heat and electricity and encouraging rural development (Lee *et al*., 2013). In western society the incentive for producing renewable energy is a sense of responsibility to combat environmental problems and climate change, especially due to increasing consumerism and waste production (McKendry, 2002b).

Fixed bed gasifiers are categorised into updraft, downdraft and crossdraft gasifyers (Puig-Arnavat *et al*., 2010). Updraft gasifiers have the oldest and simplest design. (Basu, 2010d). They are also named counter-current gasifiers, since the oxidising agent travels up, while the fuel moves downwards. Updraft gasifiers are suitable for high ash and high moisture biomasses. The disadvantage is that tar production is high and therefore less suitable for fuels with a high amount of VM. The most promising

use of the volatile gases is direct combustion in a furnace or boiler, in which case no cooling or cleaning of the gas is required (Consonni and Viganò, 2012). Downstream gas cleaning equipment is necessary for the use of the product gas in gas turbines and engines, which includes removal of particulates, tar, and trace impurities (N, S, Cl) (Siedlecki, 2011).

Downdraft (co-current) reactors are designed in a way that the gasifying agent enters at a certain height below the top, while the product gas flows downwards through a bed of hot ash, hence tars are easily cracked and their production rate is kept very low (Basu, 2010d). Hence downdraft gasifiers are suitable for internal combustion engines due to the cleanliness of the product gas (Patra *et al.*, 2016).

In crossdraft (concurrent) gasifiers air is fed from the side, while the fuel enters from the top. The product gas is released opposite the entry point of the air. This type of gasifier is suitable for fuels with a very low ash content. Tar production is also kept low and hence the gas cleaning system is simple. The biomass units are usually very small (< 10 kW_e) (Basu, 2010d).

Fluidised bed gasifiers have the advantage of excellent solid-gas mixing and temperature uniformity as already described in section 1.2.1. The production of tars lies between that for updraft and downdraft gasification. Compared to fixed bed, fluidised bed gasifiers are complex in design and operation and require additional particle size reduction to about < 10 mm (McKendry, 2002b). Two principal types of fluidised bed gasifiers exist: bubbling fluidised bed and circulating fluidised bed. Bubbling fluidised bed gasifiers are the most popular for biomass and are designed in medium size units (< 25 MWth). The bed temperature is usually kept below 900 °C for biomass to avoid ash fusion and agglomeration. Circulating fluidised bed gasifiers have a long residence time, which make them suitable for fuels containing a high amount of VM. This type of gasifier is comprised of a riser, which acts as the reactor, a cyclone and a solid recycle device. The hot gas passes through the cyclone, which collects the solid particles, and these are then returned to the bottom gasifier by a loop seal (Basu, 2010d).

1.2.3 Pyrolysis

Pyrolysis occurs at elevated temperatures between 300 °C and 700 °C in the absence of an external oxygen supply. Large complex hydrocarbon bonds in biomass break down to smaller and simpler molecules to form gas, tar and char (Basu, 2010e). Primary tar is further converted to non-condensable gases, secondary tar and char by homogenous and heterogeneous reactions (Antal and Grønli, 2003) (Figure 1-4). The product yields and compositions depend on the design of the pyrolyser (simple kiln, large pyrolysis unit), the process parameters (temperature, residence time, heating rate) and the chemical and physical properties of the feedstock (McKendry, 2002a).

Pyrolysis is generally classified as slow or fast pyrolysis, depending on the heating rate. If the time ($t_{heating}$) required to heat the fuel to the maximum pyrolysis temperature is much lower than the characteristic pyrolysis reaction time (t_r), then the pyrolysis process is considered slow pyrolysis, and vice versa. (Basu, 2010e)

- Slow pyrolysis: $t_{heating} >> t_r$
- Fast pyrolysis: $t_{heating} << t_r$

During slow pyrolysis, also known as carbonisation, the residence time of the vapours in the reactor lies between minutes and hours. This time allows the primary char and volatiles to react to form secondary char and non-condensable gases (Basu, 2010e). Secondary reactions include thermal cracking, re-polymerization, and re-condensation. The heat transfer of radiative and convective heat from the surface of biomass particle to the interior occurs through conduction and pore convection (Figure 1-5).

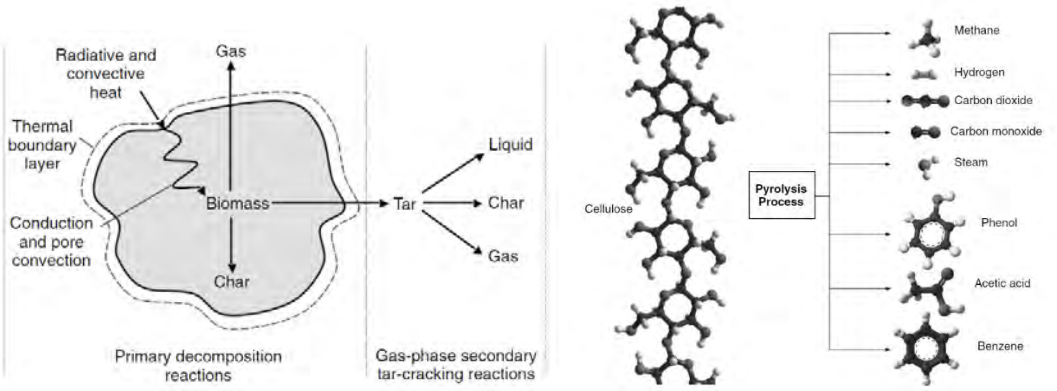

Figure 1-5: Pyrolysis in a biomass particle (left) and decomposition of large hydrocarbon molecules into smaller ones during pyrolysis (right). (Basu 2010e)

A high tar (bio-oil) yield is derived from the rapid heating during fast or flash pyrolysis, which yields higher amounts of volatiles through depolymerisation and fragmentation of cellulose, hemicellulose and lignin components (Bridgwater *et al*., 1999) (Figure 1-4). Upon condensation an aqueous phase, comprised of methanol, acetic acid, acetone, some phenols and water, and an organic phase with non-polar aliphatic and aromatic compounds are created (Azargohar *et al*., 2013). The individual biomass constituents undergo pyrolysis differently. Hemicellulose (decomposition between 150 °C - 350 °C) produces more non-condensable gases and less tar and char, while cellulose (decomposition between 275 °C - 350 °C) is the primary source of condensable vapour. Lignin decomposes under a broader temperature range (250 °C - 500 °C), producing more aromatics and char than cellulose (McKendry, 2002a). Bio-oil can be used in engines and turbines, or as a source for chemical and fuels. However, its poor thermal stability and its corrosiveness still need to be addressed and upgrading possibilities are being investigated, e.g. by lowering the oxygen content in the bio-oil and removing alkali metals by means of hydrogenation and catalytic cracking (Melligan *et al*., 2013).

Pyrolysis has largely been applied to produce bio-oil via fast pyrolysis; however, the goal of producing a char for soil amelioration and crop growth enhancement, namely biochar, is becoming more prioritised (Conte *et al*., 2015). The biochar industry is still limited to a few small enterprises selling biochar in local areas. Businesses are mainly in Europe and North America, followed by Asia and Africa. Woody biomass from forestry and other wood industries are by far the largest source of biochar. The scale and type of biochar production unit range from micro-scale cookstoves to large-scale industrial facilities. Some barriers to expand biochar production on an industrial scale include the lack of consumer awareness, technology constraints, access to financing and political issues (Jirka and Tomlinson, 2013).

The first industrial scale pyrolysis reactor in Europe for biochar production has been in operation since 2012 (Sonnenerde, 2016). The pyrolyser is a modified version of a reactor developed by PYREG GmbH in Switzerland and is in operation 24 h producing around 1.500 kg biochar a day. The woody feedstock is transferred to the reactor via a rotary feeder and heated to about 600 °C. The gas is extracted immediately, cleaned with aid of a cyclone and burned at 1200 °C to provide heat to dry the feedstock and drive the pyrolysis process. The biochar is removed from the reactor and immediately

quenched with water for it to be used for different applications, e.g. as a compost additive. The use of biochar is discussed in more detail in section 1.3.

1.3 Biochar

Biochar is the carbon rich residue of thermal treatment of an organic material under limited supply of oxygen, produced with the purpose of improving soil productivity and carbon storage (EBC, 2012). The benefits of biochar have been known for a while, leading back to pre-Columbian times, where the practices of the ancient Amerindian populations contributed to the creation of the fertile terra preta de Índio soils of the Amazon region, also known as anthropogenic "dark earth". However, recent investigations are driven by other motives such as improved waste management, energy production, mitigation of climate change and nutrient recycling (Lehmann and Joseph, 2009).

1.3.1 Biochar production and unique properties

Biochar properties are influenced by several factors, primarily the type of process (pyrolysis, gasification) (Brewer *et al*., 2009; Long *et al*., 2012), the process conditions (maximum temperature, heating rate, residence time) (Kloss *et al*., 2012; McBeath *et al*., 2014) and the physico-chemical properties of the feedstock (McBeath *et al*., 2014). Typically, slow pyrolysis is applied due to the low maximum temperature (~ 400 °C) and heating rate (< 2 °C s^{-1}), which maximises char yield (~ 50 wt.%). However, other types of processes, such as fast pyrolysis and gasification, which aim to produce a bio-oil at a fast heating rate (10-1000 °C s^{-1}) or a product gas respectively, leave a char residue, which may potentially be used as biochars (Chen *et al*., 2003). The produced biochar resembles the parent material depending on the feedstock's relative contents of biomass components (i.e., hemicellulose, cellulose, lignin, protein and ash).

The process conditions during slow pyrolysis have a significant influence on the feedstock's decomposition and hence on the biochar's final chemical and physical characteristics (Keiluweit *et al*., 2010, McBeath *et al*., 2014; Brewer *et al*., 2009). With increasing pyrolysis temperature, aliphatic compounds undergo chemical transformation to aromatic ring structures, leading to the formation of larger conjugated sheets by progressive condensation of smaller aromatic units (Figure 1-6). Abrupt changes in the physical properties of chars have been observed with regard to

crystallinity and porosity, which suggests a non-linear phase transition with increasing temperature (Keiluweit *et al*., 2010). The transformation of biomass to condensed aromatic carbon structures with high crystallinity has been seen as a key property to the biochars' carbon sequestration potential (Novotny *et al*., 2015; Budai *et al*., 2013). The chars experience several phase transitions leading from microcrystalline cellulose and amorphous lignin and hemicellulose over a large pyrogenic amorphous carbon intermediate phase towards the formation of turbostratic crystallites (Keiluweit *et al*., 2010). The transition over the temperature gradient results in a decrease of VM and subsequent weight loss of the original biomass. While higher temperatures are beneficial for carbon sequestration, lower condensed structures results in higher reactivity, which might be an interesting feature for soil application (Mukherjee *et al*., 2013).

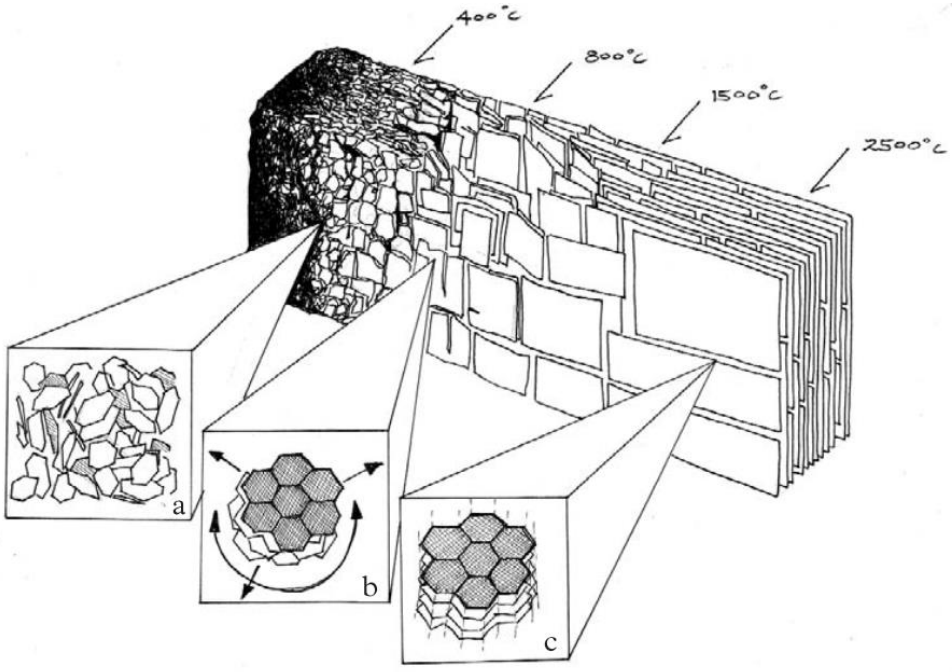

Figure 1-6: Chemical transformation of amorphous carbon to sheets of conjugated aromatic ring structures over a temperature gradient. (Lehmann and Joseph, 2009)

The proposed beneficial characteristics and functions of biochar were summarised by Manyà (2012). Biochar can be used for improving soil structure by altering physical properties, such as bulk density, pore size distribution, texture and structure. Increasing the overall surface area influences the soil native microbial communities, sorption capacity, aeration and soil water retention. High cation exchange capacity (CEC) decreases leaching and enhances the ability of the soil to adsorb and retain

cations (Uchimiya *et al*., 2012). Biochar has great potential for carbon sequestration (Mao *et al*., 2012; Singh *et al*., 2012) decreasing soil acidity (chapter 4), decreasing risk of pathogens and organic pollutants by sorption of hydrophobic organic compounds (Beesley *et al*., 2011), decreasing metal availability (Kołodyńska *et al*., 2012), decreasing waste volume and releases of GHGs (Roberts *et al*., 2010).

Even though there has been extensive discussion about the advantages of biochar there are still many research gaps to be filled (Font-Palma, 2012; Manyà, 2012). The effect of the operating conditions on biochar properties and yields has already been subject to various investigations and is fairly well understood (Enders *et al*., 2012; Wang *et al*., 2012); however, more experimental data for modelling work is needed. The relationship between biochar properties and the potentials to enhance agricultural soil is not clearly understood due to the complexity of feedstock properties and environmental factors (Joseph *et al*., 2010). Biochar has been found to either enhance or inhibit plant growth depending on its physical and chemical properties and the interaction with soils (Rillig *et al*., 2010; Luo *et al*., 2011, Uzoma *et al*., 2011). Hence different soil compositions, structures and pH values may require different biochar properties and concentrations. Agronomic responses of different crops with the same soil-biochar combination may differ (Enders *et al*., 2012). Therefore, for an effective prediction of the agronomic performance of biochars it might be necessary to define factors of a particular soil-crop-climate situation and apply biochars according to e.g. liming equivalence, buffering capacity, element content, and phytotoxicity. The long term behaviour of biochar when applied to soil is an important factor to be considered, since changes with regard to soil properties, bacterial and fungal growth, carbon mineralisation, etc. occur with time (Jones *et al*., 2012). The biochar's stability depends very much on the carbon structural properties (degree of aromaticity), but also on environmental conditions (Singh *et al*., 2012). Hence longer-term field trials and the influence on the mobility and fate of char in the environment are essential to see the long term benefits of biochar application.

1.3.2 Biochar produced from animal waste

The viability of producing biochar from waste materials is broadly discussed. Waste materials are typically inhomogeneous, and high in inorganic and moisture content (Cantrell *et al*., 2008). While the biochar community preferably focus on dry woody

biomasses as a biochar source, parties involved in waste management show a high interest in thermal treatment of waste materials for several reasons. Not only can energy be obtained from the processes, but the weight and volume of the waste material is significantly reduced (Consonni *et al*., 2005). Other benefits include elimination of pathogens and odour compounds (Arena, 2012); reduction of GHG emissions from anaerobic decomposition; reduced fuel heating requirements due to excess heat from the process; reduced nutrient run off; and potential for added income from side products. The main arguments against thermal treatment of wastes are the high tar formation (Font Palma, 2013), loss of nutrients (especially nitrogen) (Baniasadi *et al*., 2016), reliability, and capital investment (Arena, 2012).

Thermal treatment of animal manures, such as poultry litter (PL) (Abelha *et al*., 2003; Font-Palma, 2012; Kelleher *et al*., 2002), swine manure (Ro *et al*., 2009; Tsai *et al*., 2012) and cattle manure (Cantrell *et al*., 2012; Thanapal *et al*., 2012), have increasingly been subject of investigation. Valuable macro- and micronutrients can be recovered in the obtained ash and biochar fractions, especially non-volatile minerals like phosphorus (P) (Thygesen and Johnsen, 2012; Wang *et al*., 2012). However, combustion and gasification operate at high enough temperatures for the ash to cause operational problems, in particular agglomeration (Di Gregorio *et al*., 2014; Lynch *et al*., 2013). Hence, low operating temperatures may be unavoidable and pyrolysis could be seen as the preferred technology for waste treatment (see chapter 3). Furthermore, low temperatures result in higher carbon and nutrient (K, N, S) recovery (see chapter 4).

Some physico-chemical properties of manure derived biochars can be a hindrance for European Biochar Certification (EBC, 2012), however; they possess one significant advantage over lignocellulosic biochars, namely the high nutrient content and immediate fertilising effect. Fertiliser efficiency depends on pyrolysis process conditions, in particular the maximum temperature at which the biochars are produced (Subedi *et al*., 2016a - *paper II*). The process conditions, however, also impact on GHG emissions after introduction to the soil (Subedi *et al*., 2016 - *paper III*), and the biochars might result in increased emissions where high fertiliser efficiency was achieved. Lignocellulosic biochars are mainly composed of carbon, and their carbon matrix shows a unique and beneficial structure for soil amelioration as discussed in section 1.3.1. Carbon rich biochars may be enriched with nutrients to ensure instant

crop growth enhancement, where indirect effects on crop growth are not visible (Subedi *et al*., 2016a). Further information on manure derived biochars can be found in section 4.2. Section 1.3.3 describes different applications of biochar in animal farming and their simultaneous enrichment with manure nutrients.

1.3.3 Biochar usage in animal production systems

Scientists believe that biochar has to undergo transformation in the soil over decades or centuries to show a long term positive effect on soil amelioration (Mao *et al*., 2012; Singh *et al*., 2012); hence, the direct application of biochar to soil may not be economically viable. Evidence has shown that during the time of the ancient American Indians char were mixed with inorganic (e.g. ash, bones) and organic (e.g. biomass wastes, manure, excrements, urine) and introduced to infertile Ferralsols creating the fertile terra preta de Índio. (Glaser and Birk, 2012). The strong binding properties of biochar most likely developed over time through oxidation, creating a biochar acting as a nutrient store and humus stabiliser (Joseph *et al*., 2010). Therefore, biochar used in combination with nutrient rich materials in an oxidising environment might be advantageous before further applying it into agricultural field. Today, about 90% of biochar used in Europe goes into animal farming, including silage agent, feed supplement, litter additive, slurry treatment, manure composting, or water treatment in fish farming (Schmidt, 2012a).

There is increasing interest in using biochar as a stock feed additive, and investigations on this topic are increasing (McHenry, 2010; Toth and Dou, 2014; Joseph *et al*., 2015). Charcoal is known as an old remedy for digestive disorders as outlined by Gerlach and Schmidt (2012). The incidence of diarrhea rapidly decreases, toxins can be deactivated in the digestive system, feed intake is improved, allergies disappear, and the animals become calmer. The intestinal flora is positively activated, and the vitality of the animals improves markedly. Three main studies of interest were outlines by Toth and Dou (2014), namely animal performance, binding toxic substances and controlling pathogens, and reducing CH_4 production.

As a slurry additive biochar with a high specific surface area and CEC might be very efficient in binding NH_4^+ and NH_3 and other odorous and toxic substances, reduce nutrient leaching, promote soil activity and humus formation (Schmidt, 2012b). In poultry sheds the addition of highly porous biochar may serve to reduce toxic NH_3

pollution and regulate the moisture level of the litter (Gerlach and Schmidt, 2012); however further investigations are required to fully understand the benefits of biochar with regard to these applications. A study conducted by Subedi *et al*. (2015) (*paper IV*), assessing the use of biochar and hydrochar amendments to reduce the volatilization of NH_3 following slurry application revealed that NH_3 volatilization can be enhanced under certain circumstances. The attachment of microorganisms to materials with a high surface area is assumed to have a crucial impact on CH_4 emissions during AD (Adu-Gyamfi *et al*., 2012; Michaud *et al*., 2002; Michaud *et al*., 2005). For example, biochar has shown to prevent mild NH_3 inhibition through kinetic and microbiota analyses (Mumme, 2014).

Toth and Dou (2014) comment that despite the rapidly increasing number of studies devoted to biochar in animal production systems, research is still largely empirical. Only few studies have examined relevant mechanisms to explain how biochar treatments bring about the observed effects. The effects of biochar as a cow slurry additive on emissions from slurry tanks and soil-nitroen dynamics when introduced to soil in combination with slurry is reviewed in the sections 5.2 and 6.2.

1.4 The ReUseWaste project

1.4.1 Overview

The ReUseWaste Initial Training Network project was initiated to bring together research groups from universities and other institutes, agri-environmental technology companies and public regulatory authorities, located in the countries and regions of most intensive livestock production in Europe. The overall objective of ReUseWaste was to rethink the currently established manure management systems and develop and apply new technologies to improve the utilisation of manure OM and nutrients in a sustainable manner. The knowledge should provide companies with improved and new technologies to produce both bioenergy and bio-fertilisers, leading to improved soil, water and air quality. (ReUseWaste, 2016)

Figure 1-7 presents an overview of the ReUseWaste network and the objectives of the different work packages (WP), which include developing new characterisation tools for manure components (WP3), finding new technologies for treatment and separation

of manure OM and nutrients (WP4), developing new technologies for bioenergy and nutrient recovery (WP5), assessment of the performances of the manure treatment products through land recycling (WP6) and finally implementation of integrated assessments and stakeholder dialogues to integrate the gained knowledge into new manure management systems (WP7).

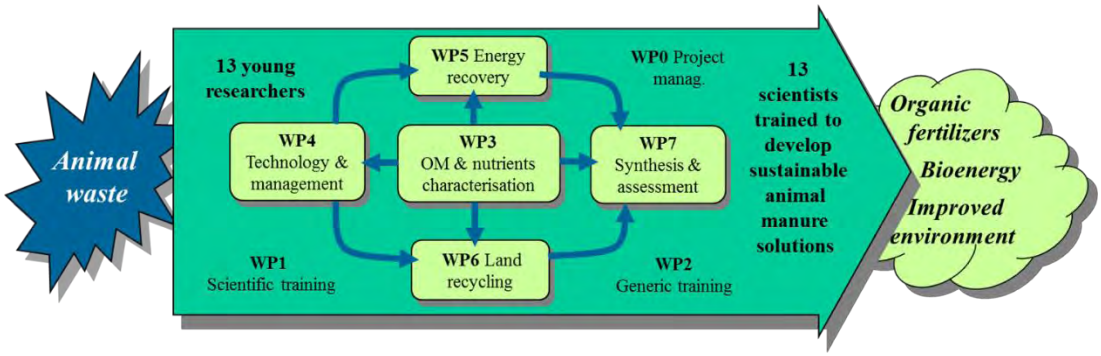

Figure 1-7: ReUseWaste project overview and objectives of each work package (WP) (ReUseWaste, 2016)

1.4.2 Collaborations between UTO and CEBAS-CSIC

The ReUseWaste network consisted of nine main partners from Denmark, The Netherlands, Portugal, Spain, Italy and Ireland, of which the University of Copenhagen, Denmark acted as the project coordinator. Collaborations between project partners was encouraged. The University of Limerick worked closely with the University of Torino (UTO), Italy, and resulted in some joint publications (see list of references *paper II, paper III* and *paper IV*) in peer-reviewed journals as listed below. Furthermore, a publication in collaboration with the 'Centro de Edafología y Biología Aplicada del Segura (CEBAS)' belonging to the 'Consejo Superior de Investigaciones Científicas (CSIC)', the Spanish National Research Council, in Murcia, Spain, is on the way.

1.4.3 Scope of Research at UL

The main aim of the research conducted at the University of Limerick (UL) was to assess substoichiometric thermochemical technologies for processing animal manure and utilising the manure treatment products in agricultural systems.

The primary focus was on biochar production and nutrient recovery from a variety of manure feedstocks using two types of processes, namely updraft gasification at pilot

scale and slow pyrolysis at laboratory scale. The effect of the process parameters on the derived biochars' physical and chemical properties and the effect of these biochars on plant growth and nutrient uptake after incorporation into soil was investigated.

Furthermore, the usability of biochar derived from virgin wood (Sitka spruce) using a uniquely designed Kon-Tiki pyrolysis kiln in two stages of the manure management chain was evaluated. The first part included an investigation in reducing NH_3 emissions when biochar was added to cow slurry during storage. The second part involved soil application of biochar mixed with cow slurry and its impact on plant growth, nitrate leaching and nitrification and denitrification behaviour using gene amplification.

The structure of the thesis is presented as follows:

Chapter 1: Introduction - introduces the topic of manure management and describes the most common manure treatment options in practice today for recycling animal manure. The focus lies on thermal treatment of different manure and lignocellulose feedstocks to produce biochar, which can be used to improve soil quality, enhance plant growth and mitigate environmental pollution in the manure management chain.

Chapter 0: Methodology - provides the reader with detailed description of the methods and operational details of the equipment used throughout the course of this research project.

Chapter 3: Updraft Gasification of Poultry Litter at Farm-Scale – A Case Study - presents a critical analysis of updraft gasification of poultry litter at farm-scale. The process performance of an existing auto-thermal updraft gasification system is demonstrated, together with the characteristics of the obtained products gas, tar and char. This chapter was published in a peer-reviewed journal (see list of references *paper I*).

Chapter 4: Manure Biochar as a Means for Closing Nutrient Cycles in Agriculture – presents the effect of thermo-chemical process type (gasification and pyrolysis) and maximum pyrolysis temperature (400 °C and 600 °C) on the physical and chemical properties of biochar using dehydrated poultry litter, cow manure and swine manure as feedstocks. Insight into the plant growth and nutrient uptake enhancement when these biochars are incorporated into soil is given.

Chapter 5: Mitigation of Ammonia Emissions during Storage of Cow Slurry amended with Biochar and Sulfuric Acid - gives insight into the effectiveness of Sitka spruce biochar, produced via a uniquely designed pyrolysis unit called Kon-Tiki kiln, to reduce ammonia emissions during the storage of cow slurry and to further investigate methane and hydrogen sulphide emissions with additional treatment with sulfuric acid.

Chapter 6: Nitrogen Dynamics in Soil treated with Slurry, Biochar and Biochar amended Slurry – describes the influence of Sitka spruce biochar on nitrate leaching from cow slurry when introduced to soil. Furthermore, nitrogen uptake to grass and changes in gene abundances in soil to evaluate nitrification (bacterial and archaeal *amoA*) and denitrification (*nosZ*) capabilities are presented.

Chapter 7: Conclusions and Recommendations for Future Work – summarises the key findings of the investigations and gives suggestions for future research work in the area.

1.5 References

Abelha, P., Gulyurtlu, I., Boavida, D., Barros, J.S., Cabrita, I., 2003. Combustion of poultry litter in a fluidised bed combustor. Fuel. 82, 687–692.

Adu-Gyamfi, N., Ravella, S.R., Hobbs, P.J., 2012. Optimizing anaerobic digestion by selection of the immobilizing surface for enhanced methane production. Bioresour. Technol. 120, 248–255.

Ågren, G.I., Wetterstedt, J.Å.M., Billberger, M.F.K., 2012. Nutrient limitation on terrestrial plant growth - modelling the interaction between nitrogen and phosphorus. New Phytol. 194, 953–960.

Antal, M.J., Grønli, M., 2003. The art, science, and technology of charcoal production. Ind. Eng. Chem. Res. 42, 1619–1640.

Arena, U., 2012. Process and technological aspects of municipal solid waste gasification. A review. Waste Manag. 32, 625–639.

Altieri, M. A., 1998. Ecological impacts of industrial agriculture and the possibilities for truly sustainable farming. Monthly Review: An Independent Socialist Magazine. 5 (3), 60–71.

Azargohar, R., Jacobson, K.L., Powell, E.E., Dalai, A.K., 2013. Evaluation of properties of fast pyrolysis products obtained, from Canadian waste biomass. J. Anal. Appl. Pyrolysis 104, 330–340.

Baniasadi, M., Tugnoli, A., Conti, R., Torri, C., Fabbri, D., Cozzani, V., 2016. Waste to energy valorization of poultry litter by slow pyrolysis. Renew. Energy 90, 458–468.

Basu, P., 2010a. Biomass Gasification and Pyrolysis - Practical Design. Elsevier Inc., Oxford, UK. 11-13.

Basu, P., 2010b. Biomass Gasification and Pyrolysis - Practical Design. Elsevier Inc., Oxford, UK. 117-121.

Basu, P., 2010c. Biomass Gasification and Pyrolysis - Practical Design. Elsevier Inc., Oxford, UK. 167-168.

Basu, P., 2010d. Biomass Gasification and Pyrolysis - Practical Design. Elsevier Inc., Oxford, UK. 170-180.

Basu, P., 2010e. Biomass Gasification and Pyrolysis - Practical Design. Elsevier Inc., Oxford, UK. 65-76.

Beesley, L., Moreno-Jiménez, E., Gomez-Eyles, J.L., Harris, E., Robinson, B., Sizmur, T., 2011. A review of biochars' potential role in the remediation, revegetation and restoration of contaminated soils. Environ. Pollut. 159, 3269–3282.

Bowen, B., Lynch, D., Lynch, D., Henihan, A.M., Leahy, J.J., McDonnell, K., 2010. Biosecurity on Poultry Farms from On-Farm Fluidized Bed Combustion and Energy Recovery from Poultry Litter. Sustainability 2, 2135–2143.

Brewer, C.E., Schmidt-rohr, K., Satrio, J.A., Brown, R.C., 2009. Characterization of Biochar from Fast Pyrolysis and Gasification Systems. Environ. Prog. Sustain. Energy 28, 386–396.

Bridgwater, A. V, Meier, D., Radlein, D., 1999. An overview of fast pyrolysis of biomass. Org. Geochem. 30, 1479–1493.

Budai, A., Zimmerman, A.R., Cowie, A.L., Webber, J.B.W., Singh, B.P., Glaser, B., Masiello, C.A., Andersson, D., Shields, F., Lehman, J., Camps Arbestain, M.C., Williams, M., Sohi, S., Joseph, S., 2013. Biochar Carbon Stability Test Method: An assessment of methods to determine biochar carbon stability. Int. Biochar Initiat.

Burns, I.G., 1992. Plant Soil - Influence of plant nutrient concentration on growth rate: Use of a nutrient interruption technique to determine critical concentrations of N, P and K in young plants. An International Journal on Plant-Soil Relationships, 142-221.

Cantrell, K., Ro, K., Mahajan, D., Anjom, M., Hunt, P.G., 2007. Role of thermochemical conversion in livestock waste-to-energy treatments: Obstacles and opportunities. Ind. Eng. Chem. Res. 46, 8918–8927.

Cantrell, K.B., Hunt, P.G., Uchimiya, M., Novak, J.M., Ro, K.S., 2012. Impact of pyrolysis temperature and manure source on physicochemical characteristics of biochar. Bioresour. Technol. 107, 419–428.

Chadwick, D., Sommer, S., Thorman, R., Fangueiro, D., Cardenas, L., Amon, B., Misselbrook, T., 2011. Manure management: Implications for greenhouse gas emissions. Anim. Feed Sci. Technol. 166-167, 514–531.

Chen, S., Kincaid, R.L., Harrison, J.H., Elliott, D.C., Brown, M.D., 2003. Value-Added Chemicals from Animal Manure. PNNL-14495. U.S. Department of Energy. Springfield. Virginia, 1-11.

Christensen, M.L., Sommer, S.G., 2013. Manure Characterisation in Inorganic Chemistry. In Sommer, S.G., Christensen, M.L., Schmidt, T., Jensen, L.S. (Eds.). Animal Manure Recycling - Treatment and Management. John Wiley and Sons Ltd. Chichester, West Sussex, UK, 41-42.

Christensen, M.L., Christensen, K.V., Sommer, S.G., 2013. Solid-liquid Separation of Animal Slurry. In Sommer, S.G., Christensen, M.L., Schmidt, T., Jensen, L.S. (Eds.). Animal Manure Recycling - Treatment and Management. John Wiley and Sons Ltd. Chichester, West Sussex, UK, p. 105.

Consonni, S., Giugliano, M., Grosso, M., 2005. Alternative strategies for energy recovery from municipal solid waste. Part A: Mass and energy balances. Waste Management 25, 123–135.

Conte, P., Schmidt, H., Cimò, G., 2015. Research and Application of Biochar in Europe of Biochar in Europe. In Guo, M., He, Z., Uchimiya, M., (Eds.). gricultural and Environmental Applications of Biochar: Advances and Barriers. SSSA Special Publication 63. Madison, Wisconsin, USA. 1–21.

Couto, N., Rouboa, A., Silva, V., Monteiro, E., Bouziane, K., 2013. Influence of the biomass gasification processes on the final composition of syngas. Energy Procedia 36, 596–606.

De Vries, J.W., Groenestein, C.M., De Boer, I.J.M., 2012. Environmental consequences of processing manure to produce mineral fertilizer and bio-energy. J. Environ. Manage. 102, 173–183.

De Vries, J.W., Groenestein, C.M., Schröder, J.J., Hoogmoed, W.B., Sukkel, W., Groot Koerkamp, P.W.G., De Boer, I.J.M., 2015. Integrated manure management to reduce environmental impact: II. Environmental impact assessment of strategies. Agric. Syst. 138, 88–99.

Di Gregorio, F., Santoro, D., Arena, U., 2014. The effect of ash composition on gasification of poultry wastes in a fluidized bed reactor. Waste Manag. Res. 32, 323–330.

EBC, 2012. European Biochar Certificate - Guidelines for a Sustainable Production of Biochar. European Biochar Foundation (EBC), Arbaz, Switzerland. Available at http://www.europeanbiochar.org/en/download. Version 6.1 of 19th June 2015

Ehlert, P.A.I., Schoumans, O.F., 2015. Products, by-products and recovered secondary materials from processed animal manure. Wageningen, Alterra Wageningen UR (University & Research centre). Alterra report 2668, 30.

Enders, A., Hanley, K., Whitman, T., Joseph, S., Lehmann, J., 2012. Characterization of biochars to evaluate recalcitrance and agronomic performance. Bioresour. Technol. 114, 644–653.

EPA, 2015. Ireland's Greenhouse Gas Emission Projections (2014-2035). Environmental Protection Agency. Available at https://www.epa.ie/pubs/reports/air/airemissions/EPA%202015%20GHG%20Projections%20Publication%20Final.pdf (accessed 01.06.2016).

EurActiv, 2012. Intensive farming: Ecologically sustainable? Available at https://www.euractiv.com/section/agriculture-food/linksdossier/intensive-farming-ecologically-sustainable/#ea-accordion-background (accessed 19.11.2016)

European Commission, 2016. Key EU Policies for Ireland. Representation in Ireland. Agriculture. Available at http://ec.europa.eu/ireland/news/key-eu-policy-areas/agriculture_en (accessed 01.06.2016).

Eurostat, 2012. Agri-environmental indicator - livestock patterns. Fact sheet. Available at http://ec.europa.eu/eurostat/statistics-explained/index.php/Agri-environmental_indicator_-_livestock_patterns#Further_Eurostat_information (accessed 01.06.2016).

Eurostat, 2015. Agriculture statistics at regional level. Eurostat regional yearbook publication. Available at http://ec.europa.eu/eurostat/statistics-explained/index.php/Agriculture_statistics_at_regional_level (accessed 01.06.2016).

FAO, 2016. Animal production. FAO's role in animal production. Food and Agriculture Organization of the United Nations. Available at http://www.fao.org/animal-production/en/ (accessed 01.06.2016).

Feilberg, A., Sommer, S.G., 2013. Ammonia and Malodorous Gases: Sources and Abatement Technologies. In Sommer, S.G., Christensen, M.L., Schmidt, T., Jensen, L.S. (Eds.). Animal Manure Recycling - Treatment and Management. John Wiley and Sons Ltd. Chichester, West Sussex, UK. 167-172.

Font-Palma, C., 2012. Characterisation, kinetics and modelling of gasification of poultry manure and litter: An overview. Energy Convers. Manag. 53, 92–98.

Font Palma, C., 2013. Modelling of tar formation and evolution for biomass gasification: A review. Appl. Energy 111, 129–141.

Gerlach, H., Schmidt H.P., 2012. Biochar in poultry farming. Ithaka Journal 1/ 2012: 262–264. Available at http://www.ithaka-journal.net/pflanzenkohle-in-der-geflugelhaltung?lang=en (accessed 01.06.2016.)

Gerlach, H., Schmidt H.P., 2012. The use of biochar in cattle farming. Ithaka Journal. Available at http://www.ithaka-journal.net/pflanzenkohle-in-der-rinderhaltung?lang=en (accessed 01.06.2016.)

Gilbert, N., 2012. One-third of our greenhouse gas emissions come from agriculture. Nature - International weekly journal of science. Available at http://www.nature.com/news/one-third-of-our-greenhouse-gas-emissions-come-from-agriculture-1.11708 (accessed 01.06.2016.)

Glaser, B., Birk, J.J., 2012. State of the scientific knowledge on properties and genesis of Anthropogenic Dark Earths in Central Amazonia (*terra preta de Índio*). Geochimica et Cosmochimica Acta. 82, 39–51.

Havlin, J.L., Tisdale, S.L., Nelson, W.L., Beaton, J.D., 1999. Soil fertility and fertilizers: an introduction to nutrient management, Sixth edit. ed. Prentice Hall, Upper Saddle River, N.J. 14-22.

Henihan, A.M., 2006. Mitigation of Organic Waste Damage Incorporating a Demonstration of a Closed Loop Conversion of Poultry Litter to Energy at the Point of Source. Submitted to the College of Science, University of Limerick. 14-16.

Hjorth, M., Christensen, K. V., Christensen, M.L., Sommer, S.G., 2010. Solid—liquid separation of animal slurry in theory and practice. A review. Agron. Sustain. Dev. 30, 153–180.

Ingram, J., 2015. Framing niche-regime linkage as adaptation: An analysis of learning and innovation networks for sustainable agriculture across Europe. J. Rural Stud. 40, 59–75.

Isaksson, J., Åsblad, A., Berntsson, T., 2013. Influence of different pretreatment methods on biomass gasification and production of fischer-tropsch crude integrated with a pulp and paper mill. Chem. Eng. Trans. 35, 559–564.

Long, J., Song, H., Jun, X., Sheng, S., Lun-Shi, S., Kai, X., Yao, Y., 2012. Release characteristics of alkali and alkaline earth metallic species during biomass pyrolysis and steam gasification process. Bioresour. Technol. 116, 278–284.

Lynch, D., Henihan, A.M., Bowen, B., Lynch, D., McDonnell, K., Kwapinski, W., Leahy, J.J., 2013. Utilisation of poultry litter as an energy feedstock. Biomass and Bioenergy 49, 197–204.

Jensen, L.S., 2013a. Animal manure residue upgrading and nutrient recovery in biofertilisers. In Sommer, S.G., Christensen, M.L., Schmidt, T., Jensen, L.S. (Eds.). Animal Manure Recycling - Treatment and Management. John Wiley and Sons Ltd. Chichester, West Sussex, UK. 302-304.

Jensen, L.S., 2013b. Animal manure residue upgrading and nutrient recovery in biofertilisers. In Sommer, S.G., Christensen, M.L., Schmidt, T., Jensen, L.S. (Eds.). Animal Manure Recycling - Treatment and Management. John Wiley and Sons Ltd. Chichester, West Sussex, UK. 276-277.

Jensen, L.S., 2013c. Animal manure residue upgrading and nutrient recovery in biofertilisers. In Sommer, S.G., Christensen, M.L., Schmidt, T., Jensen, L.S. (Eds.). Animal Manure Recycling - Treatment and Management. John Wiley and Sons Ltd. Chichester, West Sussex, UK. 296-297.

Jirka, S. and Tomlinson, T., 2013. State of the Biochar Industry - A survey of commercial activity in the biochar field. A report by the International Biochar Initiative. Available at: http://www. biochar-international. org/sites/default/files/State_of_the_Biochar_Industry_2013. pdf (accessed 01.06.2016)

Jones, D.L., Rousk, J., Edwards-Jones, G., DeLuca, T.H., Murphy, D.V., 2012. Biochar-mediated changes in soil quality and plant growth in a three year field trial. Soil Biol. Biochem. 45, 113–124.

Joseph, S., Pow, D., Dawson, K., Mitchell, D.R.G., Rawal, A., Hook, J., Taherymoosavi, S., Van Zwieten, L., Rust, J., Donne, S., Munroe, P., Pace, B., Graber, E., Thomas, T., Nielsen, S., Ye, J., Lin, Y., Pan, G., Li, L., Solaiman, Z.M., 2015. Feeding Biochar to Cows: An Innovative Solution for Improving Soil Fertility and Farm Productivity. Pedosphere 25, 666–679.

Joseph, S.D., Camps-Arbestain, M., Lin, Y., Munroe, P., Chia, C.H., Hook, J., van Zwieten, L., Kimber, S., Cowie, A., Singh, B.P., Lehmann, J., Foidl, N., Smernik, R.J., Amonette, J.E., 2010. An investigation into the reactions of biochar in soil. Aust. J. Soil Res. 48, 501-515.

Jurado, E., Antonopoulou, G., Lyberatos, G., Gavala, H.N., Skiadas, I. V., 2016. Continuous anaerobic digestion of swine manure: ADM1-based modelling and effect of addition of swine manure fibers pretreated with aqueous ammonia soaking. Appl. Energy 172, 190–198.

Keiluweit, M., Nico, P.S., Johnson, M.G., Kleber, M., 2010. Dynamic molecular structure of plant biomass-derived black carbon (biochar). Environ. Sci. Technol. 44, 1247–1253.

Kelleher, B.P., Leahy, J.J., Henihan, a M., O'Dwyer, T.F., Sutton, D., Leahy, M.J., 2002. Advances in poultry litter disposal technology - a review. Bioresour. Technol. 83, 27–36.

Kloss, S., Zehetner, F., Dellantonio, A., Hamid, R., Ottner, F., Liedtke, V., Schwanninger, M., Gerzabek, M.H., Soja, G., 2012. Characterization of Slow Pyrolysis Biochars: Effects of Feedstocks and Pyrolysis Temperature on Biochar Properties. J. Environ. Qual. 41, 990-1000.

Kołodyńska, D., Wnętrzak, R., Leahy, J.J., Hayes, M.H.B., Kwapiński, W., Hubicki, Z., 2012. Kinetic and adsorptive characterization of biochar in metal ions removal. Chem. Eng. J. 197, 295–305.

Kupper, T., Bonjour, C., Menzi, H., 2015. Evolution of farm and manure management and their influence on ammonia emissions from agriculture in Switzerland between 1990 and 2010. Atmos. Environ. 103, 215–221.

Lee, U., Balu, E., Chung, J.N., 2013. An experimental evaluation of an integrated biomass gasification and power generation system for distributed power applications. Appl. Energy 101, 699–708.

Lehmann, J., Joseph, S., 2009. In Lehmann, J., Joseph, S. (Eds.). Biochar for Environmental Management – Science and Technology: An Introduction. Earthscan. London, UK, 2-5.

Li, K., Liu, R., Sun, C., 2015. Comparison of anaerobic digestion characteristics and kinetics of four livestock manures with different substrate concentrations. Bioresour. Technol. 198, 133–140.

Li, Y., Park, S. Y., Zhu, J., 2011. Solid-state anaerobic digestion for methane production from organic waste. Renewable and Sustainable Energy Reviews. 15, 821-826.

Loo, S.V., Koppejan, J. (Eds.) 2008. The Handbook of Biomass Combustion & Co-firing. Earthscan. London, UK.

Luo, Y., Durenkamp, M., De Nobili, M., Lin, Q., Brookes, P.C., 2011. Short term soil priming effects and the mineralisation of biochar following its incorporation to soils of different pH. Soil Biology and Biochemistry, 43(11). 2304-2314.

Lynch, D., Henihan, A.M., Bowen, B., Lynch, D., McDonnell, K., Kwapinski, W., Leahy, J.J., 2013. Utilisation of poultry litter as an energy feedstock. Biomass and Bioenergy 49, 197–204.

Lynch, D., Henihan, A.M., Kwapinski, W., Zhang, L., Leahy, J.J., 2013. Ash Agglomeration and Deposition during Combustion of Poultry Litter in a Bubbling Fluidized-Bed Combustor. Energy & Fuels 27, 4684-4694.

Manyà, J.J., 2012. Pyrolysis for biochar purposes: a review to establish current knowledge gaps and research needs. Environ. Sci. Technol. 46, 7939–7954.

Mao, J.-D., Johnson, R.L., Lehmann, J., Olk, D.C., Neves, E.G., Thompson, M.L., Schmidt-Rohr, K., 2012. Abundant and stable char residues in soils: implications for soil fertility and carbon sequestration. Environ. Sci. Technol. 46, 9571–9576.

Masunga, R.H., Uzokwe, V.N., Mlay, P.D., Odeh, I., Singh, A., Buchan, D., De Neve, S., 2016. Nitrogen mineralization dynamics of different valuable organic amendments commonly used in agriculture. Appl. Soil Ecol. 101, 185–193.

McBeath, A. V., Smernik, R.J., Krull, E.S., Lehmann, J., 2014. The influence of feedstock and production temperature on biochar carbon chemistry: A solid-state 13C NMR study. Biomass and Bioenergy 60, 121–129.

McHenry, M.P., 2010. Carbon-based stock feed additives: A research methodology that explores ecologically delivered C biosequestration, alongside live weights, feed use efficiency, soil nutrient retention, and perennial fodder plantations. J. Sci. Food Agric. 90, 183–187.

McKendry, P., 2002a. Energy production from biomass (Part 2): Conversion technologies. Bioresour. Technol. 83, 47–54.

McKendry, P., 2002b. Energy production from biomass (Part 3): Gasification technologies. Bioresour. Technol. 83, 55–63.

Melligan, F., Hayes, M.H.B., Kwapinski, W., Leahy, J.J., 2013. A study of hydrogen pressure during hydropyrolysis of Miscanthus x giganteus and online catalytic vapour upgrading with Ni on ZSM-5. J. Anal. Appl. Pyrolysis 103, 369–377.

Michaud, S., Bernet, N., Buffière, P., Roustan, M., Moletta, R., 2002. Methane yield as a monitoring parameter for the start-up of anaerobic fixed film reactors. Water Res. 36, 1385–1391.

Michaud, S., Bernet, N., Buffière, P., Delgenès, J.P., 2005. Use of the methane yield to indicate the metabolic behaviour of methanogenic biofilms. Process Biochem 40, 2751–2755.

Mostofa Amin, M.G., Forslund, A., Bui, X.T., Juhler, R.K., Søren Petersen, O., 2013. Persistence and leaching potential of microorganisms and mineral N in animal manure applied to intact soil columns. Appl. Environ. Microbiol. 79, 535–542.

Mukherjee, A., Zimmerman, A.R., 2013. Organic carbon and nutrient release from a range of laboratory-produced biochars and biochar-soil mixtures. Geoderma 193-194, 122–130.

Mumme, J., Srocke, F., Heeg, K., Werner, M., 2014. Use of biochars in anaerobic digestion. Bioresour. Technol. 164, 189–197.

Narodoslawsky, M., 2013. From processes to life cycles to technology networks - New challenges for LCA in chemical engineering. Curr. Opin. Chem. Eng. 2, 282–285.

Nicholson, F.A., Chambers, B.J., Williams, J.R., Unwin, R.J., 1999. Heavy metal contents of livestock feeds and animal manures in England and Wales. Bioresour. Technol. 70, 23-31.

Novotny, E.H., Maia, C.M.B. de F., Carvalho, M.T. de M., Madari, B.E., 2015. Biochar: Pyrogenic Carbon for Agricultural Use - a Critical Review. Rev. Bras. Ciência do Solo 39, 321–344.

Oudart, D., Robin, P., Paillat, J.M., Paul, E., 2015. Modelling nitrogen and carbon interactions in composting of animal manure in naturally aerated piles. Waste Manag. 46, 588–598.

Patra, T.K., Nimisha, K.R., Sheth, P.N., 2016. A comprehensive dynamic model for downdraft gasifier using heat and mass transport coupled with reaction kinetics. Energy 116, 1230–1242.

Pels, J.R., de Nie, D.S., Kiel, J.H.A., 2005. Utilization of ashes from biomass combustion and gasification. Published at 14th European Biomass Conference & Exhibition. Paris, France. 17-21 October 2005.

Pandey, D.S., Kwapinska, M., Gómez-Barea, A., Horvat, A., Fryda, L.E., Rabou, L.P.L.M, Leahy, J.J., Kwapinski, W., 2016. Poultry Litter Gasification in a Fluidized Bed Reactor: Effects of Gasifying Agent and Limestone Addition. 30 (4), 3085–3096.

Pessuto, J., Scopel, B.S., Perondi, D., Godinho, M., Dettmer, A., 2016. Enhancement of Biogas and Methane Production by Anaerobic Digestion of Swine Manure with Addition of Microorganisms Isolated from Sewage Sludge. Process Saf. Environ. Prot. 104, 233–239.

Petersen, S.O., Sommer, S.G., Béline, F., Burton, C., Dach, J., Dourmad, J.Y., Leip, A., Misselbrook, T., Nicholson, F., Poulsen, H.D., Provolo, G., Sørensen, P., Vinnerås, B., Weiske, A., Bernal, M.P., Böhm, R., Juhász, C., Mihelic, R., 2007. Recycling of livestock manure in a whole-farm perspective. Livest. Sci. 112, 180–191.

Prapaspongsa, T., Poulsen, T.G., Hansen, J. a, Christensen, P., 2010. Energy production, nutrient recovery and greenhouse gas emission potentials from integrated pig manure management systems. Waste Manag. Res. 28, 411–422.

Puig-Arnavat, M., Bruno, J. C., Coronas, A. 2010. Review and analysis of biomass gasification models. Renewable and Sustainable Energy Reviews. 14, 2841-2851.

ReUseWaste, 2016. Project objectives. Available at http://www.reusewaste.eu/about/objectives/ (accessed 01.06.2016)

Rillig, M.C., Wagner, M., Salem, M., Antunes, P.M., George, C., Ramke, H.G., Titirici, M.M., Antonietti, M., 2010. Material derived from hydrothermal carbonization: Effects on plant growth and arbuscular mycorrhiza. Applied Soil Ecology, 45(3). 238-242.

Ro, K.S., Cantrell, K.B., Hunt, P.G., Ducey, T.F., Vanotti, M.B., Szogi, A.A., 2009. Thermochemical conversion of livestock wastes: carbonization of swine solids. Bioresour. Technol. 100, 5466–5471.

Roberts, K.G., Gloy, B. a, Joseph, S., Scott, N.R., Lehmann, J., 2010. Life cycle assessment of biochar systems: estimating the energetic, economic, and climate change potential. Environ. Sci. Technol. 44, 827–33.

Sarkar, M., Kumar, A., Tumuluru, J.S., Patil, K.N., Bellmer, D.D., 2014. Gasification performance of switchgrass pretreated with torrefaction and densification. Appl. Energy 127, 194–201.

Schmidt, H.P., 2012a. 55 Uses of Biochar. Ithaka Journal 1/ 2012: 286–289. Available at http://www.ithaka-journal.net/55-anwendungen-von-pflanzenkohle?lang=en (accessed 01.06.16)

Schmidt, H.P., 2012b. Treating liquid manure with biochar. Ithaka Journal 1/ 2012: 273–276. Available at http://www.ithaka-journal.net/gullebehandlung-durch-pflanzenkohle?lang=en (accessed 01.06.16)

SEI, 2015. Biomass Factsheet - Renewable Energy Information Office (REIO). Sustainable Energy Ireland. Available at http://www.seai.ie/uploadedfiles/RenewableEnergy/REIOBiomassFactsheet.pdf (accessed 01.06.16)

Selvatico, D., Lanzini, A., Santarelli, M., 2016. Low Temperature Fischer-Tropsch fuels from syngas: Kinetic modeling and process simulation of different plant configurations. Fuel 186, 544–560.

Siedlecki, M., De Jong, W., Verkooijen, A. H. 2011. Fluidized Bed Gasification as a Mature And Reliable Technology for the Production of BioSyngas and Applied in the Production of Liquid Transportation Fuels - A Review. Energies, 4, 389-434.

Singh, B.P., Cowie, A.L., Smernik, R.J., 2012. Biochar carbon stability in a clayey soil as a function of feedstock and pyrolysis temperature. Environ. Sci. Technol. 46, 11770–11778.

Sommer, S.G., 2013. Animal Manure – From Waste to Raw Materials and Goods. In Sommer, S.G., Christensen, M.L., Schmidt, T., Jensen, L.S. (Eds.). Animal Manure Recycling - Treatment and Management. John Wiley and Sons Ltd. Chichester, West Sussex, UK. p.1.

Sommer, S.G., Christensen, M.L., 2013. Animal Production and Animal Manure Management. In Sommer, S.G., Christensen, M.L., Schmidt, T., Jensen, L.S. (Eds.). Animal Manure Recycling - Treatment and Management. John Wiley and Sons Ltd. Chichester, West Sussex, UK. p.5.

Sommer, S.G., Feilberg, A., 2013. Gaseous Emissions of Ammonia and Malodorous Gases. In Sommer, S.G., Christensen, M.L., Schmidt, T., Jensen, L.S. (Eds.). Animal Manure Recycling - Treatment and Management. John Wiley and Sons Ltd. Chichester, West Sussex, UK. p.131.

Sommer, S.G., Clough, T.J., Chadwich, D., Peterson, S.O., 2013a. Greenhouse Gas Emissions from Animal Manures and Technologies for Their Reduction. In Sommer, S.G., Christensen, M.L., Schmidt, T., Jensen, L.S. (Eds.) Animal Manure Recycling - Treatment and Management. John Wiley and Sons Ltd. Chichester, West Sussex, UK. p.186.

Sommer, S.G., Clough, T.J., Chadwich, D., Peterson, S.O., 2013b. Greenhouse Gas Emissions from Animal Manures and Technologies for Their Reduction. In Sommer, S.G., Christensen, M.L., Schmidt, T., Jensen, L.S. (Eds.) Animal Manure Recycling - Treatment and Management. John Wiley and Sons Ltd. Chichester, West Sussex, UK. p.191.

Sommer, S.G., Ward, A.J., Leahy, J.J., 2013c. Bioenergy Production. In Sommer, S.G., Christensen, M.L., Schmidt, T., Jensen, L.S. (Eds.). Animal Manure Recycling - Treatment and Management. John Wiley and Sons Ltd. Chichester, West Sussex, UK. 252-255.

Sonnenerde, 2016. Herstellung Pflanzenkohle. Sonnenerde Gerald Dunst Kulturerden GmbH. Available at http://www.sonnenerde.at/index.php?route=common/page&id=1254 (accessed 01.06.2016)

Soti, P.G., Jayachandran, K., Koptur, S., Volin, C., 2015. Effect of soil pH on growth, nutrient uptake, and mycorrhizal colonization in exotic invasive Lygodium microphyllum. Plant Ecol. 216, pp. 989.

Subedi, R., Kammann, C., Pelissetti, S., Taupe, N., Bertora, C., Monaco, S., Grignani, C., 2015. Does soil amended with biochar and hydrochar reduce ammonia emissions following the application of pig slurry? European Journal of Soil Science. 66 (6), 1044-1053.

Subedi, R., Taupe, N., Ikoyi, I., Bertora, C., Zavattaro, L., Schmalenberger, A., Leahy, J.J., Grignani, C., 2016a. Chemically and biologically-mediated fertilising value of manure-derived biochar. Sci. Total Env. 550, 924–933.

Subedi, R., Taupe, N., Pelissetti, S., Petruzzelli, L., Bertora, C., Leahy, J.J., Grignani, C., 2016b. Greenhouse gas emissions and soil properties following amendment with manure-derived biochars: Influence of pyrolysis temperature and feedstock type. J. Environmental Management. 166, 73-83.

Tanto, M.T., Magette, W.L., 2008. Composition and Distribution of Organic Waste in Ireland: Implications for Land Application Practices. Eur. Soc. Agric. Eng. Available at http://www.cabi.org/cabdirect/FullTextPDF/2008/20083325057.pdf (accessed 01.06.2016)

Taupe, N.C., Lynch, D., Wnetrzak, R., Kwapinska, M., Kwapinski, W., Leahy, J.J., 2016. Updraft gasification of poultry litter at farm-scale – A case study. Waste Manag. 50, 324-333.

Thanapal, S.S., Annamalai, K., Sweeten, J.M., Gordillo, G., 2012. Fixed bed gasification of dairy biomass with enriched air mixture. Appl. Energy 97, 525–531.

Thygesen, O., Johnsen, T., 2012. Manure-based energy generation and fertiliser production: Determination of calorific value and ash characteristics. Biosyst. Eng. 113, 166–172.

Toth, J. D., Dou, Z., 2016. Use and Impact of Biochar and Charcoal in Animal Production Systems. In Guo, M., He, Z., Uchimiya, S.M. (Eds.). Agricultural and Environmental Applications of Biochar: Advances and Barriers, SSSA Spec. Publ. 63. SSSA, Madison, WI. 199-224.

Tsai, W.-T., Liu, S.-C., Chen, H.-R., Chang, Y.-M., Tsai, Y.-L., 2012. Textural and chemical properties of swine-manure-derived biochar pertinent to its potential use as a soil amendment. Chemosphere 89, 198–203.

Uchimiya, M., Bannon, D.I., Wartelle, L.H., 2012. Retention of Heavy Metals by Carboxyl Functional Groups of. J. Agric. Food Chem. 60, 1798–1809.

Uchimiya, M., 2014. Changes in nutrient content and availability during the slow pyrolysis of animal wastes. In He, Z., Zhang, H. (Eds.) Applied manure and nutrient chemistry for sustainable agriculture and environment. Springer Dordrecht Heidelberg New York London, p. 55

UN, 2015. World Population Prospects: The 2015 Revision, World Population 2015 Wallchart. ST/ESA/SER.A/378. United Nations, Department of Economic and Social Affairs, Population Division. Available at https://esa.un.org/unpd/wpp/publications/Files/World_Population_2015_Wallchart.pdf (accessed 01.06.2016)

Uzoma, K.C., Inoue, M., Andry, H., Fujimaki, H., Zahoor, a., Nishihara, E., 2011. Effect of cow manure biochar on maize productivity under sandy soil condition. Soil Use Manag. 27, 205–212.

Wang, C., Lu, H., Dong, D., Deng, H., Strong, P.J., Wang, H., Wu, W., 2013. Insight into the effects of biochar on manure composting: Evidence supporting the relationship between N2O emission and denitrifying community. Environ. Sci. Technol. 47, 7341–7349.

Wang, T., Camps-Arbestain, M., Hedley, M., Bishop, P., 2012. Predicting phosphorus bioavailability from high-ash biochars. Plant Soil 357, 173–187.

Wang, Y., Lai, N., Zuo, J., Chen, G., Du, H., 2016. Characteristics and trends of research on waste-to-energy incineration: A bibliometric analysis, 1999–2015. Renewable and Sustainable Energy Reviews. 66, 95–104.

Werther, J., Saenger, M., Hartge, E. U., Ogada, T., Siagi, Z. 2000. Combustion of agricultural wastes. Progress in Energy and Combustion Science, 26. 1-27.

Williams, P.T. 2005. Waste Treatment and Disposal, Sussex, Wiley & Sons.

Ye, Z., Xiu, S., Shahbazi, A., Zhu, S., 2012. Co-liquefaction of swine manure and crude glycerol to bio-oil: model compound studies and reaction pathways. Bioresour. Technol. 104, 783–787.

Yin, C., Rosendahl, L.A., Kær, S.K., 2008. Grate-firing of biomass for heat and power production. Progress in Energy and Combustion Science. 34, 725-754.

Yin, S., Dolan, R., Harris, M., Tan, Z., 2010. Subcritical hydrothermal liquefaction of cattle manure to bio-oil: Effects of conversion parameters on bio-oil yield and characterization of bio-oil. Bioresour. Technol. 101, 3657–3664.

Yoder, J., Galinato, S., Granatstein, D., Garcia-Pérez, M., 2011. Economic tradeoff between biochar and bio-oil production via pyrolysis. Biomass and Bioenergy 35, 1851–1862.

Xiu, S., Shahbazi, A., Shirley, V., Cheng, D., 2010. Hydrothermal pyrolysis of swine manure to bio-oil: Effects of operating parameters on products yield and characterization of bio-oil. J. Anal. Appl. Pyrolysis 88, 73–79.

Xue, G., Kwapinska, M., Horvat, A., Kwapinski, W., Rabou, L.P.L.M., Dooley, S., Czajka, K.M., Leahy, J.J., 2014. Gasification of torrefied Miscanthus×giganteus in an air-blown bubbling fluidized bed gasifier. Bioresour. Technol. 159, 397–403.

2. Materials and Methods

This chapter provides the reader with a detailed description of the methods and operational details of the equipment used throughout the course of this research project.

2.1. Sampling

Sampling of the solid samples was carried out in accordance with BS EN 14778:2011. Numerous subsamples were taken from stock piles at different positions or depths due to the variability of moisture and ash contents in the pile. The samples were stored in freezer bags at -20 °C and mixed thoroughly before analysis.

2.2. Proximate Analysis

Proximate analysis involved the determination of moisture, ash, volatile matter (VM) and fixed carbon (FC) content according to standards methods (BS EN 14774-3:2009, I.S. EN 14775:2009, I.S. EN 15148:2009).

2.2.1. Moisture

Once manure samples are dried the moisture content can still change during storage and treatment practices depending on its hygroscopic nature. Therefore, the moisture content was completed alongside other analytical measurements.

Procedure:

At least three replications were performed each time. A crucible was dried at 105 ± 2 °C for at least two hours and subsequently cooled to room temperature in a desiccator. Around 1 g of each manure sample was added to the crucible and weighted to an accuracy of 0.1 mg. For biochar samples the weight was 0.5 g each. The crucibles containing the samples were heated over night at 105 ± 2 °C left to cool to room temperature the following day in a desiccator and finally the crucibles containing the dry sample were weighed and the moisture content determined following equation 2.1.

Calculation:

$$MC = \frac{(m_3 - m_1)}{(m_2 - m_1)} x\ 100 \qquad \textit{equation 2.1}$$

Where:
MC = moisture content at 105 °C (wt%)$_{ar}$
m_1 = mass of empty crucible (g)
m_2 = mass of empty crucible and initial sample (g)
m_3 = mass of empty crucible and dried sample (g)

The moisture content of the tar samples was determined by Karl Fischer titration (Mettler Toledo DL 31). The samples were titrated using Hydranal Composite 5 and Methanol-Chloroform (3:1) was used as a solvent.

2.2.2. Ash

Procedure:

At least three replications were carried out for each solid or liquid sample. Prior to ash content determination the moisture content was analysed according to section 2.2.1. The porcelain crucible and samples were heated in a furnace from room temperature to 250 ± 10 °C at a heating rate of 5 °C min^{-1} with a residence time of 60 min. Then the furnace was raised to 550 ± 10 °C at a heating rate of 5 °C min^{-1} and kept at this temperature level for at least 120 min (overnight for biochar samples) until complete combustion was achieved. The crucible was allowed to cool in the furnace until 105 °C and then placed in a desiccator to cool to room temperature before weighing to the nearest 0.1 mg.

Calculation:

$$Ash = \frac{(m_3 - m_1)}{(m_2 - m_1)} \; x \; 100 \; x \; \frac{100}{100 - MC} \qquad \textit{equation 2.2}$$

Where:
Ash = ash content on dry basis (wt.%)$_{db}$
m_1 = mass of empty crucible (g)
m_2 = mass of empty crucible and initial sample (g)
m_3 = mass of empty crucible and ashed sample (g)
MC = moisture content (wt.%) of the initial sample

2.2.3. Volatile Matter

The volatile matter (VM) represents the gas released, excluding moisture, from a solid biofuel when heated to 900 °C in absence of air for seven minutes.

Procedure:

A silica volatile matter crucible plus lid was baked out in a heated furnace at 900 °C for 7 min and cooled to room temperature in a desiccator. An amount of 1 g ± 0.1 g of dried test sample was weighed to the nearest 0.1 mg into the crucible. The crucible was covered with the lid and then inserted into the preheated furnace (900 ± 10 °C)

for seven minutes. The crucible was then removed from the furnace and cooled to room temperature first outside and then inside a desiccator before weighing it.

Calculation:

$$VM = \left[\frac{100\,(m_2 - m_3)}{m_2 - m_1} - MC\right] x\ \left(\frac{100}{100 - MC}\right) \qquad \textit{equation 2.3}$$

Where:
VM = volatile matter (wt.%)$_{db}$
m_1 = mass of empty crucible and lid (g)
m_2 = mass of empty crucible and lid plus initial sample (g)
m_3 = mass of empty crucible and lid plus final sample (g)
MC = moisture content (wt.%)$_{ar}$

2.2.4. Fixed Carbon

The fixed carbon (FC) content was calculated by subtracting the moisture, ash and volatile matter content from 100% according to equation 2.4.

$$FC = 100 - (MC + Ash + VM) \qquad \textit{equation 2.4}$$

Where:
FC = fixed carbon (wt.%) $_{db}$
MC = moisture content (wt.%)$_{ar}$
Ash = ash content (wt.%)$_{db}$
VM = volatile content (wt.%)$_{db}$

2.3. Ultimate Analysis

Ultimate analysis included the determination of the elemental composition of the solid and liquid samples. This required a variety of different analytical techniques depending on the type of element.

2.3.1. Determination of Carbon, Hydrogen, Nitrogen, Sulphur and Oxygen Content

The analysis was conducted according to BS EN 15104:2011 to determine the C, H, N, S and O content of the solid and liquid samples. The instrument used was an Elemental Vario EL Cube analyser using sulfanilic acid as a standard. Oxygen was calculated by difference, subtracting the percentage of C, H, S and ash from 100%.

A basic schematic of the instrument is given in Figure 2-1.

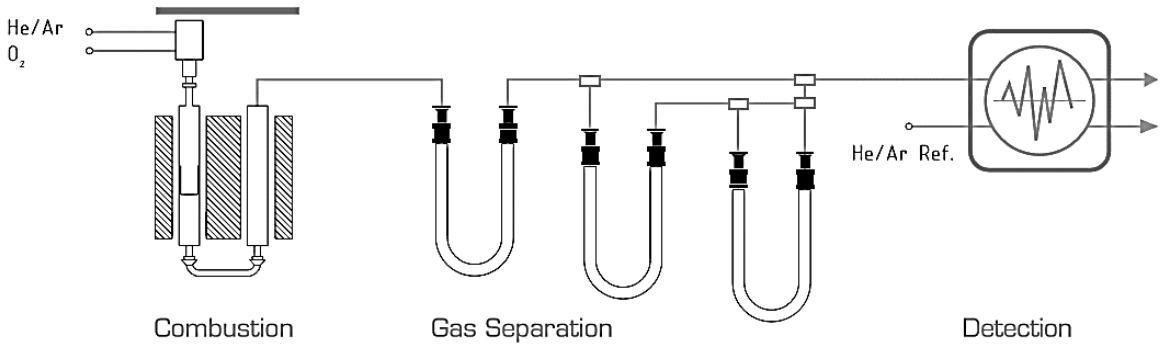

Figure 2-1: Schematic of elemental analyser (Elementar, 2016)

Procedure:

Approximately 10 mg of finely ground sample was weighted to the nearest 0.01 mg into an aluminium boat, which was then sealed carefully, formed to a ball shape, and placed into an integrated carousel. Each sample entered a ball valve, flushed with helium gas to remove atmospheric nitrogen and then dropped into a combustion tube. Catalytic combustion of the samples was carried out at 1150 °C with oxygen and tungsten trioxide (WO_3). Furthermore, WO_3 is used to prevent the formation of non-volatile sulphates and bind alkali metals, which interfere with the results and damage the instrument. Then the gases passed through a reduction tube using helium as a carrier gas, where compounds such as NO_x and SO_3 were reduced to N_2 and SO_2 by hot copper wires. Excess oxygen was adsorbed, while volatile halogen compounds were trapped by silver wool at the entrance to the reduction tube. Water was removed with Sicapent (phosphorus pentoxide). The formed analysis gases (CO_2, H_2O, and SO_2) were separated by adsorption to three separate columns, while N_2 entered the thermal conductivity detector (TCD) directly. The trapped gases were desorbed one by one from the columns by heat exposure, which are then also detected and quantified using the TCD. (Elementar, 2016)

2.3.2. Determination of Chlorine Content

The amount of chloride in the solid samples was measured according to BS EN 14582:2007. In brief a sample was oxidised in a bomb calorimeter and the halogen was absorbed in 0.2 M KOH and detected using a chloride ion selective electrode.

Procedure:

Approximately 1 g of pelleted sample was weighed to the nearest 0.1 mg and combusted in an oxygen bomb calorimeter (as described in section 2.6.5) which contained 20 ml of 0.2 M KOH as absorbent. The solution was carefully collected at the end of each run and transferred to a suitable volumetric flask and made up to the mark. Care was taken to ensure the calorimeter was completely rinsed with water so as not to exclude any chloride containing solution.

A chloride ion selective electrode, Thermo Scientific Orion ISE meter, was used to quantify the chloride in the solutions by direct calibration. For the calibration curve standard solutions between 2 and 2500 ppm of dried NaCl were prepared using deionised water. An ion strength adjuster (ISA Cat.No.940011) was added to all solutions (2 ml ISA in 100 ml sample solution) to ensure that the samples and standards had similar ionic strengths. All solutions were stirred in a beaker and after a few minutes a steady reading was achieved and the signal recoded in mV.

2.3.3. Determination of Phosphorus Content (UV-VIS)

Phosphate concentrations were determined sing a UV-VIS-4000, Varian Spectrophotometer, using the stannous chloride method. Molybdophosphoric acid is formed and reduced by stannous chloride to intensely coloured molybdenum blue.

Procedure:

For the ammonium molybdate reagent 25 g of ammonium molybdate was dissolved in 175 ml distilled water. A volume of 280 ml of concentrated sulfuric acid was carefully added to 400 ml distilled water, left to cool and finally mixed with the ammonium molybdate solution. For the stannous chloride reagent 2.5 g stannous chloride was mixed with 100 ml glycerol, heated until dissolved and then kept warm to remain in liquid state. Standards of P concentrations ranging from 0.1 to 1.0 ppm were prepared by diluting a stock solution of 50 ppm (0.22 g H_3PO_4 in 1 L H_2O). For the colour development 4 ml molybdate reagent and 10 drops of stannous chloride reagent were added to the solution. The samples were measured photometrically after 10 min at 690 nm.

2.3.4. Flame Assisted Atomic Absorption Spectroscopy (FA-AAS)

The determination of some inorganic elements in the solid samples was performed using a Varian Spectra AA-220 after the samples were acid digested as described in section 2.3.5 or leached from the solid samples. Hollow cathode lamps, which emit light at the characteristic wavelength of an element, have been developed to use with FA-AAS. Every element has a characteristic wavelength at which light is absorbed most strongly.

Procedure:

Water leaching was performed by weighing approximately 3 g of finely ground char or manure feedstock (± 0.001 g) into a beaker containing 50 ml of distilled water. The samples were vacuum filtrated through a Whatman grade 1 filter paper. Prior to analysis, standard solutions of each element, together with any necessary ionisation suppressants, were prepared. The solutions were aspirated into a flame, either air/acetylene or nitrous oxide/acetylene flames depending on the element. The flame containing the atomised vapour of the solution, absorbed radiation from the hollow cathode lamp. The relationship of concentration and absorption follows that of Lambert Beer's Law (equation 2.5).

$$A = \varepsilon \, x \, c \, x \, d \qquad \textit{equation 2.5}$$

Where:
A = absorption
ε = molar absorptivity co-efficient (M^{-1} cm^{-1})
c = concentration (M)
d = path length (cm)

2.3.5. Inductively Coupled Plasma - Optical Emission Spectrometry (ICP-OES)

Inductively Coupled Plasma - Optical Emission Spectrometry (ICP-OES) is widely used for inorganic analysis. A plasma is created when a high frequency electric current is applied to a work coil at the tip of a torch tube. Argon is supplied to the coil and ionised using the electromagnetic field and plasma is generated. The samples are introduced to the plasma in an atomised state through a narrow tube. The high electron density and high temperature (10 000 °C) in the plasma supplies energy to excite the atoms of the samples. Emission rays are released when the excited atoms return back

to ground state and the emission rays corresponding to the photon wavelength are measured. The type of element is determined based on the position of the photon rays, while the content of the element is determined based on the intensity of the rays. (Chemiasoft, 2014)

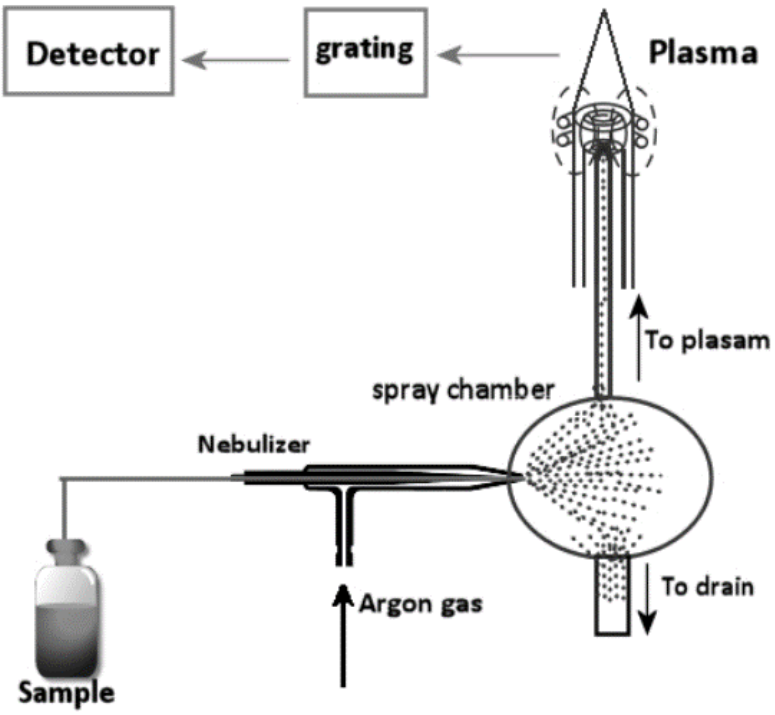

Figure 2-2: Schematic of ICP-OES (Chemiasoft, 2014)

Procedure:

The determination of inorganic elements in the solid samples was performed in the "Centro de Edafología y Biología Aplicada del Segura" (CEBAS), Murcia, using a ICP-OES, Thermo Elemental Co. Iris Intrepid II XDL after the samples were acid digested. Milled manure feedstock (0.1 g ± 0.0001g) was digested in 2 ml H_2O_2 and 8 ml HNO_3 in a microwave digester. The biochars were ashed at 500 °C for 8 h according to the modified dry ash method by Enders *et al*. (2012) prior to digestion in 3 ml HNO_3 and 9 ml HCl. The samples were filtered and diluted to 25 ml with ultrapure water before subject to ICP-OES.

2.4. Texture Characterisation and Morphology

2.4.1. Scanning Electron Microscopy combined with Energy Dispersive Spectroscopy (SEM-EDS)

During Scanning Electron Microscopy - Energy Dispersive Spectroscopy (SEM-EDS) the sample is bombarded with accelerated and focused electrons to generate a variety of signals at different depths, for example secondary electrons (for SEM image) and X-rays (for elemental analysis). These signals from the secondary electrons can be used to generate an image which can reveal the morphological and topographical features of the sample. The X-rays emitted from the samples have the characteristics of the parent elements and can be used to provide analysis of the elemental composition of the samples.

Procedure:

The solid samples were crushed, placed onto carbon tabs, and coated with gold to decrease charging. The analysis was performed using an Ultra-High-Resolution Analytical FE-SEM SU-70 (Hitachi), and a Large Area EDS Silicon Drift Detector, (Oxford Instruments) equipped with INCA software. The accelerating voltage was 15.0 kV and the working distance for the EDS analysis was 15 mm.

2.4.2. Specific Surface Area (SSA) and Pore Size Distribution

Brunauer, Emmet and Teller developed the equation for the specific surface area for solids (equation 2.6), which is an extension of the Langmuir theory and is applicable to the multilayer adsorption following the assumptions that (1) the gas molecules will physically adsorb to a solid surface in infinite layers, that (2) the layers do not interact and that (3) the Langmuir theory can be applied to each layer.

$$\frac{p}{n_m(p_o - p)} = \frac{(C_a - 1)p}{V_m C_a p_o} + \frac{1}{V_m C_a}$$

equation 2.6

Where:
n_m = number of molecules adsorbed at pressure p and constant temperature (77.4 °K)
p = partial vapour pressure of adsorbate gas in equilibrium with the surface (Pa)
p_0 = saturation pressure at the measurement temperature (Pa)
V_m = volume of gas adsorbed (monolayer) at STP per unit mass of adsorbent (ml)
C_a = constant relating to the free energy of adsorption (dimensionless)

A straight line is produced by plotting $p/n_m(p_0-p)$ against p/p_0, with a slope equal to $(C_a-1)/(V_mC_a)$ and an intercept of $1/(V_mC_a)$. The surface area (S_{BET}) can be calculated according to equation 2.7.

$$S_{BET} = \frac{V_m N A_m}{V_{mol}}$$

equation 2.7

Where:
N = Avogadro's constant (6.023×10^{23} mol^{-1})
V_{mol} = the molar volume of adsorbate at STP (22.4 l mol^{-1})
A_m = cross sectional area of adsorbed gas (for N_2 = 0.162 nm^2)

Two common techniques for describing porosity are the determination of total pore volume and pore size distribution. The distribution of pore volume with respect to pore size is called a pore size distribution.

Procedure:

The multipoint Brunauer-Emmett-Teller - N_2 specific surface area (BET-N_2 SSA) was determined from the N_2 adsorption-desorption isotherm of the biochar sample by means of a Micrometric Tri-Star BET system in a relative pressure range (p/p_0) from 0.05 to 0.30. The samples (0.1 g ± 0.0001 g) were degassed prior to analysis under vacuum at 200 °C for 15 h. Nitrogen was used as the sorbent gas, and the process took place at - 196 °C. The pore size distribution of the Sitka spruce biochar was measured using an Quantachrome Autosorb AS-1 instrument and calculated from the desorption isotherm using the Barrett-Joyner-Halenda (BJH) theory.

2.5. Surface functionality

2.5.1. Fourier Transform Infrared Spectroscopy (FTIR)

The vibrational spectrum obtained by Fourier transform infrared spectroscopy (FTIR) is a unique physical property, which is widely used to characterise molecules. The infrared spectrum can be used as a fingerprint for identifying unknown functional groups by comparison with previously recorded reference spectra. The infrared spectrum is formed as electromagnetic radiation is absorbed. The frequencies correlate to the vibration of specific chemical bonds from within the molecule. The contributing

energy possessed by a molecule includes electronic, vibrational, rotational and translational energy (Coates, 2000).

Procedure:

Samples were ground finely before analysis using an Agilent Cary 630 FTIR Spectrometer.

2.5.2. Cross-Polarization and Magic Angle Spinning Nuclear Magnetic Resonance Spectroscopy (CPMAS ^{13}C-NMR)

The principle behind Nuclear Magnetic Resonance spectroscopy (NMR) is that nuclei have spin and are electrically charged. When an external magnetic field is applied, energy is transferred from the ground level to a higher energy level. The wavelength at which the energy transfer takes place corresponds to radio frequencies. When the spin returns to the ground level, energy is emitted at the same frequency. The signal that matches this transfer is measured and processed in order to produce an NMR spectrum.

Procedure:

Solid-state ^{13}C NMR experiments were carried out in the "Instituto de Pesquisas Jardim Botânico do Rio de Janeiro" by Dr. Etelvino Novotny using a VARIAN INOVA spectrometer at ^{13}C and ^{1}H frequencies of 100.5 and 400.0 MHz, respectively. The techniques used were variable amplitude cross-polarization (VACP); chemical shift anisotropy (CSA) with total suppression of spinning side bands (TOSS); and recoupled dipolar dephasing (DD) experiments. A JACKOB-SEN 5 mm magic-angle spinning double-resonance probe head was used for (VACP) experiments at spinning frequencies of 13 kHz. Typical CP times of 1 ms, acquisition times of 13 ms, and recycle delays of 500 ms were used. The CP time was chosen after variable contact time experiments, and the recycle delays in CP experiments were chosen to be five times longer than the longest ^{1}H spin–lattice relaxation time (T_{1H}) as determined by inversion-recovery experiments.

2.6. Chemical and Physical Properties

2.6.1. Bulk Density

The bulk density was determined using a modified version of the standard procedure ISO/TC238:2011, using a 100 ml cylinder.

Principle:

A 100 ml cylinder was filled to the mark with solid sample, knocked on a flat horizontal surface three times and the weight of the sample was measured.

2.6.2. Ash Melting Behaviour

An important factor governing gasification of fuels is the behaviour of the mineral matter during heat exposure. Thermal gravimetric analysis (TGA) monitors weight changes in a material as a function of temperature or time under a controlled atmosphere. Weight changes depend on the material's thermal stability and propensity to decomposition involving dehydration, volatilisation and oxidation. Differential thermal analysis (DTA) measures the difference in temperature between a sample and a reference material (alumina) as a function of temperature and time. During changes in a material's physical or chemical state, heat is either absorbed (endothermic) or liberated (exothermic). These thermal reactions in the material will result in a change in temperature, which is recorded. The latent heat of fusion of the material is proportional to the area under the melting endotherm. The mean value of the endotherm peak temperature can be used to measure the melting point (Dodd and Thonge, 1987).

Procedure:

Poultry litter was ashed at 550 °C in a muffle furnace to a constant weight using standard conditions. A test sample (50 mg) was weighed to the nearest 0.1 mg, and placed in a platinum/rhodium crucible. The reference material (alumina) was placed in a second crucible and placed into the instrument. The ash fusion point of the ash was then determined using a Stanton Redcroft STA 1640 combined differential thermal analyser DTA/TGA, operated with a nitrogen flow rate of 500 ml min^{-1} and at a heating rate of 10 °C min^{-1}.

2.6.3. Determination of pH

The pH was determined according to ISO 10390:2005 using a CyberScan pH 510 calibrated pH meter. The pH values of the biochar and soil samples were measured in a 0.01 M $CaCl_2$ solution (1 wt.%) after shaking for 2 h at 100 rpm.

2.6.4. Cation Exchange Capacity (CEC)

The cation exchange capacity (CEC) represents the total quantity of negative charges available to attract cations in solution. It is one of the most important chemical properties of soils and strongly influences surface and organic matter.

Procedure:

The CEC of biochar was evaluated based on the replacement of Na^+ with NH_4^+. The method was adopted from Uzoma *et al*. (2011). One gram of biochar was weighed with a precision of 0.01 g into a centrifuge tube; 20 ml of sodium acetate solution (1.0 M) was added, and shaken for 1 h at 16 rpm to saturate the exchange sites. The biochar solution was transferred to a solid phase extraction column with cotton wool and leached another two times with 20 ml of the same sodium acetate solution. The excess sodium acetate was then removed by leaching slowly with 30 ml of ethanol (96%) and repeated three to four times until the solution reached a conductivity of < 40 µS cm^{-1}. Ammonium acetate solution (30 ml, 1.0 M) was added to the column to replace the adsorbed Na^+ and the leaching process was repeated three times. The extract was transferred to a 100 ml flask and filled to the mark with ammonium acetate solution (1.0 M). The extracts were stored in a fridge until analysed for Na content using FA-AAS. The feedstocks and soils were analysed based on the same method with slight modifications. The feedstocks (1 g) were mixed well with activated carbon (2.0 g) before adding 20 ml of sodium acetate solution (1.0 M). The leaching steps were carried out with vacuum filtration through an ash-less quantitative filter paper (DP 5895 110). The soils (4.0 g) were shaken for 5 min at 16 rpm in 30 ml sodium acetate solution (1.0 M) and centrifuged at 7400 rpm for 5 min in place of leaching though the columns.

2.6.5. Gross Calorific Value

The higher heating value (HHV), also known as gross calorific value or gross energy, of a fuel is defined as the amount of heat released from combustion and the products

have returned to the original temperature. The HHV takes into account the latent heat of vaporisation of water in the combustion products. The lower heating value (LHV), also known as net calorific value, of a fuel is defined as the amount of heat released from combustion and returned to the temperature of the combustion products to 150 °C. Hereby it is assumed that the latent heat of vaporisation of water in the reaction products is not recovered. (Hydrogen Analysis Resource Center, 2015)

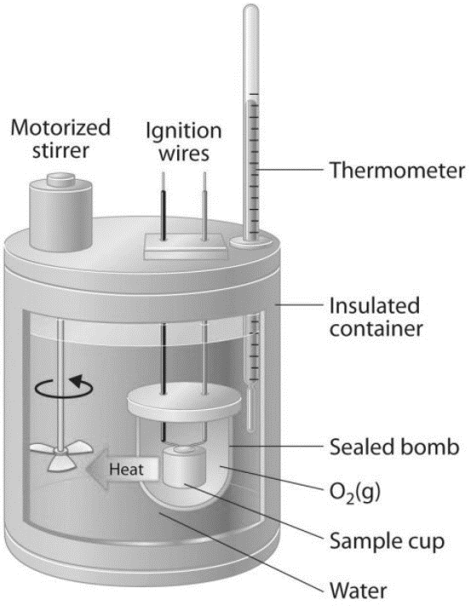

Figure 2-3: Schematic of bomb calorimeter (Averill and Eldredge, 2007)

Procedure:

The HHV was determined using an oxygen bomb calorimeter 6200 No. 442 M from Parr instruments Company according to BS EN 14918:2009. The HHV of certified benzoic acid was determined before the pelletised samples. Combustion took place in a high pressure oxygen environment. The HHV was then calculated considering the temperature rise and mean effective heat capacity of a water surrounding the combustion vessel (Figure 2-3). Approximately 1 ± 0.1 g of sample was pelleted using a 13 mm die press. The pellet was weighed to the nearest 0.1 mg and placed in a metal crucible. An ignition wire was fastened to two electrodes and the hanging part of the wire was positioned in a way that was just touching the pellet. The bomb was sealed and charged with oxygen to a pressure 3.0 ± 0.2 MPa. The bomb was mounted in the calorimeter containing 2000 g of water. The leads for the ignition circuit were connected to the bomb. The calorimeter was closed and the cooling water, temperature control and stirrers turned on. The ignition button was pressed and the water

temperature was automatically measured by the calorimeter. At the end of the test, which lasted about 8 min, the bomb was removed from the calorimeter, the pressure released slowly under the fume hood and the bomb dismantled. The interior of the bomb was examined for any unburned sample. The software provided the HHV_{ar}.

Calculations:

Gross calorific value:

$$Q_g = \left[\frac{(C\ x\ \Delta T) - (Q_f + Q_i)}{m}\right]$$

equation 2.8

Where
Q_g = HHV at constant volume of the fuel as analysed (J g^{-1})
C = mean effective heat capacity of the calorimeter (J K^{-1})
ΔT = corrected temperature rise (K)
Q_f = contribution from combustion of the fuse (J)
Q_i = contribution from oxidation of the ignition wire (J)
m = mass of sample (g)

Effective heat capacity:

$$C = \frac{(m_{ba}\ x\ q_{v,ba})}{\theta}$$

equation 2.9

Where:
m_{ba} = mass of benzoic acid (g)
$q_{v,ba}$ = certified HHV at constant volume of benzoic acid (J g^{-1})

The lower heating value (LHV) of the solids was calculated according to *equation 2.10* to *equation 2.14* (ECN Phyllis 2, 2015).

$$HHV_{ar} = HHV_{dry}\ x\ \left(1 - \frac{MC}{100}\right) \qquad \textit{equation 2.10}$$

$$HHV_{dry} = HHV_{daf}\ x\ \left(1 - \frac{Ash}{100}\right) \qquad \textit{equation 2.11}$$

$$LHV_{dry} = HHV_{dry} - 2.443\ x\ 8.936\frac{H}{100} \qquad \textit{equation 2.12}$$

$$LHV_{ar} = LHV_{dry}\ x\ \left(1 - \frac{MC}{100}\right) - 2.442\ x\ \frac{MC}{100} \qquad \textit{equation 2.13}$$

$$LHV_{ar} = HHV_{ar} - 2.442\ x\ \left\{8.936\ x\ \frac{H}{100}\ x\ \left(1 - \frac{MC}{100}\right) + \frac{MC}{100}\right\} \qquad \textit{equation 2.14}$$

Where:
HHV = Higher Heating Value (MJ kg^{-1})
LHV = Lower Heating Value (MJ kg^{-1})
MC = moisture content at 105 °C $(wt\%)_{ar}$
Ash = ash content on dry basis $(wt.\%)_{db}$
H = mass fraction of hydrogen $(wt.\%)_{db}$

2.6.6. Particle Size Distribution

The solid sample were sieved using a Retsch AS 200 sieve shaker. The sieves (Endecotts Ltd.) were 200 mm in diameter and 25 mm in height. The five sizes used were 5.0, 2.8, 1.0, 0.5, and 0.25 mm. A known weight of solid samples was placed into the shaker and shaken for 45 min at an amplitude of 60. The fractions were weighed and reported as weight percent (wt.%).

2.6.7. GC-MS

Gas Chromatography and Mass Spectrometry (GC-MS) is used to analyse volatile and semi-volatile compounds, also found in bio-oil. Separation of the compounds occurs in the GC and the MS provides detailed structural information to identify and quantify them. The sample is in the vapour form and a mobile phase, usually an inert or unreactive gas such as helium nitrogen, carries it through a stationary phase. The stationary phase is a microscopic layer of liquid or polymer on an inert solid support, called a column. Through interaction with the column the sample is separated and eluted form the column at a specific time called retention time, which depends on the column and sample properties as well as the temperature gradient. Upon exiting the sample is fragmented by ionisation and the fragments are sorted by mass to form a fragmentation pattern. The fragmentation pattern for a given component of sample is unique and therefore often referred to as a molecular fingerprint. (Hussain and Khushnuma, 2014)

Procedure:

Organic compounds were extracted using methanol-chloroform (3:1) and analysed using an Agilent 7890A GC fitted with an HP-5MS capillary column (30m x 0.25mm, 0.25µm film thickness) and coupled with hyperbolic quadrupole mass selective detector MSD 5975C. The carrier gas was helium (1.2 ml min^{-1}), and 0.8 µl of sample was manually injected in splitless mode with an injector temperature at 300 ºC. The

oven temperature initiated at 30 ºC for 5 min after which the temperature was increased to 180 ºC at 5 ºC min^{-1}, and from 180 to 300 ºC at 8 ºC min^{-1}. The MSD was tuned using the auto tune function. ChemStation RTE integrator was applied to integrate the total ion current chromatograms merging every peak with an area greater than 0.1% of the largest peak in the chromatogram.

2.7. Soil properties

2.7.1. Water Holding Capacity

The maximum water holding capacity (WHC) was measured gravimetrically according to Ahn *et al*., (2009). A soil aliquot (100 g) was weight to a precision of 0.1 g, transferred into a beaker and soaked in distilled water for one day. The excess water was then drained through a filter paper (Whatman #2). The sample saturated with water (S_2) was weighed and the WHC calculated according to equation 2.15.

Calculation:

$$WHC = \frac{(S_2 - S_1) + MC * S_1}{(1 - MC) * S_1} \qquad \textit{equation 2.15}$$

Where:
S_1 = soil aliquot (g)
S_2 = sample saturated with water (g)
MC = moisture content (wt.%)
WHC = Water holding capacity ($g_{water}\ g_{soil}^{-1}$)

2.7.2. Particle size analysis

The soils contents of sand (50-2000 µm), silt (2-50 µm), and clay (< 2 µm) were determined according to Reeuwijk (2002).

Procedure:

Soil samples were weight (20 g) into a 1 L beaker. Organic matter was removed from the samples by treating them with 15 ml H_2O and 15 ml H_2O_2 (30%) overnight. The following day the samples were treated with additional 10 ml H_2O_2 and water was added to a volume of 300 ml. The samples were heated to 80 °C for 2 h and cooled to room temperature. After the soils had settled water was siphoned off with a pipette. To remove carbonates, the soil residues were treated with 30 ml HCl (1.0 M). Water was added to 250 ml and the suspensions exposed to 80 °C for 15 min. The

suspensions were then left overnight. The following day water was siphoned off and the samples washed with water another two times to remove salts. The following day 20 ml dispersing agent (sodium hexametaphosphate 4% and soda 1%) was added to the suspensions and made up to a volume of 400 ml with water. The suspensions were then shaken overnight in 1 L polyethylene bottles at 30 rpm. The following day the suspensions were passed through a 50 µm sieve and transferred to a 1 L sedimentation cylinder which were filled to the mark with water. The cylinders were mixed and placed on the table. Immediately 20 ml of suspension was taken from the centre of the cylinder using a 20 ml full pipette. After 5.5 hours another 20 ml sample was taken at 7 cm height. The three collected samples (including the retained samples < 50 µm) were dried at 105 °C.

Calculations:

Clay (< 2 µm) = (H x 50) – (Z x 50)	(K)	*equation 2.16*
Silt (2-20 µm) = (F x 50) – (Z x 50) – K	(P)	*equation 2.17*
Sand (> 50 µm) = weighed	(N)	*equation 2.18*

Where:
F = weight 20 ml pipette aliquot of fraction < 50 µm (g)
H = weight 20 ml pipette aliquot of fraction < 2 µm (g)
Z = weight 20 ml pipette aliquot of blank (g)
K = weight of clay in the soil sample (g)
P = weight of silt in the soil sample (g)
N = weight of sand in the soil sample (g)

Total Sample weight = K + P + N (g)

2.7.3. DNA Isolation

DNA Isolation was carried out using a PowerSoil DNA Isolation Kit purchased from MO BIO laboratories, USA. The solutions were provided were:

- C1: contained disruption agents required for complete cell lysis
- C2: contained a reagent to precipitate non-DNA organic and inorganic material including humic substances, cell debris, and proteins
- C3: was a second reagent to precipitate additional non-DNA material
- C4: was used to adjust the DNA solution salt concentrations to allow binding of DNA

- C5: was an ethanol based wash solution used to clean the DNA that is bound to the silica filter membrane
- C6: sterile elution buffer

Soil samples (0.25 g) were added to the PowerBead Tubes provided and vortexed gently to mix. Solution C1 (60 µl) was added and vortexed briefly. The PowerBead Tubes were secured horizontally using the MO BIO Vortex Adapter tube holder and vortexed at maximum speed for 10 min. The tubes were centrifuged at 10,000 x g for 30 seconds at room temperature and the supernatant (480 µl) was transferred to a clean 2 ml Collection Tube. Solution C2 (250 µl) was added to the tube vortexed for 5 seconds and incubated at 4 °C for 5 min. The tubes were centrifuged at room temperature for 1 minute at 10,000 x g. The supernatant (600 µl) was transferred into a 2 ml Collection Tube. Solution C3 (200 µl) was added, vortexed briefly and incubated at 4 °C for 5 minutes. The tubes were centrifuged at room temperature for 1 min at 10,000 x g. The supernatant (670 µl) was transferred into a clean 2 ml Collection Tube. Solution C4 was shaken, 1200 µl added to the supernatant and vortexed for 5 s. An amount of 675 µl were loaded onto a Spin Filter and centrifuged at 10,000 x g for 1 min at room temperature. The flow through was discarded, 675 µl of supernatant added to the Spin Filter and centrifuged at 10,000 x g for 1 min at room temperature. The remaining supernatant was loaded onto the Spin Filter and centrifuged at 10,000 x g for 1 min at room temperature. Solution C5 (500 µl) was added and centrifuged at room temperature for 30 s at 10,000 x g. The flow through was discarded, the tubes centrifuged again at room temperature for 1 min at 10,000 x g. The spin filter was carefully placed in a clean 2 ml Collection Tube and 100 µl of Solution C6 was added to the centre of the white filter membrane. The tubes were centrifuged at room temperature for 30 s at 10,000 x g, the Spin Filter discarded and the DNA in the tube was stored at -20 °C before further use. The DNA recovery was determined spectrophotometrically at 260 nm using an Eon plate reader (Biotek) and diluted with H_2O to a concentration of 10 ng μl^{-1}.

2.7.4. Endpoint polymerase chain reaction (PCR)

Endpoint PCR was carried out to identify the presence of the targeted RNA bands. The PCR reaction mixtures for bacterial *amoA*, archeal *amoA* and *nosZ* were as follows:

	Conc.:	*(µl)*	*X fold: 11*
Buffer	*10X*	*2.5*	*27.5*
Betaine	*5M*	*5*	*55*
dNTP-Mix	*10mM*	*0.5*	*5.5*
forward	*50 pmol/ µl*	*0.2*	*2.2*
reverse	*50 pmol/ µl*	*0.2*	*2.2*
H_2O		*16*	*176*
Template		*0.5*	*5.5*
Taq	*5U/ µl*	*0.1*	*1.1*
			275 µl total
			25 µl per reaction

The gel (1.5% agarose) for electrophorese was prepared by carefully heating 0.6 g Agarose with 40 g of buffer (TAE IX) for 2 min and replacing the evaporated water. Safe view nucleic acid stain (2 µl) was added to the gel after 2 min of cooling. The liquid gel was poured into a horizontal electrophoresis gel tray with a comb to create sample wells. After the gel had solidified the gel was placed into a electrophoresis tank and covered with buffer solution (TAE IX). Each sample (5 µl) was mixed with a tracking dye (1 µl) and transferred into the sample wells with aid of a micropipette. A blank and a gene runner were also included. The samples were run for 30 min at 100 V.

The samples with the most RNA were purified using the Thermo Scientific GeneJET PCR Purification Kit as follows: 20 µl of binding buffer was added to 20 µl PCR Product and transferred to the GeneJET purification column. The column was centrifuged for 1 min and the flow-through discarded. Wash Buffer (700 µl) was added to the column and centrifuged for 1 min. The flow-through was discarded and the column centrifuged a second time for 1 min to remove any residual wash buffer. The column was transferred to a clean 1.5 ml microcentrifuge tube, elution buffer (50 µl) was added to the centre of the column membrane and centrifuged for 1 min. The GeneJET purification column was discarded and the purified DNA stored at -20 °C.

The purified RNA was determined with a Qubit Fluorometric Quantitation. First the working solution was prepared by mixing the Qubit dsDNA HS Buffer with Qubit dsDNA HS Reagent (1:200). Each sample (2 µl) was added to the working solution (198 µl) to a final volume of 200 µl. The samples were vortexed and incubated at room temperature for 2 min before reading the samples. The quantified sample was diluted

to make up standards for the quantification with qPCR. The copy number was determined at scienceprimer.com.

2.7.5. Real-time / quantitative PCR (qPCR)

The qPCR was performed using the KAPA SYBR FAST qPCR Kit Master Mix. The qPCR was run with standards obtained after the Endpoint PCR with a concentration between 10^1 and 10^6 copies per µl a 96-Well PCR Plates using a LightCycler 480 Real-Time PCR System (Roche). The bacterial and archeal *amoA* genes were amplified using the primers amoA1F and amoA2R (Rotthauwe *et al*., 1997) and amo19F (Leininger *et al*., 2006) and crenamoA616r48x (Schauss *et al*., 2008) respectively. The *nosZ* gene was amplified using the primers nosZ2F and nosZ2R (Henry *et al*., 2006).

Bacterial *amoA* and *nosZ:*

Reaction mixture	*Conc.*	*Vol. (µl)*	*Thermal profile*
2X Master mix		*5.0*	*95 °C – 3 min*
Betaine	*5 M*	*5.0*	*95 °C – 3 s*
amoA1F	*5 µM*	*0.1*	*60 °C – 20 s*
amoA2R	*5 µM*	*0.1*	*72 °C – 20 s*
H_2O		*1.8*	*Cycles: 45*
Template DNA		*1.0*	

Archeal *amoA:*

Reaction mixture	*Conc.*	*Vol. (µl)*	*Thermal profile*
2X Master mix		*5.0*	*95 °C – 3 min*
Betaine	*5 M*	*5.0*	*95 °C – 3 s*
amo19F	*5 µM*	*0.1*	*55 °C – 20 s*
crenamoA616r48x	*5 µM*	*0.1*	*72 °C – 20 s*
H_2O		*1.8*	*Cycles: 40*
Template DNA		*1.0*	

2.8. Updraft Gasification Unit

2.8.1. Gasification process and operation

The updraft gasification unit consisted of a feed hopper, fixed bed reactor, two scrubber units, a storage tank, and cooling system (Figure 2-4). The feedstock was transferred from the hopper to the top of the reactor by means of a motorised screw feeder. The feedstock was continuously rotated downwards at approximately 5 rpm using steel impellers. Two induced draft fans located downstream from the gasifier pulled the gasification medium air from the bottom of the reactor through the gasification system generating the updraft. The speed of the fans controlled the air flow rate and air intake to maintain a bed temperature. Two thermocouples were placed inside the reaction zone of the reactor to measure the temperature. The gasifier was preheated with propane gas which was initially maintained as the feedstock was added until auto-thermal conditions were achieved. Tar and water condensed on the cold surfaces of metal packing in two water cooled scrubber units and were collected in a storage tank. The product gas passed through an additional air cooled heat exchanger with the aim of lowering the moisture content in the gas before flaring in a gas burner. The residual char passed through a grate at the base of the gasifier and was augered into a sealed collection drum.

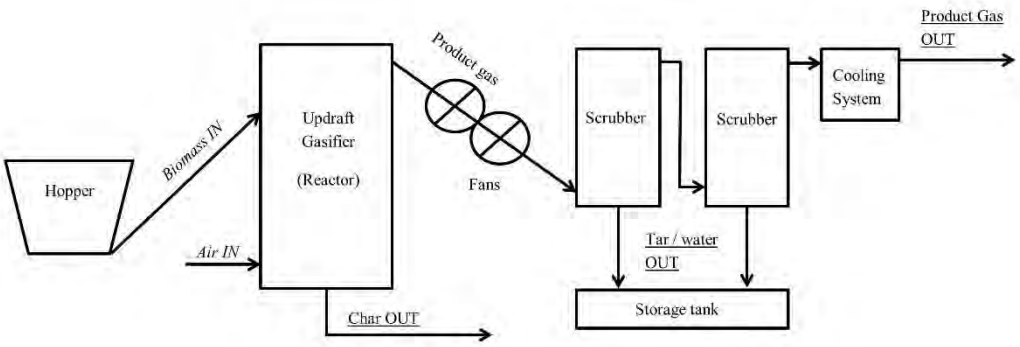

Figure 2-4: Schematic of the updraft gasification system, presenting the hopper, reactor, scrubber units and the cooling system. The main input (IN) and output (OUT) flows are highlighted.

2.8.2. Mass and Energy Balance

Data collected from analysing the feedstock and end-products (Table 2-1) were used to develop mass and energy balances to calculate the operating and performance parameters.

Table 2-1: Summary of methods used for the mass balance calculation

	Flow rate (kg h^{-1}) or (MJ h^{-1})	**Elemental composition (wt.%) or (vol.%)**	**Energy content (MJ kg^{-1})**
Input Feedstock	Measured by the software	As described in section 2.2.1, 2.2.2, and 2.3.1	Bomb calorimeter
Input air	According to nitrogen[1] 100% - ($N_{OUT} - N_{PL}$)	Assume = 21 vol.% oxygen and 79 vol.% nitrogen	Assumed = 0
Output char	measured gravimetrically every 30 min	As described in section2.2.1, 2.2.2, and 2.3.1	Bomb calorimeter
Output oil	measured gravimetrically every 30 min	As described in section 2.2.1, 2.2.2, and 2.3.1	*equation 2.19*
Output gas	Flow meter Testo 350 XL	Micro-GC	*equation 2.20*

[1] *assuming that nitrogen is inert and does not take part in the reactions.*

The average feed rate of the biomass was regulated by the software. The flow rates of the char and the tar/water emulsion were determined several times by measuring the mass output during a time period of 30 minutes. A Testo 350 XL was used to measure gas temperature (°C) and gas velocity (m s^{-1}) from which the flow rate of the cooled product gas (kg h^{-1}) was determined. Producer gas was sampled after the cooling system using Tedlar gas sampling bags and its composition analysed using an Agilent micro-GC 3000. The GC was equipped with a thermal conductivity detector for the determination of permanent gases. Module A of the GC was fitted with a Plotu column of 30 μm/32 μm/8 m and Pre Col: PLOTQ 10 μm/320 μm/1 m, using helium as the carrier gas, to analyse CO_2, ethylene, ethane, and acetylene. Module C was fitted with Molsieve 12 μm/320 μm/10 m and Pro Col PLOTU 30 μm/320 μm/3 m columns, and used argon as the carrier gas, to separate and detect H_2, O_2, N_2, CH_4, and CO. Module B was not used during this study. The chromatograph was calibrated with a standard gas mixture every day of analysis. The NH_3 concentration in the gas samples was measured using a Kitagawa AP-1 gas detector tube system fitted with a Gastec No. 3H ammonia detector tube with a measuring range 0.20-32%. The HHV and LHV of the gas were calculated according to equation 2.19 and equation 2.20 (Basu, 2010a).

$$HHV = (39.80CH_4 + 12.63CO + 12.78H_2 + 63.04C_2H_4 + 69.73C_2H_6 + 58.09C_2H_2)/100$$

equation 2.19

$$LHV = (35.84CH_4 + 12.63CO + 10.79H_2 + 59.07C_2H_4 + 63.79C_2H_6 + 56.11C_2H_2)/100$$

equation 2.20

Where:
HHV = Higher Heating Value (MJ kg^{-1})
LHV = Lower Heating Value (MJ kg^{-1})
CH_4, CO, H_2, C_2H_4, C_2H_6, C_2H_2 = vol. ratio of each gas specie

For the mass balance all volumetric flow rates (m^3 h^{-1}) were converted to mass flow rates (kg h^{-1}) using the density for each individual gas specie (Appendix I). For the energy balance the mass balance was used as a base, and including the LHV of the ingoing and product streams.

2.8.3. Process Performance Parameters

Equivalence Ratio (ER)

The equivalence ratio (ER) is a key parameter for dictating the gasification performance. It is defined as the ratio between the oxidant content in the oxidant supply and that required for complete stoichiometric combustion (Arena, 2012). To calculate the ER, the theoretical (also stoichiometric) air requirement of the fuel is to be determined first. The stoichiometric air (A_{stoich}) refers to the air, which contains the right amount of oxygen for complete combustion of the fuel, while taking into account the oxygen already present in the fuel. To calculate the A_{stoich} we followed the calculations given by (Basu, 2010b). From the elemental analysis of the fuel and the mass flow rate (kg h^{-1}), the molar feed rate of the fuel (mol h^{-1}) was determined, from which it was possible to determine the oxygen required to convert C into CO_2, hydrogen to H_2O and sulphur to SO_2 (equation 2.21). The ER is then calculated by dividing the actual air to fuel ratio (A_{actual}/F) by the stoichiometric air to fuel ratio (A_{stoich}/F) (equation 2.22). The A/F values are calculated by dividing the actual or stoichiometric air input (kg h^{-1}) by the fuel input (kg h^{-1}_{db}).

$$A_{stoich} = \frac{32C}{12} + 8H + S - O \qquad \textit{equation 2.21}$$

$$\frac{A_{actual}}{A_{stoich}} = ER \qquad \textit{equation 2.22}$$

$$gasification\ ER < 1.0 \qquad \textit{equation 2.23}$$

$$combustion\ ER > 1.0 \qquad \textit{equation 2.24}$$

Carbon Conversion Efficiency (CCE)

The carbon conversion efficiency (CCE) is a measure of chemical efficiency of the process, by providing information of unconverted material. The CCE is determined by dividing the mass flow of carbon (kg h^{-1}) in the syngas, excluding dust and tar, by the initial biomass carbon input (kg h^{-1}), where C is the carbon fraction and Q is the flow rate.

$$CCE = \frac{Q_{syngas}\, C_{syngas}}{Q_{fuel}\, C_{fuel}} \qquad \textit{equation 2.25}$$

Cold Gas Efficiency

The cold gas efficiency (CGE) is one of the most important process parameters for gasification. The CGE does not take into account the gas sensible heat, but only the potential chemical energy. was determined as the ratio between the chemical energy in the product gas and the input energy from the feedstock, where LHV_{gas} and LHV_F are the LHVs (MJ kg^{-1}) of the clean product gas and feedstock respectively, and the F_{IN} and Gas_{OUT} are the input and output streams (kg h^{-1}) of the feedstock on a dry basis (db) and product gas respectively.

$$CGE = \frac{LHV_{gas}\ x\ Gas_{OUT}}{LHV_F\ x\ F_{IN}} \qquad \textit{equation 2.26}$$

Specific Energy

The specific energy was expressed as the chemical energy of the product gas for 1 kg of feedstock (ar), where the specific energy (MJ kg^{-1}) is the product of the LHV of the gas (MJ kg^{-1}) and the product gas output (kg h^{-1}) divided by the feedstock input (kg $h^{-1}{}_{ar}$).

$$Specific\ energy = \frac{LHV_{gas}\ x\ Gas_{OUT}}{F_{IN}} \qquad \textit{equation 2.27}$$

2.9. Pyrolysis Units

2.9.1. Pyromaat Augur Pyrolysis Reactor

Swine manure biochar was produced at ECN, The Netherlands, using a slow augur pyrolysis unit named Pyromaat (Figure 2-5). Pyromaat is an indirectly heated screw conveyer reactor, in which the biomass is moved down the reactor length at a fixed speed using a screw thread feeder. It is electrically heated at 25 kWth and is able to convert typically 5 kg h^{-1} of fuel in an O_2-free atmosphere at temperatures up to 600 °C (De Wild, et.al. 2011). Solid fuel residence time was 1 hour. The slow pyrolysis biochars were produced at 400 °C and 600 °C. A small input flow of inert gas was used to facilitate the product gas flow and avoid tar condensation on the produced char.

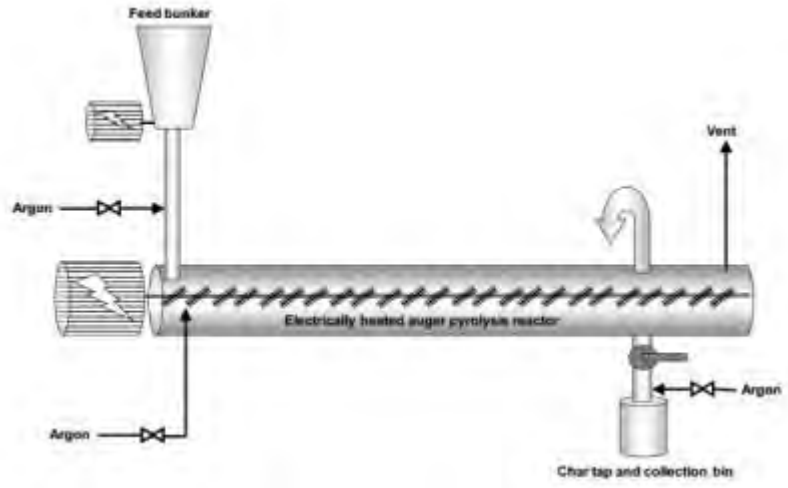

Figure 2-5: Schematic Layout of Pyromaat Augur Pyrolysis Reactor (De Wild, et.al. 2011).

2.9.2. Batch Pyrolysis Unit

Figure 2-6 shows a schematic of the laboratory scale pyrolysis unit. The slow pyrolysis process was conducted in batch mode in the absence of an inert gas. The reactor was cylindrical with a diameter of 9 cm and length of 15 cm. The containers had small holes on the caps and along the reactor walls, which served to release any vapours generated during pyrolysis. The vapours forced the remaining oxygen out of the reactor. The manure biomass was completely filled to the top (about 320 g for poultry

litter and 100 g for cow manure per batch) to avoid any oxygen to enter the container. The reactor was placed in a muffle furnace and heated from room temperature to the maximum temperature at a heating rate of 20 °C min^{-1} with a residence time of 1 hour. The maximum temperatures were chosen to be 400 °C and 600 °C. After heating was terminated the reactor was left to cool to room temperature in the muffle furnace.

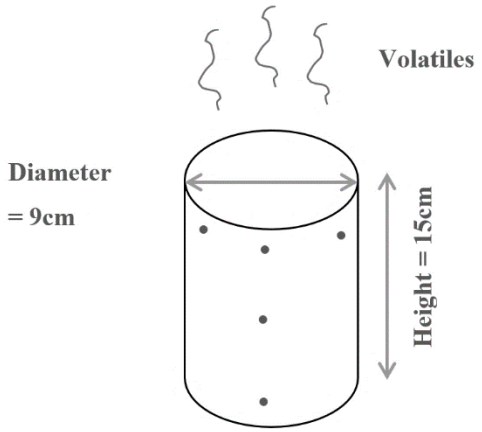

Figure 2-6: Schematic of pyrolyser operated in batch mode

2.9.3. Kon-Tiki Kiln

The Kon-Tiki Open Fire Kiln was developed by the Ithaka Institute, a non-profit research institute based in Valais, Switzerland. The design is a large inverted cone of a volume of 850 L, which is filled with the biomass feedstock. After lighting the biomass, the charring process begins. After the biomass is charred to about two thirds of its height, another layer of biomass is added, which will create a low oxygen environment in the lower layer of the kiln. A vortex is created by the shape of the cone, which prevents smoke formation by burning the condensable and non-condensable gases. The design was inspired by the Japanese Moki Kiln (Figure 2-7).

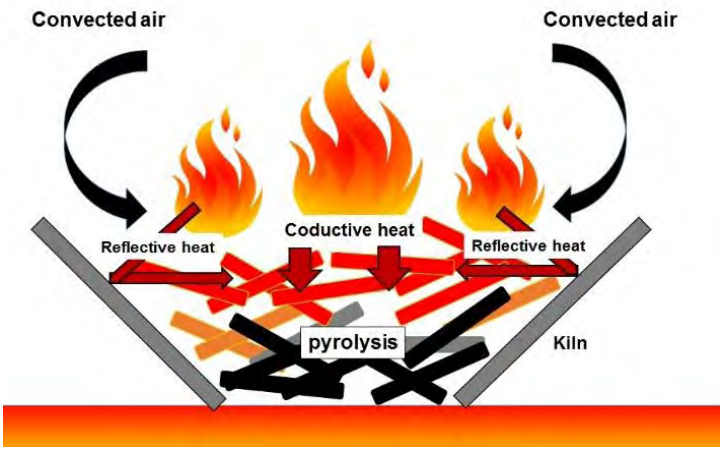

Figure 2-7: The Japanese Cone Kiln (the Moki Kiln)

2.10. References

Ahn, H.K., Sauer, T.J., Richard, T.L., Glanville, T.D., 2009. Determination of thermal properties of composting bulking materials. Bioresour. Technol. 100, 3974-3981.

Arena, U., 2012. Process and technological aspects of municipal solid waste gasification. A review. Waste Manag. 32, 625–639.

BS EN 14778:2011. Solid biofuels - Sampling: methods for sampling.

BS EN 14774-3:2009. Solid biofuels - Determination of moisture content - Oven dry method. Moisture in general analysis sample.

BS EN 15104:2011. Solid biofuels - Determination of total content of carbon, hydrogen and nitrogen.

BS EN 14582:2007. Characterization of waste - Halogen and sulfur content - Oxygen combustion in closed systems and determination methods.

BS EN 14775:2009 - Solid biofuels. Determination of ash content.

BS EN 14918:2009 - Solid biofuels. Determination of calorific value.

Basu, P., 2010a. Biomass Gasification and Pyrolysis - Practical Design. Elsevier Inc., Oxford, UK. p.221

Basu, P., 2010b. Biomass Gasification and Pyrolysis - Practical Design. Elsevier Inc., Oxford, UK. p.199

Chemiasoft, 2014. Available at http://www.chemiasoft.com/chemd/node/52 (accessed 10.07.16).

Coates, J., 2000. Interpretation of Infrared Spectra, A Practical Approach. In Meyer, R.A. (Ed.). Encyclopedia of Analytical Chemistry. John Wiley & Sons Ltd. Chichester, UK. 10815–10837.

De Wild, P.J., Reith, H., Heeres, H.J. 2011. Biomass pyrolysis for chemicals.

Biofuels.2(2), 185 - 208.

Dodd, J. W. and Thonge, K. H. (1987). Thermal Methods, Chichester: Wiley.

ECN Phyllis 2, 2015. Available at https://www.ecn.nl/phyllis2/Home/Help (accessed 22.10.15).

Elementar, 2016. Elementar Analysensysteme GmbH. Available at http://www.elementar.de/en/products/vario-serie/vario-el-cube.html (accessed 07.06.2016)

Enders, A., Lehmann, J., 2012. Comparison of Wet-Digestion and Dry-Ashing Methods for Total Elemental Analysis of Biochar. Commun. Soil Sci. Plant Anal. 43, 1042–1052.

Henry, S., Bru, D., Stres, B., Hallet, S., Philippot, L. 2006. Quantitative detection of the *nosZ* gene, encoding nitrous oxide reductase, and comparison of the abundances of 16S rRNA, *narG*, *nirK*, and *nosZ* genes in soils. Appl Environ Microbiol 72, 5181–5189.

Hydrogen Analysis Resource Center, 2015. Available at http://hydrogen.pnl.gov/tools/lower-and-higher-heating-values-fuels (accessed January 2015)

Hussain, S. Z., Khushnuma, M. 2014. GC-MS: Principle, Technique and its application in Food Science. Review Article. Int. J. Curr. Sci. 13, 116-126.

I.S. EN 15148:2009. Solid biofuels - Determination of the content of volatile matter.

ISO/TC238:2011. Solid biofuels - Determination of bulk density.

ISO 10390:2005. Soil quality - Determination of pH.

Leininger, S., Urich, T., Schloter, M., Schwark, L., Qi, J., Nicol, G.W., Prosser, J.I., Schuster, S.C., Schleper, C., 2006. Archaea predominate among ammonia-oxidizing prokaryotes in soils. Nature. 442, 806–809.

Reeuwijk, L.P., 2002. In Reeuwijk (Ed.). Procedures for soil analysis. Sixth edit. ed. International Soil Reference and Information Centre. ISSN 0923-3792: no.9. Food and Agriculture Organization of the United Nations. Wageningen, The Netherlands.

Rotthauwe, J.H., Witzel, K.P., Liesack, W. 1997. The ammonia monooxygenase structural gene *amoA* as a functional marker: molecular fine-scale analysis of natural ammonia-oxidizing populations. Appl. Environ. Microbiol. 63, 4704–4712.

Schauss, K., Focks, A., Leininger, S., Kotzerke, A., Heuer, H., Thiele-Bruhn, S., *et al*. 2008. Dynamics and functional relevance of ammonia-oxidizing archaea in agricultural soil. Environ Microbiol. 11(2), 446-456.

Uzoma, K.C., Inoue, M., Andry, H., Fujimaki, H., Zahoor, a., Nishihara, E., 2011. Effect of cow manure biochar on maize productivity under sandy soil condition. Soil Use Manag. 27, 205–212.

3. Updraft Gasification of Poultry Litter at Farm-Scale – A Case Study

The content of this chapter has been published in the Elsevier journal 'Waste management'.

Taupe, N.C., Lynch, D., Wnetrzak, R., Kwapinska, M., Kwapinski, W., Leahy, J.J., 2016. Updraft gasification of poultry litter at farm-scale – A case study. Waste Manag. 50, 324-333

The chapter proposes a critical analysis of updraft gasification of PL at farm-scale. The aim is to evaluate the process performance of an existing updraft gasification system and to characterise the side products for their practical use.

3.1. Abstract

Farm and animal wastes are increasingly being investigated for thermochemical conversion, such as gasification, due to the urgent necessity of finding new waste treatment options. We report on an investigation of the use of a farm-scale, auto-thermal gasification system for the production of a heating gas using poultry litter (PL) as a feedstock. The gasification process was robust and reliable. The PL's ash melting temperature was 639 °C, therefore the reactor temperature was kept around this value. As a result of the low reactor temperature the process performance parameters were low, with a cold gas efficiency (CGE) of 0.26 and a carbon conversion efficiency (CCE) of 0.44. The calorific value of the clean product gas was 3.39 MJ m^{-3}_{N} (LHV). The tar was collected as an emulsion containing 87 wt.% water and the extracted organic compounds were identified. The residual char exceeds thresholds for Zn and Cu to obtain European biochar certification; however, has potential to be classified as a pyrogenic carbonaceous material (PCM), which resembles a high nutrient biochar.

3.2. Introduction

The livestock sector is one of the fastest growing subsectors of the agricultural economy driven by growing population and demand for animal protein; however, it faces several challenges in terms of its effect on the natural environment upon which production depends. In particular, it has to adapt to a policy context requiring it to improve its environmental performance and mitigate its impact on climate change.

Poultry was responsible for 33% of the global meat in 2010 (MacLeod *et al*., 2013) and now accounts for over 80% of the entire world's livestock (FAO, 2015). The poultry sector's growth over the recent decades has moved away from traditional farming practices towards industrialisation, geographical concentration and intensification. A direct consequence of these structural changes is that far more waste is produced than can be managed by land disposal. This has given rise to a number of environmental concerns, including bad odours, pathogens, water eutrophication, volatilisation of ammonia (NH_3) and emissions of greenhouse gases (De Vries *et al*., 2012).

At a European Union (EU) level reuse and recycling of wastes are now encouraged over land disposal and legislative restrictions have been introduced. The most significant is the Nitrates Directive (EC, 1991), which aims to protect waters against pollution from nitrates. The choice of waste treatment technologies depends on several factors, e.g. the waste's properties and availability, the desired end products and their economic value. Energy conversion technologies have the advantage of recycling nutrients and recovering energy at the same time. Energy recovery is significant for countries like Ireland. According to Sustainable Energy Ireland (SEI) Ireland imports 86% of its fuels making it the most import dependent country in the EU (SEI, 2015). Furthermore, developments in biomass to energy conversion technologies using e.g. poultry litter (PL), animal slurry and manure, spent mushroom compost and straw would provide a valuable source of employment in rural areas in Ireland. While wet wastes such as cattle manure and pig manure are suitable for bio-chemical conversion, e.g. anaerobic digestion, low moisture wastes such as PL and spent mushroom compost can be subject to thermal treatment, such as combustion, pyrolysis and gasification.

Poultry litter, the waste from broiler production, can vary significantly in its physical and chemical composition depending on its origin and the management practices of the farm. It consists of bedding material (BM), faeces, urine, feathers and waste feed. Poultry litter is the most suitable manure feedstock for thermal conversion processes, since its comparably low moisture content reduces the need for pre-treatment (Lynch *et al*., 2013a). However, some inorganic species, in particular alkali and earth alkali metals ionically bonded with chlorine, cause operational problems, which need to be addressed (Di Gregorio *et al*., 2014; Font Palma and Martin, 2013a; Lynch *et al*., 2013b).

Recently, the European Commission (EC) decided to allow PL to be used as a fuel for on-farm combustion under existing animal by-product regulations (Commission Regulations (EU) No 592/2014). On-farm application offers several advantages for farmers, mainly to have the benefit of handling their own waste and to produce heat for the poultry sheds in winter and a natural fertiliser without having to pay expensive waste disposal and transportation costs. Furthermore, the excess product gas can be easily distributed to other sites in the vicinity. Combustion of PL is already successfully being applied on farm-scale (BHSL, 2011), using the energy for heating the poultry sheds and the residual ash in the PK fertilising industry.

Gasification is a thermochemical treatment technology which transforms the solid manure biomass into a gaseous energy carrier called “syngas” or “product gas” under sub stoichiometric oxygen conditions (Arena, 2012). This means that the oxygen supply is lower than that required for complete combustion. Gasification offers some advantages over conventional combustion as highlighted by Basu (2010a); the gas volume is less, which requires smaller equipment, the gas can be easily transported and gas handling is easier compared to a solid biomass. In addition, the gas could be distributed to individual houses or units to be used as a fuel for cooking or heating. Gasification produces less NO_x and SO_x emissions due to the lower oxygen supply and operating temperature; however undesired gaseous species, which occur in a reducing environment, might be formed, such as H_2S, HCl, carbonyl sulphides (COS), HCN, and NH_3. Depending on the final application of the product gas, gas cleaning units are required. In particular, for gas turbines and engines there are defined limits for contaminants, including tar, dust, alkalis, heavy metals, H_2S and HCl. For large scale operations the installation of a product gas cleaning unit is economically feasible.

Nevertheless, Lee *et al*. (2013) demonstrated the possibility of generating electricity from biomass using a trailer-scale integrated system for distributed energy and rural applications. For their engine application they installed a cyclone, cooling tower and two filters to clean the gas of dust particles and tars.

Scientific literature on PL gasification is still fairly limited since PL is an unconventional fuel to gasify owing to its high ash content. In fact, the use of PL for thermal treatment might have to be seen primarily as a waste treatment option, while producing energy as a useful side product, rather than aiming to achieve high process performance. The critical focus of scientific investigations has been to understand and mitigate operational difficulties related to ash during fluidised bed gasification (Di Gregorio *et al*., 2014; Font Palma and Martin, 2013a). Priyadarsan *et al*. (2004) performed a study on updraft gasification of poultry manure and concluded that a high alkali content in the feedstock leads to ash agglomeration in the fuel bed. Font Palma and Martin (2013b) used chemical equilibrium modelling to design compact reactors to suit on-site applications for heat and power generation from PL. Their optimised configuration achieved modelled electrical efficiencies of between 26% and 33.5%.

Selecting the right type of gasifier depends on the capital, operating and maintenance costs, the size, simplicity and feedstock properties and pre-treatment (drying, separation, size, reduction, pelletisation). Updraft gasifiers are the oldest and simplest design. They are also known as counter current gasifiers, since the oxidising agent travels upwards and the bed of fuel moves down. They are considered suitable for gasifying feedstocks with relatively high moisture and ash content (50 wt.% and 15 wt.% respectively), have a high thermal efficiency due to low exit gas temperature, and have a low ash carryover due to the filtering effect of the fuel bed (McKendry, 2002; Priyadarsan *et al*., 2004). The simple reactor design and low investment make this type of technology very attractive for on-farm application; however, the technology has several disadvantages which have to be addressed before application, such as poor temperature control and tar formation.

There are relatively few reports in the scientific literature of the operation of on-farm gasification of PL. This paper proposes a critical analysis of updraft gasification of PL at farm-scale. The aims were to evaluate the process performance of an existing

updraft gasification system, to characterise the side products and give suggestions for their practical use.

3.3. Methodology

3.3.1. Gasification process and operation

A schematic of the on-farm updraft gasification system is presented in Figure 3-1. The fixed bed reactor was cylindrical in shape with an average feed rate of 40 kg h^{-1}. The feedstock was transferred from a hopper to the top of the reactor by means of a motorised screw feeder. The reactor was filled to the top with PL, which was continuously rotated downwards at approximately 5 rpm using steel impellers. Two induced draft fans located downstream from the gasifier pulled the gasification medium air from the bottom of the reactor through the gasification system generating the updraft, which also resulted in a slight pressure drop. The speed of the fans controlled the air flow rate and air intake to maintain a bed temperature between 580 °C and 680 °C. Two thermocouples were placed inside the reaction zone of the reactor to measure the temperature. The gasifier was preheated with propane gas which was initially maintained as the feedstock was added until auto-thermal conditions were achieved. Tar and water condensed on the cold surfaces of metal packing in two water cooled scrubber units and were collected in a storage tank. The gas entered the first scrubber at around 85 °C and exited it around 50 °C; the gas exited the second scrubber at around 32 °C. The product gas passed through an additional air cooled heat exchanger with the aim of lowering the moisture content in the gas before flaring in a gas burner. A Testo 350 XL was used to measure the flow rate of the cooled product gas, being 28.8 Nm^3 h^{-1} at 12.3 °C. The residual unconverted solid char passed through a grate at the base of the gasifier and was augered into a sealed collection drum. The flow rates of the char and the tar/water emulsion were determined several times by measuring the mass output during a time period of 30 minutes. A more detailed description of the gasifier and the process can be found in Joseph *et al*. (2012). The gasifier operated for 14 hours on each of three consecutive days and > 560 kg of litter was gasified. The results present an average of measurements conducted on these three days.

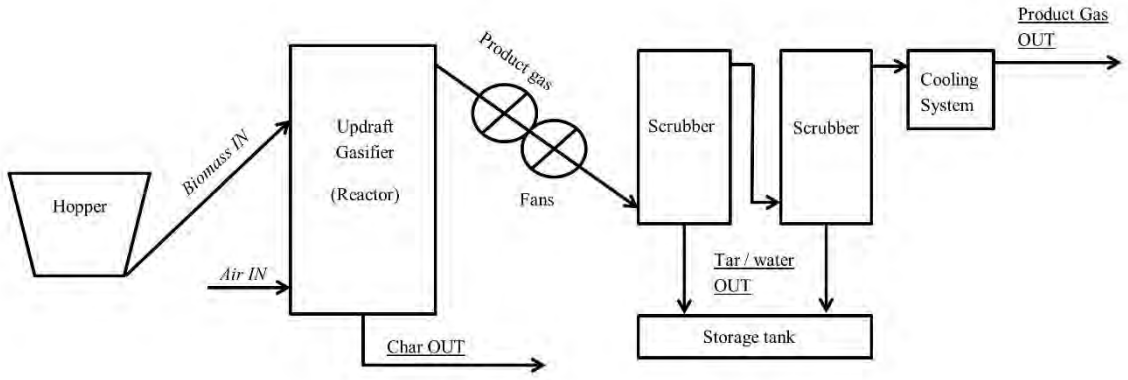

Figure 3-1: Schematic of the updraft gasification system, presenting the hopper, reactor, scrubber units and the cooling system. The main input (IN) and output (OUT) flows are highlighted.

3.3.2. Feedstock and product characterisation

Wood shavings from Sitka spruce trees were used as a BM prior to the stocking of birds on the broiler farm. The broiler chickens were fed a conventional diet suitable to their age. In the first 3 weeks the chickens were fed so-called "starter feed", between 3-6 weeks they were fed "grower feed" and between 6-8 weeks they were fed "fattener/finisher feed". The poultry sheds were cleaned professionally according to the guidelines for approval of breeding farms under Council Directive 2009/158/EC. A representative sample of PL and BM were collected from stock piles in the farm's storage shed according to BS EN 14778 (2011). Numerous subsamples were taken at different positions and depths. Several char samples were taken from the collection drum. The samples were stored in airtight bags. The solids were mixed thoroughly and ground when necessary before analysis. The condensed product gas impurities were sampled from the storage tank after the two scrubber units as a tar / water emulsion.

Proximate analysis involved the determination of moisture, ash, volatile matter (VM) and fixed carbon (FC) content according to standard methods (BS EN 14774-1, I.S. EN 14775:2009, I.S. EN 15148:2009). The FC content was calculated by subtracting the moisture, ash and VM content from 100%. Ultimate analysis was conducted to determine the elemental composition of the solid and liquid samples. Carbon, hydrogen, nitrogen and sulphur were analysed with an Elemental Vario EL Cube analyser. Oxygen was calculated by difference. The amount of chlorine in the solid samples was measured using a chloride ion selective electrode following oxidation in

a bomb calorimeter and absorption of the halogen in KOH (0.2 M) (BS EN 14582:2007). Inorganic constituents were measured using inductively coupled plasma optical emission spectrometry (ICP-OES, Thermo Elemental Co. Iris Intrepid II XDL) after nitric acid and hydrogen chloride (HNO_3-HCl) digestion in a microwave oven. Bulk density (BD) was analysed using a modified version of a standard method (ISO/TC238), using a 100 ml volumetric flask instead of a 5 litre measuring container specified in the standard procedure. The particle size distribution was measured with a stainless steel sieve shaker using 5.0, 2.8, 1.0, 0.5, and 0.25 mm sieves.

Thermal analyses of the PL ash produced at 550 °C was carried out using a TGA/DSC 9 instrument (Setaram Labsys, USA) operated with a nitrogen flow rate of 500 ml min^{-1} and at a heating rate of 10 °C min^{-1}. The higher heating value (HHV) was determined using an oxygen bomb calorimeter 6200 No. 442 M from Parr instruments Company. The lower heating value of the solids was corrected for hydrogen (equation 3.1) (ECN Phyllis 2, 2015).

$LHV_{dry} = HHV_{dry} - 2.443 \times 8.936 \times (H/100)$ *equation 3.1*

Scanning electron microscopy (SEM) combined with energy dispersive spectroscopy (EDS) was used to analyse the composition and morphology of the PL char. The PL char was crushed, placed onto carbon tabs, and coated with gold to mitigate charging. The analysis was performed using an Ultra-High-Resolution Analytical FE- SEM SU- 70 (Hitachi), and a Large Area EDS Silicon Drift Detector, (Oxford Instruments) equipped with INCA software. The accelerating voltage was 15.0 kV and the working distance for the EDS analysis was 15 mm.

The water content of the tar / water emulsion was determined by Karl Fischer titration (Mettler Toledo DL 31). The samples were titrated using Hydranal Composite 5 and methanol-chloroform (3:1) was used as a solvent. The pH was determined using an Orion 420 pH meter. Organic compounds were extracted using methanol-chloroform (3:1) and analysed using an Agilent 7890A GC fitted with an HP-5MS capillary column (30m x 0.25mm, 0.25µm film thickness) and coupled with hyperbolic quadrupole mass selective detector MSD 5975C. The carrier gas was helium (1.2 ml min^{-1}), and 0.8 µl of sample was manually injected in splitless mode with an injector temperature at 300 ºC. The oven temperature initiated at 30 ºC for 5 min after which the temperature was increased to 180 ºC at 5 ºC min^{-1}, and from 180 to 300 ºC

at 8 ºC min^{-1}. The MSD was tuned using the auto tune function. ChemStation RTE integrator was applied to integrate the total ion current chromatograms merging every peak with an area greater than 0.1% of the largest peak in the chromatogram.

Producer gas was sampled after the cooling system using Tedlar gas sampling bags and its composition analysed using an Agilent micro-GC 3000. The NH_3 concentration in the gas samples was measured using a Kitagawa AP-1 gas detector tube system fitted with a Gastec No. 3H ammonia detector tube with a measuring range 0.2%-32%. The HHV and LHV of the gas were calculated according to equation 3.2 and 3.3 (Basu, 2010e).

$$HHV = (39.80CH_4 + 12.63CO + 12.78H_2 + 63.04C_2H_4 + 69.73C_2H_6 + 58.09C_2H_2)/100$$

equation 3.2

$$LHV = (35.84CH_4 + 12.63CO + 10.79H_2 + 59.07C_2H_4 + 63.79C_2H_6 + 56.11C_2H_2)/100$$

equation 3.3

Data collected from analysis of the feedstock and product were used to develop mass and energy balances and flow analysis to calculate the operating and performance parameters. The equivalence ratio (ER) was calculated by dividing the actual air to fuel ratio (A/F_{actual}) by the stoichiometric air to fuel ratio (A/F_{stoich}) according to Basu (2010d). The carbon conversion efficiency (CCE) was determined by dividing the mass flow of carbon (kg h^{-1}) in the scrubbed product gas by the initial biomass carbon input (kg h^{-1}). The cold gas efficiency (CGE) was the ratio of the chemical energy in the product gas to the input energy from the PL according to equation 3.4, where LHV_{gas} and LHV_{PL} are the LHVs (MJ kg^{-1}) of the clean product gas and PL respectively, and the PL_{IN} and Gas_{OUT} are the input and output streams (kg h^{-1}) of the feedstock on a dry basis (db) and product gas respectively.

$$\mathrm{CGE} = \frac{\mathrm{LHV_{gas}\ x\ Gas_{OUT}}}{\mathrm{LHV_{PL}\ x\ PL_{IN}}}$$

equation 3.4

The specific energy was expressed as the chemical energy of the product gas for 1 kg of as received (ar) PL feedstock according to equation 3.5, where the specific energy

(MJ kg^{-1}) is the product of the LHV of the gas (MJ kg^{-1}) and the product gas output (kg h^{-1}) divided by the PL input (kg h^{-1}) (ar).

$$\text{Specific energy} = \frac{\text{LHV}_{\text{gas}} \text{ x } \text{Gas}_{\text{OUT}}}{\text{PL}_{\text{IN}}} \qquad \textit{equation 3.5}$$

Equation 3.6 was used to calculate the percentage mass balance closure (MBC) with the average values from steady state being used for the calculations.

$$\text{MBC} = (\text{OUT/IN}) * 100 \qquad \textit{equation 3.6}$$

3.4. Results and Discussion

3.4.1. Suitability of poultry litter for updraft gasification

The chemical and physical properties of a feedstock are essential to the design of any gasification unit. Arena (2012) outlined some significant feedstock properties recommended for updraft gasification, which were used to compare against the PL feedstock used in this study (Table 3-1). The proximate analysis and elemental composition of the feedstock are discussed later.

Moisture content and BD were within the limits recommended by Arena (2012). The moisture content was 30.2 wt.% (ar). In general, updraft gasifiers cope very well with moisture contents up to 50.0 wt.% (ar), as the feedstock dehydrates in the drying zone at the top of the reactor. Poultry litter rarely exceeds this value, since poultry sheds are usually ventilated thoroughly to keep the BM between 20 and 25 wt.% (Fairchild and Czarick, 2011). This precaution is important for bird welfare by avoiding exposure to harmful microorganisms. Miles *et al*. (2011) reported a critical moisture level between 37.4% and 51.1% litter moisture, at which ammonia (NH_3) emissions are at their maximum, and recommend moisture contents of litter below or above these values. The BD of PL (ar) was 411.2 kg m^{-3}, which is in agreement with Singh *et al*. (2008) and Coloma (2005) who reported values of 466.7 kg m^{-3} (ar) and between 410.0 and 434.9 kg m^{-3} (ar) respectively.

The ash content in the PL feedstock was higher than the guideline advocated by Arena (2012), Table 3-1. Generally, the ash content can vary significantly depending on the feed, type of birds, moisture content, type of the BM and animal husbandry practice. Lynch *et al*. (2013a) measured ash contents of between 5.95 to 15.15 wt.% (ar) in PL

samples from Irish broiler production facilities. Font Palma and Martin (2013b) used a mineral content of 21.6 wt.% (db) for their modelling work on fluidised bed gasification, which was a compilation of other published work. Di Gregorio *et al*. (2014) reported values of 17.2 and 25.1 wt.% (ar) of ash in Italian poultry manure, while Priyadarsan *et al*. (2004) reported an unusually high ash content of 43.9 wt.% (ar) in the PL used in their updraft gasifier experiments. Their samples were collected as wet-cake close to the water dispensers in the poultry shed. High ash content feedstocks, such as PL, make low temperature operation conditions unavoidable during gasification as high temperatures in the oxidation zone leads to ash melting, clinkering and slagging problems due to alkali oxides and other salts, which produce eutectic mixtures with low melting points (Lynch *et al*., 2013b). In our study, softening of PL ash occurred at 639 °C as shown by the melting endotherm of the differential scanning calorimetric thermograph (Figure 3-2). Operational temperatures above or close to this temperature were considered not suitable.

Table 3-1 presents the particle size distribution of the PL with an estimated average particle size of 2.1 mm, which was similar to PL used in other studies (Di Blasi, 2009; Singh *et al*., 2008). Finer particles offer less resistance for condensable gases to escape to the surrounding environment, which then undergo secondary cracking (Basu, 2010b). Priyadarsan *et al*. (2004) found that smaller particle sizes of poultry manure have a higher peak-temperature propagation rate compared to larger particles during fixed bed gasification. They explained this observation by the larger surface area of the smaller particles and the faster reaction rates. They also reported the peak temperatures to be higher for smaller particles; however, the particle size did not significantly affect the product gas composition or heating value of the product gas.

Table 3-1: Physical and chemical properties of the PL feedstock used in this study compared to the recommended requirements for suitable feedstock for updraft gasification given by Arena (2012). The particle size distribution is also included.

	Poultry Litter	**Requirements for up-draft**
Moisture content [wt.%] (ar[1])	30.2 ± 0.5	< 50
Ash content [wt.%] (db[2])	19.8 ± 0.3	< 15
BD[3] [kg m^{-3}] (ar)	411.2 ± 11.9	> 400
Ash melting point [°C]	639	> 1000
Particle size [mm]	< 10	< 100
Average particle size [mm]	2.1	
Particle size > 5 mm [wt.%]	9	
Particle size 2.8 mm - 5 mm [wt.%]	18	
Particle size 1 mm - 2.8 mm [wt.%]	36	
Particle size 0.5 mm - 1 mm [wt.%]	17	
Particle size 0.25 mm - 0.5 mm [wt.%]	9	
Particle size < 0.25 mm [wt.%]	11	

[1] *as received*
[2] *dry basis*
[3] *bulk density*

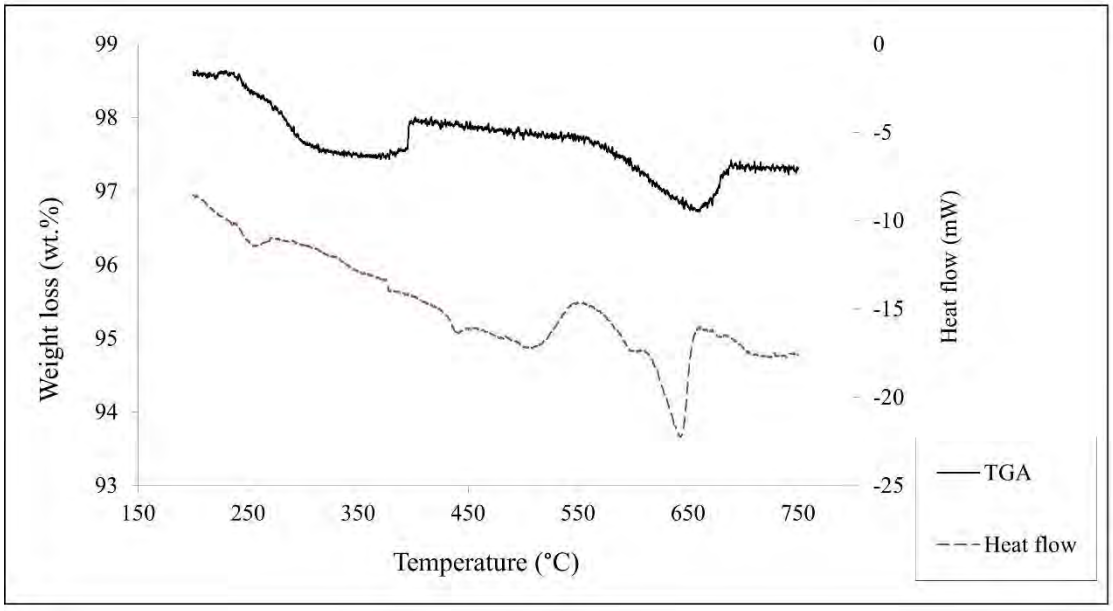

Figure 3-2: Weight loss and heat flow of PL ash using thermogravimetric analysis (TGA) with a nitrogen flow rate of 500 ml min^{-1} and at a heating rate of 10 °C min^{-1}

3.4.2. System analysis and process performance

To assess the performance of the gasification process a conventional mass and energy balance was established in which the main input and output streams were considered. Figure 3-3 presents the mass and energy flows to scale. Detailed information about the mass and energy balance can be found in the Appendix I.

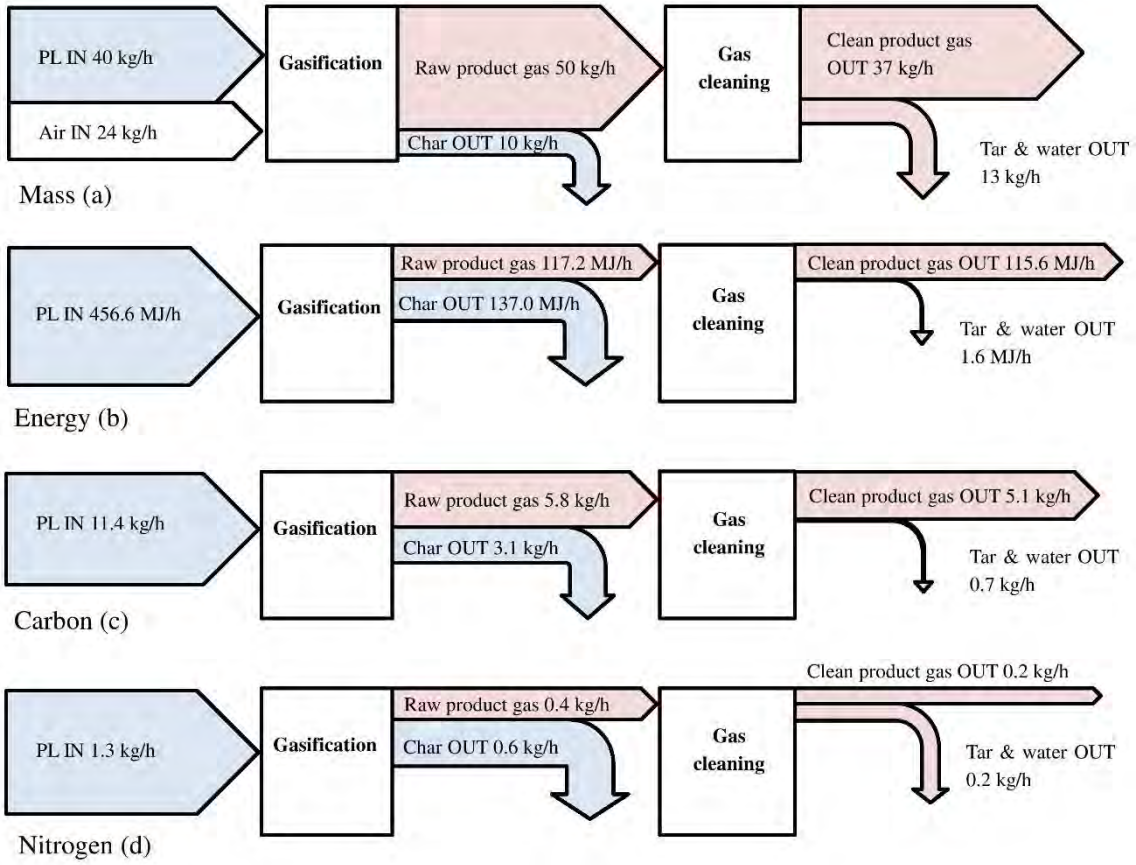

Figure 3-3: Flow chart (a) of the mass balance in kg h^{-1}(ar), (b) of the energy balance in MJ h^{-1} (calculated based on LHV) and (c and d) of the carbon and nitrogen balance in kg h^{-1} (ar). Flow chart (d) excludes inert nitrogen from the gasification air.

The mass balance in Figure 3-3 (a) shows, that solid PL and air were converted to raw product gas and char. After gas cleaning the product gas yield represented 57.8 wt.% of the total input streams with an estimated LHV of 3.39 MJ m^{-3}_N based on the measured gas composition (Table 3-4). The unconverted char accounted for 15.6 wt.% and the tar / water emulsion for 20.3 wt.% of the total input streams. The char and tar / water residues made up 58.3 wt.% of the initial PL input.

The energy balance in Figure 3-3 (b) reveals that 55.7% of the original LHV was stored in the products. The remaining 44.3% of the energy was therefore used to

evaporate the moisture and dry the feedstock, for heating the feedstock to the reactor temperature, as well as thermal losses to the environment. Heat losses could be reduced significantly by insulating the main reactor and pipes. The excess heat could be used for drying the PL prior to gasification to improve the overall gasification efficiency and reduce the moisture content in the gas. However, during such pre-drying volatile organic compounds (VOCs) can be volatilised from the fuel, which have to be captured by an additional air pollution control system (McKendry, 2002). The char residue represented 30.0% of the initial energy input and the gas only 25.7%. The tar / water emulsion contained 87 wt.% water and hence its LHV was very low (1.6 MJ kg^{-1}).

The carbon balance in Figure 3-3 (c) demonstrates that a significant quantity of carbon remained unconverted in the char (27.2 wt.%), while 44.7 wt.% was converted to lower molecular weight gaseous products. Considering the MBC of only 78.1 wt.% for carbon (Table 3-3), it was assumed that the 21.9 wt.% of undetected carbon formed the main component of the un-measured tar, which accumulated on the walls of the pipes and scrubber units. Carbon in the air input was neglected in our calculations. An amount of 46.2 wt.% of nitrogen remained in the char (Figure 3-3 (d)), while 15.4 wt.% was trapped in the tar/water emulsion and 15.4 wt.% left the system as product gas. A total of 23.1 wt.% nitrogen was not detected, which could be attributed to inaccurate NH_3 measurements with the Kitagawa AP-1 gas detector tubes or organic nitrogen compounds as part of the unmeasured tar in the scrubber units. Also most of the sulphur remained to 51.4 wt.% in the char and only 0.2 wt.% was trapped in the tar phase (not shown in the figure), hence 48.6 wt.% of sulphur is potentially emitted as H_2S and COS.

The gasification experiments were performed during late winter when the ambient temperature was around freezing (0 – 4 ºC), typical of operating conditions when the demand for heat are highest. The reactor achieved temperatures of between 580 and 680 ºC during steady state operation, which are considered low for gasification (temperatures normally exceed 700 ºC); however, the low temperature was deemed necessary in order to avoid ash agglomeration. For auto-thermal gasification the temperature is normally controlled by selecting the appropriate ER value. The induced draft fan at the outlet of the reactor regulated the ER by constantly adjusting the air flow to maintain the temperature. The air input was consequently difficult to measure

accurately, and so was calculated based on the nitrogen input and output flows of the system. The calculated air input was used to determine the ER value (0.15) in Table 3-2, which was lower than the values normally associated with biomass gasification. The low ER resulted in low partial oxidation of the PL providing less heat for gasification and creating an environment typical of pyrolysis (see section 3.4.4). As a result of the low temperature the gasification process performance was low, as can be seen by a CGE of 0.26, a CCE of 0.44 (Table 3-2) and resulting in a significant quantity of unconverted char as discussed earlier. The CGE and specific energy were low compared to Di Gregorio *et al*. (2014), who reported a CGE of 0.33 to 0.44 and specific energy of 3.64 to 4.86 MJ kg^{-1}_{waste} during fluidised bed gasification of PL at temperatures between 700 and 760 ºC. The overall power output in our study was 32.6 kWh_{th}.

Table 3-2: Operating and performance parameters

Parameter	**value**
T_{air}[1] [°C]	0-4
T_{bed}[2] [°C]	580-680
$T_{product\ gas\ OUT}$[3] [°C]	11.0-13.2
A/F^{4}_{stoich}	5.29-5.31
A/F_{actual}	0.75-0.96
Equivalence ratio (ER)	0.13-0.17
Cold gas efficiency (CGE)	0.25-0.26
Carbon conversion efficiency (CCE)	0.44-0.46
Specific energy [MJ kg_{PL}^{-1}]	2.88-2.98
Average power output [kWh_{th}]	32.0-33.1

[1] *temperature of the gasifying medium (air) entering the reactor*
[2] *bed temperature in the reaction zone*
[3] *temperature of cooled product gas*
[4] *air to fuel ratio*

The MBC is presented in Table 3-3. The values emphasise how well the input and the output components fulfil the principle of mass conservation. Nitrogen was introduced to the reactor as N_2 in air as well as in form of protein and inorganic nitrogen in PL, which was converted to heterocyclic nitrous compounds in tar, amine and amid residues from the feedstock and volatile gases, such as N_2 and NH_3. Gaseous nitrogen is chemically inert and is therefore commonly used as an indicator for the uncertainty of measurements during gasification experiments. Consequently, the nitrogen input by air was calculated according to all nitrogen input and output streams. For this reason,

nitrogen closure equalled 100%. The oxygen closure was 100.6%, which included the calculated oxygen in air, and total oxygen in PL, char, tar/water and gas. Hydrogen balance is generally difficult to close since it is included in many minor-products, some of which were not measured in the gas phase. There are gaseous compounds which were not detected, such as H_2S and light hydrocarbons, which influenced S and C output. Tar composition, flow rate, as well as losses on surfaces of the gasification system can have a significant influence on the mass balance closure and might also be responsible for the ash closure of 94.0%.

Table 3-3: Mass balance closure (MBC)

Component	MBC [wt.%]
H	66
C	78
O	101
S	52
N	100
Ash	94

3.4.3. Product gas, and condensed hydrocarbons and water

Table 3-4 presents the product gas composition together with data from other reports of PL gasification. The experimental data show that H_2 and CO concentrations were lower and CO_2 concentration was higher compared to previously reported product gas composition from updraft gasification of poultry manure, with CH_4 concentration similar to reported values (Priyadarsan *et al*., 2004). As already discussed in section 3.4.2, the ER regulates the temperature and therefore the exothermic and endothermic reactions. The results suggest that the low ER and hence low temperature did not provide sufficient energy for endothermic reactions to take place. The CO_2 from combustion would not react with char resulting in low H_2 and CO concentrations. Generally, with increasing ER the CO content increases due to the water gas reaction ($C + H_2O \leftrightarrow CO + H_2$) and the Boudouard reaction ($C + CO_2 \leftrightarrow 2CO$) (Basu, 2010c). Hydrogen content also increases with higher temperatures because oxygen preferentially reacts with carbon to form CO_2 rather than H_2 to form water (Arena, 2012). The CO_2 values observed were nevertheless comparable with the results obtained from FBG of PL (Dayananda and Sreepathi, 2013; Di Gregorio *et al*., 2014). Air was introduced at the base of the reactor as a gasification medium; however, some

air might have entered the system at the feed inlet diluting the product gas with nitrogen and oxygen.

The only trace impurity measured was NH_3, of which only 1 vol.% was detected in the gas. A larger amount of NH_3 is assumed to have dissolved in the residual tar / water emulsion. Other trace impurities containing N, S and Cl, such as HCN, H_2S and HCl should be addressed before using the product gas in gas engines or turbines. Furthermore, the application of an air pollution control system for flue gas cleaning after combustion of the product gas should be considered carefully to avoid harmful emissions such as NO_x, SO_x, dioxins and furans.

Table 3-4: Clean product gas composition [vol.%] from updraft gasification of poultry litter as a function of process conditions in comparison with previous studies

	Updraft Continuous[1]	Updraft Batch[2]	FBG Continuous[3]	FBG Batch[4]	Typical[5]
Temperature [°C]	580-680	817	700-770	800	
ER	0.13-0.17	0.34	0.32 - 0.40	0.16	
Ash [wt.%] (ar)	19.8 ± 0.3	44	25.1	34.8	
O_2	4.6-6.3				
N_2	54.9-56.2				40-50
CH_4	0.99-1.04	0.9-1.4	2.02-2.24	1.1	3-5
CO_2	18.7-19.1	3.7-11.0	19.61-21.56	22	10-15
CO	12.1-13.4	28.1-28.4	4.76-6.86	16.8	10-15
H_2	3.3-5.0	6.1-7.3	4.61-7.17	2.9	15-20
NH_3	0.9-1.1		0.1 – 0.7		
C_nH_m	1.1-1.2 (Ethylene)		0.9-1.15		
Heating value [MJ m^{-3}_N]	3.30-3.76 (HHV) 3.16-3.62 (LHV)	4.3-4.6 (HHV)	2.8 (LHV)		4-6 (HHV)

[1] Experimental data
[2] Priyadarsan et al., 2004
[3] Di Gregorio et al., 2014
[4] Dayananda and Sreepathi, 2013
[5] Typical product gas composition (McKendry, 2002)

The residual tar / water emulsion was dark grey in appearance, a mixture of water, tar, fine ash and char particles with a moisture content of 87 wt.% (ar). The ash content was 0.73 wt.% (ar) which would originate from fly ash and dust particles in the gas captured together with the tar in the scrubber units. The pH was high (9.6) compared to a typical pyrolysis oil and the nitrogen content in the emulsion was 1.2 wt.% (ar) or 9.2 wt.% (db). Most results published on the properties of PL tar originate from fast

pyrolysis experiments (Agblevor *et al*., 2010; Das *et al*., 2009; Mante and Agblevor, 2012; Monreal and Schnitzer, 2011; Schnitzer *et al*., 2007). Agblevor *et al*. (2010) measured a pH of 6.2 ± 0.1 for broiler litter biocrude oil from fast pyrolysis with a nitrogen content of 4.94-7.23 wt.% (db). In addition, they used starter turkey litter and hardwood bedding as a feedstock with biocrude oil pHs of 4.2 and 2.7 respectively. They reported a strong correlation between the wood content of the litters and the pH. Wnetrzak *et al*. (2013) observed a nitrogen content of 3.87 wt.% (ar) or 9.04 wt.% (db) and a considerably high pH value of 9.12 for the bio-liquid from the pyrolysis of the solid fraction recovered from centrifugation of anaerobically digested pig slurry. The authors attributed the high pH to the formation of low molecular weight organic bases formed due to the reaction of NH_3 with the organic species in the liquid fraction. Their results are very similar to our findings and suggest that organic species like amines found in the tar/water emulsion (Table 3-5) could be responsible for the high pH value. Alkali metals present in the tar/water emulsion could also contribute to an increase in pH; however, their concentration was not determined during the experiment.

The main organic compounds in the tar fraction were identified using gas chromatography-mass spectrometry (GC-MS) and are listed in Table 3-5. They include organic compounds which might be attractive in the chemical industry, such as phenolics and other low molecular weight (MW) compounds, while others might have the potential to be upgraded to a bio-fuel (paraffins). Monreal and Schnitzer (2011) successfully produced a colourless refined bio-oil with diesel qualities by upgrading and refining a raw pyrolytic PL bio-oil by means of extraction with n-hexane. The refined bio-oil accounted for 10 wt.% of the raw bio-oil and consisted of n-alkanes, alkenes, steroids and sterols, which were also partly identified in the gasification tar/water emulsion. Bio-oil consists of more than 500 individual compounds (Monreal and Schnitzer, 2011) and a wider suite of analytical techniques are required in order to identify the full range of molecules in the tar/water emulsion, such as ^{1}H, ^{13}C or ^{15}N nuclear magnetic resonance spectroscopy (NMR), high performance liquid chromatography (HPLC) and perhaps size exclusion chromatography (SEC) for high MW compounds. Other investigations have shown that bio-oils can be separated into phases of different polarities, one containing a high carbon content with non-polar aromatic compounds and a high calorific value, while the other containing a high nitrogen content with more aliphatic compounds

(Schnitzer *et al*., 2007; Singh *et al*., 2010). These results suggest that a separation of the tar/water emulsion into a nitrogen rich aqueous phase and carbon rich tar phase could upgrade the emulsion for use as both a fertiliser and energy feedstock respectively. To avoid the complex and expensive product gas cleaning a simple steam Rankine cycle for electricity generation has been suggested previously (Di Gregorio *et al*., 2014), where the hot product gas is sent directly to a suitable burner for complete exploitation of the energy content of the tar. The halogenated organics however are potential precursors for the formation of dioxins at higher temperatures (McKay, 2002; Tsai and Wu, 2013), which is why post combustion treatment of the gases may be required. Discussions about using gasification and pyrolysis tar as a natural pesticide are still at an early stage and need additional research.

Table 3-5: Gas chromatography-mass spectrometry (GC-MS) analysis of extracted organic compounds from the tar / water emulsion using methanol-chloroform (3:1) as a solvent. The area represents the relative peak area of the chromatogram.

Composition	**Peak Area [%]**
Normal paraffins	3.7
Iso paraffins	11.4
Cyclo paraffins	24.4
Mono aromatics	0.9
Di aromatics	3.6
Poly aromatics	1.6
Organic acids	2.4
Alcohols	8.8
Aldehydes	0.2
Amides	1.9
Amines	3.4
Esters	0.5
Indenes	2.9
Ketones	3.7
Olefins	11
Phenolics	2.9
Organo nitriles	2.6
Halogen containing organics	5.8
Oxygenates	0.8
Others	7.5

3.4.4. Poultry litter conversion to char

During auto-thermal gasification air provides thermal energy by partial ($C + 0.5\ O_2 \rightarrow CO$, -111 kJ mol^{-1}) and complete ($C + O_2 \rightarrow CO_2$, -394 kJ mol^{-1}) oxidation of the char produced from pyrolysis. This thermal energy is needed for the endothermic gasification reactions. Char gasification is the slowest of the gasification reactions and governs the overall conversion rate. The reactivity of the char varies greatly, depending on porosity, crystal structure of the carbon and catalytic effects of ash components (Higman and van der Burgt, 2007). We estimated the amount of oxygen required to provide sufficient thermal energy for gasification according to calculations by Basu (2010c). Heat is required for drying the feedstock, to raise the feedstock to the reaction temperature and drive the water-gas gasification reaction ($C + H_2O \rightarrow CO + H_2$, $+131$ kJ mol^{-1}). Furthermore, the gasifier must provide energy to compensate for the heat lost through the reactor walls. According to Basu (2010c) the amount of oxygen required was 9.7 kg h^{-1}; however, in our case, the air oxygen input to the reaction zone was only 5.0 kg h^{-1}. Taking into account the high amount of unconverted char and the low gasification performance parameters, we reason that there was only enough energy provided for pyrolysis. In fact, “auto-thermal pyrolysis” might be a more appropriate classification.

Table 3-6 presents the main chemical and physical characteristics of the BM, PL feedstock and char. The moisture content of the initial BM increased three fold after poultry production to 30.2 wt.% (ar) in PL. The 7.8 wt.% of moisture in the char was captured from the atmosphere’s humidity. The ash content of the char was almost three fold higher than the original PL due to the loss of volatile organic compounds and the relative non-volatility of the ash species. The VM content decreased from 94.1 wt.% (daf) in the feedstock to 58.6 wt.% (daf) in the char as a result of this phenomenon. The still noticeably high VM content of the char shows that some of the PL remained unconverted, indicating that the process operation could be improved to increase the gas yield. The BD increased while the HHV and LHV decreased with increasing ash content. The heating value of the PL, however, was less than the char despite the lower ash content, which is attributed to the higher moisture and lower FC content.

Table 3-6: Proximate analysis, heating values (HVV, LHV), bulk density (BD) and elemental composition of the bedding material (BM), poultry litter (PL) and char on an as received (ar), dry basis (db), or dry ash free basis (daf). Char properties are compared with the basic and premium quality grade biochar ($BC_{basic/premium}$) specified in the guidelines for the European Biochar Certificate (EBC, 2012)

Sample		BM	PL	Char	Limits[2]
Proximate analysis	Moisture [wt.%] (ar)	10.6 ± 0.1	30.2 ± 0.5	7.8 ± 0.2	
	Ash [wt.%] (db)	3.2 ± 0.2	19.8 ± 1.3	54.8 ± 3.7	
	VM [wt.%] (daf)	91.2 ± 1.6	94.1 ± 0.6	58.6 ± 2.1	
	FC [wt.%] (daf)	8.7	5.9	41.4	
Heating value	HHV [MJ kg^{-1}] (ar)	17.4 ± 0.3	12.8 ± 0.3	14.3 ± 0.2	
	LHV [MJ kg^{-1}] (ar)	16.6	11.4	13.7	
Bulk density	BD [g ml^{-1}] (ar)	62 ± 9.03	411.2 ± 11.9	501 ± 17.2	
Ultimate analysis	H [wt.%] (db)	5.9 ± 0.1	5.0 ± 0.2	1.6 ± 0.02	
	C [wt.%] (db)	46.8 ± 0.4	40.9 ± 0.8	33.1 ± 0.2	> 50
	N [wt.%] (db)	0.4 ± 0.04	4.6 ± 0.1	6.4 ± 0.03	
	S [wt.%] (db)	0.03 ± 0.003	0.47 ± 0.1	0.7 ± 0.1	
	O [wt.%] (db)	43.6 ± 0.5	29.2 ± 0.9	3.3 ± 0.4	
	P [g kg^{-1}] (db)	0.135 ± 0.009	9.12 ± 0.29	29.3 ± 1.4	
	K [g kg^{-1}] (db)	6.77 ± 0.01	33.4 ± 0.2	87.8 ± 1.8	
	Na [g kg^{-1}] (db)	0.07 ± 0.01	3.08 ± 0.08	10.4 ± 0.3	
	Ca [g kg^{-1}] (db)	1.61 ± 0.09	13.5 ± 1.1	44.1 ± 2.2	
	Cl [g kg^{-1}] (db)	0.4 ± 0.1	2.1 ± 0.2	1.2 ± 0.5	
	Mg [g kg^{-1}] (db)	0.350 ± 0.014	5.95 ± 0.21	18.3 ± 0.6	
	Fe [mg kg^{-1}] (db)	75.6 ± 8.5	933 ± 19	2389 ± 19	
	Mn [mg kg^{-1}] (db)	21.8 ± 1.1	499 ± 29	1577 ± 57	
	Zn [mg kg^{-1}] (db)	5.30 ± 0.31	412 ± 13	1229 ± 10	400/400
	Cu [mg kg^{-1}] (db)	3.09 ± 0.19	122 ± 6.5	273 ± 9	100/100
	B [mg kg^{-1}] (db)	< DL[1]	55.8 ± 2.5	148 ± 9	
	Al [mg kg^{-1}] (db)	< DL	0.32 ± 0.03	1.12 ± 0.10	
	Pb [mg kg^{-1}] (db)	< DL	0.93 ± 0.23	0.87 ± 0.16	150/120
	Cd [mg kg^{-1}] (db)	< DL	0.48 ± 0.02	1.03 ± 0.05	
	Ni [mg kg^{-1}] (db)	4.16 ± 0.88	27.3 ± 3.7	21.6 ± 1.5	50/30
	Cr [mg kg^{-1}] (db)	8.26 ± 0.57	4.61 ± 0.8	16.1 ± 3.3	90/80

[1] *detection limit*
[2] *thresholds for $BC_{basic/}BC_{premium}$ certification*

The elemental composition of the PL and char is very much in agreement with previous findings (Cantrell *et al*., 2012; Di Gregorio *et al*., 2014). Many of these elements are added to poultry feed and excreted if not fully digested (Bolan *et al*., 2010). In char these elements provide a valuable source of nutrients. Phosphorus and potassium recovery were 100 wt.% and 88 wt.% respectively. The nitrogen content is recovered by 28wt.% in the char. Even though the nitrogen would be incorporated in the aromatic char structure forming heterocyclic aromatic char compounds (Knicker, 2010), some of it might still be plant available. The PL's chlorine content was recovered by 19 wt.% in the char, the remaining chlorine most likely carried over into the gas phase. During combustion of the gases the possible dioxin and polychlorinated biphenyl (PCB) formation (McKay, 2002) could be considered a problem as discussed in section 3.4.3.

The presence of ash forming elements with respect to their predisposition to association and reactivity is perhaps the most important indicator of the propensity for ash related problems. These elements have been well investigated (Billen *et al*., 2014; Lynch *et al*., 2013b; Nzihou and Stanmore, 2013; Zevenhoven *et al*., 2012) and identified primarily as alkali elements, alkali earth metals, P, S and Cl. Priyadarsan *et al*. (2004) performed updraft gasification experiments using two feedstocks of the same ash content, but with a difference in Na and K content of 63.5 wt.% combined. The higher alkali contents led to ash agglomeration in the fuel bed and resulted in a lower peak temperature and peak-temperature propagation rate compared to the lower alkali feedstock. The PL feedstock in our experiment contained a combined Na and K content of 3.5 wt.% (db), similar to their lower concentrated fuel of 2.9 wt.% (db), whereas ash agglomeration problems were significantly more noticeable with the higher concentrated fuel containing 7.3 wt.% (db) Na and K. Di Gregorio *et al*. (2014) compared two PL batches and found a reduction of LHV_{gas}, CGE and specific energy for the batch with the higher concentrations of Ca, P and K. They also highlight the importance of these elemental species in the feedstock as being responsible for coating formation. The found Ca content of 93.2 g kg^{-1} was seven times higher than our PL, while the found K content of 14.7 g kg^{-1} was less than half of our PL. Concentrations of P were similar.

The gasification char appeared to be a mixture of uncharred PL feedstock, char, and white ash particles. The composition of the gasification char is a clear indication of

the uneven temperature distribution in the gasifier. Cold surfaces at the outer limits of the reactor resulted in unconverted or torrefied PL, while some of the PL was completely oxidised in the hottest zone, in the heart of the gasifier. Figure 3-4 depicts four SEM images of the obtained char. Images (a) and (b) show the morphological pore structure of a char particle, while image (c) and (d) present a white ash particle. A small ash particle, which was attached to the char's surface (image b, area 1), was analysed for its elemental composition using EDS (Table 3-7). The high potassium, sulphur and chlorine contents of the ash particle (Table 3-7, area 1) compared to the char surface (Table 3-7, area 2) suggests a particle composition of potassium sulphates and potassium chlorides. An average elemental composition of the char's surface is presented in Table 3-7 (area 3 and 4). The elemental composition of the white ash particle in Table 3-8 suggests a composition of calcium carbonate ($CaCO_3$), which is formed in the presence of CaO and CO_2. It has to be noted that the EDS results are qualitative only, since the interaction volume of the SEM might be larger than the particles, resulting in errors.

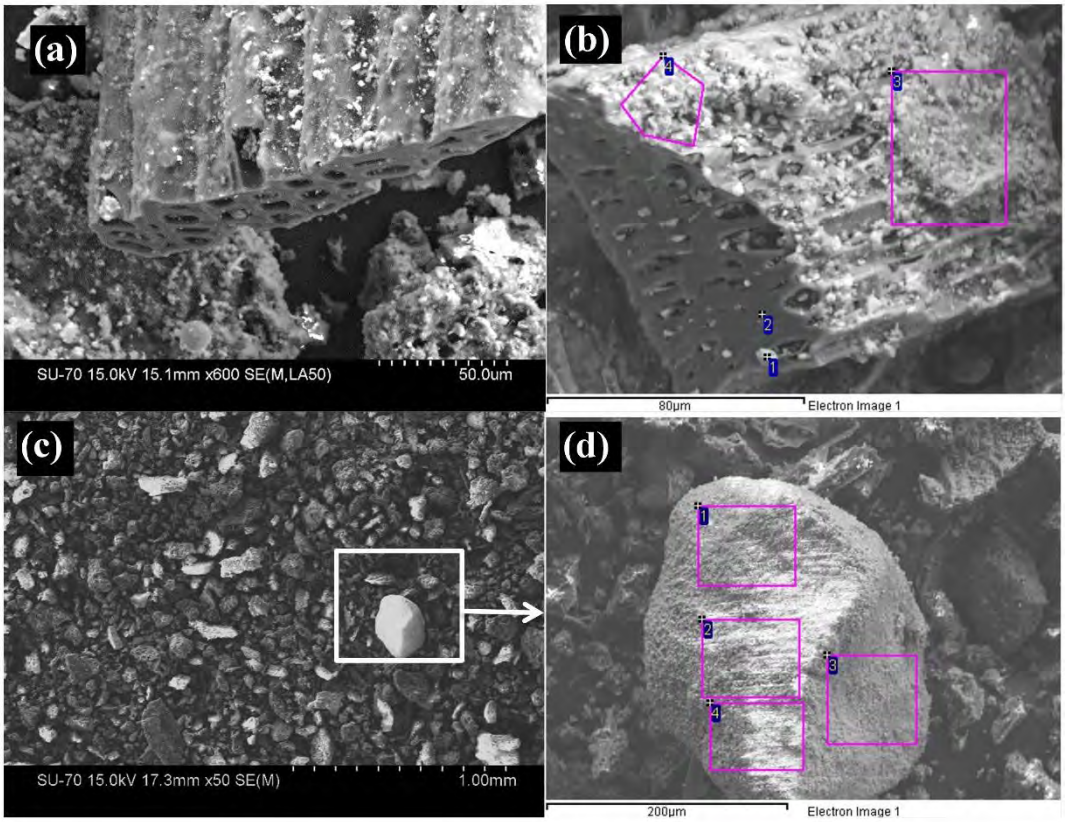

Figure 3-4: Scanning electron microscopy (SEM) images of PL char showing the porosity and structure of the char (a and b) and ash particle (c and d). The selected areas of interest in (b and d) were subject to energy dispersive spectroscopy (EDS) analysis. Image (d) is a close up of image (c).

Table 3-7: Scanning electron microscopy combined with energy dispersive spectroscopy (SEM-EDS) analysis of an ash particle (area 1), the char carbon matrix (area 2), and the surface of a char particle (area 3 and 4). The image is presented in Figure 3-4 (b).

Area	C	O	Na	Mg	Si	P	S	Cl	K	Ca	Mn	Total
	(wt.%)											
1	40	10	0.6	0.0	0.0	1.5	**3.4**	**5.5**	**39**	0.0	0.0	100
2	**85**	7.3	0.4	0.0	0.0	0.6	0.8	0.4	5.4	0.0	0.0	100
3	42	31	1.6	1.0	0.6	2.8	0.7	2.7	13	3.8	0.2	100
4	51	25	1.7	1.3	0.2	2.6	0.6	3.9	12	2.1	0.2	100

Table 3-8: Scanning electron microscopy combined with energy dispersive spectroscopy (SEM-EDS) analysis of an ash particle. The image is presented in Figure 3-4 (image d).

Area	C	O	Na	Mg	Si	P	S	Cl	K	Ca	Mn	Total
	(wt.%)											
1	12	**52**	0.2	0.5	0.2	0.4	2.3	0.3	2.2	**30**	0.0	100
2	11	**53**	0.2	0.4	0.2	0.7	1.0	0.3	1.9	**32**	0.0	100
3	17	**40**	0.3	0.5	0.2	1.3	0.8	0.5	3.7	**36**	0.0	100
4	10	**51**	0.2	0.4	0.1	0.4	0.8	0.2	1.7	**35**	0.0	100

Research into PL char is increasing and discussed as a potential biochar. Huang *et al*. (2015) performed a techno-economic analysis of an integrated pyrolysis and gasification process to produce biochar from poultry litter together with heat and power using different scenarios. Overall they conclude that the production of biochar is technically and economically feasible, however gate fees, carbon credits and renewable obligation certificates (ROC) have a significant impact on the breakeven selling price of biochar produced. Their study was based in the United Kingdom and the results may not be transferable to other countries such as the Republic of Ireland. To ensure quality based control of biochar production on a European scale, guidelines to obtain the European biochar certificate are published and now obligatory for the use of biochar in agriculture in Switzerland (EBC, 2012). The heterogeneous nature of the char obtained might make it difficult to obtain biochar certification. In fact, the carbon content of the gasification char was too low (< 50 wt.%$_{db}$) for it to be certified as a

biochar; however, it may be classified as pyrogenic carbonaceous material (PCM) and marketed as such if it could comply with all other threshold criteria. The threshold for heavy metals was not met for Zn and Cu in our case (1229 and 273 g t^{-1}), which allows maximum values of 400 g t^{-1} and 100 g t^{-1} respectively. Zn and Cu are important enzyme cofactors and are required in trace amounts in PL feed (Acamovic, 2001); however, these elements are often added in excess of the recommended daily allowance as they are difficult to absorb (Sistani and Jeffrey, 2005). In depth analysis of biochar properties, especially quantitative analysis of polycyclic aromatic hydrocarbons (PAH) and polychlorinated biphenyls (PCB), are necessary to evaluate the potential of gasification biochar and will be investigated in the future.

3.5. Conclusions

The updraft gasification process underwent a critical evaluation and analysis of the products char, tar and gas was performed. In general, the gasifier seemed suitable for on-farm application due to its simple reactor design and application. The gas composition and heating value were comparable with previous studies; however, the cold gas efficiency revealed its low conversion efficiency. This was however unavoidable due to the low operation temperature necessary for preventing agglomeration as shown by its low ash melting point. An additional consequence of the low reactor temperature was the high amount of remaining char, which was heterogeneous in nature due to the uneven bed temperature. The char exceeded the concentration limits for Zn and Cu in order for it to qualify for European biochar certification. For future research we suggest that the focus should be on obtaining, a higher quality biochar, since a certified biochar might be easier to market rather than undergoing an expensive upgrading and refining process to improve the tar quality. It should be possible to achieve this by management of the overall poultry production chain including amending the poultry feed supplements to exclude Zn and Cu, or alternatively blending of the poultry litter with dry lignocellulosic biomass prior to gasification.

3.6. Acknowledgement

Financial support for this work is gratefully acknowledged from the People Programme (Marie Curie Actions) of the European Union's Seventh Framework Programme FP7/2007-2013/ under REA grant agreement n° [289887], and from Enterprise Ireland Competence Centre for Biorefining & Bioenergy (CC/2009/1305A) and INTERREG IVB NEW REsource Innovation Network for European Waste Project number 317J-RENEW as research. Furthermore, we would like to thank Prof. M. Pilar Bernal and the Centro de Edafología y Biología Aplicada del Segura, CSIC, Campus Universitario de Espinardo, 30100, Murcia, for their contribution.

3.7. References

Acamovic, T., 2001. Commercial application of enzyme technology for poultry production. Worlds. Poult. Sci. J. 57, 225-242.

Agblevor, F.A., Beis, S., Kim, S.S., Tarrant, R., Mante, N.O., 2010. Biocrude oils from the fast pyrolysis of poultry litter and hardwood. Waste Manag. 30, 298–307.

Arena, U., 2012. Process and technological aspects of municipal solid waste gasification. A review. Waste Manag. 32, 625–39.

Basu, P., 2010a. Biomass Gasification and Pyrolysis - Practical Design. Elsevier Inc., Oxford, UK. pp.20

Basu, P., 2010b. Biomass Gasification and Pyrolysis - Practical Design. Elsevier Inc., Oxford, UK. p.75

Basu, P., 2010c. Biomass Gasification and Pyrolysis - Practical Design. Elsevier Inc., Oxford, UK. p.127

Basu, P., 2010d. Biomass Gasification and Pyrolysis - Practical Design. Elsevier Inc., Oxford, UK. p.199

Basu, P., 2010e. Biomass Gasification and Pyrolysis - Practical Design. Elsevier Inc., Oxford, UK. p.221

BHSL, 2011. Poultry Case Studies. Available at http://www.bhsl.com/poultry-home-page/case-studies/ (accessed 10.22.15).

Billen, P., Creemers, B., Costa, J., Van Caneghem, J., Vandecasteele, C., 2014. Coating and melt induced agglomeration in a poultry litter fired fluidized bed combustor. Biomass and Bioenergy 69, 71–79.

Bolan, N.S., Szogi, A.A., Chuasavathi, T., Seshadri, B., Rothrock, M.J., Panneerselvam, P., 2010. Uses and management of poultry litter. Worlds. Poult. Sci. J. 66, 673–698.

Cantrell, K.B., Hunt, P.G., Uchimiya, M., Novak, J.M., Ro, K.S., 2012. Impact of pyrolysis temperature and manure source on physicochemical characteristics of biochar. Bioresour. Technol. 107, 419–428.

Coloma, A., 2005. Treatment of Poultry Litter by Screening. M.Sc. Thesis, Clemson University, Clemson, SC.

Comission Regulation (EU) No 592/2014 of 3 June 2014.

Das, D.D., Schnitzer, M.I., Monreal, C.M., Mayer, P., 2009. Chemical composition of acid-base fractions separated from biooil derived by fast pyrolysis of chicken manure. Bioresour. Technol. 100, 6524–6532.

Dayananda, B.S., Sreepathi, L.K., 2013. A Study on Gasification of Chicken Litter with Saw Dust in A Laboratory Scale Fluidized Bed Gasifier. Int. J. Innov. Res. Sci. Eng. Technol. 2, 3901–3907.

De Vries, J.W., Groenestein, C.M., De Boer, I.J.M., 2012. Environmental consequences of processing manure to produce mineral fertilizer and bio-energy. J. Environ. Manage. 102, 173–183.

Di Blasi, C., 2009. Combustion and gasification rates of lignocellulosic chars. Prog. Energy Combust. Sci. 35, 121–140.

Di Gregorio, F., Santoro, D., Arena, U., 2014. The effect of ash composition on gasification of poultry wastes in a fluidized bed reactor. Waste Manag. Res. 32, 323–330.

EBC (2012) 'European Biochar Certificate - Guidelines for a Sustainable Production of Biochar.' European Biochar Foundation (EBC), Arbaz, Switzerland. http://www.europeanbiochar.org/en/download. Version 6.1 of 19th June 2015

ECN Phyllis 2, 2015. Available at https://www.ecn.nl/phyllis2/Home/Help (accessed 10.22.15).

Fairchild, B., Czarick, M., 2011. Poultry Housing Tips. Univ. Georg. Coll. Agric. Environ. Sci. 23.

FAO, 2015. Environment Statistics - The Food and Agriculture Organization of the United Nations. Available at http://www.fao.org/economic/ess/environment/en/ (accessed 10.22.15).

Font Palma, C., Martin, A.D., 2013a. Inorganic constituents formed during small-scale gasification of poultry litter: A model based study. Fuel Process. Technol. 116, 300–307.

Font Palma, C., Martin, A.D., 2013b. Model based evaluation of six energy integration schemes applied to a small-scale gasification process for power generation. Biomass and Bioenergy 54, 201–210.

Higman, C., van der Burgt, M., 2007. Gasification, 2nd ed. Elsevier. p.38

Huang, Y., Anderson, M., McIlveen-Wright, D., Lyons, G.A., McRoberts, W.C., Wang, Y.D., Roskilly, A.P., Hewitt, N.J., 2015. Biochar and renewable energy generation from poultry litter waste: A technical and economic analysis based on computational simulations. Appl. Energy 1–8.

Joseph, P., Tretsiakova-McNally, S., McKenna, S., 2012. Characterization of cellulosic wastes and gasification products from chicken farms. Waste Manag. 32, 701–709.

Knicker, H., 2010. "Black nitrogen" – an important fraction in determining the recalcitrance of charcoal. Org. Geochem. 41, 947–950.

Lee, U., Balu, E., Chung, J.N., 2013. An experimental evaluation of an integrated biomass gasification and power generation system for distributed power applications. Appl. Energy 101, 699–708.

Lynch, D., Henihan, A.M., Bowen, B., Lynch, D., McDonnell, K., Kwapinski, W., Leahy, J.J., 2013a. Utilisation of poultry litter as an energy feedstock. Biomass and Bioenergy 49, 197–204.

Lynch, D., Henihan, A.M., Kwapinski, W., Zhang, L., Leahy, J.J., 2013b. Ash Agglomeration and Deposition during Combustion of Poultry Litter in a Bubbling Fluidized-Bed Combustor. Energy & Fuels 27, 4684–4694.

MacLeod, M., Gerber, P., Mottet, A., Tempio, G., Falcucci, A., Opio, C., Vellinga, T., Henderson, B., Steinfeld, H., 2013. Greenhouse gas emissions from pig and chicken supply chains – A global life cycle assessment. Food and Agriculture Organization of the United Nations (FAO), Rome.

Mante, O.D., Agblevor, F.A., 2012. Storage stability of biocrude oils from fast pyrolysis of poultry litter. Waste Manag. 32, 67–76.

McKay, G., 2002. Dioxin characterisation, formation and minimisation during municipal solid waste (MSW) incineration: review. Chem. Eng. J. 86, 343–368.

McKendry, P., 2002. Energy production from biomass (Part 3): Gasification technologies. Bioresour. Technol. 83, 55–63.

Miles, D.M., Rowe, D.E., Cathcart, T.C., 2011. High litter moisture content suppresses litter ammonia volatilization. Poult. Sci. 90, 1397–1405.

Monreal, C.M., Schnitzer, M., 2011. Production of a refined biooil derived by fast pyrolysis of chicken manure with chemical and physical characteristics close to those of fossil fuels. J. Environ. Sci. Health. B. 46, 630–637.

Nzihou, A., Stanmore, B., 2013. The fate of heavy metals during combustion and gasification of contaminated biomass - a brief review. J. Hazard. Mater. 256-257, 56–66.

Priyadarsan, S., Annamalai, K., Sweeten, J.M., Mukhtar, S., Holtzapple, M.T., 2004. Fixed-bed gasification of feedlot manure and poultry litter biomass. Am. Soc. Agric. Eng. 47, 1689–1696.

Schnitzer, M.I., Monreal, C.M., Facey, G.A., Fransham, P.B., 2007. The conversion of chicken manure to biooil by fast pyrolysis I. Analyses of chicken manure, biooils and char by ^{13}C and ^{1}H NMR and FTIR spectrophotometry. J. Environ. Sci. Health. B. 42, 71–7.

SEI (Sustainable Energy Ireland): Biomass Factsheet - Renewable Energy Information Office (REIO) Available at http://www.seai.ie/uploadedfiles/RenewableEnergy/REIOBiomassFactsheet.pdf (accessed 10.22.15).

Singh, K., Risse, L.M., Das, K.C., Worley, J., Thompson, S., 2010. Effect of Fractionation and Pyrolysis on Fuel Properties of Poultry Litter. J. Air Waste Manage. Assoc. 60, 875–883.

Singh, K., Risse, M., Worley, J., Das, K.C., Thompson, S., 2008. Effect of fractionation on fuel properties of poultry litter. Am. Soc. Agric. Biol. Eng. 60, 875–883.

Sistani, K., Jeffrey, N., 2005. Trace Metal Accumulation, Movement, and Remmediation in Soils Receiving Animal Manure. In Prasad, M.N.V, Sajwan, K.S., Naidu, R., (eds.) Trace Elements in the Environment (Biogeochemistry, Biotechnology, and Bioremdiation). CRC Press.

Tsai, W.-T., Wu, P.-H., 2013. Environmental Concerns About Carcinogenic Air Toxics Produced from Waste Woods as Alternative Energy Sources. Energy Sources, Part A Recover. Util. Environ. Eff. 35, 725–732.

Wnetrzak, R., Kwapinski, W., Peters, K., Sommer, S.G., Jensen, L.S., Leahy, J.J., 2013. The influence of the pig manure separation system on the energy production potentials. Bioresour. Technol. 136, 502–508.

Zevenhoven, M., Yrjas, P., Skrifvars, B.-J., Hupa, M., 2012. Characterization of Ash-Forming Matter in Various Solid Fuels by Selective Leaching and Its Implications for Fluidized-Bed Combustion. Energy & Fuels 26, 6366–6386.

4. Manure Biochar as a Means for Closing Nutrient Cycles in Agriculture

The content of this chapter will be submitted to the Elsevier journal Chemosphere by N.C. Taupe, C. Dela Piccolla, A. Santos, M.P. Bernal, W. Kwapinski, M.H.B. Hayes, J.J. Leahy.

This study aims to provide a cradle to cradle perspective on recycling nutrients from dehydrated animal manure by producing biochar.

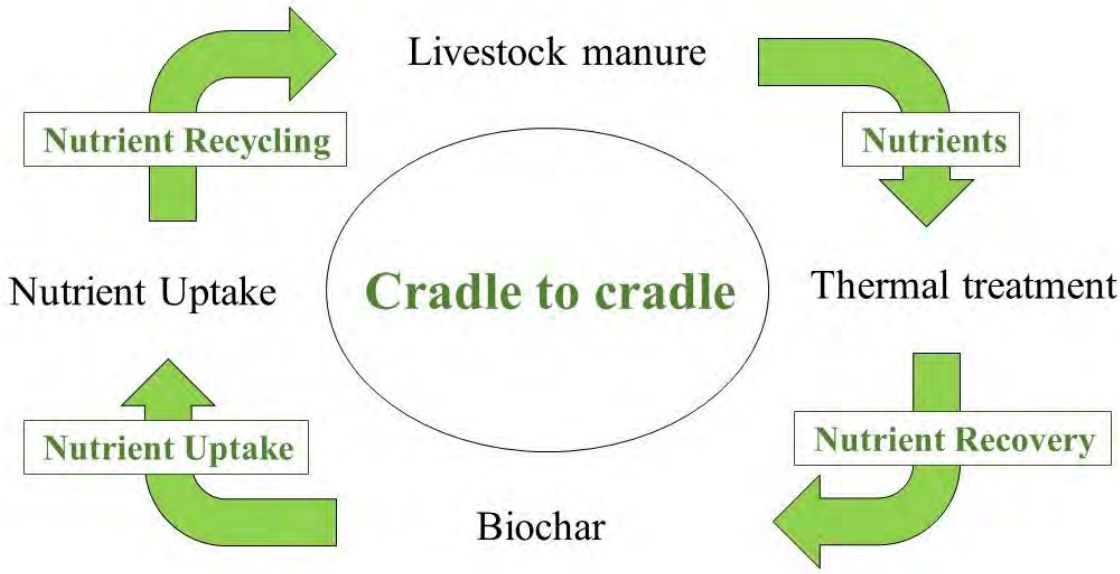

4.1. Abstract

Animal manure is giving rise to several environmental problems in areas of intensive livestock production. Thermal treatment of dehydrated manure feedstocks provides benefits as a waste treatment option, such as the elimination of pathogens, significant reduction of waste by weight and volume, and consecutive concentration of nutrients in the solid residue. This study aims to provide a cradle to cradle perspective on recycling nutrients from dehydrated animal manure by producing biochar by updraft gasification and/or slow pyrolysis. The study encompassed a detailed analysis of the biochars' physicochemical properties, including recovery rates of nutrients and heavy metals (HM), as well as pot trials to determine nutrient uptake and plant growth of lettuce (*Lactuca sativa)*. The results revealed that most macro- and micronutrient were recovered to > 90% in the biochars with the exception of N (28% - 54%), and S (37% - 62%). Recoveries of some HM were low, for example Pb (12% - 31%), and Ni (21% - 28%), and this demonstrates an advantage with regard to soil application. Nitrogen, P, K concentrations in biochar generally exhibited highly significant ($p < 0.01$) correlation on the accumulation of these nutrients in lettuce for all treatments. Overall, nutrient uptake to lettuce was highest for poultry litter (PL), followed by swine manure (SM) and cow manure (CM) biochars when applied to soil at a rate of 2 wt.%. Biochars produced by slow pyrolysis of PL exhibited a higher nutrient uptake than biochar produced from updraft gasification of PL with the exception of P and K uptake, which were not significantly affected by process type. Furthermore, biochars produced at 400 °C resulted in higher nutrient uptake efficiencies and HM accumulation in lettuce than biochars produced at 600 °C. Other results highlight the importance of careful selection of process conditions for biochar production. The results of this study might offer useful data on thermal treatment of animal manure for future modelling work and life cycle assessment.

4.2. Introduction

Over application of animal manure onto agricultural land to improve soil fertility and to dispose of accumulating waste causes several environmental problems; these include bad odours, introduction of pathogens, water eutrophication through leaching of nitrate and phosphate to surface water, volatilisation of ammonia, and emissions of greenhouse gases (De Vries *et al*., 2012; Prapaspongsa *et al*., 2010). This common practice is not sustainable in the long term and therefore systematic changes throughout the manure management chain are being investigated (Hou *et al*., 2014). These include manure treatment for improved nutrient use efficiency and energy recovery. Within the European Union (EU) these changes must operate within the framework of the Nitrates Directive (01/676/EEC; EC, 1991) and the Water Framework Directive (2000/60/EC; EC 2000).

Thermo-chemical conversion of animal manure has several advantages as a treatment option, including a significant reduction of waste in mass and volume, the eliminating of pathogens and malodour compounds, and reduced harmful emissions from anaerobic decomposition (Arena, 2012). Combustion is the most developed and frequently used technology. However, a high alkali metal content in the biomass ash can result in agglomeration and operational problems at high temperatures (Lynch *et al*., 2013). Compared to woody biomasses, manure contains a high ash content which makes low temperature operation appropriate. Gasification (550 °C - 900°C) and pyrolysis (380 °C – 600 °C) operate at relatively low temperatures compared to combustion (850 °C - 1200 °C) under sub stoichiometric oxygen or a totally inert environment respectively (McKendry, 2002) and may be good alternatives to combustion. The high and constantly varying moisture content in animal manure, however, may pose a challenge for thermal treatment at low temperatures, as a high moisture content delays combustion and causes the furnace temperature to decrease. Low operating temperature further delays combustion and decreases the furnace temperature eventually leading to operational failure (Orang and Tran, 2015). A previous study showed how a high moisture content in manure negatively affects the energy balance during pyrolysis (Wnetrzak *et al*., 2013). Nevertheless, the investigation presented in chapter 3 showed that auto-thermal updraft gasification of PL at temperatures below the ash melting point (639 °C) is a reliable process, producing a low calorific value gas, with a tar and char residue.

During pyrolysis the manure undergoes dehydration and de-volatilisation of its volatile organic compounds, leaving a char residue concentrated with ash and highly stable carbon. When applied to soil, the carbon contributes to the soil organic matter depending on immobilisation and aging processes. The ash is composed of valuable nutrients and heavy metals (HM), which can be phytotoxic at elevated concentrations (He *et al*., 2005; Islam *et al*., 2007). Plants that grow in metal-polluted soils exhibit metal accumulation, altered metabolism, and lower biomass production (Nagajyoti *et al*., 2010). Nutrient recovery in the residue is of big concern (Wise *et al*., 2009; Prapaspongsa *et al*., 2010), in particular N and S, as these are lost when exposed to high temperatures (Lang *et al*., 2005). Furthermore, the behaviour of the nutrients and of the HM once applied to soil is of importance (Verheijen *et al*., 2010; Prendergast-Miller *et al*., 2014). The total nutrient content may not reflect nutrient availability. Availability of nutrients in biochar amended soils depends on the applied pyrolysis process conditions (e.g. maximum temperature), the chemical state of the element, crop demands and the soil properties (Lehmann and Joseph, 2009). The nutrient availability determines nutrient uptake by crops used for human consumption or animal feed thereby closing the nutrient cycle.

Literature is scarce on chars produced by gasification; hence one objective of this study was to compare two different thermal treatment technologies (slow pyrolysis and updraft gasification) using poultry litter (PL) as a feedstock to obtain a nutrient rich biochar for crop growth enhancement. The second objective was to evaluate three manure types, namely PL, cow manure (CM) and swine manure (SM), as feedstocks for biochar production via slow pyrolysis at two maximum pyrolysis temperatures (400 °C and 600 °C). The first part of the chapter focuses on the physical and chemical characteristics of the obtained chars to investigate the influence of feedstock type, treatment technology and process conditions on char formation and energy and nutrient recovery. The second part discusses the influence of char application to soils on plant yield response and nutrient and HM uptake. We hypothesised that process type and operating conditions significantly influence char properties. Furthermore, we believe that manure biochars improve plant growth and nutrient uptake depending on the direct supply of nutrients to the soils and indirect effects such as liming.

4.3. Methodology

4.3.1. Feedstock sampling and biochar production

Poultry litter was obtained from the storage shed of a broiler farm in County Monaghan, Ireland. The standard procedure for sampling from stock piles, according to BS EN 14778 (2011), was followed. A more detailed description of the PL sampling procedure, bedding material used in the poultry sheds, and the updraft gasification process used to produce PLgas can be found in chapter 3 (section 3.3.1). Cow manure was sampled from pasture grazed suckler cows. On the day of sampling, the manure samples were analysed for their moisture content as received (ar). The samples were air-dried for two days and subsequently oven dried at 60 °C. Biochars were produced by means of slow pyrolysis in batch mode to maximum temperatures of 400 °C and 600 °C, with a heating rate of 20 °C min^{-1} and a residence time of 1 h after reaching maximum temperature. The pyrolysis container was cylindrical with a total volume of 1000 ml. Air was present in the system initially, but as the volatile vapours were emitted the air was displaced and pyrolysis took place. Swine manure biochars (SM_{BC}) were provided from the Energy Research Centre of the Netherlands (ECN), where the solid fraction of digested SM dried at 40 °C was used as a feedstock. The SM_{BC} were produced continuously at 400 °C and 600 °C with a residence time of 30 min in a slow pyrolysis reactor (auger pyrolysis unit called Pyromaat), an indirectly heated screw conveyer reactor.

4.3.2. Feedstock and biochar characterisation

Proximate analysis, including moisture, ash and volatile matter (VM) content, was carried out according to BS EN 14774-1, I.S. EN 14775:2009, and I.S. EN 15148:2009. The fixed carbon (FC) content was then calculated by difference. Ultimate analysis (CHNS+O) was carried out by means of an Elementar Vario EL Cube analyser. Total nutrients and HM concentrations were quantified using inductively coupled plasma optical emission spectrometry (ICP-OES, Thermo Elemental Co. Iris Intrepid II XDL). For the ICP-OES analysis, 0.1 g of milled manure feedstock was digested in 2 ml H_2O_2 and 8 ml HNO_3 in a microwave digester. The biochars were ashed at 500 °C for 8 h according to the modified dry ash method by Enders *et al*. (2012) prior to digestion in 3 ml HNO_3 and 9 ml HCl. The samples were

filtered and diluted to 25 ml with ultrapure water. Biochar available phosphorus was extracted with 2% formic acid and determined by UV/VIS spectroscopy following the procedure by Wang *et al*. (2012).

The higher heating value (HHV) was determined using an oxygen bomb calorimeter 6200 No. 442 M from Parr instruments Company. The HHV and lower heating value (LHV) of the solids in their different states were calculated according to ECN Phyllis 2, (2015) (equation 4.1 – 4.3), where MC = moisture content in the sample.

$HHV_{ar} = HHV_{dry}$ x (1- MC/100) *equation 4.1*

$LHV_{dry} = HHV_{dry}$ - 2.442 x 8.936 x H/100 *equation 4.2*

$LHV_{ar} = HHV_{ar}$ - 2.442 x (8.936 x H/100 x (1 - MC/100) + MC/100) *equ. 4.3*

The elemental recoveries (R) were calculated as the product of the ratio of their concentration in char and feedstock (C_C/C_f), and the char yield (equation 4.4). The char yields (Y_c) are expressed as a percentage ratio of char mass divided by feedstock mass (m_c/m_f).

$$R = (C_C/C_f)*Y_c \qquad \textit{equation 4.4}$$

Water leaching of HMs was performed by weighing approximately 3 g of finely ground char or manure feedstock (± 0.001 g) into a beaker containing 50 ml of distilled water. Iron, Mn, Zn, and Cu were quantified in the leachate with flame assisted atomic absorption spectroscopy (FA-AAS) using a Varian Spectra AA-220.

The multipoint Brunauer-Emmett-Teller - N_2 surface area (BET-N_2 SA) of the biochar samples was analysed by means of a Gemini 2375 V5.01 surface area analyser (Micromeritics Instrument Co., USA). The bulk density was determined using a modified version of the standard procedure ISO/TC 238 WG 4, using a 100 ml cylinder. The pH values of the biochars were measured in a 0.01 M $CaCl_2$ solution (1 wt.%) after shaking for 2 h at 100 rpm using an Orion 420 pH meter. The results are expressed as the average of three measurements.

Scanning electron microscopy (SEM) combined with energy dispersive spectroscopy (EDS) was used to analyse the composition and morphology of the PL char. The PL char was crushed, placed onto carbon tabs, and coated with gold to mitigate charging.

The analysis was carried out using an Ultra-High-Resolution Analytical FE- SEM SU- 70 (Hitachi), and a Large Area EDS Silicon Drift Detector, (Oxford Instruments) equipped with INCA software. The accelerating voltage was 15.0 kV and the working distance for the EDS analysis was 15 mm.

Fourier transform infrared (FTIR) spectra were obtained using an Agilent Cary 630 FTIR Spectrometer. Solid-state ^{13}C NMR experiments were carried out using a VARIAN INOVA spectrometer at ^{13}C and ^{1}H frequencies of 100.5 and 400.0 MHz, respectively. The techniques used were variable amplitude cross-polarization (VACP); chemical shift anisotropy (CSA) with total suppression of spinning side bands (TOSS); and recoupled dipolar dephasing (DD) experiments. A JACKOB-SEN 5 mm magic-angle spinning double-resonance probe head was used for (VACP) experiments at spinning frequencies of 13 kHz. Typical CP times of 1 ms, acquisition times of 13 ms, and recycle delays of 500 ms were used. The CP time was chosen after variable contact time experiments, and the recycle delays in CP experiments were chosen to be five times longer than the longest ^{1}H spin–lattice relaxation time (T_{1H}) as determined by inversion-recovery experiments.

The CEC of biochar was evaluated based on the replacement of Na^+ with NH_4^+, using the method from Uzoma *et al*. (2011). Biochar (1.0 ± 0.01) was weighed into a centrifuge tube; 20 ml of sodium acetate solution (1.0 M) was added, and shaken for 1 h at 16 rpm to saturate the exchange sites. The biochar solution was transferred to a solid phase extraction column with cotton wool and leached another two times with 20 ml of the same sodium acetate solution. The excess sodium acetate was then removed by leaching slowly with 30 ml of ethanol (96%) and repeated three to four times until the solution reached a conductivity of < 40 µS cm^{-1}. Ammonium acetate solution (30 ml, 1.0 M) was added to the column to replace the adsorbed Na^+ and the leaching process was repeated three times. The extract was transferred to a 100 ml flask and filled to the mark with ammonium acetate solution (1.0 M). The extracts were stored in a fridge until analysed for Na content using FA-AAS. The feedstocks were analysed based on the same method with slight modifications. The feedstocks (1.0 ± 0.01 g) were mixed well with activated carbon (2.0 ± 0.01 g) before adding 20 ml of sodium acetate solution (1.0 M) and the leaching steps were carried out by vacuum filtration through an ash-less quantitative filter paper (DP 5895 110).

4.3.3. Plant growth experimental setup

For each treatment air dried soil (350 g) was mixed well with 7 g of char (approximately 2 wt.%). The soil-char mixture was transferred to a pot, which was sealed at the base with a plastic bag. The treatments were replicated five times and arranged in a completely randomised design in a naturally lighted glasshouse. Three to four lettuce seeds (*Lactuca sativa)* were placed on the surface of the soil and gently pushed to a depth of about 2 cm. Throughout the experiment the soil moisture was maintained at 70 wt.% of maximum water holding capacity (WHC) (procedure in section 4.3.4) by weighing the pots every two to three days and replenishing the water lost. First germination occurred after seven to eight days. The seedlings were thinned down to one per pot after 20 days. The plants were harvested after six weeks. The leaves were washed with distilled water, dried in paper bags for 2 days at 60 °C and weighed (± 0.001 g). The samples were stored in a freezer at -20 °C before further analysis.

4.3.4. Soil and plant analysis

Two soils were used in this experiment, namely soil 1 (loam soil) and soil 2 (sandy loam soil). The soils' taxonomy (sand, silt, and clay content) was determined according to Reeuwijk (2002). The soils were ground finely and analysed for their carbon and nitrogen content using an Elementar Vario EL Cube analyser. The maximum WHC was measured gravimetrically according to Ahn *et al*. (2009). The pH was determined in the same way as the biochar samples (section 4.3.2). For analysis of the CEC the soils (4.0 ± 0.01 g) were shaken for 5 min at 16 rpm in 30 ml of a sodium acetate solution (1.0 M) and centrifuged at 7400 rpm for 5 min followed by the procedure outlined in section 4.3.2.

The total elemental composition of the soils was determined following the procedure for biochars and the plants' elemental composition was quantified following the procedure for manure feedstocks outlined in section 4.3.2 for three replicates. The total nutrient accumulation by plants (mg pot^{-1}) was calculated as the product of the nutrient concentration (mg g^{-1}) and the lettuce dry yield (g). Nutrient uptake efficiency (UE) was calculated according to equation 4.5.

$$UE = \frac{NU_t - NU_c}{N_{BC}}$$ *equation 4.5*

where,

NU_t Nutrient uptake (mg pot^{-1}) to lettuce for BC treated soils

NU_c Nutrient uptake (mg pot^{-1}) to lettuce for the control soil

N_{BC} Nutrient supplied to the soil with biochar

4.3.5. Statistical analysis

All results on dry biomass yield, nutrient concentration, and nutrient uptake for lettuce from different biochar treatments of soil were analysed using a one-way ANOVA (IBM SPSS statistics22). A Shapiro-Wilk's test ($p > 0.05$) showed that the results were approximately normally distributed. The results were tested for homoscedasticity using the Leven's test. The data violating the model assumption were logarithmically transformed before analysed by ANOVA. A Tukey's HSD post-hoc test was applied for pairwise comparison to assess significant differences ($p < 0.05$) between treatment means. Contrasts of the means were used to test the effects biochar feedstock, process type and pyrolysis temperature on nutrient uptake. A Pearson bivariate correlation analysis was performed to assess the correlation of the biochar and soil properties with grass yield and nutrient uptake.

4.4. Results and Discussion

4.4.1. Feedstock and biochar characteristics

The physico-chemical properties of the manure feedstocks and biochars (Table 4-1) provide information about the degree of carbonisation from pyrolysis and gasification and furthermore are important characteristics for soil amelioration and crop growth.

The moisture contents of the biochars varied according to their different hygroscopic properties. Biochars produced at 600 °C (BC600) were expected to be more hydrophobic than biochars produces at 400 °C (BC400) due to the loss of labile aliphatic compounds with increasing temperatures, which also reflects the results of the polarity index (Table 4-1). Cow manure biochars (CM_{BC}) and SM biochars (SM_{BC}) confirmed this assumption, while the opposite was the case for PL biochars (PL_{BC}). This suggests that physical interactions of water vapour with biochar compounds other than the organic matrix may take place, for instance the contribution of the ash content might be considerable. PLgas possessed the highest hygroscopic moisture of all PL_{BC} and the highest ash content. A significant correlations existed between moisture and VM contents ($n = 10$, $p < 0.01$, $r = 0.90$), but not between ash and moisture.

Release of VM with increasing pyrolysis temperature resulted in a simultaneous increase in the relative ash and FC contents. PL_{BC} and SM_{BC} had similar ash contents, and CM_{BC} contained about two thirds of these amounts. The VM and FC contents are also expressed on a dry and ash free basis (daf), in order to estimate the extent of carbonisation of the organic matter under different process conditions. The samples SM_{BC} and CM_{BC} had similar proportions of VM_{daf} and FC_{daf} suggesting similar carbonisation behaviours; however, PL_{BC} showed a higher proportion of VM_{daf} and lower proportion of FC_{daf} indicating lower carbonisation. A direct comparison of PL and CM can be made as the process conditions were the same. The decrease in VM_{daf} for PL when pyrolysing at 400 °C (30.2 wt.%) was smaller than for CM (53.2 wt.%). Pyrolysis at 600 °C resulted in a VM_{daf} loss of 63.7 wt.% and 75.5 wt.% for PL and CM, respectively. This observation might be attributed to the higher bulk density of the PL compared to CM (Table 4-1) which would have influenced convection within the pores. It has previously been suggested that particle density can be used to estimate the charring temperature (Brewer *et al*., 2009). Hence a higher maximum temperature

or longer residence time should be considered for PL feedstocks, although the maximum temperature has been shown to be more important than residence time in determining the chemical nature of chars (Brewer *et al*., 2011; Cimò *et al*., 2014). It should also be noted that biochar contains both primary and secondary char derived from the deposition of organic vapours (tars) onto the solid. A low gas flow (as was the case for PL and CM in the batch pyrolysis reactor) increases the interaction of reactive VM with the solid residue and produces additional char (Antal and Grønli, 2003).

PLgas had the highest ash content of all PL_{BC}. The FC_{daf} content was an intermediate between PL400 and PL600 presumably because the VM_{daf} loss during updraft gasification (35.5 wt.%) was lower than pyrolysis at 600 °C (63.7 wt.%) but higher than 400 °C (30.2 wt.%). The sample PLgas was heterogeneous in nature compared to PL400 and PL600; and as the PL feedstock was partially combusted to supply heat for the auto-thermal gasification process, small white ash particles were present in the char. Furthermore, some of the PL feedstock was incompletely carbonised due to the uneven temperature distribution in the updraft gasification reactor as described in chapter 3. Fluidised bed gasification might produce a more homogenous char as a result of improved mass and energy transfer within the bed and subsequently uniform heat distribution.

Table 4-1: Physico-chemical properties of the bedding material used in the poultry sheds, manure feedstocks and biochar samples

Samples[1]	MC	Ash	VM	FC	VM	FC	C[2]	C:N	(O+N)/C	BD	SA	pH	CEC
	(wt.%$_{ar}$)	(wt.%$_{db}$)			(wt.%$_{daf}$)		(wt.%$_{db}$)		polarity	(g ml^{-1})	(m^2 g^{-1})		(mmol$_c$ kg^{-1})
BM	10.6 ± 0.1	3.2 ± 0.2	88.4	8.4	91.2	8.7	46.8 ± 0.4	ND	0.71	62 ± 9.0	ND	ND	ND
PL	9.9 ± 0.1	19.8 ± 1.3	75.5	4.7	94.1	5.9	40.9 ± 0.8	8.9	0.62	411 ± 12	3.7	6.89	70.2 ± 5.3
PL400	4.8 ± 0.2	28.8 ± 0.8	45.5	25.7	63.9	36.1	47.2 ± 0.8	8.6	0.31	407 ± 10	5.5	7.53	70.3 ± 3.2
PL600	5.9 ± 0.3	41.9 ± 1.1	17.7	40.4	30.4	69.6	48.5 ± 2.2	11.5	0.12	453 ± 5.9	7.4	10.77	39.7 ± 4.9
PLgas	7.8 ± 0.2	54.8 ± 3.4	26.5	18.7	58.6	41.4	42.4 ± 0.2	9.9	0.23	501 ± 7.0	6.7	11.35	75.1 ± 2.9
CM	10.2 ± 0.8	9.08 ± 0.8	83.3	6.6	92.7	7.4	48.3 ± 0.4	28.4	0.60	108 ± 8.1	4.1	6.08	53.2 ± 2.8
CM400	5.6 ± 0.2	21.9 ± 1.4	30.8	47.3	39.5	60.5	58.1 ± 0.7	24.2	0.19	139 ± 1.0	11.7	7.61	52.1 ± 5.0
CM600	4.5 ± 0.1	27.2 ± 2.2	12.5	60.3	17.2	82.8	67.5 ± 0.2	32.1	0.07	153 ± 8.2	25.7	9.88	11.2 ± 0.5
SM	ND	ND	ND	ND	ND	ND	ND	ND	ND	ND	ND	ND	ND
SM400	5.4 ± 0.1	32.5 ± 0.2	24.5	43.0	36.3	63.7	52.2 ± 3.3	20.9	0.16	283 ± 6.3	5.1	8.98	91.4 ± 3.2
SM600	3.7 ± 0.02	40.4 ± 0.4	11.0	48.6	18.4	81.6	57.9 ± 1.3	32.2	0.07	300 ± 6.9	13.2	9.88	36.3 ± 5.8

Abbreviations: BM = bedding material, PL = poultry litter, PLgas = biochar from updraft gasification of PL, CM = cow manure, SM = swine manure, MC = moisture content, VM = volatile matter, FC = fixed carbon, BD = bulk density, SA = Multipoint Brunauer-Emmett-Teller - N_2 (BET-N_2) surface area, CEC = cation exchange capacity, ar = as received, db = dry basis, daf = dry ash free basis, ND = not determined

[1] Letters refer to manure feedstock and numbers refer to maximum pyrolysis temperature (°C)

[2] Total

The Van Krevelen Diagram plots the molar H:C ratio against the O:C ratio to evaluate the transformation of the complex biomass structure into a more stable aromatic structure arising from H and O losses. The diagram (Figure 4-1) clearly shows that lower carbonisation occurred for PL400 compared to CM400 and SM400 products. Again, this could be explained by the lower charring efficiency of the higher density PL feedstock and the mass loading into the reactor, which influence the heat and mass transfer during pyrolysis. Budai *et al*. (2013) recommended a H:C_{org} limit of 0.7 (or H:C limit of 0.6) to distinguish between "somewhat thermochemically altered" and "thermochemically converted" biomasses. The thermochemically converted chars have a proportion of fused aromatic ring structures high enough to contribute to carbon sequestration. All the biochars, except PL400, are close to or below the 0.6 threshold. The general agreement is that biochars produced at 600 °C are more suitable for carbon sequestration. The properties of gasification chars are likely to change according to the process type, e.g. fluidised bed as opposed to fixed bed, and this requires further investigation.

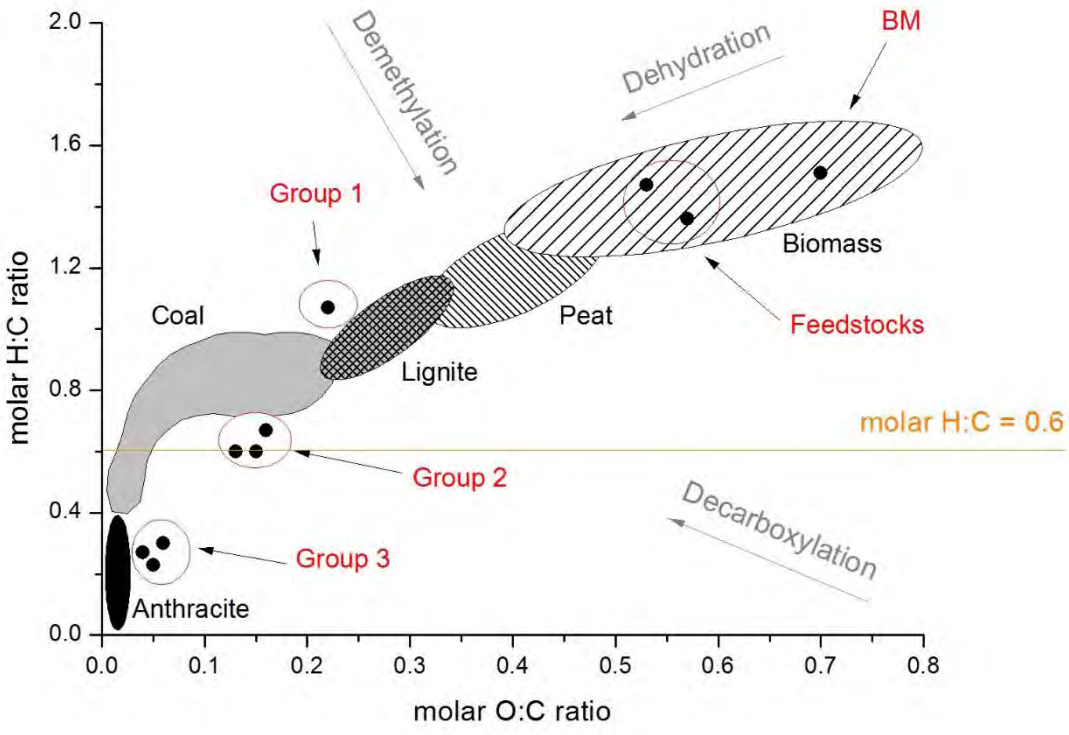

Figure 4-1: Van Krevelen diagram: Feedstocks (PL and CM), Group 1 (PL400) Group 2 (CM400, SM400, PLgas), Group 3 (PL600, CM600, SM600). Abbreviations same as in Table 4-1.

The FTIR spectra (Figure 4-2) provided information about the functional group chemistry and helped to understand the behaviour of these groups during pyrolysis and gasification. Overlapping of inorganic and of organic vibration signals was expected due to the heterogeneous nature of the samples. Identification of functional groups was based on the assignments provided in Cantrell *et al*. (2012) and Coates (2000). The broad band at about 3242 cm^{-1} was associated with the stretching vibration of hydrogen bonded hydroxyl (O-H) and was found mainly in the feedstocks with higher moisture content. Aliphatic functional groups were present in the feedstocks as shown by the C-H stretching vibration at 2925 cm^{-1} (asymmetric) and 2854 cm^{-1} (symmetric). These bands disappeared for CM400, but not PL400 and SM400, which suggests that carbonisation was more complete for CM400. A sharp N-C=O stretching band associated with the carbonyl stretching vibration in peptide bonds was observed for PL at 1629 cm^{-1} and to a lesser extent in CM. The signal decreased for BC400 and was hardly noticeable for BC600 and PLgas. The sharp signal at 1402 cm^{-1} suggests - CH_3 bending of trimethyl bonds in the feedstocks, however for the biochar samples the signal is more likely to be attributed to mineral species. The sharp band at 1324 cm^{-1} could be associated with the O-H bending vibration in phenolic compounds, as these would have been lost with increasing pyrolysis temperature and are therefore not visible in BC600 and PLgas. The intense peak at 1007 cm^{-1} also decreased during pyrolysis and is attributed to the C-O stretching vibration of carbohydrates, such as cellulose, hemicellulose and the methoxy groups of lignin. However, for BC600 and PLgas asymmetric and symmetric stretching of PO_2 and $P(OH)_2$ in phosphates between 1100 cm^{-1} and 950 cm^{-1} is more likely, as the decomposition temperature of hemicellulose and cellulose lies below 400 °C and the decomposition temperature of lignin below 600 °C (McKendry, 2002). The sharp signal at 1402 cm^{-1} and the signal at 877 cm^{-1} might be attributed to inorganic species, for example carbonate ions for the latter.

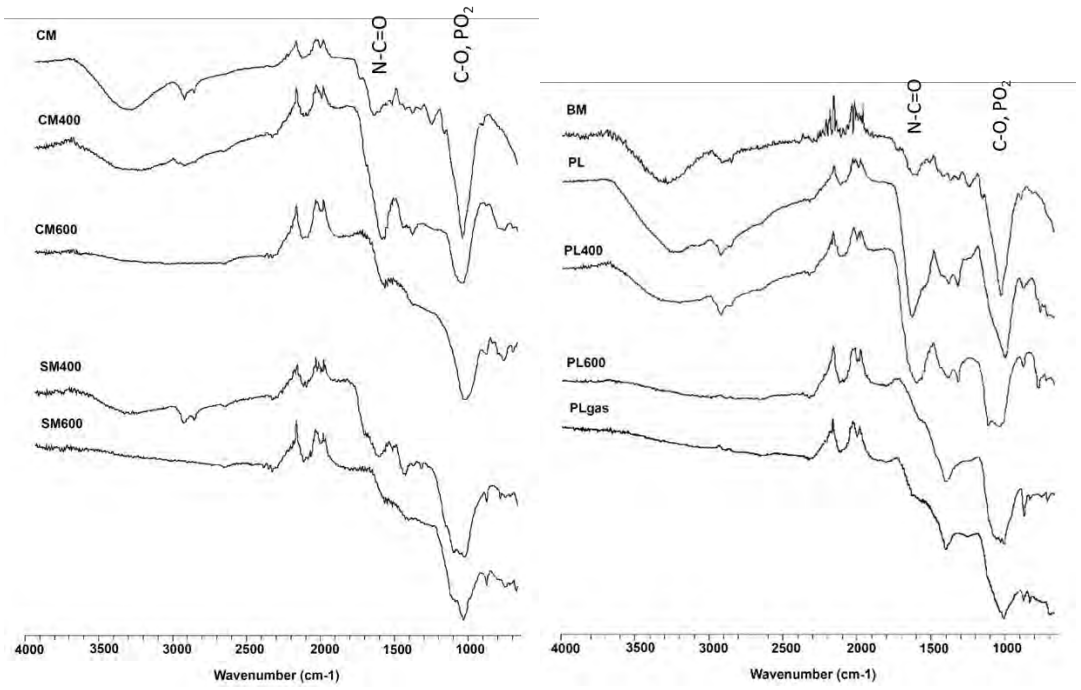

Figure 4-2: FTIR spectra. Abbreviations same as in Table 4-1.

Figure 4-3 shows the ^{13}C (CP/MAS) NMR spectra of the manure derived biochars. These were compared with the spectra in Cimò *et al*. (2014) and McBeath *et al*. (2014). The signals between 0 and 50 ppm were assigned to alkyl carbons and were found in all BC400 and PLgas. The peaks at 31 ppm and 24 ppm were attributed to methylene chains ($-CH_2-$), and 14 ppm to methyl groups terminating alkyl chains (Cimò *et al*., 2014). In PL400 and PLgas the peak at 31 ppm was the most intense of the three, which indicates the presence of alkyl species that have not been altered, such as highly ordered crystalline and amorphous cellulose, but also waxes and long chain fatty acids. In CM400 and SM400 the alkyl peaks had similar peak areas suggesting the majority of alkyl carbon to be in short side-chains attached to, or bridges between, aromatic structures (McBeath *et al*., 2014). The aromatic carbon region between 110 ppm and 160 ppm (Cimò *et al*., 2014) was detected in all biochar samples and became increasingly dominant with increasing pyrolysis temperature; being most dominant in CM600. The spectra also contained prominent spinning sidebands (SSBs) associated with the aromatic peak (marked with an asterisk). McBeath *et al*. (2014) attributed a sharp peak at 169 ppm to carbonates and these were most likely present in our samples however the peak was not visible due to overlapping by the broad aromatic carbon peak. The sample PL400 had the strongest signals for oxygen-containing groups,

indicating incomplete carbonisation. One signal was visible in the carbohydrate region (60 ppm – 110 ppm) at ~ 73 ppm assigned to C-2, C-3 and C-5 in amorphous cellulose, hemicellulose and cellulose oligomers (Cimò *et al*., 2014). Anomeric carbon may be responsible for the signal at 105 ppm in PL400, which confirmed the presence of crystalline cellulose at 73 ppm. Also tannins were detected at 110 ppm. The signal around 160 ppm was assigned to aromatic C–O (phenolic and aromatic ether moieties of lignin origin), which was present in PL400, most likely derived from the bedding material. This signal was also visible in SM400. The signal around 170 ppm (C=O) showed the presence of carbonyl, carboxylic groups, amides and esters, confirming the presence of amides by FTIR (Figure 4-2). The NMR spectra revealed differences between biochars derived from PL and biochars derived from CM and SM. The different carbonisation behaviours due to different mass loadings into the reactor were discussed above. However, differences in feedstock compositions may also play a role, as PL is a mixture of bedding material and manure, while CM and SM are composed of digested grass or excreted animal feed. Internal digestion may result in a manure with less VM.

The NMR spectra reflects the previous grouping of the biochars in the Van Krevelen Diagram (Figure 4-1): (1) PL400, (2) CM400, SM400, PLgas and (3) PL600, CM600, SM600. Group 1 representing PL400 presumably had characteristics similar to the original feedstock owing to the oxygenated functional groups found in the NMR spectrum and the fact that most functional groups observed by FTIR for PL were still present in PL400. Group 2 have two alkyl and aryl peaks, of which aryl is more dominant in the pyrolysis chars (CM400 and SM400), while for the updraft gasification char (PLgas) the alkyl and aryl peak were very similar in intensity. This is validated by the distribution of VM and FC content amongst these samples (Table 4-1). The FTIR spectrum of PLgas was more similar to BC600 than the pyrolysis chars in group 2 owing to the lack of N-C=O stretching of peptide bonds and the C-H stretches of aliphatics. Biochars of group 3 (BC600) had all been converted to polycyclic aromatic structures with simultaneous loss of aliphatic chains, carbohydrates and N-containing organic compounds.

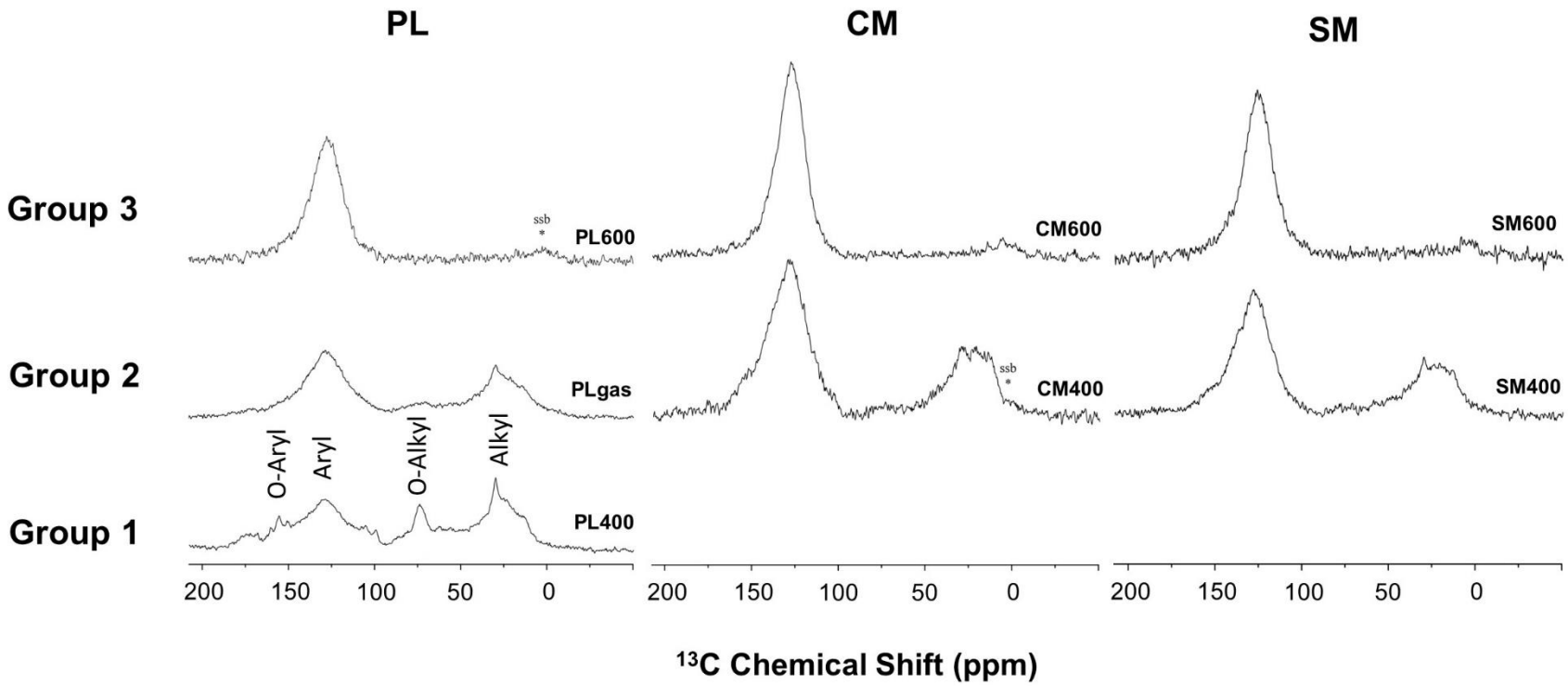

Figure 4-3: ^{13}C direct polarization (CP/MAS) NMR spectra at a magic angle spinning (MAS) frequency of 13 kHz. Grouped biochar samples: Group 1 (PL400) Group 2 (CM400, SM400, PLgas), Group 3 (PL600, CM600, SM600). Abbreviations same as in Table 4-1.

Brewer *et al*. (2011) compared biochar chemical properties derived from grass and wood waste using different thermochemical processes (fast pyrolysis, slow pyrolysis and gasification) for the purpose of selecting biochars for field studies. They concluded that fast pyrolysis and gasification chars differ physically and chemically from traditional chars prepared by slow pyrolysis. Fast pyrolysis biochars showed the strongest ^{13}NMR signals for oxygen-containing groups. The gasification char showed by far the lowest aromatic C-H signal, which was in agreement with our results (with the exception of PL400). Furthermore, the gasification char from Brewer *et al*. (2011) showed relatively sharp COO signals compared to the pyrolysis chars, which were not observed in our case. It should be noted that the gasifier in their study was in fact a bubbling fluidised bed reactor as opposed to the updraft gasifier in our study. Both used air as a gasification medium, but fluidised bed gasification offers better contact between the gasification medium and the solids, which likely results in surface oxidation. Overall PLgas shared features of both PL400 and PL600, but was less aromatic than PL600. This would be considered a disadvantage for carbon sequestration.

Cimò *et al*. (2014) investigated the effect of pyrolysis temperature and residence time on the biochar properties of poultry manure and found that the char's chemical composition is dependent on production temperature rather than on residence time. With regard to production temperature, their findings conform with our results, as biochars produced at 350 °C and 450 °C showed abundance of alkyl groups, while at 600 °C mainly aromatic groups were found. The different charring behaviour of PL400 could be attributed to the different mass load into the pyrolysis vessel and hence convection in the pores. This resulted in different pyrolysis efficiencies and structural properties of the biochars. At higher volumes the residence time might play a bigger role, since a residence time of 30 min was sufficient to carbonise the feedstock in a 300 ml pyrolysis vessel (Cimò *et al*., 2014), while a residence time of 1 h produced poorly carbonised chars when using a 1000 ml pyrolysis vessel.

Some biochar properties may have a strong influence on the agronomic performance of soils, such as pH, CEC, surface area and porosity. Even though correlations between biochars' functional groups and the biochar's pH have been reported previously (Li *et al*., 2013), the high ash content in the manure feedstocks might have a more significant effect on the pH, considering that alkali and alkaline-earth metals are separated from

the organic matrix during pyrolysis (Abe *et al*. 1998). The high pH of biochars has been seen to be a beneficial feature for neutralising soil acidity (Cao and Harris, 2010). The pH is influenced by the content and composition of the mineral fraction and changes once incorporated into the soil, as the minerals dissolve and ions are exchanged on the surfaces of the surrounding clay particles (Joseph *et al*., 2010).

The CEC gives information about the retention of cationic nutrients and their availability for plant uptake (Havlin *et al*., 1999a). Pyrolysis at 400 °C did not have an influence on the original feedstocks' CEC, but it decreased with further increasing pyrolysis temperature (Table 4-1). This was also observed by Kloss *et al*. (2012), who linked the decrease of CEC and simultaneous negative surface charge density to a decrease of surface functional groups with rising temperature. The opposite effect has also been reported whereby the CEC increased with increased SA at higher temperatures (Lehmann, 2007). Gaskin *et al*. (2008) showed that biochar derived from PL had a higher CEC than peanut hull and pine chips and associated this with higher concentrations of nutrients in PL. Mészáros *et al*. (2007) suggested that K, Mg, Na, and P in the biomass may be the cause of catalytic formation of oxygen groups on the biochar surface at low pyrolysis temperatures (e.g. carboxyls, lactones, and phenols), which have Brønsted acidic properties. In our case we also observed a higher CEC for PL_{BC} and SM_{BC} which have a relatively high ash content compared to CM_{BC}. However, the NMR spectra do not confirm presence of carboxylic, lactone or phenolic groups in these biochars, suggesting that other interactions must influence the CEC results, for example adsorption of cations onto the negative charges on the surfaces of ash particles.

Biochar's SA is also known to vary with feedstock properties and pyrolysis conditions, with instrumental features such as outgassing conditions and the type of adsorbate gas (e.g. N_2, CO_2) also affecting the SA results (Mc Laughlin *et al*., 2012). The BET-N_2 SA of the biochars (Table 4-1), while low, increased with increasing pyrolysis temperature and was highest for CM_{BC} and lowest for PL_{BC}, possibly owing to the high proportion of ash relative to char present in PL_{BC}. Our results are in accordance with scientific literature on manure derived biochars using slow pyrolysis (Cantrell *et al*., 2012; Cao and Harris, 2010; Jin *et al*., 2016). Keiluweit *et al*. (2010) observed a significant increase in the BET-N_2 SA between 400 °C and 600 °C for wood-derived biochars (from 28.7 $m^2\ g^{-1}$ to 392 $m^2\ g^{-1}$ respectively) and grass-derived biochars (from

8.7 m^2 g^{-1} to 75 m^2 g^{-1} respectively). In our study the increase in BET-N_2 SA from 400 °C to 600 °C was more apparent for CM_{BC} and SM_{BC} than for PL_{BC}, most likely owing to the less pyrolysed PL feedstock as discussed above and the influence of the relative high ash content. Tsai *et al*. (2012) found that the biggest increase in BET- N_2 SA of SM biochar in their study occurred between 600 °C and 700 °C (from 3.4 m^2 g^{-1} to 59 m^2 g^{-1} respectively). Lima *et al*. (2009) recorded a decrease in BET-N_2 SA from 238 m^2 g^{-1} to 199 m^2 g^{-1} for PL_{BC} produced at 700 °C and 800 °C respectively and Qiu and Guo (2010) recorded a BET-N_2 SA of 403 m^2 g^{-1} for granular activated carbon generated from pelletised PL following steam-activation. It appears that biochar derived from manure and litter can in fact possess a variety of BET- N_2 SAs depending on the selection of process conditions and biochar post treatment (e.g. steam activation).

The macro pores often present in biochar are considered to provide a habitat for microorganisms, which are beneficial for plant growth. It is well established that pores develop upon release of volatiles, which can condense at low temperatures clogging pores and reducing the total SA (Pignatello *et al*., 2006); however, it seems reasonable to assume that melting ash particles also contribute to pore blockage. Raveendran *et al*. (1995) observed that biochar SA increased with prior demineralisation for twelve biomass feedstocks. Figure 4-4 displays SEM images of PL600, CM600 and SM600 with the corresponding EDS analysis for PL600 (Table 4-2). The char's structure resembles that of the original PL with its heterogeneous composition of mainly bedding material and manure, but also remnants of hair, feathers and feed. Accordingly, the surface of the charred bedding material was mainly composed of carbon (Area 1,), with some small ash particles containing macro- and micronutrients (Area 2 and 3, Table 4-2). The catalytic effect of some alkali (Na, K) and alkaline- earth metals (Ca, Mg) during thermal treatment has to be considered (Mitsuoka *et al*., 2011; Müller-Hagedorn *et al*., 2003). Joseph *et al*. (2010) reported that the interfaces between minerals and the amorphous carbon in biochars can result in a high defect structure, including nanoscale pores, where reactions might occur preferentially thereafter. Similar observations were made for SM600 (Figure 4-4). The SEM image revealed the presence of small ash particles on the carbon surface as well as pores of about 1 µm or less. Once the biochar is incorporated into the soil the SA may change due to the water soluble salts being washed away leaving a reactive

biochar. High mineral ash biochars have been shown to oxidise faster than low mineral ash biochars (Joseph *et al*., 2010). Furthermore, Amonette *et al*. (2006) proposed that the mineral matter in the biochar provides nutrients for microorganisms to grow faster as well as catalysing the breakdown of organic matter.

Table 4-2: Scanning electron microscopy combined with energy dispersive spectroscopy (SEM-EDS) analysis of ash particles and char surface of poultry litter biochar produced at 600 °C. The mean values of the points selected in Figure 4-4 (bottom, left) are as follows: Area 1 = average (3, 8, 10, 11). Area 2 = (average 2, 5, 6). Area 3 = average (4, 7, 9).

Area	**C**	**O**	**Na**	**Mg**	**P**	**S**	**Cl**	**K**	**Ca**	**Mn**	**Fe**	**Cu**	**Zn**	**Total**
	(wt.%)													(wt.%)
1	81	15	0.2	0.0	0.2	0.4	0.2	2.6	0.0	0.0	0.1	0.6	0.0	100
2	72	19	0.4	0.5	1.0	0.4	0.5	3.8	1.4	0.0	0.1	0.4	0.0	100
3	52	26	1.7	3.7	5.0	0.3	0.6	6.8	1.3	0.2	0.1	0.0	0.8	100

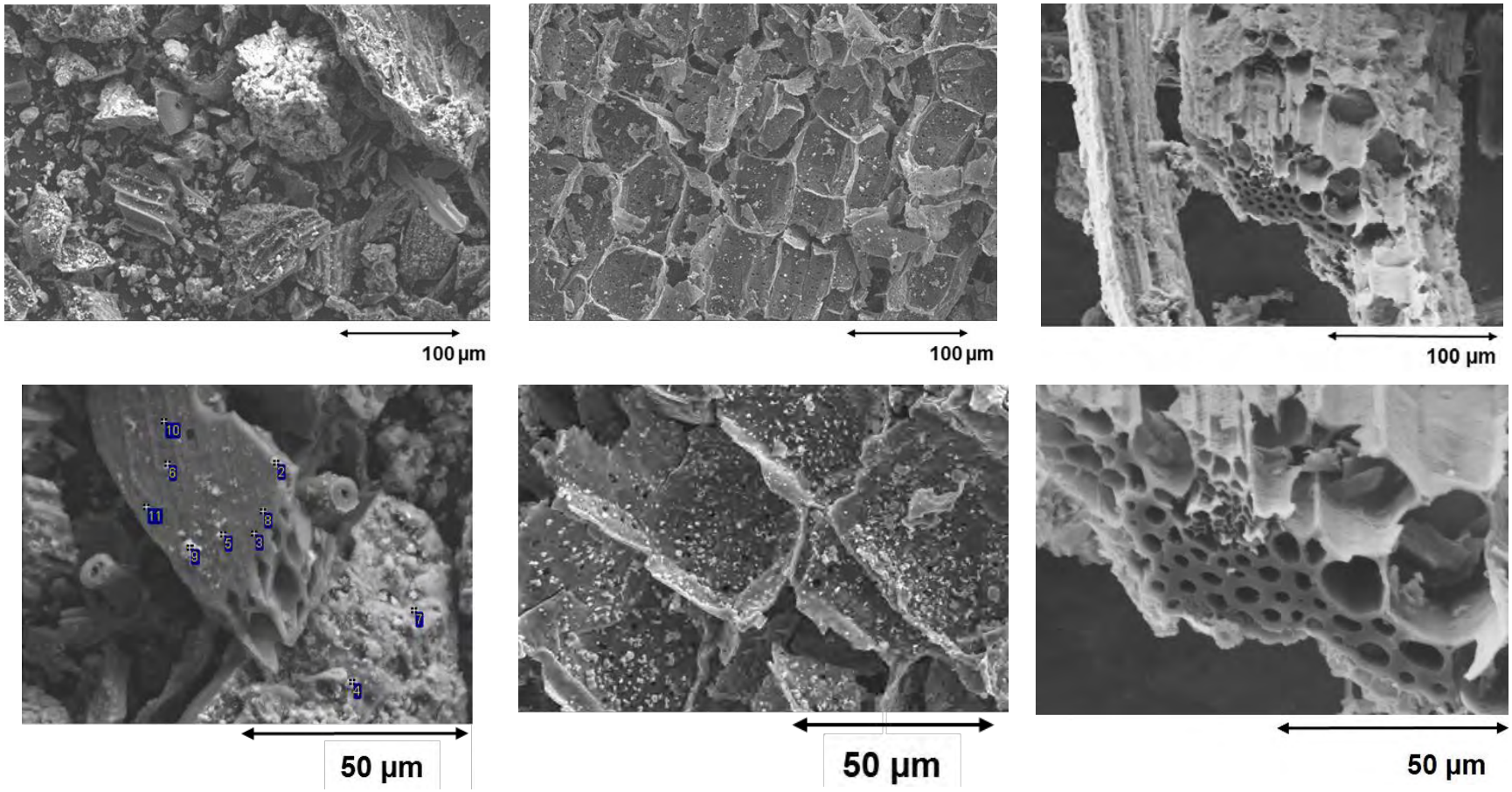

Figure 4-4: Scanning electron microscopy (SEM) image (10.0 kV) of biochars produced at 600 °C. Left to right: poultry litter biochar, swine manure, cow manure. The selected areas of interest encompass ash particles and char surfaces and were subject to energy dispersive spectroscopy (EDS) analysis.

4.4.2. Energy recovery

Table 4-3 shows the mass yields, heating values and energy recovered in the biochars from updraft gasification of PL and slow pyrolysis of dried PL and CM. Due to the fact that the SM_{BC} samples were received after pyrolysis the study did not include the recovery values associated with this feedstock. As the biochar yield decreased with increasing temperature, so did the energy recovered in the biochar. The remaining energy was converted to condensable and non-condensable gases (not measured in our study), or consumed for driving the pyrolysis process. Combusting the pyrolysis gas to provide heat for drying the manure feedstocks would increase the energy use efficiency. Generally, the heating values of the biochars were higher than the original manure feedstocks. This can be explained by the loss of VM and an increase in energy dense FC content. However, with a relative increase in ash content (BC600) the heating values decreased concurrently. The heating values for the dried CM were higher than for PL; however, if the initial moisture content of 86.3 $wt\%_{ar}$ in CM as opposed to 30.2 $wt\%_{ar}$ in PL is considered, then the heating value of CM decreases to 2.6 MJ kg^{-1} and the heating value of PL decreases to 12.8 MJ kg^{-1}, while their LHV decrease to 0.47 MJ kg^{-1} and 11.4 MJ kg^{-1} respectively. This indicates the importance of the drying step for the overall energy balance of thermochemical conversion processes. Manure types with a high moisture content, in particular SM, might undergo pre-treatment (e.g. anaerobic digestion), and solid-liquid separation before the solid fraction is subject to thermal treatment. All these steps require energy. Wnetrzak *et al*., (2013) concluded that the type of pre-treatment influences the composition of the separated solid fractions and subsequently the properties of the pyrolysis products, which results in both positive and negative energy balances.

Table 4-3: Biochar yield and energy recovery (%) in the biochars after pyrolysis and gasification of PL and CM

Samples	Biochar Yield	HHV	LHV	Energy recovered in biochars
	$(wt.\%)_{db}$	$(MJ\ kg^{-1})_{db}$		$(\%)_{db}$
PL	-	18.0 ± 0.3	16.9	-
PL400	50.7	20.9 ± 0.6	20.0	57.9
PL600	35.0	20.7 ± 0.2	20.4	39.6
PLgas	33.4	15.5 ± 0.2	15.1	28.2
CM	-	18.8 ± 0.3	17.6	-
CM400	45.7	25.0 ± 0.2	24.3	60.8
CM600	34.3	24.7 ± 0.4	24.4	45.2

Abbreviations same as in Table 4-1 as well as HHV = Higher heating value, LHV = Lower heating value

4.4.3. Nutrient recovery

The ash in livestock manure is composed of a variety of different elements, which include macro- (N, P, K, S, Ca, Mg) and micronutrients (Fe, Mn, Zn, Cu and B), and other alkali and HM (Na, Al, Pb, Cd, Ni, Cr). The concentration of these elements in the manure feedstocks and their derived biochars (Table 4-4) were compared with the mandatory limit values for Zn, Cu, Pb, Cd, Ni, and Cr laid down in the sewage sludge directive (SSD; 86/278/EEC; EC, 1986) to protect soil, surface and ground water in accordance with Directives 75/440/EEC and 80/68/EEC, as some HMs may be toxic to plants and humans after consumption. The European Biochar Certificate (EBC) also limits the HM content able to be applied to land with biochar. The results show that all biochars comply with the limits of the SSD, however the EBC thresholds were not met for Zn in the cases of PL_{BC} and SM_{BC}, Cu for any biochar and Cd is at the limit for the premium quality grade biochar ($BC_{premium}$) in the case of PLgas. Similar findings have been reported previously for PL (Lynch *et al*., 2014). One way to counteract the high Zn and Cu concentration is to alter the animal feed, which is often amended with Zn and Cu as important enzyme cofactors (Sistani and Jeffrey, 2005).

Furthermore, according to the existing European Biochar Certification scheme (EBC, 2012), the carbon content of a biochar should account for at least 50 $wt.\%_{db}$. This threshold was not met for PL_{BC} (Table 4-1) and must therefore be classified as a pyrogenic carbonaceous material (PCM). Depending on its intended use, a carbon

content below 50 wt.% might not mean a diminished quality of the char. In order to achieve a desired biochar classification, the PL feedstock could be blended before pyrolysis with a low ash biomass. For simplicity we are continuing to label the manure chars as “biochars” throughout this chapter.

Nutrient recovery in biochar after pyrolysis has been shown to vary amongst feedstocks and reactor design (Wise *et al*., 2009). Nutrients recovered at more than 90 wt.% included P, Ca, Mg, Na, Mn, and Zn, and to some extent K, Fe, and Cr (Table 4-4). Nitrogen recoveries ranged from 28 - 54 wt.%, and S from 37 - 62 wt.%. Recoveries of some volatile HM were very low, e.g. Pb recoveries ranged from 12 - 31 wt.%, and Ni recoveries ranged from 21 - 28 wt.%. The volatility of HM during thermal treatment is important for downstream processing of the ash and gas cleaning and has hence previously been subject to investigation during fluidised bed combustion of PL (Lynch *et al*., 2014). The results suggest that plant nutrients, including P, K, Ca, Mg, Na, Fe, Mn, Zn, and Cr, are recovered to a higher degree in the biochar than volatile toxic HM, such as Pb, Ni and to a certain extent Cd, and this might be beneficial for the biochars as a soil additive and biofertiliser.

Table 4-4: Macro-, micronutrients and heavy metals (HM) in the bedding material used in the poultry sheds, manure feedstocks and biochar samples. HM concentrations are compared with the thresholds of the Sewage Sludge Directive and the guidelines for European Biochar Certification (EBC, 2012). Nutrient recovery (%) in the biochars after pyrolysis and gasification of poultry litter and cow manure are presented below, taking into account the biochar yield.

Samples	N	P	P^2	K	S	Ca	Mg	Na	Fe	Mn	Zn	Cu	B	Al	Pb	Cd	Ni	Cr
	(g kg^{-1})											(mg kg^{-1})						
BM	4.4	0.13	ND	6.8	0.35	1.6	0.35	0.07	0.08	0.02	0.005	1.8	2.4	< DL	< DL	< DL	2.5	4.4
PL	52.2	9.7	6.2	33.4	7.8	15.2	6.0	3.3	0.93	0.50	**0.41****	**122****	55.8	0.3	0.9	0.5	27.3	5.3
PL 400	55.3	17.1	11.3	54.2	9.4	29.5	10.7	6.3	1.60	0.95	**0.76****	**159****	91.8	0.7	< DL	0.8	11.2	9.8
PL 600	42.1	27.6	9.9	79.0	9.4	40.0	17.0	9.8	2.20	1.47	**1.09****	**241****	133	0.9	< DL	0.9	16.7	13.2
PL gas[1]	43.0	29.3	12.4	87.8	8.6	44.1	18.3	10.4	4.30	1.58	**1.23****	**274****	148	1.1	0.9	1.0*	21.6	19.3
CM	19.0	2.3	1.97	9.0	1.2	4.1	2.9	3.4	1.8	0.10	0.07	**163****	10.4	1.2	5.4	0.2	11.9	5.2
CM 400	24.0	5.2	4.7	18.1	1.3	9.0	6.5	7.3	3.83	2.21	0.14	**207****	9.80	5.7	1.4	0.2	7.2	9.9
CM 600	21.4	7.0	6.0	24.3	1.6	12.0	8.5	9.3	3.73	3.11	0.19	**290****	14.7	5.6	2.2	0.1	7.9	10.5
SM 400	24.6	17.9	10.7	24.0	2.8	23.5	11.7	31.1	4.02	0.43	**0.44****	**128****	79.1	1.1	2.0	0.2	11.2	14.3
SM 600	18.3	31.0	13.1	28.5	4.8	29.8	22.3	37.1	5.08	0.61	**0.62****	**139****	88.2	1.7	3.9	0.2	12.7	18.8
SSD thresholds											*2.50*	*1000*			*750*	*20*	*300*	
BC_{basic}*											***0.40****	***100****			***150****	***1.5****	***50****	***90****
$BC_{premium}$**											***0.40*****	***100*****			***120*****	***1.0*****	***30*****	***80*****
	Recovery (%)																	
PL 400	54	> 90		82	62	> 90	> 90	> 90	87	> 90	> 90	66	83	> 90	< DL	82	21	> 90
PL 600	28	> 90		83	42	> 90	> 90	> 90	83	> 90	> 90	69	83	> 90	< DL	67	21	87
PL gas	28	> 90		88	37	> 90	> 90	> 90	85	> 90	> 90	75	89	> 90	31	72	27	> 90
CM 400	58	> 90		> 90	53	> 90	> 90	> 90	> 90	> 90	> 90	58	43	> 90	12	59	28	87
CM 600	39	> 90		> 90	47	> 90	> 90	> 90	70	> 90	> 90	61	49	> 90	14	21	23	69

*Abbreviations same as in Table 4-1 as well as DL = detection limit, SSD = Sewage Sludge Directive (thresholds), BC_{basic} = Basic quality grade biochar, BC_{prem} = Premium quality grade biochar. [1]Presented in chapter 3, [2]Available phosphorus: determined using 1 wt.% formic acid, *above BC_{basic} threshold, **above $BC_{premium}$ threshold (EBC, 2012).*

4.4.4. Plant growth and nutrient uptake

All biochar treated soils significantly increased dry plant biomass compared to the controls in soil 1 and soil 2, with the exception of CM600 which showed no significant growth improvement compared to the control in soil 2 (Figure 4-5). The impact of pyrolysis temperature on the biochars' performance on plant yield was not significant, except for SM_{BC} in soil 1, where the SM400 treatment performed significantly better than SM600. Nevertheless, the CM400 and SM400 treatments gave higher plant yields than CM600 and SM600, respectively, when comparing the mean values in both soils. The opposite was the case for PL_{BC}, where PL600 produced higher plant yields than PL400. Excessive HM and low P and K plant uptake (Table 4-8) might explain the low dry biomass for PL400 compared with PL600 amended soil 1. Soils amended with PLgas produced lower yields compared to pyrolysis derived PL_{BC}; however not significantly. Also Subedi *et al*. (2016a) found that manure biochar resulted in higher root biomass turnover when added to acidic soils, with positive effects for low temperature PL biochars, both on crop growth and soil chemical properties, and to a lesser extent for low temperature SM biochars.

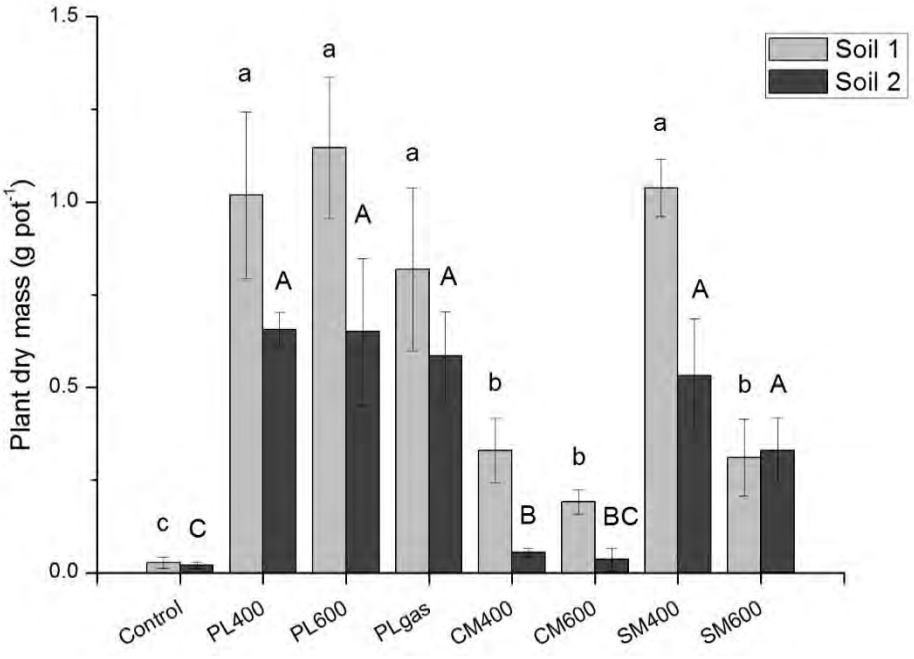

Figure 4-5: Effects of biochar amendment in two different soils on plant shoot biomass (db). Error bars represent standard error of the means (n = 5). Different small letters indicate significant differences ($p < 0.05$) in soil 1, while different capital letters indicate significant differences ($p < 0.05$) in soil 2. Abbreviations are the same as Table 4-1.

The increase in plant yield could be attributed to several factors, such as addition of organic carbon and available plant nutrients, pH, as well as an improvement of the soils' physical and biological properties. Nitrogen is in most cases the plant nutrient that has the largest influence on crop dry matter (Jensen, 2013b), which was also found by Chan *et al*. (2008), who attributed the yield increase after soil amendment with PL biochar to be largely due to the ability of the biochar to increase N availability of the applied N fertiliser. They assigned the additional observed yield increase to higher available P content in biochars produced at lower temperatures. Also Abbasi and Anwar (2015) showed that PL biochar alone or in combination with N fertiliser increased plant growth and biomass production. The rise in pH of the acidic soils (Table 4-5) show the liming effect of the biochars. In our study lettuce yield did not correlate with N content in the biochars or pH of the soils according to the Pearson bivariate correlation analysis, and hence we assume that a combination of factors was responsible for the plant response.

An increase in C:N ratio is known to shift the equilibrium from mineralisation and immobilisation of N in the soil (Havlin *et al*., 1999b), reducing available N for the plants. The calculated C:N ratios were higher in soil 2 than soil 1 (Table 4-5), higher in BC600 than BC400 and higher in CM and SM than PL, which might explain the results obtained for the plant dry yields; however, a significant correlation between the lettuce yields and C:N ratios of the soils was not found. The content of volatiles and the recalcitrant nature of C and N in the biochar matrix and soil would have impacted on the degree of mineralisation and immobilisation. Furthermore, an increase of soil pH was observed for all biochar treatments to values between 5 and 6 in soil 1 and 4 and 6 in soil 2 (Table 4-5), and this pH range (around pH 5.5) might have made P, K and other micronutrients (Mn, Fe, Cu, Zn, B) more available influencing plant yield.

Table 4-5: Properties and elemental composition of soil 1 and soil 2 as well as pH and C:N ratios of biochar treated soils

Soil properties	**Soil 1**	**Soil 2**	**Soil elements**	**Soil 1**	**Soil 2**	**Biochar treated soil**	**pH[1] (soil 1)**	**pH[1] (soil 2)**	**C:N[2] (soil 1)**	**C:N[2] (soil 2)**
C (g kg^{-1})	57.6 ± 6.2	25.5 ± 1.3	P (g kg^{-1})	0.5	0.4	Control	4.70	3.27	18.6	23.2
N (g kg^{-1})	1.2 ± 0.5	0.9 ± 0.1	K (g kg^{-1})	40.7	27.2	PL400	5.35	4.57	15.9	15.8
WHC (g_{water} g_{soil}^{-1})	0.58 ± 0.03	0.42 ± 0.01	S (g kg^{-1})	0.4	0.3	PL600	5.69	4.99	17.1	18.1
CEC ($mmol_c$ kg^{-1})	90.0 ± 2.2	45.4 ± 1.9	Ca (g kg^{-1})	2.2	1.9	PLgas	5.99	5.60	16.7	17.3
Sand (wt.%)	37.6 ± 0.8	55.6 ± 1.1	Mg (g kg^{-1})	4.9	3.5	CM400	4.97	4.03	19.3	23.5
Silt (wt.%)	36.4 ± 2.0	24.5 ± 1.2	Na (g kg^{-1})	1.3	0.7	CM600	5.32	4.26	20.2	25.7
Clay (wt.%)	26.0 ± 1.2	19.9 ± 1.9	Fe (g kg^{-1})	< DL	< DL	SM400	5.24	4.04	18.9	22.5
			Mn (g kg^{-1})	0.5	0.4	SM600	5.22	4.04	20.0	25.4
			Zn (g kg^{-1})	0.1	< DL					
			Cu (mg kg^{-1})	17.4	15.0					
			Pb (mg kg^{-1})	31.1	24.8					
			Cd (mg kg^{-1})	0.6	0.4					
			Cr (mg kg^{-1})	0.1	0.1					

Abbreviations same as in Table 4-1. CEC = cation exchange capacity, WHC = Water holding capacity, DL = detection limit
[1] pH measured in 1 wt.% 0.01 M $CaCl_2$
[2] based on calculation

The nutrient concentrations in the lettuce leaves varied amongst the different biochar treatments for soil 1 (Table 4-6). Some macro- (N, S) and micronutrients (Zn, Cu, B) were most concentrated in the plants from the control soil. Other macronutrient (P and K) concentrations were highest in the plants from PLgas treatments and were lowest in the control. Calcium and Mn showed the highest concentration for SM600 treatments and Mg was not significantly different for any of the treatments. Some HM such as Fe and Cr concentrations were significantly higher in PL400 compared to the other treatments. The nutrient concentrations in lettuce leaves varied amongst the different treatments for soil 2 (Table 4-7) in a similar way as for soil 1. Some exceptions were Na, which showed the highest concentration in SM400 treatments and Fe which had the highest concentration in the control. In general, P, S, Mg, Na and B concentration were higher for soil 2, while K and Ca concentrations were higher for soil 1.

The control, CM_{BC} and SM600 treatments exhibited significantly lower P (and K with the exception of SM600) concentrations than the other treatments in soil 1, and this reflects clearly the plant growth response (Figure 4-5). Soil 2 gave very similar results. Even though statistically no significant correlation was found between these factors it is reasonable to assume that the addition of P and K with PL_{BC} and SM_{BC} played a significant role for enhancing lettuce growth. Concentrations for Fe, Mn, Zn, and Cu in lettuce were compared with the limits laid out by the Food and Agriculture Organisation of the United Nations and the World Health Organisation (FAO/WHO, 2001). Concentrations for Fe, Mn and Zn were above the thresholds in lettuce grown in the control soil, which might be attributed to the low biomass yield and the subsequent accumulation of metals in the plant. The only two biochar treatments above the thresholds for Fe and Mn were PL400 and SM600 as a result of the direct available HM supply to the soil with biochar addition. The availability of HM is discussed in more detail below.

Table 4-6: Average elemental concentration in the lettuce leaves in soil 1. *Concentrations of some micronutrients (Fe, Mn, Zn, and Cu) are compared with the thresholds of the Food and Agriculture Organisation of the United Nations and World Health Organisation (FAO/WHO).*

Treatment	**N**	**P**	**K**	**S**	**Ca**	**Mg**	**Na**	**Fe**	**Mn**	**Zn**	**Cu**	**B**	**Cr**
	(g kg^{-1})							**(mg kg^{-1})**					
Control	60.9 a	0.58 b	31.7 cd	2.69 ab	6.37 a	2.70 bc	6.08 ab	**1549 a***	**1076 a***	**315 a***	60.29 a	66.9 a	0.01 b
PL400	48.8 ab	2.91 a	53.2 ab	2.28 ab	3.48 cd	3.28 ab	3.45 bc	**682 b***	226 d	60.3 bcd	13.9 b	48.6 b	32.0 a
PL600	37.2 b	3.22 a	63.04 a	1.06 ab	3.10 d	3.00 bc	3.55 bc	357 b	174 d	43.1 de	12.2 b	43.8 bc	3.58 b
PLgas	42.5 ab	3.75 a	62.0 a	3.51 a	2.66 d	2.89 bc	2.21 c	327 b	165 d	54.8 cd	11.3 b	36.5 bcd	5.95 b
CM400	37.7 b	1.40 b	28.2 d	1.87 ab	4.06 bcd	2.72 bc	7.86 a	411 b	339 cd	35.9 d	7.96 b	27.6 cd	< DL
CM600	44.2 ab	0.98 b	31.8 cd	0.43 b	2.69 d	1.86 d	3.65 bc	356 b	717 b	78.8 b	8.79 b	27.0 d	< DL
SM400	31.5 b	3.04 a	44.0 bc	1.28 ab	5.99 ab	3.90 a	1.81 c	214 b	198 d	75.4 b	8.40 b	32.8 bcd	1.77 b
SM600	30.4 b	1.47 b	41.0 bcd	2.31 ab	5.51 abc	2.37 cd	2.22 c	146 b	**543 bc***	73.4 bc	8.66 b	38.7 bcd	3.34 b
Limits*								**425.5***	**500.0***	**99.4***	**73.3***		

Abbreviations same as Table 4-1
** FAO/WHO limits*

Table 4-7: Average elemental concentration in the lettuce leaves in soil 2. *Concentrations of some micronutrients (Fe, Mn, Zn, and Cu) are compared with the thresholds of the Food and Agriculture Organisation of the United Nations and World Health Organisation (FAO/WHO).*

Treatment	**N**	**P**	**K**	**S**	**Ca**	**Mg**	**Na**	**Fe**	**Mn**	**Zn**	**Cu**	**B**	**Cr**
	(g kg^{-1})							**(mg kg^{-1})**					
Control	62.3 a	0.77 e	34.7 d	6.94 a	8.82 ab	2.96 a	8.32 a	**493 b***	471 ab	80.8 a	17.8 a	31.9 a	16.1 ab
PL400	47.9 b	1.60 bc	58.9 abc	1.63 c	5.48 bc	2.96 a	2.60 c	**1089 a***	188 bc	55.2 ab	11.7 ab	28.2 a	30.0 a
PL600	33.3 d	1.86 ab	65.6 ab	1.33 c	4.28 c	2.70 a	3.07 bc	395 b	114 c	39.3 b	5.78 b	25.1 a	7.00 ab
PLgas	40.7 bcd	2.11 a	67.1 a	1.44 c	4.52 bc	2.71 a	4.15 bc	220 b	92.5 c	34.6 b	6.75 b	26.3 a	4.03 ab
CM400	41.6 bcd	1.02 de	48.7 c	1.36 c	7.03 abc	2.87 a	4.67 bc	146 b	268 abc	46.4 b	10.2 b	27.5 a	1.67 b
CM600	43.4 bc	0.91 de	49.4 c	1.37 c	6.85 abc	2.52 a	5.71 b	131 b	297 abc	44.9 b	5.12 b	29.6 a	2.22 b
SM400	38.5 cd	1.83 ab	53.5 bc	1.76 c	6.53 bc	3.82 a	2.55 c	235 b	255 abc	55.9 ab	8.01 b	24.4 a	1.85 b
SM600	43.6 bc	1.32 cd	52.1 c	3.80 b	11.0 a	4.14 a	4.96 bc	**611 b***	429 ab	56.6 ab	8.63 b	32.5 a	9.22 ab
Limits								**425.5***	**500.0***	**99.4***	**73.3***		

Abbreviations same as Table 4-1
** FAO/WHO limits*

To compensate for the so-called “Steenberg effect”, where growth increases more rapidly than nutrient concentrations, the total nutrient uptake in the dry lettuce biomass was calculated per pot (Table 4-8 and Table 4-9). A significant correlations existed between N uptake by lettuce and biochar N contents ($n = 21$, $p < 0.01$, $r = 0.86$ for soil 1 and $r = 0.86$ for soil 2), P uptake and biochar P contents ($n = 21$, $p < 0.05$, $r = 0.49$ for soil 1 and $p < 0.01$, $r = 0.62$ for soil 2), P uptake and P (available) contents ($n = 21$, $p < 0.05$, $r = 0.50$ for soil 1 and $p < 0.01$, $r = 0.60$ for soil 2) as well as K uptake and biochar K contents ($n = 21$, $p < 0.01$, $r = 80$ for soil 1 and $r = 0.79$ for soil 2).

Contrasts of the means show that the uptake of nutrients to lettuce depended on the soil type and the nature of the biochar applied to the soil, influenced by the feedstock and process type and pyrolysis temperature. Biochar application resulted in a pH increase in soil 1 and soil 2 (Table 4-5), which was expected to positively influence uptake of alkali metals (Ca, K, Mg) and P. The uptake of macronutrients in soil 1 was significantly higher in lettuce for all biochar amendments compared to the control (Table 4-8), as was the uptake of micronutrients and HMs for all PL_{BC} treatments. Also for CM_{BC} and SM_{BC} treatments micronutrient and HM uptake was significantly higher compared to the control with the occasional exception for Fe, Mn, Cu, Al and Cr. The CM_{BC} amended soil 2 (Table 4-9) performed less well than in soil 1, as nutrient uptake was not significantly different to the control. Only PL_{BC} treatments showed significantly higher uptake of all nutrients in soil 2. Overall, nutrient uptake was in the order PL > SM > CM.

When comparing the effect of process type on biochar effectiveness, PL_{BC} derived from pyrolysis significantly increased N uptake in both soils compared to PLgas from updraft gasification. The uptake of P and K remained unaffected in both soils. The remaining macro- and micronutrient uptake was significantly enhanced in soil 1 for PL_{BC} while in soil 2 Ca, Mg, Fe, Mn were not significantly affected. With regard to the maximum pyrolysis temperature used for biochar production, N uptake in soil 1 was significantly higher in all BC400 than BC600 treatments. CM400 and SM400 treatments significantly increased P and K uptake compared to CM600 and SM600 treatments, while the opposite was the case for PL400 and PL600. Also Na uptake was significantly increased using PL600 as opposed to PL400. The uptake of all other macro- and micronutrients was either significantly improved or remained the same for BC400 as opposed to BC600 treatments. In soil 2 the difference between the two

pyrolysis temperatures was not as apparent as in soil 1, however the trends were the same. The nutrient uptake for all CM_{BC} treatments were not significantly different to the control. We conclude that PL_{BC} produced via pyrolysis resulted in a higher nutrient uptake then PLgas treatments and BC400 performed better at nutrient uptake than BC600 treatments.

The UE of all macro- and micronutrients (Table 4-10) gave information about the uptake of nutrients compared to the initial concentration of nutrients supplied to the soil. It was observed that SM400 treatments were most effective with regard to uptake of macronutrients, while PL400 treatments were in most cases most effective with regard to micro-nutrient and HM uptake. Generally, N, P and K UE decreased with increasing pyrolysis temperature, except for PL_{BC} and CM_{BC} in soil 2, where N UE was higher for PL600 and CM600 than PL400 and CM400. It should be noted that the UE of all nutrients was low, which indicates that nutrients were supplied in excess of the requirements for lettuce and hence application rate should be considered carefully.

The results (Table 4-10) suggest that biochars produced at 600 °C can contain a similar amount of available N compared to biochars produced at 400 °C or make N in soil more available through microbial processes. Some manure feedstocks contain a high proportion of inorganic N, which might not react with the organic carbon of the manure and incorporate it into the biochar structure as heterocyclic N during pyrolysis or gasification, making it available at all pyrolysis temperatures if not emitted as ammonia. Also Gunes *et al*. (2014) found that poultry manure biochar performed better or equal with regard to N, P and K nutrition compared to the original poultry manure feedstock, suggesting that pyrolysis did not affect N availability. The distribution of inorganic and organic N in the original feedstock and their chemical transformation during pyrolysis and gasification would be worth investigating in the future.

The results on nutrient UE (Table 4-10) might provide a more meaningful comparison of the nutrient availability compared to the results presented on nutrient uptake according to the biochar application rate (2 wt.%, Table 4-8 and Table 4-9), as the nutrient UE compensates for differences in the amount of nutrients applied to the soil.

Table 4-8: Average elemental uptake by lettuce leaves in soil 1 (n=3). Contrasts are calculated for three different manure feedstocks, two different process types and two different pyrolysis temperatures.

Treatment	N	P	K	S	Ca	Mg	Na	Fe	Mn	Zn	Cu	B	Cr
	(mg pot^{-1})							(µg pot^{-1})					
Control	1.67 e	0.02 d	0.93 d	0.18 e	0.24 e	0.08 d	0.22 f	13.2 b	12.7 d	2.18 d	0.48 d	0.86 c	0.42 b
PL400	55.9 a	1.87 b	69.1 ab	1.91 a	6.41 ab	3.46 ab	3.03 bc	1180 a	219 ab	64.2 a	13.7 a	32.9 a	34.7 a
PL600	42.3 b	2.37 a	83.3 a	1.69 ab	5.45 ab	3.44 ab	3.90 ab	508 ab	145 abc	50.0 ab	7.34 bc	31.9 a	8.96 ab
PLgas	41.5 b	2.14 ab	68.9 ab	1.46 b	4.61 bc	2.76 b	4.21 a	220 ab	95.9 bcd	35.4 bc	6.72 bc	26.8 a	3.84 b
CM400	17.6 c	0.43 c	20.5 c	0.57 d	2.95 cd	1.21 c	1.96 de	61.5 b	113 bcd	19.8 cd	4.32 bcd	11.6 b	0.71 b
CM600	8.94 de	0.19 cd	10.2 cd	0.28 de	1.39 de	0.51 cd	1.16 ef	26.7 b	61.0 cd	9.3 d	1.07 d	6.09 bc	0.46 b
SM400	41.4 b	1.96 b	57.4 b	1.89 a	7.01 a	4.10 a	2.74 cd	253 ab	274 a	60.0 a	8.60 ab	26.3 a	1.98 b
SM600	10.5 cd	0.33 cd	13.4 cd	1.01 c	2.89 cd	1.10 c	1.36 e	174 b	119 bcd	15.0 cd	2.27 cd	7.82 b	2.40 b
Control													
PL x C	**94.9****	**4.20****	**150****	**3.23****	**11.4****	**6.73****	**6.49****	**1662****	**338****	**109****	**20.1****	**63.1****	**42.9***
PLgas x C	**39.8****	**2.12****	**67.9****	**1.28****	**4.38****	**2.68****	**3.99****	207	83.3	**33.3****	**6.24****	**25.9****	3.41
CM x C	**23.1****	**0.57****	**28.9****	**0.49***	**3.87****	**1.56***	**2.68****	61.7	149	**24.7***	4.42	**15.9****	0.32
SM x C	**48.6****	**2.26****	**68.9****	**2.53****	**9.43****	**5.04****	**3.67****	400	**367****	**70.6****	**9.91****	**32.4****	3.20
Feedstock													
PL x CM	**71.7****	**3.63****	**121****	**2.74****	**7.51****	**5.18****	**3.81****	**1600****	**189****	**85.2****	**15.6****	**47.2****	**42.5****
PL x SM	**46.3****	**1.95****	**81.5****	**0.70****	**1.96***	**1.69****	**2.82****	**1262****	-29.0	**39.2****	**10.1****	**30.7****	**39.3****
CM x SM	**-25.4****	**-1.68****	**-40.1****	**-2.04****	**-5.56****	**-3.49****	**-0.99***	-338	**-218****	**-46.0****	**-5.48***	**-16.4****	-2.88
Treatment technology													
PL x PLgas	**15.3****	-0.037	14.70	**0.67****	**2.63***	**1.37***	**-1.48****	**1248***	**172***	**43.3****	**7.57****	**11.2****	**36.0***
Temperature													
PL400 x PL600	**13.7****	**-0.50****	**-14.2****	0.22	0.96	0.02	**-0.87****	**672***	73.7	**14.1***	**6.34****	1.07	**25.8****
CM400 x CM600	**8.61****	**0.24***	**10.3***	**0.29***	**1.56***	**0.70***	**0.81****	**34.8****	52.4	**10.5***	**3.25***	**5.47***	0.25
SM400 x SM600	**30.8****	**1.63****	**44.0****	**0.89****	**4.12****	**3.00****	**1.38****	**78.6**	**155****	**45.0****	**6.33****	**18.5****	-0.75

*Abbreviations same as Table 4-1. * significant to 5%. ** significant to 1%*

Table 4-9: Average elemental uptake by lettuce leaves in soil 2 (n=3). Contrasts are calculated for three different manure feedstocks, two different process types and two different pyrolysis temperatures.

Treatment	N	P	K	S	Ca	Mg	Na	Fe	Mn	Zn	Cu	B	Cr
	(mg pot^{-1})							(µg pot^{-1})					
Control	1.29 e	0.01 b	0.65 c	0.05 b	0.13 c	0.06 c	0.12 b	31.6 b	21.9 c	1.66 c	1.23 d	1.36 c	0.25 b
PL400	32.3 a	1.93 a	35.2 ab	1.52 a	2.31 ab	2.18 ab	2.26 ab	450 a	151 ab	40.0 ab	9.20 ab	32.2 a	21.5 a
PL600	29.0 ab	2.67 a	51.7 a	0.89 ab	2.59 ab	2.50 a	2.97 a	262 ab	149 ab	34.6 ab	9.69 a	34.8 a	2.76 b
PLgas	24.5 bc	2.19 a	35.4 ab	0.50 ab	1.55 bc	1.75 ab	1.05 ab	186 ab	95.4 abc	29.3 b	6.92 abc	21.0 b	1.96 b
CM400	2.36 e	0.09 b	1.77 c	0.12 b	0.26 c	0.17 c	0.49 b	94.3 b	21.2 c	1.66 c	0.58 d	1.72 c	< DL
CM600	2.65 e	0.06 b	1.87 c	0.02 b	0.17 c	0.11 c	0.18 b	22.7 b	41.3 bc	4.22 c	0.53 d	1.60 c	< DL
SM400	19.4 c	1.96 a	27.7 b	0.78 ab	3.75 a	2.44 a	1.12 ab	135 ab	125 abc	47.3 a	5.28 bc	20.5 b	1.03 b
SM600	11.1 d	0.55 b	15.2 bc	0.98 ab	2.26 ab	0.95 bc	0.93 ab	60.1 b	190 a	28.5 b	3.43 cd	15.8 b	0.98 b
Control													
PL x C	**58.8****	**4.58****	**85.6****	**2.31****	**4.64****	**4.57****	**4.99****	**649****	**256****	**61.7****	**16.4****	**64.2****	**23.7****
PLgas x C	**27.9****	**2.42****	**41.6****	**1.65***	**5.75****	**3.27****	1.81	132	**271****	**62.9****	**6.25****	**33.6****	1.51
CM x C	2.44	0.13	2.33	0.04	0.16	0.16	0.43	53.9	19	-6.98	-1.35	0.60	-0.50
SM x C	**23.2****	**2.18****	**34.7****	0.45	**1.42***	**1.69****	0.93	154	73	**22.9****	**5.69****	**19.6****	1.71
Feedstock													
PL x CM	**56.3****	**4.45****	**83.3****	**2.28****	**4.48****	**4.41****	**4.56****	**595****	**238****	**68.7****	**17.8****	**63.6****	**24.2****
PL x SM	**30.9****	**2.16****	**44.0****	0.7	-1.11	**1.30***	**3.18****	**517****	-14.7	-1.24	**10.2****	**30.6****	**22.2****
CM x SM	**-25.5****	**-2.30****	**-39.2****	**-1.62****	**-5.59****	**-3.11****	-1.38	-77.8	**-252****	**-69.9****	**-7.60****	**-33.0****	-2.01
Treatment Technology													
PL x PLgas	**12.4****	0.22	16.1	**1.41***	1.81	1.20	**3.12****	341	109	**15.9***	**5.05***	**25.0****	**20.3****
Temperature													
PL400 x PL600	**3.29***	**-0.74***	**-16.4***	0.63	-0.28	-0.32	-0.71	**189***	1.94	5.34	-0.48	-2.60	**18.7****
CM400 x CM600	-0.29	0.03	-0.10	-0.10	0.09	0.06	0.31	71.6	-20.1	-2.56	0.06	0.12	0.05
SM400 x SM600	**8.23****	**1.35****	12.5	-0.20	**1.49****	**1.49****	0.18	74.7	-65.3	**18.9****	1.86	4.73	0.05

*Abbreviations same as Table 4-1. * significant to 5%. ** significant to 1%*

Table 4-10: Uptake efficiency for macro- and micro nutrients to lettuce leaves for soil 1 and soil 2

Treatment	N	P	K	S	Ca	Mg	Na	Fe	Mn	Zn	Cu	B	Cr
Soil 1	**UE (%)**												
PL400	14.0	1.5	18.0	9.4	1.6	3.8	3.9	11.0	17.6	3.9	5.6	2.1	50.0
PL600	13.8	1.2	14.9	7.9	1.2	3.1	2.2	1.6	4.8	1.7	2.8	0.7	9.2
PLgas	13.2	1.0	11.1	7.3	0.9	3.1	0.5	0.5	1.9	1.0	1.7	0.6	3.0
CM400	9.5	1.1	15.5	29.8	1.8	3.8	0.2	0.0	0.3	10.3	12.1	5.6	0.4
CM600	4.9	0.3	5.5	10.3	0.5	1.6	2.0	0.0	0.1	3.6	3.5	0.6	0.0
SM400	23.1	1.6	33.6	34.6	2.4	3.1	7.8	0.1	8.0	8.5	6.5	1.5	1.2
SM600	6.9	0.2	6.2	7.9	0.5	0.7	2.1	0.1	3.8	2.4	1.3	0.3	1.5
Soil 2	**UE (%)**												
PL400	8.0	1.6	9.1	2.2	1.1	2.8	4.9	3.7	1.9	0.7	0.7	4.8	31.0
PL600	9.4	1.4	9.2	1.3	0.9	2.1	4.2	1.5	1.2	0.4	0.5	3.6	2.7
PLgas	7.7	1.1	5.7	0.7	0.5	1.3	1.3	0.9	0.7	0.3	0.3	1.9	1.5
CM400	0.6	0.2	0.9	0.8	0.2	0.2	0.7	0.2	0.0	0.0	-0.4	0.5	< DL
CM600	0.9	0.1	0.7	-0.3	0.0	0.1	0.1	0.0	0.1	0.2	-0.3	0.2	< DL
SM400	10.5	1.6	16.1	3.7	2.2	2.9	4.6	0.4	3.4	1.5	0.5	3.5	0.8
SM600	7.7	0.3	7.3	2.8	1.0	0.6	2.1	0.1	3.9	0.6	0.2	2.3	0.6

Abbreviations same as Table 4-1 as well as UE = Uptake efficiency (nutrient uptake/nutrient concentration applied)

Our results were in agreement with other studies reported in the literature. Nigussie *et al*. (2012) found that biochar application to soil produced from maize stalk increased N, P, K content in lettuce (*lactuca sativa*) while reduced Cr uptake significantly from Cr polluted soils. They attributed the nutrient availability increase to either directly added nutrients to the soils as well as increased microbial activity of microorganisms involved in N, P, S transformations. They postulated that a reduction of Cr in plant tissue was due to the adsorption capacity of the biochar, which might explain the significantly higher Cr uptake in PL400, the least carbonised biochar. Other literature suggests that despite the increased HM content in biochars (e.g. Fe, Zn, Cu, Mn, Pb, Cd and Cr) with increasing pyrolysis temperature, the availability of these HM is reduced (Cely *et al*., 2015; Gunes *et al*., 2015, 2014; Liu *et al*., 2014; Park *et al*., 2011; Yuan *et al*., 2015). This was also observed in our study, where the hydro-solubility of some HM (Fe, Mn, Zn and Cu) was reduced with increasing charring temperature (Appendix II). This might be explained by the formation of insoluble phases via precipitation to amorphous crystals involving P and organo-metallic complexes (Cao and Harris, 2010; Zornoza *et al*., 2016), e.g. the formation of whitlockite (Cao and Harris, 2010; Liang *et al*., 2014) or the formation of pyrophosphate (House, 2008). This would also explain the reduced UE of P (Table 4-10) with increasing process temperature. In their review paper, Keiluweit *et al*., (2009) mention evidence of the capacity of aromatic pi-systems within organic compounds to adsorb to minerals. They found that polar interactions, cation-pi interactions and pi-pi electron donor-acceptor interactions appear in addition to hydrophobic interactions.

Heavy metals can accumulate and migrate in soils affecting regional eco-safety and posing a threat to animals and plants; therefore, the dose at which manure biochars are introduced to soils should be considered carefully. Application in regular intervals in small doses might prevent HM accumulation and enhance nutrient use efficiency while gradually contributing to the soil organic carbon pool. Generally, it is believed that biochar application in soil at first results in a priming effect, where nutrients are released from the ash and immobilisation of N and P takes place. With aging in soil the less labile fraction is oxidised and becomes reactive, being as effective as humified organic matter, for carbon storage and reactions in soils.

4.5. Conclusions

This chapter gave a cradle to cradle perspective on using dry animal manure for recovering nutrients in the remaining biochars from updraft gasification and slow pyrolysis for their subsequent use as fertilisers. The results suggest that the process conditions for pyrolysing animal manure should be considered carefully taking into account the bulk density and proximate and ultimate analysis of the manure or litter. Solid-state ^{13}C NMR was broadly in agreement with the Van Krevelen parameter for classifying biochar and may offer a reasonable alternative analytical technique for biochar classification. Mostly, plant nutrients were recovered to a higher degree in the biochar compared to volatile toxic HMs and this results in an improved biochar quality. However, under the current European guidelines for biochar certification (EBC) manure chars cannot meet the set thresholds unless blended with a low ash biomass or through alterations of the content of nutrients in animal feed. Despite these marketing restrictions, manure chars proved to be an effective way of improving biomass yield and supplying nutrients to the soil and crops. Nutrient uptake was highest for PL, followed by SM and CM treatments. Biochars produced via slow pyrolysis of PL resulted in a higher nutrient uptake than biochar produced from updraft gasification with the exception of P and K uptake, which were not affected by process type. Biochars produced at low pyrolysis temperature contributed to short term soil fertility, while biochars produced at high temperatures possessed a recalcitrant aromatic carbon structure and reduced HM availability to plants. The results of this study could be beneficial for decision making with regard to improving the agricultural management chain.

4.6. Acknowledgement

Financial support for this work is gratefully acknowledged from the People Programme (Marie Curie Actions) of the European Union's Seventh Framework Programme FP7/2007-2013/ under REA grant agreement n° [289887]. Furthermore, we would like to thank Cristiano Dela Piccolla from the Universidade de São Paulo, São Paulo, Piracicaba, Brazil, as well as Prof. M. Pilar Bernal and Dr. André Santos from the Centro de Edafología y Biología Aplicada del Segura, CSIC, Campus Universitario de Espinardo, 30100, Murcia, Spain, for their contribution.

4.7. References

Abbasi, M.K., Anwar, A.A., 2015. Ameliorating effects of biochar derived from poultry manure and white clover residues on soil nutrient status and plant growth promotion - greenhouse experiments. PLoS ONE 10 (6): e0131592. 1-18.

Abe, F., 1998. The thermochemical study of forest biomass. Forest. Prod. Chem. 45, 1–95.

Ahn, H.K., Sauer, T.J., Richard, T.L., Glanville, T.D., 2009. Determination of thermal properties of composting bulking materials. Bioresour. Technol. 100, 3974-3981.

Amonette, J.E., Joseph, S. 2009. Characteristics of biochar: Microchemical properties. In Lehmann, J., Joseph, S. (Eds.) Biochar for environmental management: Science and technology. Earthscan. London, UK. 33-52.

Antal, M.J., Grønli, M., 2003. The art, science, and technology of charcoal production. Ind. Eng. Chem. Res. 42, 1619–1640.

Arena, U., 2012. Process and technological aspects of municipal solid waste gasification. A review. Waste Manag. 32, 625–639.

Bai, S.H., Xu, C.-Y., Xu, Z., Blumfield, T.J., Zhao, H., Wallace, H., Reverchon, F., Van Zwieten, L., 2014. Soil and foliar nutrient and nitrogen isotope composition ($\delta^{15}N$) at 5 years after poultry litter and green waste biochar amendment in a macadamia orchard. Environ. Sci. Pollut. Res. 22, 3803–3809.

Brewer, C.E., Schmidt-rohr, K., Satrio, J.A., Brown, R.C., 2009. Characterization of Biochar from Fast Pyrolysis and Gasification Systems. Environ. Prog. Sustain. Energy 28, 386–396.

Brewer, C.E., Unger, R., Schmidt-Rohr, K., Brown, R.C., 2011. Criteria to Select Biochars for Field Studies based on Biochar Chemical Properties. BioEnergy Res. 4, 312–323.

Budai, A., Zimmerman, A.R., Cowie, A.L., Webber, J.B.W., Singh, B.P., Glaser, B., Masiello, C.A., Andersson, D., Shields, F., Lehman, J., Camps Arbestain, M.C., Williams, M., Sohi, S., Joseph, S., 2013. Biochar Carbon Stability Test Method: An assessment of methods to determine biochar carbon stability. Int. Biochar Initiat.

Cantrell, K.B., Hunt, P.G., Uchimiya, M., Novak, J.M., Ro, K.S., 2012. Impact of pyrolysis temperature and manure source on physicochemical characteristics of biochar. Bioresour. Technol. 107, 419–428.

Cao, X., Harris, W., 2010. Properties of dairy-manure-derived biochar pertinent to its potential use in remediation. Bioresour. Technol. 101, 5222–5228.

Cely, P., Gascó, G., Paz-Ferreiro, J., Méndez, A., 2015. Agronomic properties of biochars from different manure wastes. J. Anal. Appl. Pyrolysis 111, 173–182.

Chan, K.Y., Van Zwieten, L., Meszaros, I., Downie, a., Joseph, S., 2008. Using poultry litter biochars as soil amendments. Aust. J. Soil Res. 46, 437-444.

Cimò, G., Kucerik, J., Berns, A.E., Schaumann, G.E., Alonzo, G., Conte, P., 2014. Effect of heating time and temperature on the chemical characteristics of biochar from poultry manure. J. Agric. Food Chem. 62, 1912–1918.

Clough, T., Condron, L., Kammann, C., Müller, C., 2013. A Review of Biochar and Soil Nitrogen Dynamics. Agronomy 3, 275–293.

Coates, J., 2000. Interpretation of Infrared Spectra, A Practical Approach. In Meyer, R.A. (Ed.). Encyclopedia of Analytical Chemistry. John Wiley & Sons Ltd. Chichester, UK. 10815–10837.

De Vries, J.W., Groenestein, C.M., De Boer, I.J.M., 2012. Environmental consequences of processing manure to produce mineral fertilizer and bio-energy. J. Environ. Manage. 102, 173–183.

EBC, 2012. European Biochar Certificate - Guidelines for a Sustainable Production of Biochar. European Biochar Foundation (EBC), Arbaz, Switzerland. Available at http://www.europeanbiochar.org/en/download. Version 6.1 of 19th June 2015

EC, 2000. Directive 2000/60/EC of the European Parliament and of the Council of 23 October 2000 establishing a framework for the Community action in the field of water policy.

EC, 1991. Council Directive 91/676/EEC of 12 December 1991 concerning the protection of waters against pollution by nitrates from agricultural sources.

EC, 1986. Directive 86/278/EEC of 12 June 1986 on the protection of the environment, and in particular of the soil, when sewage sludge is used in agriculture. Off. J. Eur. Commun. L. 181, 6-12.

ECN Phyllis 2, 2015. Available at https://www.ecn.nl/phyllis2/Home/Help (accessed 10.22.15).

Enders, A., Lehmann, J., 2012. Comparison of Wet-Digestion and Dry-Ashing Methods for Total Elemental Analysis of Biochar. Commun. Soil Sci. Plant Anal. 43, 1042–1052.

FAO/WHO, 2001. Codex Alimentarius Commission. Food additives and contaminants. Joint FAO/WHO food standards programme, ALINORM 01/12A:1-289.

Gaskin, J.W., Steiner, C., Harris, K., Das, K.C., Bibens, B., 2008. Effect of low-temperature pyrooysis conditions on biochar for agricultural use. Soil Sci. Soc. Am. J. 51, 2061–2069.

Gunes, A., Inal, A., Taskin, M.B., Sahin, O., Kaya, E.C., Atakol, A., 2014. Effect of phosphorus-enriched biochar and poultry manure on growth and mineral composition of lettuce (Lactuca sativa L. cv.) grown in alkaline soil. Soil Use Manag. 30, 182-188.

Gunes, A., Inal, A., Sahin, O., Taskin, M.B., Atakol, O., Yilmaz, N., 2015. Variations in mineral element concentrations of poultry manure biochar obtained at different pyrolysis temperatures, and their effects on crop growth and mineral nutrition. Soil Use Manag. 31, 429–437.

Havlin, J.L., Tisdale, S.L., Nelson, W.L., Beaton, J.D., 1999a. Soil fertility and fertilizers: an introduction to nutrient management, Sixth edit. ed. Prentice Hall, Upper Saddle River, N.J. 14-22.

Havlin, J.L., Tisdale, S.L., Nelson, W.L., Beaton, J.D., 1999b. Soil fertility and fertilizers: an introduction to nutrient management, Sixth edit. ed. Prentice Hall, Upper Saddle River, N.J. p.111

He, Z.L., Yang, X.E., Stoffella, P.J., 2005. Trace elements in agroecosystems and impacts on the environment. J. Trace Elem. Med. Biol. 19, 125–140.

Hilscher, A., Knicker, H., 2011. Carbon and nitrogen degradation on molecular scale of grass-derived pyrogenic organic material during 28 months of incubation in soil. Soil Biol. Biochem. 43, 261–270.

Hou, Y., Velthof, G. L., Oenema, O., 2014. Mitigation of ammonia, nitrous oxide and methane emissions from manure management chains: a meta-analysis and integrated assessment. Global Change Biology 21 (3), 1293–1312.

Islam, E.U., Yang, X., He, Z., Mahmood, Q., 2007. Assessing potential dietary toxicity of heavy metals in selected vegetables and food crops. J. Zhejiang Univ. Sci. B 8, 1–13.

Jensen, L.S., 2013a. Animal manure residue upgrading and nutrient recovery in biofertilizers. In Sommer, S.G., Christensen, M.L., Schmidt, T., Jensen, L.S. (Eds.). Animal Manure Recycling - Treatment and Management. John Wiley and Sons Ltd. Chichester, West Sussex, UK. 302-303.

Jensen, L.S., 2013b. Animal manure residue upgrading and nutrient recovery in biofertilizers. In Sommer, S.G., Christensen, M.L., Schmidt, T., Jensen, L.S. (Eds.). Animal Manure Recycling - Treatment and Management. John Wiley and Sons Ltd. Chichester, West Sussex, UK. p.297.

Jensen, L.S., 2013c. Animal manure residue upgrading and nutrient recovery in biofertilizers. In Sommer, S.G., Christensen, M.L., Schmidt, T., Jensen, L.S. (Eds.). Animal Manure Recycling - Treatment and Management. John Wiley and Sons Ltd. Chichester, West Sussex, UK. p.302.

Jin, Y., Liang, X., He, M., Liu, Y., Tian, G., Shi, J., 2016. Manure biochar influence upon soil properties, phosphorus distribution and phosphatase activities: A microcosm incubation study. Chemosphere 142, 128–135.

Joseph, S.D., Camps-Arbestain, M., Lin, Y., Munroe, P., Chia, C.H., Hook, J., van Zwieten, L., Kimber, S., Cowie, A., Singh, B.P., Lehmann, J., Foidl, N., Smernik, R.J., Amonette, J.E., 2010. An investigation into the reactions of biochar in soil. Aust. J. Soil Res. 48, 501-515.

Keiluweit, M., Kleber, M., 2009. Molecular-Level Interactions in Soils and Sediments: The Role of Aromatic π-systems. Environ. Sci. Technol. 43, 3421–3429.

Keiluweit, M., Nico, P.S., Johnson, M.G., Kleber, M., 2010. Dynamic molecular structure of plant biomass-derived black carbon (biochar). Environ. Sci. Technol. 44, 1247–1253.

Kloss, S., Zehetner, F., Dellantonio, A., Hamid, R., Ottner, F., Liedtke, V., Schwanninger, M., Gerzabek, M.H., Soja, G., 2012. Characterization of Slow Pyrolysis Biochars: Effects of Feedstocks and Pyrolysis Temperature on Biochar Properties. J. Environ. Qual. 41, 990-1000.

Knicker, H., 2010. "Black nitrogen" – an important fraction in determining the recalcitrance of charcoal. Org. Geochem. 41, 947–950.

Lang, T., Jensen, A.D., Jensen, P.A., 2005. Retention of organic elements during solid fuel pyrolysis with emphasis on the peculiar behavior of nitrogen. Energy & Fuels 19, 1631–1643.

Lehmann, J. 2007. Bio-energy in the black. Front. Ecol. Environ. 5, 381–387.

Lehmann, J., Joseph, S., 2009. In Lehmann, J., Joseph, S. (Eds.). Biochar for Environmental Management – Science and Technology: An Introduction. Earthscan. London, UK. 1-12.

Lynch, D., Henihan, A.M., Kwapinski, W., Zhang, L., Leahy, J.J., 2013. Ash Agglomeration and Deposition during Combustion of Poultry Litter in a Bubbling Fluidized-Bed Combustor. Energy & Fuels 27, 4684–4694.

Lynch, D., Low, F., Henihan, A.M., Garcia, A., Kwapinski, W., Zhang, L., Leahy, J.J., 2014. Behavior of Heavy Metals during Fluidized Bed Combustion of Poultry Litter. Energy & Fuels 28, 5158−5166.

Li, X., Shen, Q., Zhang, D., Mei, X., Ran, W., Xu, Y., Yu, G., 2013. Functional Groups Determine Biochar Properties (pH and EC) as Studied by Two-Dimensional ^{13}C NMR Correlation Spectroscopy. PLoS One. 8 (6), 1-7.

Li-Xian, Y, L. Guo-Liang, T. Shi-Hua, S. Gavin, H. Zhao-Huan. 2007. Salinity of animal manure and potential risk of secondary soil salinization through successive manure application. Sci. Total Environ. 183, 106-114.

Liang, Y., Cao, X., Zhao, L., Xu, X., Harris, W., 2014. Phosphorus Release from Dairy Manure, the Manure-Derived Biochar, and Their Amended Soil: Effects of Phosphorus Nature and Soil Property. J. Environ. Qual. 43, 1504–1509.

Lima, I.M., Boateng, A.A., Klasson, K.T., 2009. Pyrolysis of broiler manure: Char and product gas characterization. Ind. Eng. Chem. Res. 48, 1292–1297.

Liu, T., Liu, B., Zhang, W., 2014. Nutrients and Heavy Metals in Biochar Produced by Sewage Sludge Pyrolysis: Its Application in Soil Amendment. Polish J. Environ. Stud. 23, 271–275.

McBeath, A. V., Smernik, R.J., Krull, E.S., Lehmann, J., 2014. The influence of feedstock and production temperature on biochar carbon chemistry: A solid-state ^{13}C NMR study. Biomass and Bioenergy 60, 121–129.

McKendry, P., 2002. Energy production from biomass (Part 2): Conversion technologies. Bioresour. Technol. 83, 47–54.

Mc Laughlin, H., Shields, F.E., Jagiello, J., Thiele, G., 2012. Analytical Options for Biochar Adsorption and Surface Area. Char Charact. 1–19.

Mészáros, E., Jakab, E., Várhegyi, G., Bourke, J., Manley-Harris, M., Nunoura, T., Antal, M.J., 2007. Do all carbonized charcoals have the same chemical structure? Implications of thermogravimetry: Mass spectrometry measurements. Ind. Eng.Chem. Res. 46, 5943–5953.

Mitsuoka, K., Hayashi, S., Amano, H., Kayahara, K., Sasaoaka, E., Uddin, M.A., 2011. Gasification of woody biomass char with CO_2: The catalytic effects of K and Ca species on char gasification reactivity. Fuel Process. Technol. 92, 26–31.

Müller-Hagedorn, M., Bockhorn, H., Krebs, L., Müller, U., 2003. A comparative kinetic study on the pyrolysis of three different wood species. J. Anal. Appl. Pyrolysis 68-69, 231–249.

Nagajyoti, P.C., Lee, K.D., Sreekanth, T.V.M., 2010. Heavy metals, occurrence and toxicity for plants: A review. Environ. Chem. Lett. 8, 199–216.

Nigussie, A., Kissi, E., Misganaw, M., Ambaw, G., 2012. Effect of Biochar Application on Soil Properties and Nutrient Uptake of Lettuces (Lactuca sativa) Grown in Chromium Polluted Soils 12, 369–376.

Orang, N., Tran, H., 2015. Effect of feedstock moisture content on biomass boiler operation. Bioenergy 14 (10), 629–637.

Park, J.H., Choppala, G.K., Bolan, N.S., Chung, J.W., Chuasavathi, T., 2011. Biochar reduces the bioavailability and phytotoxicity of heavy metals. Plant Soil 348, 439–451.

Pignatello, J.J., Kwon, S., Lu, Y., 2006. Effect of natural organic substances on the surface and adsorptive properties of environmental black carbon (Char): Attenuation of surface activity by humic and fulvic acids. Environ. Sci. Technol. 40, 7757–7763.

Prapaspongsa, T., Poulsen, T.G., Hansen, J.A, Christensen, P., 2010. Energy production, nutrient recovery and greenhouse gas emission potentials from integrated pig manure management systems. Waste Manag. Res. 28, 411–422.

Prendergast-Miller, M.T., Duvall, M., Sohi, S.P., 2014. Biochar-root interactions are mediated by biochar nutrient content and impacts on soil nutrient availability. Eur. J. Soil Sci. 65, 173–185.

Qiu, G., Guo, M., 2010. Quality of poultry litter-derived granular activated carbon. Bioresour. Technol. 101, 379–386.

Raveendran, K., Ganesh, A., Khilar, K.C., 1995. Influence of mineral matter on biomass pyrolysis characteristics. Fuel 74, 1812–1822.

Reeuwijk, L.P., 2002. In Reeuwijk (Ed.). Procedures for soil analysis. Sixth edit. ed. International Soil Reference and Information Centre. ISSN 0923-3792: no.9. Food and Agriculture Organization of the United Nations. Wageningen, The Netherlands.

Sistani, K., Jeffrey, M., 2005. In Prasad, M.N.V., Sajwan, K.S., Naidu, R. (Eds.). Trace Metal Accumulation, Movement, and Remediation. Soils Receiving Animal Manure. CRC Press. 689-706.

Subedi, R., Taupe, N., Ikoyi, I., Bertora, C., Zavattaro, L., Schmalenberger, A., Leahy, J.J., Grignani, C., 2016a. Chemically and biologically-mediated fertilizing value of manure-derived biochar. Sci. Total Environ. 550, 924–933.

Subedi, R., Taupe, N., Pelissetti, S., Petruzzelli, L., Bertora, C., Leahy, J.J., Grignani, C., 2016b. Greenhouse gas emissions and soil properties following amendment with manure-derived biochars: Influence of pyrolysis temperature and feedstock type. J. Environ. Manage. 166, 73–83.

Tsai, W.-T., Liu, S.-C., Chen, H.-R., Chang, Y.-M., Tsai, Y.-L., 2012. Textural and chemical properties of swine-manure-derived biochar pertinent to its potential use as a soil amendment. Chemosphere 89, 198–203.

Uzoma, K.C., Inoue, M., Andry, H., Fujimaki, H., Zahoor, A., Nishihara, E., 2011. Effect of cow manure biochar on maize productivity under sandy soil condition. Soil Use Manag. 27, 205–212.

Verheijen, F.G.A., Jeffery, S., Bastos, A.C., van der Velde, M., and Diafas, I., 2009. Biochar Application to Soils - A Critical Scientific Review of Effects on Soil Properties, Processes and Functions. EUR 24099 EN, Office for the Official Publications of the European Communities, Luxembourg, 149pp.

Wang, T., Camps-Arbestain, M., Hedley, M., Bishop, P., 2012. Predicting phosphorus bioavailability from high-ash biochars. Plant Soil 357, 173–187.

Wise, J., Vietor, D., Provin, T., Capareda, S., Munster, C., Boatengc, A., 2012. Mineral Nutrient Recovery from Pyrolysis Systems. Environ. Prog. Sustain. Energy 31, 251–255.

Wnetrzak, R., Kwapinski, W., Peters, K., Sommer, S.G., Jensen, L.S., Leahy, J.J., 2013. The influence of the pig manure separation system on the energy production potentials. Bioresour. Technol. 136, 502–508.

Yuan, H., Lu, T., Huang, H., Zhao, D., Kobayashi, N., Chen, Y., 2015. Influence of pyrolysis temperature on physical and chemical properties of biochar made from sewage sludge. J. Anal. Appl. Pyrolysis 112, 284–289.

Zornoza, R., Moreno-Barriga, F., Acosta, J.A., Muñoz, M.A., Faz, A., 2016. Stability, nutrient availability and hydrophobicity of biochars derived from manure, crop residues, and municipal solid waste for their use as soil amendments. Chemosphere 144, 122–130.

5. Mitigation of ammonia emissions during storage of cow slurry amended with biochar and sulfuric acid

This chapter gives insight into the effectiveness of Sitka spruce biochar, produced via a uniquely designed pyrolysis unit, namely Kon-Tiki kiln, to reduce ammonia, methane and hydrogen sulphide emissions during the storage of cow slurry.

5.1. Abstract

Biochar, a porous recalcitrant carbon rich material derived from pyrolysis, has gained attraction as an amendment to mitigate some of the environmental problems associated with animal slurry handling, including harmful emissions. The aim of this study was to evaluate the potential of Sitka spruce biochar, produced via a uniquely designed pyrolysis unit called Kon-Tiki kiln, to reduce ammonia (NH_3) emissions during the storage of cow slurry and to further investigate pollution swapping through methane (CH_4) and hydrogen sulphide (H_2S) emissions. Two other treatments, namely the addition of sulfuric acid to reduce the slurry pH to 5.5 and a combination of biochar and acid, were included as a comparison. Biochar neither decreased nor increased NH_3 emissions, while sulfuric acid and the combined acid and biochar treatment decreased NH_3 emissions by about 50% during a storage period of 49 days. Biochar addition resulted in inconsistent CH_4 fluxes, which were both increased and decreased compared to un-amended slurry. No H_2S emissions were observed for biochar treated slurry as opposed to both acidified treatments. Biochar changed the physico-chemical characteristics of cow slurry by increasing total carbon (TC), dry matter (DM), and the C:N ratio with visual evidence of altered aeration properties and microbial activity. Even though biochar could not compete with acidification as a NH_3 or CH_4 mitigation option during slurry storage, biochar had the advantage of not increasing H_2S emissions. The benefits of biochar in terms of altering slurry physico-chemical properties and shifting microbial communities for a significantly longer storage period should be subject to further investigation.

5.2. Introduction

Livestock production systems have undergone substantial changes in the past decades towards large and intensive farming practices as a result of the radical increasing population and meat consumption worldwide. As a consequence, manure is accumulating in specific areas causing regional and global environmental problems. Some consequences are groundwater eutrophication through nitrate and phosphate leaching (Sørensen and Jensen, 2013), emissions of ammonia (NH_3), greenhouse and malodorous gases (Feilberg and Sommer, 2013a; Sommer *et al*., 2013a).

Mitigation of NH_3 emissions are of particular concern as they pose health risks to humans and animals (Schiffman *et al*., 2006) and at the same time nitrogen, a valuable nutrient, is lost to the atmosphere. In addition, NH_3 may cause acidification and eutrophication (Bouwman *et al*., 2002) and may undergo transformation to nitrous oxide (N_2O) (Avrahami *et al*., 2002) when deposited from the air into water and soils. In 2011 agriculture accounted for 93.3% of the total NH_3 emissions in the European Union (EU), and three quarters were attributed to manure management (Eurostat, 2012). Hence, the EU has set NH_3 emission limits and NH_3 was also included in the Convention on Long-range Transboundary Air Pollution (CLRTP) by the United Nations (UN). NH_3 emissions occur during all stages of animal manure handling, namely animal houses, storage, and application (Kai *et al*., 2008). Slurry characteristics that determine NH_3 volatilisation include the total concentration of ammoniacal nitrogen (TAN = NH_4^+ + NH_3), pH, temperature, the surface area and turbulences in slurry or air (Sommer and Feilberg, 2013).

Likewise, considerable amounts of methane (CH_4) emissions may be emitted from manure or slurry storage. CH_4 belongs to the greenhouse gases (GHG) emitted from livestock along with carbon dioxide (CO_2) and N_2O. The global warming potential of CH_4 and N_2O are around 25 and 298 times higher than CO_2 over a 100-year time period respectively (IPCC, 2014). Enteric fermentation and manure together account for approximately 80% of agricultural CH_4 emissions and about 35% to 40% of the total anthropogenic CH_4 emissions (Steinfeld *et al*., 2006). CH_4 is produced in anaerobic environments and involves hydrolysis and degradation of higher molecular weight organic compounds to e.g. long-chain acids and alcohols, which are broken down into short-chain acids and finally CO_2 and CH_4 during fermentation (Sommer *et al*.,

2013b). The formation of CH_4 is dependent on the surrounding environment, such as temperature, and the physical and chemical properties of the manure (Sommer *et al*. 2013b). Also microorganisms can be a significant factor effecting GHG emissions depending on the source of nutrients available to them. CH_4 production in the slurry most likely depends on the activity of slow-growing acetotrophic methanogens (Sommer *et al*. 2013b)

Some mitigation measures for NH_3 and CH_4 from animal manure and slurry are already common practices in some European countries, for example covering of the storage tanks (Williams and Nigro, 1997; Berg *et al*., 2003) and diet manipulation (Feilberg and Sommer, 2013b). Other treatment options are being investigated, such as temperature control (Van der Stelt *et al*., 2007; Panetta *et al*., 2005), stirring (Panetta *et al*., 2005), oxidising agents (McCrory and Hobbs, 2001), enzymatic and bacterial preparations (Van der Stelt *et al*., 2007), urease inhibitors (Panetta *et al*., 2005), slurry acidification (Petersen *et al*., 2012; Panetta *et al*., 2005), and binding additives such as zeolite (Jaramillo and Chandross, 2004) and other adsorbents (Van der Stelt *et al*., 2007).

Investigations have shown the addition of acids to slurries to be very effective and economically worthwhile in mitigating NH_3 and CH_4 (Wang *et al*., 2014). Acids shift the equilibrium from NH_3 to NH_4^+, contributing to the fertiliser value of the slurry, and reduce CH_4 emissions as acidic environments below 6.5 are not appropriate for methanogenic activity. Most studies have been conducted using strong acids, but also base precipitating salts and easily fermenting materials are under investigation (Fangueiro *et al*., 2015). Sulfuric acid is the only acid used on a commercial scale. In Denmark the in-house acidification systems has been introduced, where slurry accumulating under slatted floors is adjusted to pH 5.5. This system has been approved as Best Available Technology (BAT) in Denmark (Dai and Blanes-Vidal, 2013; Kai *et al*., 2008). The disadvantage of using sulfuric acid is its hazardous properties and foaming of slurry during acidification. Other acids have also been investigated (Regueiro *et al*., 2016), and the use of aluminium sulfate has shown interesting results, however the effects using this additive are still unclear.

The addition of natural materials may also alter NH_3 and CH_4 emissions by their adsorbing properties and chemical alterations. Luo *et al*. (2004) attributed the

beneficial effect of organic-rich materials, such as pine bark, sawdust and wood shavings, in reducing NH_3 emissions to direct sorption of NH_4^+ or NH_3, or enhanced microbial N immobilisation. Amon *et al*., (2006) found that covering cow slurry with a layer of chopped straw instead of a wooden lid increased CH_4 emissions by 21.7% and concluded that the straw serves as an additional carbon source for methanogens. Furthermore, covering the slurry store with a layer of chopped straw lead to a dramatic increase in net total N_2O emissions. Conversely Yamulki (2006) found that straw addition to farmyard manure reduced both CH_4 and N_2O emissions and commented that additives with high carbon contents could reduce GHG emissions due to changes in dry matter (DM) content, C:N ratio and aeration of the manure.

Biochar is gaining attraction to be used for different purposes in agriculture, e.g. as a silage agent, feed additive, litter additive or slurry treatment (Schmidt, 2014a). Biochar is a product of pyrolysis of a carbon rich biomass and often possesses a high surface area and porosity. The reaction of NH_3 with the surface groups on biochar has been known for a while (Holmes and Beebe, 1957). NH_3 can react with carboxylic groups on the biochar's surface, either as a Brøwnsted or Lewis acid, to form an ammonium salt or an amide respectively (Figure 5-1).

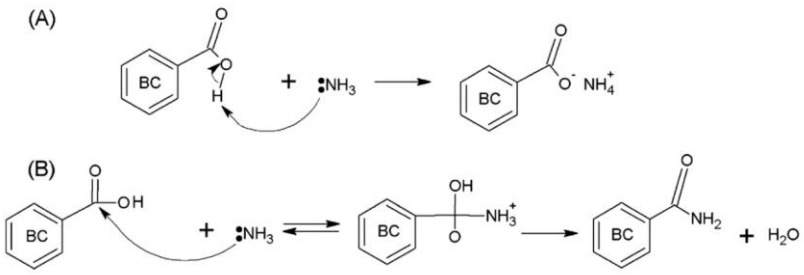

Figure 5-1: Biochar reaction with ammonia (Spokas et al., 2012)

The sorption of NH_4^+ or NH_3 to biochar depends on the biochar's surface chemistry and its physical properties such as surface area and pore structure (Spokas *et al*., 2012). These properties again depend on the process conditions, such as pyrolysis temperature, heating rate and residence time, and the physical and chemical properties of the original feedstock (Keiluweit *et al*., 2010). Activation of biochar using acids, bases or steam to create and alter surface functional groups can positively affect sorption of NH_4^+ (Reddy, 2012). The cation exchange capacity (CEC) of a biochar has found to be the most important property for NH_4^+ or NH_3 sorption (Gai *et al*., 2014;

Zeng *et al*., 2013), but also other effects might play a role, such as electrostatic exchange with other cationic species on the surface of the char (Hale *et al*., 2013). Biochar has been shown to be efficient in adsorbing NH_3 in the gas phase (Asada *et al*., 2002; Asada *et al*., 2006; Iyobe *et al*., 2004). Taghizadeh-Toosi *et al*. (2012a) found that biochar was able to capture NH_4^+ generated from ruminant urine-N and demonstrated the bioavailability of the adsorbed NH_4^+ using isotopic labelling with ^{15}N during plant growth and nutrient uptake experiments (Taghizadeh-Toosi *et al*., 2012b). Furthermore, biochar may affect ammonia-oxidising and denitrification bacteria in the slurry (Song *et al*., 2013; Wei *et al*., 2014) by altering its physico-chemical properties, such as aeration, C:N ratio and pH.

While there are many studies on the effects of concentration, temperature and pH on NH_4^+ and NH_3 sorption to biochar in aqueous solutions (Chintala *et al*., 2013; Gai *et al*., 2014; Hale *et al*., 2013; Zeng *et al*., 2013), few studies exist for real scale slurry addition. Haeni *et al*. (2012) investigated the effect of adding biochar and acid activated biochar to cow slurry on the release of NH_3 emission during storage. Non-activated biochar both increased and decreased NH_3 emissions slightly. The authors found a significant reduction of NH_3 emissions when acid activated biochar was amended to slurry, however the results did not reveal whether surface functional groups or the porous structure of the biochar were responsible for the NH_3 sorption or if simply the pH reduction reduced NH_3 emissions.

The boom in biochar research in recent years has provided the scientific community with a broad understanding of different production methods and application opportunities of biochar, however there still remain uncertainties about the effectiveness of biochar, in particular as the properties of biochar are prone to change with changing environment. If biochar is to become more commercially available in the future, it seems reasonable that research goals should revolve around factors like feedstock availability, end use, available technologies and infrastructure. Reddy (2012) commented that "*The definition of biochar is more about its creation and intended application rather than what it is composed of."*

In our study biochar was produced from Sitka spruce, the most common tree species in the Republic of Ireland, occupying 52.4% of its forest area (Statistics, 2014). The pyrolysis unit was developed in Switzerland with the focus on its simple and cheap

design and elimination of harmful emissions arising from the process. The main objective of this study was to evaluate the potential of Sitka spruce biochar to reduce NH_3 emissions during storage of cow slurry. Two further treatments, namely acidification to pH 5.5 with sulfuric acid and a mixture of the two additives, were included as a comparison. We hypothesised that biochar addition would reduce NH_3 emissions from stored cow slurry as a result of its morphology and surface functionality and in addition increase CH_4 emissions due to the addition of carbon with biochar. In addition, we looked at the effect of the adding sulfuric acid on CH_4 and H_2S emissions, keeping in mind the risk of pollution swapping when adding either a carbon and/or sulphur rich source to stored cow slurry.

5.3. Methodology

5.3.1. Biochar production and characterisation

Biochar was produced from Sitka spruce wood using an 850 L Kon-Tiki Open Fire Kiln, developed by the Ithaka Institute, a non-profit research foundation based in Valais, Switzerland. The Kon-Tiki was named after the Inca sun god (Con Tici Viracocha) and was designed after a Japanese Cone Kiln (the Moki Kiln) (Taylor, 2014). The Moki Kiln is a shallow cone of about 45° angle, as illustrated in Figure 5-2. The air is convected in a way to maintain combustion above the feedstock. Pyrolysis is driven by radiant, reflected and conducted heat. The gases emitted from the biomass during pyrolysis are consumed by the flames resulting in clean smokeless combustion. Char is preserved in the lower layer in the oxygen free zone. The cone kiln belongs to a category called Cavity Kilns or Top Lit Open Burn Kilns as opposed to retorts and microgasifiers. The method is cheap, simple and robust (Schmidt, 2014b).

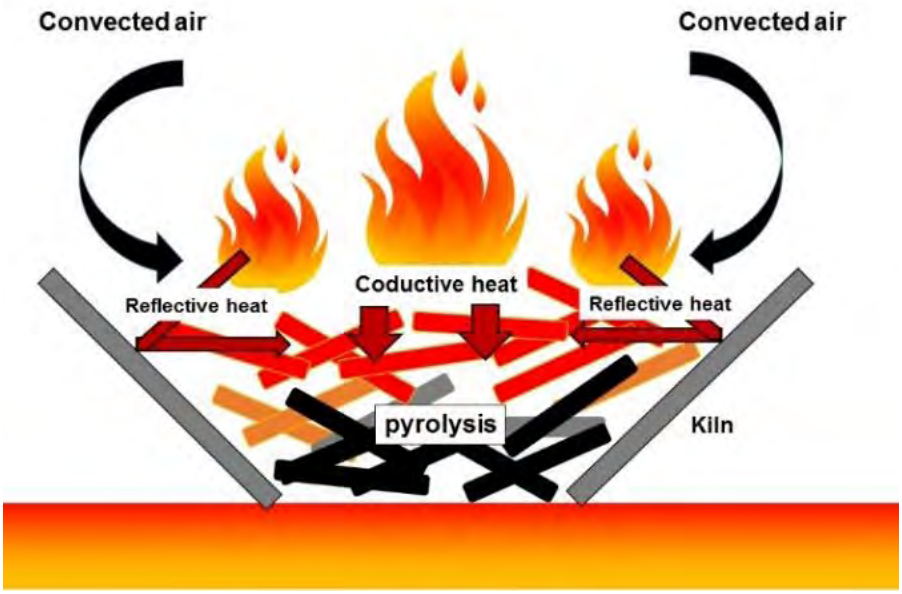

Figure 5-2: The Japanese Cone Kiln (the Moki Kiln) (Schmidt, 2014b)

The biochar was characterised fully complying with the guidelines for European biochar certification (EBC, 2012). A summary of the results and list of standard procedures are presented in Table 5-1.

The cation exchange capacity (CEC) of biochar was evaluated via Na^+ replacement with NH_4^+. The method was adopted from (Uzoma *et al*., 2011). Approximately 1 g of biochar was weighed with a precision of 0.01 g and transferred into a centrifugation tube with 20 ml of sodium acetate solution (1 N). The solution was shaken for 1 h at 16 rpm to saturate the exchange sites. The biochar solution was transferred to a Buchner funnel and vacuum filtrated through an ashless quantitative filter paper (DP 5895 110). The biochar was washed twice with the same sodium acetate solution (1 N). The excess sodium acetate was removed by washing with 30 ml of ethanol (96%) and repeated four to five times until the solution reached a conductivity of < 40 µS cm^{-1}. To replace the adsorbed Na^+ 30 ml of ammonium acetate was added to the funnel and filtered three times. The extract was transferred to a 100 ml flask and filled up with ammonium acetate solution before quantification of the Na with flame assisted atomic absorption spectroscopy (FA-AAS) using a Varian Spectra AA-220.

Major and minor elements in the biochar were quantified using inductively coupled plasma optical emission spectrometry (ICP-OES, Thermo Elemental Co. Iris Intrepid II XDL). The biochar (0.1 g) was ashed at 500 °C for 8 h according to the modified dry ash method by Enders *et al*. (2012) and digested in 3 ml HNO_3 and 9 ml HCl. The

samples were filtered, diluted to 25 ml with ultrapure water, and analysed with ICP- OES.

Scanning electron microscopy (SEM) was used to analyse the morphology of the char. The biochar was crushed, placed onto carbon tabs, and coated with gold to mitigate charging. The analysis was performed using an Ultra-High-Resolution Analytical FE- SEM SU-70 (Hitachi). The accelerating voltage was 20.0 kV. For evaluating the presence of functional groups in the char, a sample was ground finely before analysis using an Agilent Cary 630 Fourier transform infrared spectrometer (FTIR).

The multipoint Brunauer-Emmett-Teller - N_2 surface area (BET-N_2 SA) was determined from the N_2 adsorption-desorption isotherm of the biochar sample using a Quantachrome Autosorb AS-1 instrument in a relative pressure range (p/p_0) from 0.05 to 0.30. The samples (0.100 g) were degassed prior to analysis under vacuum at 200 °C for 15 h. Nitrogen was used as the sorbent gas, and the process took place at - 196 °C. The pore volume and pore size distribution were calculated from the desorption isotherm using the Barrett-Joyner-Halenda (BJH) theory.

5.3.2. Slurry characterisation

Slurry from grass fed cattle was sampled from an outdoor storage tank in Co. Kerry, Ireland in late spring of 2015, which had been stored for more than four months over the winter period. The slurries were analysed before and after the experiment for their moisture (according to BS EN 14774-1), organic matter (OM) (according to I.S. EN 14775:2009), and total carbon (TC) and total nitrogen (TN) content using an Elemental Vario EL Cube analyser.

*Table 5-1: Biochar characteristics on an as received (ar.) and dry basis (db.). * Limits are taken from EBC (2012)*

Parameter	Unit	Standards	Limits*	ar.	db.
Bulk Density	g cm^{-3}	EN 15103:2009 (E)		460	-
Specific Surface Area (BET-N_2)	m^2 g^{-1}	ISO 9277:2010 (E)		-	267
True Density	g cm^{-3}	ISO 5072:2013 (E)		-	1.77
Total water	wt.%	I.S. EN 14774-2:2009		69.1	-
Ash Content (550 °C)	wt.%	I.S. EN 14775:2009		-	5.4
Volatile matter (VM)	wt.%	I.S. EN 15148:2009		-	7.0
Fixed carbon (FC)	wt.%	100% – Ash_{db} – VM_{db}		-	88.9
Hydrogen	wt.%	EN 15104:2011 (E)		0.38	1.07
Carbon	wt.%	EN 15104:2011 (E)	>50	25.83	84.9
Nitrogen	wt.%	EN 15104:2011 (E)		0.12	0.41
Oxygen	wt.%	Calculated		2.24	7.25
Polarity index (O+N)/C (molar)		Calculated			0.07
Carbonate as CO_2	wt.%	ISO 925: 1997 (E)		0.72	2.32
Carbon Organic	wt.%	Calculated		30.88	84.3
Ratio H:C (molar)		Calculated	<0.6	0.15	0.15
Ratio H:C organic (molar)		Calculated	<0.7	0.15	0.15
Ratio O:C organic (molar)		Calculated	<0.4	0.06	0.06
Sulphur (total)	wt.%	EN 15289:2011 (E)		0	0
pH (0.01 M $CaCl_2$)		ISO 10390:2005		9.15	-
Electrical Conductivity	µS cm^{-1}	ISO 11265:1994 (E)		1024	-
Salt Content	g kg^{-1}	I.S. EN 772-5-2002		1.195	3.87
Salt content cal. with bulk density	g l^{-1}	Calculated		0.549	1.78
Cation exchange capacity	$mmol_c$ kg^{-1}	Na^+ replacement with NH_4^+		25.5	25.5
Major elements					
Phosphorus (P)	g kg^{-1}	EN 15290:2011 (E)			1.67
Magnesium (Mg)	g kg^{-1}	EN 15290:2011 (E)			2.41
Calcium (Ca)	g kg^{-1}	EN 15290:2011 (E)			20.9
Potassium (K)	g kg^{-1}	EN 15290:2011 (E)			2.98
Sodium (Na)	g kg^{-1}	EN 15290:2011 (E)			0.99
Iron (Fe)	g kg^{-1}	EN 15290:2011 (E)			0.41
Sulfur (S)	g kg^{-1}	EN 15290:2011 (E)			0.44
Minor Elements					
Lead (Pb)	g t^{-1}	EN 15297:2011 (E)	120		0.92
Cadmium (Cd)	g t^{-1}	EN 15297:2011 (E)	1		0
Copper (Cu)	g t^{-1}	EN 15297:2011 (E)	100		31.3
Nickel (Ni)	g t^{-1}	EN 15297:2011 (E)	30		2.95
Zinc (Zn)	g t^{-1}	EN 15297:2011 (E)	400		131
Chromium (Cr)	g t^{-1}	EN 15297:2011 (E)	80		2.42
Boron (B)	g t^{-1}	EN 15297:2011 (E)			27.2
Manganese (Mn)	g t^{-1}	EN 15297:2011 (E)			222

5.3.3. Slurry amendment and storage

Slurries were weighed into 5 L cylindrical glass containers of 17 cm diameter and a height of 22 cm to equal weights of 4.3 kg, with three replicates of each treatment: S (slurry), SB (slurry amended with biochar), SpH (acidified slurry), SpHB (acidified slurry amended with biochar). Biochar was crushed, sieved to particle size < 5 mm and weighed to a final concentration of 3.5 wt.%$_{ar}$ (or 1.1 wt.%$_{db}$) of SB and SpHB treatments one day before acidification and starting the storage period. For acidification concentrated sulfuric acid was added dropwise to SpH (1.0 wt.%) and SpHB (1.0 wt.%) to decrease the pH to 5.5. The slurries were stirred carefully during acidification to avoid excessive foaming.

The storage containers remained undisturbed for 49 days. A schematic of the continuous gas flow experiment is presented in Figure 5-3. The slurry containers were weighed before and after the storage period to determine the weight loss. Furthermore, the headspace (approximately 1 L) and temperature were measured before gas sampling as the volume changed during the storage period. The temperature of the slurries ranged between 16 ºC and 18 ºC throughout the experiment, which was measured with a conventional glass thermometer. The pH was monitored weekly after gas sampling for CH_4 using an Orion 420 pH meter.

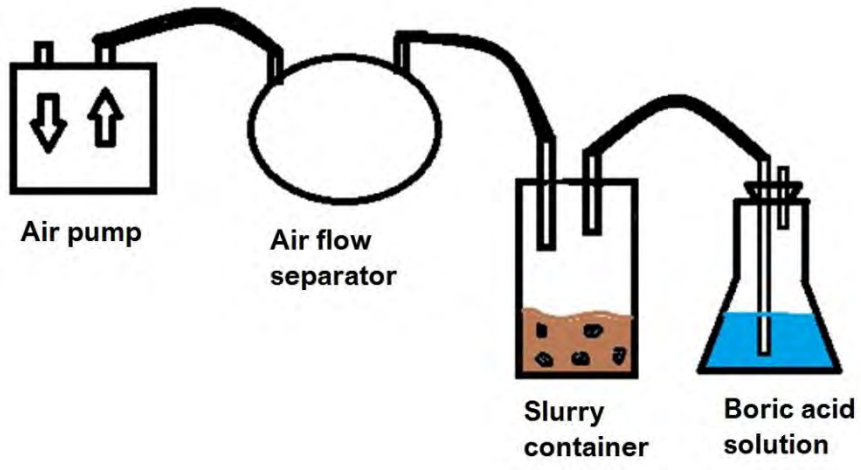

Figure 5-3: Schematic of the continuous gas flow experiment

5.3.4. Gas analysis

The containers were sealed at the top with a screw cap GL45, which fitted a Dreschel bottle head. An air flow of 40 ml min^{-1} was established across the slurry surface. An air pump pumped air into an air separator, which distributed the air amongst all treatments. The flow rate of the air to each individual container was measured with aid of an air flow meter (CSI 6000 Flowmeter, Ellutia) and adjusted accordingly using high-density polyethylene stopcocks. The air then holding the anaerobically produced gas was bubbled into an acid trap comprised of a saturated solution of boric acid solution (H_3BO_3). The boric acid captures the NH_3, forming an ammonium-borate complex, according to equation 5.1 and 5.2. The boric acid solution was saturated to ensure that all NH_3 emissions were captured in the solution and replaced every seven days.

$$NH_3 + H_3BO_3 \rightleftharpoons NH_4^+ + H_2BO_3^- \qquad \textit{equation 5.1}$$

$$\{H[B(OH)_4] + NH_3 \rightarrow NH_4[B(OH)_4]\} \qquad \textit{equation 5.2}$$

The equivalent point of an aliquot of each borate solution (20 ml) was determined using standardised 0.005 M HCl. The HCl solution was standardised with a known concentration of sodium carbonate and the blank was subtracted from the results. The amount of NH_3 captured in solution was equivalent to the titration volume of the HCl solution required according to equation 5. Equation 5.3 and 5.4 present the titration reactions.

$$H_2BO_3^- + H^+ \rightleftharpoons H_3BO_3 \qquad \textit{equation 5.3}$$

$$\{NH_4[B(OH)_4] + HCl \rightarrow (NH_4)Cl + H[B(OH)_4]\} \qquad \textit{equation 5.4}$$

$$NH_3\ (mol) = HCl\ (mol\ L^{-1}) \times \text{Titre volume (L)} \qquad \textit{equation 5.5}$$

For measuring CH_4 emissions the Drechsel heads were replaced by an airtight lid to create a steady state. A septum in the lid served as a gas sampling port. Gas samples were drawn from the containers using a 100 ml glass syringe at time 0 (t_0) and after two hours (t_2). After each sampling the withdrawn air was replaced within the headspace by an identical volume of atmospheric air in order to minimize any pressure reduction. The gas samples were injected immediately into an Agilent Micro-GC 3000. The Micro-GC was equipped with a thermal conductivity detector for the

determination of permanent gases. The column was a PLOT U column of 12 µm/320 µm/10 m and Pre Col PLOT U 30 µm/320 µm/3 m column, using argon as the carrier gas to determine CH_4. The chromatograph was calibrated regularly with a standard gas mixture. The gas remaining in the syringe after GC analysis was injected into a hydrogen sulphide (H_2S) portable detector to trace any H_2S emitted from the treatments.

Concentrations of CH_4 were converted to flux per kg of slurry per hour:

$$CH_4\ flux\ = \frac{(ct_1 - ct_0) * HV * d}{t * s} \qquad \textit{equation 5.6}$$

where CH_4 flux is the CH_4 evolution rate (µg kg^{-1} h^{-1}); $ct_{0,1}$ (µg) are the CH_4 concentrations in the sampled air; HV (m^3) is the headspace volume; d (g m^{-3}) is the volume to mass coefficient, which depends on the temperature, pressure and molar weight of the gas species according to the ideal gas law; t (h) is the elapsed time and s (m^2) is the slurry surface area.

5.3.5. Statistical analysis

Data obtained on the properties of cow slurries before and after storage, cumulative NH_3 emissions, and cumulative CH_4 fluxes were analysed using a one-way ANOVA (IBM SPSS statistics22). A Shapiro-Wilk's test ($p > 0.05$) showed that the results were approximately normally distributed. The results were tested for homoscedasticity using Leven's test. Means were partitioned using a Tukey's HSD post-hoc test to assess significant differences ($p < 0.05$) between treatment means.

5.4. Results and Discussion

5.4.1. Biochar properties

The properties of the Sitka spruce biochar are presented in Table 5-1. The high moisture content (69 wt.%) is the results of quenching the biochar with water to terminate the pyrolysis process. It is the general agreement that moist biochar is easier to handle compared to dry biochar, e.g. during application to soil; however moist conditions may attract bacterial or fungal growth during storage. The biochar complied with the required threshold values for premium grade European biochar certification (EBC, 2012). The requirements include a carbon content above 50 $wt.\%_{db}$ and a

maximum concentration for heavy metals which comply with Switzerland's Chemical Risk Reduction Act.

The FTIR spectrum in Figure 5-4 provides information about the biochar's functional group chemistry. The signals around 1500 cm^{-1}**,** 1400 cm^{-1} and 880 cm^{-1} might be attributed to C–C stretch and C–H "oop" of aromatic components respectively. The peak around 1000 cm^{-1} is likely attributed to the C-O stretching vibration of alcohols, carboxylic acids, esters or ethers (Coates, 2000). The presence of carboxylic functional groups has been shown to be an important feature for NH_4^+ sorption as these groups influence the CEC. Gai *et al*. (2014) suggested that the CEC of biochar was the dominant factor affecting NH_4^+ sorption, as opposed to specific surface area and pore structures, which followed different trends. In their study CEC decreased with increasing charring temperature as acidic functional groups were lost. The low molar H:C and O:C ratios as well as the high fixed carbon (FC) content of the biochar (Table 5-1) indicate a high degree of carbonisation and a shift from aliphatic to aromatic functionality with a high carbon sequestration potential (Keiluweit *et al*., 2010; Budai *et al*., 2013). The high degree of aromaticity and extent of carbonisation is also supported by the biochar's polarity index of 0.07 (Table 5-1), which conforms with the highly aromatic manure chars presented in chapter 4 (section 4.3.2) as opposed the original Sitka spruce feedstock (polarity index = 0.71). The temperature was hence assumed to be in the higher pyrolysis range (~700 °C). Functional groups such as carboxylic acid or carbonyl groups may develop over time due to weathering in an oxidising environment such as soil (Joseph *et al*., 2010). This might also affect the anion exchange capacity (AEC) and consequently the NO_3^- adsorption capacity, as these properties correlate with basic functional groups, for example heterocyclic functional groups containing O or N (Darvell *et al*., 2012). Lawrinenko (2014) conducted an in depth investigation on the AEC of biochar and concluded that the AEC in the studied biochar was primarily due to oxonium groups. Changes in physical chemical properties of biochar in an anaerobic environment such as stored slurry is still unreported.

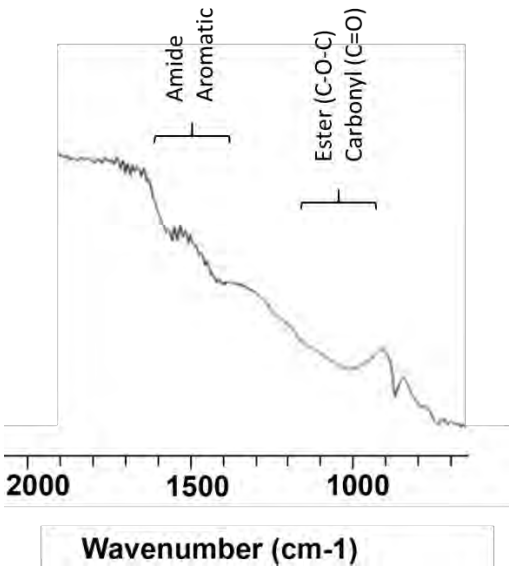

Figure 5-4: FTIR spectrum of Sitka Spruce biochar

The morphology of biochar depends to a large extent on the original feedstock and pyrolysis system (Downie *et al*., 2009). The SEM image (Figure 5-5) reveals the porous honeycomb-like structure of the biochar with pores of around 10 µm in diameter. The morphology resembles the typical structure of a physically activated carbon, derived from the capillary structure of the raw carbonaceous material (Wildman and Derbyshire, 1991).

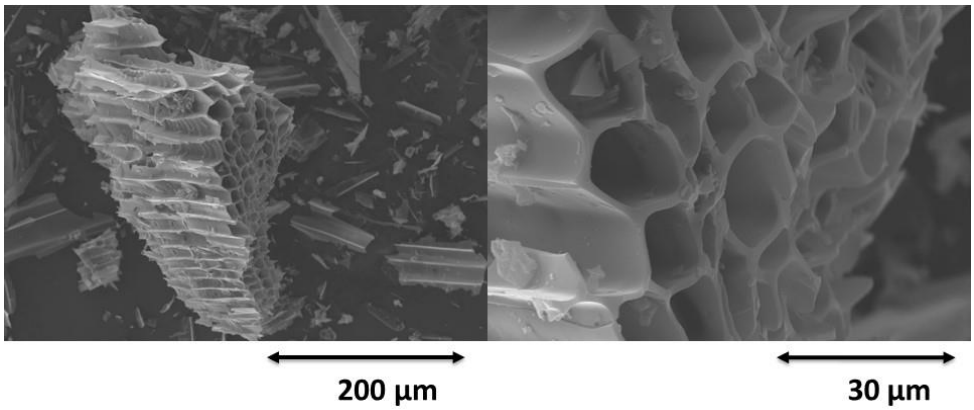

Figure 5-5: Scanning electron microscopy (SEM) image (20.0 kV) of the Sitka spruce biochar

These macro-pores (> 50nm) serve as a feeder to meso- (2 nm – 50 nm) and micro-pores (< 2 nm) (Fukuyama *et al*., 2001), which were also present in the biochar as revealed by the pore size distribution (Appendix III). These micro-pores likely contribute considerably to the high surface area of the biochar (267 $m^2 g^{-1}$) (Table 5-1).

Macro-pores are relevant to soil functions such as aeration, hydrology and movement of the roots (Downie *et al*., 2009). Furthermore, the pores' dimension is suitable to provide a habitat for a vast variety of soil microbes (Thies and Rillig, 2009).

5.4.2. Slurry properties

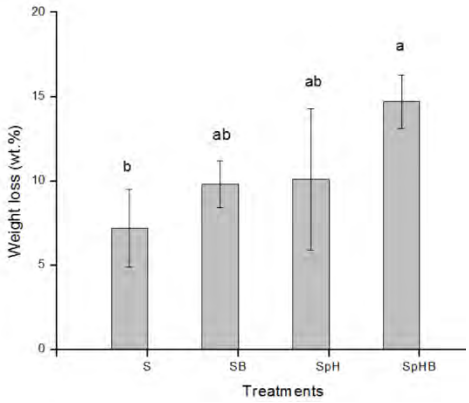

Figure 5-6: Weight loss of cow slurries during storage. S (slurry), SB (slurry amended with biochar), SpH (acidified slurry), SpHB (acidified slurry amended with biochar). Different small letters indicate significant differences ($p < 0.05$) ($n = 3$).

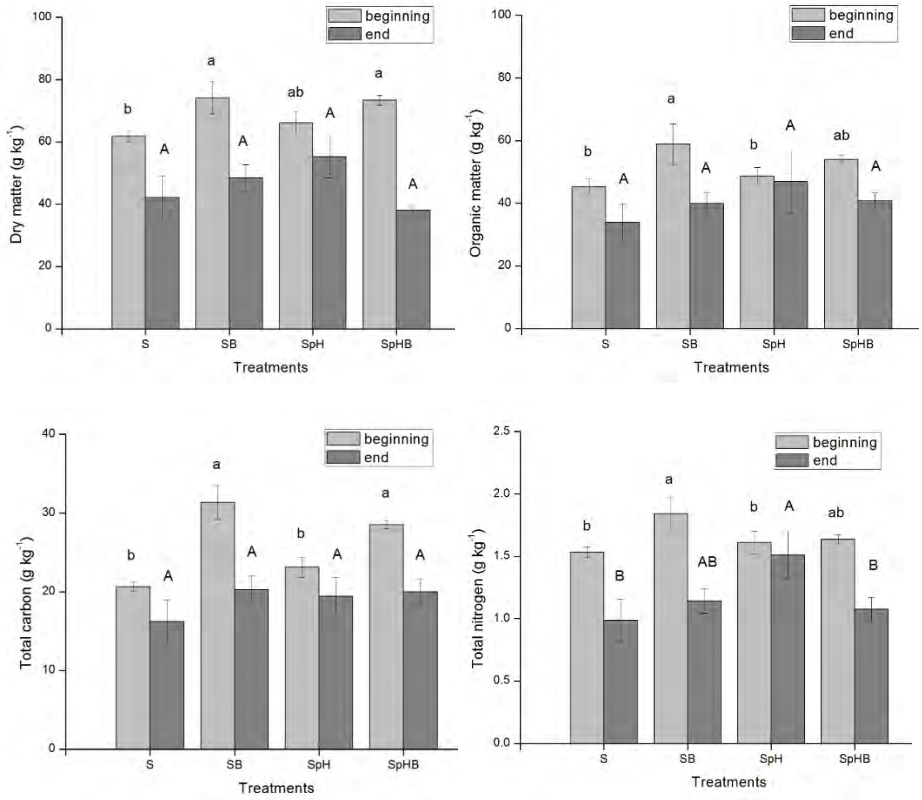

Figure 5-7: Properties of cow slurries. Abbreviations same as Figure 5-6. Different small letters indicate significant differences ($p < 0.05$) before, different capital letters indicate significant differences ($p < 0.05$) after slurry storage.

The pH of the cow slurry (7.25 ± 0.06) did not change within one day of biochar addition (7.22 ± 0.05). A rise in pH was expected when adding biochar with a pH of 9.15; however, the buffering capacity of the slurry might have prevented the pH increase. The weight loss and properties of the cow slurries at the beginning and at the end of the storage period are presented in Figure 5-6 and Figure 5-7. The total weight loss was higher for acidified slurry (SpH and SpHB) compared to non-acidified slurry (S and SB) treatments. Biochar addition also increased weight loss, but was only significant when in combination with acid. Biochar addition increased DM content by about 20 wt.% and 11 wt.% for SB and SpHB respectively. The OM and TC contents were significantly increased in the biochar amended slurries than in the slurries without biochar at the beginning of the storage period for both acidified and non-acidified slurries, while a significant increase was the case with TN for non -acidified slurries only. After 49 days the DM and OM contents of all samples had decreased as a result of water evaporation, biomass decomposition, and subsequent gaseous losses. The lowest decrease in DM content was observed for SpH (16 wt.%), followed by S (32 wt.%) and SB (35 wt.%), and the highest decrease was observed for SpHB (48 wt.%) and was significant only for S, SB and SpHB. The same phenomenon was observed for OM, where the lowest decrease was observed for SpH (4 wt.%), followed by S and SpHB (25 wt.%) and the highest decrease was observed for SB (32 wt.%). A higher loss of TC was encountered for SB (35 wt.%) and SpHB (30 wt.%) compared to S (21 wt.%) and SpH (16 wt.%). The TN content decreased by about 35 wt.% for all treatments except for SpH where a lower decrease of 6 wt.% was observed.

The results suggest that biochar alone changed the slurry characteristics by increasing DM, OM, TC, and TN consequently. Biochar addition resulted in higher TC and OM loss over the time of the storage period. Acidification resulted in the lowest loss of DM, OM, TC, and TN, which suggests inhibition of microbial decomposition of OM. However, biochar addition and subsequent acidification resulted in higher decreases of DM, OM, TC and TN than acidification alone. In general biochar addition appeared to accelerate decomposition of OM.

5.4.3. pH value and temperature

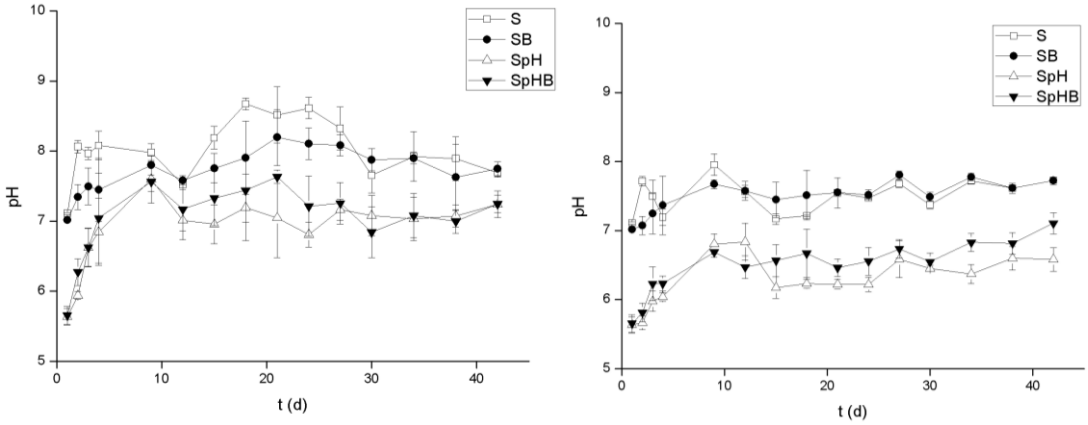

Figure 5-8: pH evolution at slurry surface (left) and at base of slurry container (right) of S (slurry), SB (slurry amended with biochar), SpH (acidified slurry) and SpHB (acidified slurry amended with biochar)

In general pH evolution for non-acidified slurries (S and SB) and acidified slurries (SpH and SpHB) behaved similarly (Figure 5-8). The pH was higher at the surface of the treatments than at the base of the slurry container with a difference in pH of about 0.5, possibly due to the rise of NH_3 to the surface. Canh *et al*. (1998) reported that pH in stored slurry is related to the distance from the surface. In the first 9 days of the experiment the pH increased from 7 and stabilised between 7.5 for S and SB and increased from 5.5 and stabilised between 6.5 and 7.0 for SpH and SpHB respectively. It was noticed that pH evolution of S and SB behaved very similarly, while SpHB showed a slightly higher pH than the SpH at the base of the container after 49 days. The rise of pH over time can be explained by the buffer components in the slurry, such as ammonium and carbonates. Also changes in volatile fatty acids concentration, emissions of H_2S from sulfuric acid, and mineralisation occur increasing the pH again. Overall biochar had no significant effect on pH evolution in SB compared to S, however an increase in pH was observed for SpHB compared to SpH.

5.4.4. Ammonia emissions

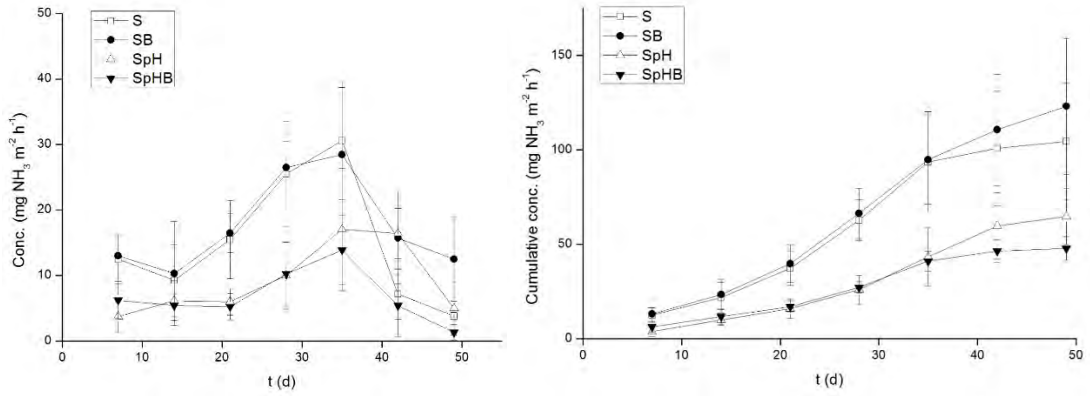

Figure 5-9: NH_3 emissions (left) and cumulative NH_3 emissions (right) over a seven-week period of S (slurry), SB (slurry amended with biochar), SpH (acidified slurry) and SpHB (acidified slurry amended with biochar)

Figure 5-9 illustrates total NH_3 emissions and the cumulative NH_3 emissions for all treatments. Acidification reduced cumulative NH_3 emissions by about 50 wt.% (not significant according to Tukey's HSD post-hoc test), while biochar had no influence on cumulative NH_3 evolution over a 49-day time period. This indicates that biochar was not effective in binding TAN either by adsorption nor through other mechanisms. Even though biochar has shown to be an effective sorbent for NH_4^+ and NH_3 in aqueous solutions (Gai *et al*., 2014; Zeng *et al*., 2013; Hale *et al*., 2013), the addition to cow slurry on the other hand shows little evidence of adsorption. Slurry is composed of a variety of organic compounds ranging from long chain polymers to short chain low molecular weight molecules and some of these might clog the biochar pores. Eykelbosh *et al*. (2015) found that biochar-amended soil preferentially retained high-molecular weight, humic-like DOC species, but did not retain low-weight amino acid-like species. Furthermore, divalent cations such as Ca^{2+} and Mg^{2+}, present in solution might compete with NH_4^+ for the adsorption sights. Our results confirm the findings by Haeni *et al*. (2012), who found no significant influence of biochar on NH_3 emissions; in fact, in their study biochar altered NH_3 emissions both ways, but only slightly.

NH_3 accounted for approximately 15 wt.% and 19 wt.% of TN loss for S and SpH respectively, while NH_3 accounted for 10 wt.% and 7 wt.% of TN loss for SB and SpHB respectively. This indicates that other N-containing gasses, e.g. N_2O, might have occurred in higher amounts. A finding worth mentioning is the fact that biochar

amended slurries, in particular SB, developed a high amount of foam throughout, but particularly at the beginning of the storage period, which suggests strongly that biochar changed the aeration properties of the slurry. Foaming might induce the release of air trapped in the biochar pores or carbonates present in the biochar forming carbonic acid. This might also explain the buffering effect when biochar was added to the slurry, with no increase in pH observed. An investigation on N_2O formation with biochar addition to animal slurry should be considered as N_2O emissions occur when both aerobic and anaerobic conditions coexist in manure as a by-product of the nitrification and denitrification process (Loyon *et al*., 2007). Additives with carbon contents have previously been reported to both increase N_2O emissions (Amon *et al*., 2006) and reduce N_2O emissions of slurry stores (Yamulki, 2006) depending on the DM content, C:N ratio and aeration of manure.

5.4.5. Methane emissions

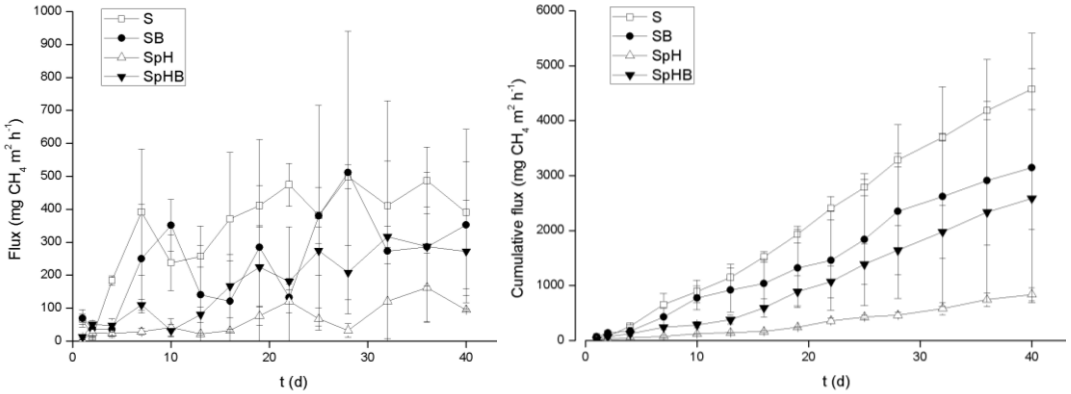

Figure 5-10: CH_4 fluxes (left) and cumulative CH_4 fluxes (right) over a seven-week period of S (slurry), SB (slurry amended with biochar), SpH (acidified slurry) and SpHB (acidified slurry amended with biochar)

Figure 5-10 presents the CH_4 fluxes and cumulative CH_4 fluxes of the slurry treatments. Acidification reduced the cumulative CH_4 fluxes by about 82% (SpH) and 43% (SpHB) as a result of the lower pH; it is known that the ideal pH range for CH_4 production lies between 6 and 8 (Sommer *et al*., 2013b). SpHB caused higher CH_4 fluxes compared to SpH, which might have been the result of acid hydrolysis of the labile carbon compounds within the biochar, making them available for methanogens. SB treatments resulted in contradictory results. All replicates showed different values, ranging from CH_4 fluxes higher than slurry alone to fluxes as low as acidified slurry. We originally hypothesised that biochar would potentially increase CH_4 emissions due

to the additional carbon present in the slurry. However, two of the three replicates reduced cumulative CH_4 fluxes compared to slurry alone (38% and 81%), while one replicate increased cumulative CH_4 fluxes by 25% at the end of the storage period.

The reduction of CH_4 emissions might be the consequence of the change in aeration properties when treating slurry with biochar, with subsequent development of aerobic sites and a higher CO_2 release. Furthermore, a shift in microbial communities may have a significant impact. The application of biochar to paddy soils has previously been shown to significantly decrease CH_4 emissions, which resulted from an increase in methanotropic probacterial abundances and decreased ratios of methanogenic to methanotropic abundances (Feng *et al*., 2012). Also Liu *et al*. (2011) found a 51% to 91% decrease in CH_4 emissions in paddy soils upon biochar addition and suggested that biochar might inhibit methanogenic activity or stimulate methylotrophic activity. On the other hand, Singla *et al*. (2014) found a significantly increased CH_4 flux compared to untreated paddy soil and a further increase with increased biochar concentration. The authors found no differences in methanogenic archaeal diversity and attributed the increased CH_4 fluxes to variation in the soil variables. Zhang *et al*. (2010) also reported an increase in CH_4 emissions in paddy soil under biochar amendments. An observation worth mentioning, is that after the storage period a white mold had grown on the surface of slurry alone (S), while for biochar treatments (SB) any sign of mold was absent. This suggests that the biochar does effect the abundance of organisms. Further investigations are required to fully understand the impact of biochar on microbial communities in slurry and the subsequent influence on GHG emissions, in particular long-term studies are required. Furthermore, investigation of biochar to reduce odour compounds during slurry storage and the effect of emissions after the storage period, e.g. during land application, are necessary.

5.4.6. Hydrogen sulphide emissions

Some H_2S emissions were detected in the range of 5 ppm – 50 ppm for the acidified treatments SpH and SpHB (results not shown) and were not detected for S and SB treatments throughout the storage period. The H_2S emissions were observed in the first week for SpH treatments, while H_2S emissions for SpHB treatments were slightly delayed and were only found from week four onwards. The previous results in sections 5.4.4 and 5.4.5. indicate that biochar cannot compete with slurry acidification for

reducing NH_3 and CH_4 emissions; however, with the drawback of potential H_2S emissions arising from sulfuric acid in an anaerobic environment.

5.5. Conclusions

This study is one of the first to investigate the influence of biochar on NH_3, CH_4 and H_2S emissions from stored cow slurry and provides insight into the potential benefits of biochar as an amendment. Biochar was not able to compete with sulfuric acid as a mitigation option for NH_3 and CH_4 emissions, since biochar had no or inconsistent impacts on these emissions. Acidification however resulted in elevated H_2S emissions. Other benefits (or drawbacks) might arise from biochar amendments, as biochar affected some physico-chemical characteristics of cow slurry, in particular TC and DM content, aeration properties, and C:N ratios. The influence of biochar on microbial abundances and long-term research is necessary to fully understand the effectiveness of biochar to mitigate environmental pollution during storage of animal slurry.

5.6. Acknowledgement

Financial support for this work is gratefully acknowledged from the People Programme (Marie Curie Actions) of the European Union's Seventh Framework Programme FP7/2007-2013/ under REA grant agreement n° [289887], and from the SEAI under the Energy Research, Development & Demonstration (RD&D) Programme. A special thanks to Alberto Garcia and Ray McInerney for their contribution.

5.7. References

Amon, B., Kryvoruchko, V., Amon, T., Zechmeister-Boltenstern, S., 2006. Methane, nitrous oxide and ammonia emissions during storage and after application of dairy cattle slurry and influence of slurry treatment. Agric. Ecosyst. Environ. 112, 153–162.

Asada, T., Ishihara, S., Yamane, S., Toba, T., Yamada, A., Oikawa, K., 2002. Science of bamboo charcoal: Study of carbonizing temperature of bamboo charcoal and removal of harmful gases. J. Health. Sci. 48, 473–479.

Asada, T., Ohkubo, T., Kawata, K., Oikawa, K., 2006. Ammonia adsorption on bamboo charcoal with acid treatment. J. Health Sci. 52, 585–589.

Avrahami, S., Conrad, R., Braker, G., 2002. Effect of soil ammonium concentration on N_2O release and on the community structure of ammonia oxidizers and denitrifiers. Appl. Environ. Microbiol. 68, 5685–5692.

Berg, W., Türk, M., Hellebrand, H.J., 2006. Effects of acidifying liquid cattle manure with nitric of lactic acid on gaseous emissions. Work. Agric. Air Qual. 492–498.

Bouwman, A.F., Van Vuuren, D.P., Derwent, R.G., Posch, M., 2002. A Global Analysis of Acidification and Eutrophication of Terrestrial Ecosystems. Water, Air, and Soil Pollution. 141 (1), 349–382.

Budai, A., Zimmerman, A.R., Cowie, A.L., Webber, J.B.W., Singh, B.P., Glaser, B., Masiello, C.A., 2013. Biochar Carbon Stability Test Method: An assessment of methods to determine biochar carbon stability. International Biochar Initiative. September 20, 2013.

Canh, T.T., Aarnink, A.J.A., Schutte, J.B., Sutton, A., Langhout, D.J., Verstegen, M.W.A., 1998. Dietary protein affects nitrogen excretion and ammonia emission from slurry of growing-finishing pigs. Livestock Production Science. 56, 181-191.

Chintala, R., Mollinedo, J., Schumacher, T.E., Papiernik, S.K., Malo, D.D., Clay, D.E., Kumar, S., Gulbrandson, D.W., 2013. Nitrate sorption and desorption in biochars from fast pyrolysis. Microporous Mesoporous Mater. 179, 250–257.

Coates, J., 2000. Interpretation of Infrared Spectra, A Practical Approach. In Meyer, R.A. (Ed.) Encyclopedia of Analytical Chemistry, John Wiley & Sons Ltd, Chichester. 10815–10837.

Dai, X.R., Blanes-Vidal, V., 2013. Emissions of ammonia, carbon dioxide, and hydrogen sulfide from swine wastewater during and after acidification treatment: Effect of pH, mixing and aeration. J. Environ. Manage. 115, 147–154.

Darvell, L.I., Brindley, C., Baxter, X.C., Jones, J.M., Williams, A., 2012. Nitrogen in Biomass Char and Its Fate during Combustion: A Model Compound Approach.

Downie, A., Crosky, A., Munro, P., 2009. Physical properties of biochar. In: Lehmann, J., Joseph, S. (Eds.), Biochar for Environmental Management: Science and Technology. Earthscan, London, 13-22.

EBC, 2012. 'European Biochar Certificate - Guidelines for a Sustainable Production of Biochar.' European Biochar Foundation (EBC), Arbaz, Switzerland. http://www.europeanbiochar.org/en/download. Version 6.1 of 19th June 2015

Eurostat, 2012. Agri-environmental indicator - ammonia emissions. Available at http://ec.europa.eu/eurostat/statistics-explained/index.php/Agri-environmental_indicator_-_ammonia_emissions (accessed 25.05.2016).

Enders, A., Lehmann, J., 2012. Comparison of Wet-Digestion and Dry-Ashing Methods for Total Elemental Analysis of Biochar. Commun. Soil Sci. Plant Anal. 43, 1042–1052.

Eykelbosh, A.J., Johnson, M.S., Couto, E.G., 2015. Biochar decreases dissolved organic carbon but not nitrate leaching in relation to vinasse application in a Brazilian sugarcane soil. Journal of Environmental Management. 149, 9–16.

Fangueiro, D., Hjorth, M., Gioelli, F., 2015. Acidification of animal slurry - a review. J. Environ. Manage. 149, 46–56.

Feilberg, A., Sommer, S.G., 2013a. Ammonia and Malodorous Gases: Sources and Abatement Technologies. In Sommer, S.G., Christensen, M.L., Schmidt, T., Jensen, L.S. (Eds.). Animal Manure Recycling - Treatment and Management. John Wiley and Sons Ltd. Chichester, West Sussex, UK. 153-176.

Feilberg, A., Sommer, S.G., 2013b. Ammonia and Malodorous Gases: Sources and Abatement Technologies. In Sommer, S.G., Christensen, M.L., Schmidt, T., Jensen, L.S. (Eds.). Animal Manure Recycling - Treatment and Management. John Wiley and Sons Ltd. Chichester, West Sussex, UK. 171-172.

Feng, Y., Xu, Y., Yu, Y., Xie, Z., Lin, X., 2012. Mechanisms of biochar decreasing methane emission from Chinese paddy soils. Soil Biol. Biochem. 46, 80–88.

Fukuyama, K., Kasahara,Y., Kasahara, N., Oya, A., Nishikawa, K., 2001. Small-angle X- ray scattering study of the pore structure of carbon fibers prepared from a polymer blend of phenolic resin and polystyrene. Carbon. 39, 287–290.

Gai, X., Wang, H., Liu, J., Zhai, L., Liu, S., Ren, T., Liu, H., 2014. Effects of feedstock and pyrolysis temperature on biochar adsorption of ammonium and nitrate. PLoS One 9, 1–19.

Haeni, C., Kupper, T., Jocher, M., Neftel, A., Sintermann, J., 2012. Amendment of biochar to slurry: A possibility to mitigate ammonia emissions? Emission of Gas and Dust from Livestock. June 10-13, 2012. Saint-Malo, France.

Hale, S.E., Alling, V., Martinsen, V., Mulder, J., Breedveld, G.D., Cornelissen, G., 2013. The sorption and desorption of phosphate-P, ammonium-N and nitrate-N in cacao shell and corn cob biochars. Chemosphere 91, 1612–1619.

Holmes, J.M., Beebe, R.A., 1957. An example of desorption hysteresis at low relative pressures on a non-porous adsorbent: ammonia on graphitized carbon black. J Phys Chem. 61(12),1684–1686.

IPCC, 2014. Myhre, G., Shindell, D., Bréon, F.-M., Collins, W., Fuglestvedt, J., Huang, J., Koch, D., Lamarque, J.-F., Lee, D., Mendoza, B., Nakajima, T., Robock, A., Stephens, G., Takemura, T., Zhang, H., 2013. Anthropogenic and Natural Radiative Forcing. In Stocker, T.F., Qin, D., Plattner, G.-K., Tignor, M., Allen, S.K., Boschung, J., Nauels, A., Xia, Y., Bex, V., Midgley, P.M. (Eds.). Climate Change 2013: The Physical Science Basis. Contribution of Working Group I to the Fifth Assessment Report of the Intergovernmental Panel on Climate Change. Cambridge University Press, Cambridge, United Kingdom and New York, NY, USA.

Iyobe T., Asada T., Kawata K., Oikawa K., 2004. Comparison of removal efficiencies for ammonia and amine gases between woody charcoal and activated carbon. J. Health Sci. 50, 148–153.

Jaramillo, E., Chandross, M., 2004. Adsorption of Small Molecules in LTA Zeolites. 1. NH_3, CO_2, and H_2O in Zeolite 4A. J. Phys. Chem. B. 108 (52), 20155–20159.

Joseph, S.D., Camps-Arbestain, M., Lin, Y., Munroe, P., Chia, C.H., Hook, J., van Zwieten, L., Kimber, S., Cowie, a., Singh, B.P., Lehmann, J., Foidl, N., Smernik, R.J., Amonette, J.E., 2010. An investigation into the reactions of biochar in soil. Aust. J. Soil Res. 48, 501-515.

Kai, P., Pedersen, P., Jensen, J.E., Hansen, M.N., Sommer, S.G., 2008. A whole-farm assessment of the efficacy of slurry acidification in reducing ammonia emissions. Eur. J. Agron. 28, 148–154.

Keiluweit, M., Nico, P.S., Johnson, M.G., Kleber, M., 2010. Dynamic molecular structure of plant biomass-derived black carbon (biochar). Environ. Sci. Technol. 44, 1247–1253.

Lawrinenko, M., 2014. Anion exchange capacity of biochar. Graduate Theses and Dissertations. Paper 13685.

Liu, Y.X., Yang, M., Wu, Y.M., Wang, H.L., Chen, Y.X., Wu, W.X., 2011. Reducing CH_4 and CO_2 emissions from waterlogged paddy soil with biochar. Journal of Soils and Sediments 11, 930-939.

Luo, J., Kulasegarampillai, M., Bolan, N., Donnison, A., 2004. Control of gaseous emissions of ammonia and hydrogen sulphide from cow manure by use of natural materials. New Zeal. J. Agric. Res. 47, 545–556.

Loyon, L., Guiziou, F., Beline, F., Peu, P., 2007. Gaseous emissions (NH_3, N_2O, CH_4, CO_2) during pig slurry biological aerobic treatment and treatment by-product storages. Biosyst. Eng. 97, 472-480.

McCrory, D.F., Hobbs, P.J., 2001. Additives to Reduce Ammonia and Odor Emissions from Livestock Wastes. American Society of Agronomy, Crop Science Society of America, Soil Science Society. Published in J. Environ. Qual. 30, 345–355.

Panetta, D.M., Powers, W.J., Lorimor, J.C., 2005. Management strategy impacts on ammonia volatilization from swine manure. J. Environ. Qual. 34, 1119–1130.

Petersen, S.O., Andersen, A.J., Eriksen, J., 2012. Effects of Cattle Slurry Acidification on Ammonia and Methane Evolution during Storage. J. Environ. Qual. 41, 88-94.

Reddy, G.B., Cyrus, J.S., 2012. Ammonia capture and adsorption characteristics of biochar. Land grant and sea grant national water conference. May 20-24, 2012. Marriott Waterfront, Portland, Oregon.

Regueiro, I., Coutinho, J., Fangueiro, D., 2016. Alternatives to sulfuric acid for slurry acidification: impact on slurry composition and ammonia emissions during storage. J. Clean. Prod. 131, 296-307.

Schiffman, S.S., Auvermann, B.W., Bottcher, R.W., 2006. Health effects of aerial emissions from animal production and waste management systems. In Rice, J.M., Caldwell, D.F., Humenik, F.J. (Eds.). Animal Agriculture and the

Environment: National Center for Manure and Animal Waste Management White Papers. St. Joseph, Michigan: ASABE . 225-262.

Schmidt, H.P., Wilson, K., 2014a. The 55 uses of biochar. The Biochar Journal. Arbaz, Switzerland. ISSN 2297-1114. Available at www.biochar-journal.org/en/ct/2 Version of 12th May 2014. Accessed: 29.05.2016

Schmidt, H.P., Taylor, P., 2014b. Kon-Tiki - the democratization of biochar production. The Biochar Journal. Arbaz, Switzerland. Available at ISSN 2297-1114 www.biochar-journal.org/en/ct/39 Version of 29th November 2014. Accessed: 30.05.2016

Singla, A., Dubey, S.K., Singh, A., Inubushi, K., 2014. Effect of biogas digested slurry-based biochar on methane flux and methanogenic archaeal diversity in paddy soil. Agric. Ecosyst. Environ. 197, 278–287.

Sommer, S.G., Clough, T.J., Chadwich, D., Peterson, S.O., 2013a. Greenhouse Gas Emissions from Animal Manures and Technologies for Their Reduction. In Sommer, S.G., Christensen, M.L., Schmidt, T., Jensen, L.S. (Eds.). Animal Manure Recycling - Treatment and Management. John Wiley and Sons Ltd. Chichester, West Sussex, UK. 177-194.

Sommer, S.G., Clough, T.J., Chadwich, D., Peterson, S.O., 2013b. Greenhouse Gas Emissions from Animal Manures and Technologies for Their Reduction. In Sommer, S.G., Christensen, M.L., Schmidt, T., Jensen, L.S. (Eds.). Animal Manure Recycling - Treatment and Management. John Wiley and Sons Ltd. Chichester, West Sussex, UK. 179-180.

Sommer, S.G., Feilberg, A., 2013. Gaseous Emissions of Ammonia and Malodorous Gases. In Sommer, S.G., Christensen, M.L., Schmidt, T., Jensen, L.S. (Eds.). Animal Manure Recycling - Treatment and Management. John Wiley and Sons Ltd. Chichester, West Sussex, UK. 131-152.

Song, Y., Zhang, X., Ma, B., Chang, S.X., Gong, J., 2013. Biochar addition affected the dynamics of ammonia oxidizers and nitrification in microcosms of a coastal alkaline soil. Biol. Fertil. Soils 50, 321–332.

Sørensen, P., Jensen, L.S., 2013. Nutrient Leaching and Runoff from Land Application of Animal Manure and Measures for Reduction. In Sommer, S.G., Christensen, M.L., Schmidt, T., Jensen, L.S. (Eds.). Animal Manure Recycling - Treatment and Management. John Wiley and Sons Ltd. Chichester, West Sussex, UK. 195-210.

Spokas, K. a., Novak, J.M., Venterea, R.T., 2012. Biochar's role as an Alternative N-fertilizer: Ammonia Capture. Plant Soil. 350, 35–42.

Statistics, 2014. Ireland's Forests - Annual Statistics. Department of Agriculture, Food and the Marine. Availabale at http://www.agriculture.gov.ie/media/migration/forestry/forestservicegeneralinformation/Annual%20Forest%20Sector%20Statistics%202014.pdf (accessed 25.06.2016).

Steinfeld, H., Gerber, P., Wassenaar, T., Castel, V., Rosales, M. And de Haan, C.,

2006. Livestock's Long Shadow: Environmental Issues and Options, FAO, Rome.

Taghizadeh-Toosi, A., Clough, T.J., Sherlock, R.R., Condron, L.M., 2012a. A wood based low-temperature biochar captures NH_3-N generated from ruminant urine-N, retaining its bioavailability. Plant Soil. 353, 73–84.

Taghizadeh-Toosi, A., Clough, T.J., Sherlock, R.R., Condron, L.M., 2012b. Biochar adsorbed ammonia is bioavailable. Plant Soil. 350, 57–69.

Taylor, 2014. Biochar Makers for the Biochar Gardener and Small Farmer. By The Biochar Revolution. Monday, January 26, 2015. Available at http://www.thebiocharrevolution.com/blog/biochar-makers-for-the-biochar-gardener-and-small-farmer (accessed 25.06.2016)

Thies, J.E., Rillig, M.C., 2009. Characteristics of Biochar: Biological Properties. In: Lehmann, J., Joseph, S. (Eds.), Biochar for Environmental Management: Science and Technology. Earthscan, London, 86-88.

Uzoma, K.C., Inoue, M., Andry, H., Fujimaki, H., Zahoor, a., Nishihara, E., 2011. Effect of cow manure biochar on maize productivity under sandy soil condition. Soil Use Manag. 27, 205–212.

Van der Stelt, B., Temminghoff, E.J.M., Van Vliet, P.C.J., Van Riemsdijk, W.H., 2007. Volatilization of ammonia from manure as affected by manure additives, temperature and mixing. Bioresour. Technol. 98, 3449–3455.

Wang, K., Huang, D., Ying, H., Luo, H., 2014. Effects of acidification during storage on emissions of methane, ammonia, and hydrogen sulfide from digested pig slurry. Biosyst. Eng. 122, 23–30.

Wei, L., Shutao, W., Jin, Z., Tong, X., 2014. Biochar influences the microbial community structure during tomato stalk composting with chicken manure. Bioresour. Technol. 154, 148–154.

Williams, A. G., Nigro, E., 1997. Ammonia and Odour Control from Animal Production Facilities. Proceedings of a Conference held in Vinkeloord, The Netherlands. 6 - 10 October 1997. 421-428.

Wildman, J., Derbyshire, F., 1991. Origins and functions of macroporosity in activated carbons from coal and wood precursors. Fuel 70, 655–661.

Yamulki, S., 2006. Effect of straw addition on nitrous oxide and methane emissions from stored farmyard manures. Agric. Ecosyst. Environ. 112, 140–145.

Zeng, Z., Zhang, S., Li, T., Zhao, F., He, Z., Zhao, H., Yang, X., Wang, H., Zhao, J., Rafiq, M.T., 2013. Sorption of ammonium and phosphate from aqueous solution by biochar derived from phytoremediation plants. J. Zhejiang Univ. Sci. B. 14, 1152–1161.

Zhang, A.F., Cui, L.Q., Pan, G.X., Li, L.Q., Hussain, Q., Zhang, X.H., Zheng, J.W., Crowley, D., 2010. Effect of biochar amendment on yield and methane and nitrous oxide emissions from a rice paddy from Tai Lake plain, China. Agriculture Ecosystems & Environment. 139, 469-475.

6. Nitrogen dynamics in soil treated with slurry, biochar and biochar amended slurry

This chapter describes the effect of Sitka spruce biochar on influencing nitrate leaching, nitrogen uptake to grass and gene abundances (*amoA* and *nosZ*) when added to cow slurry and introduced to soil.

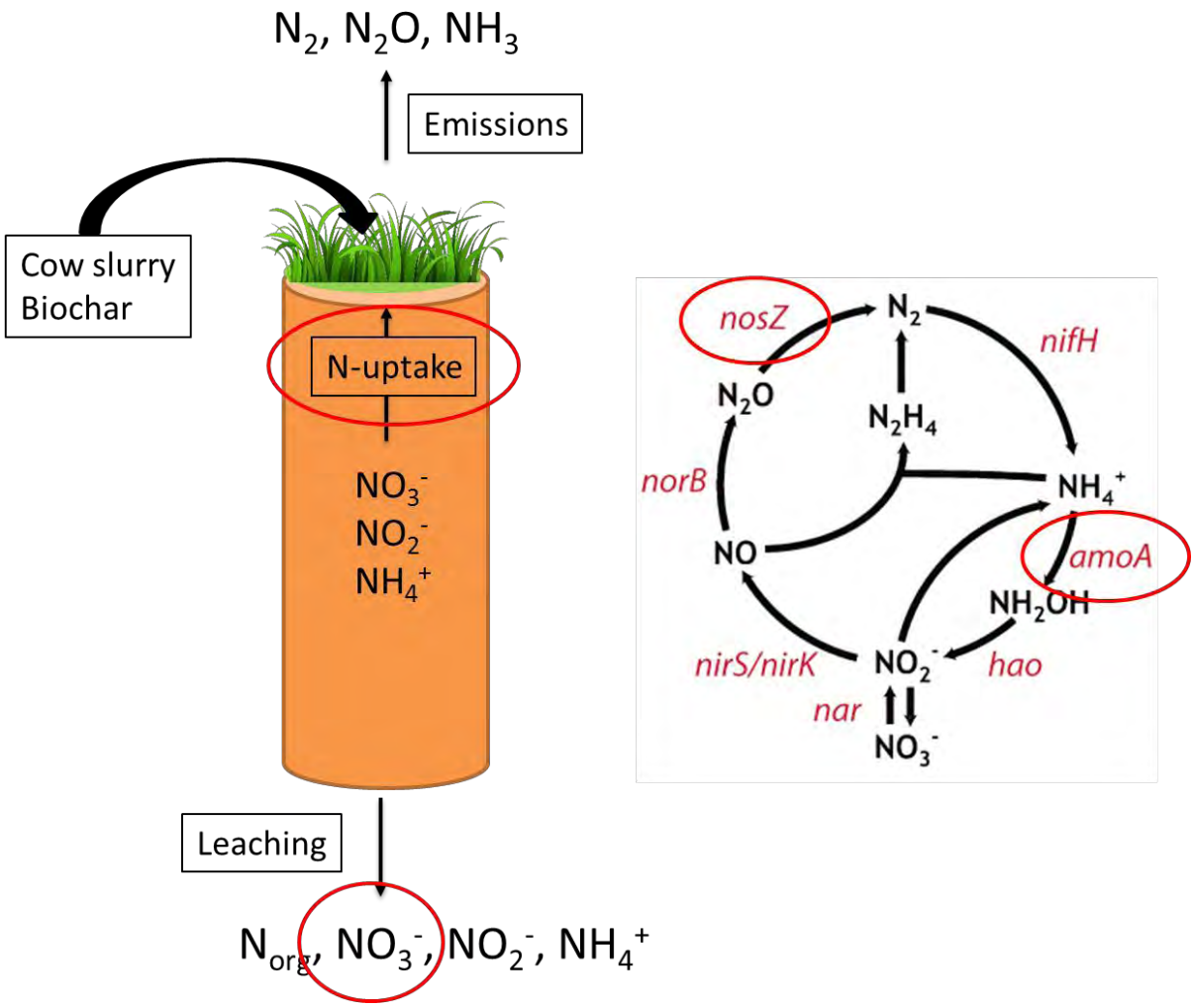

6.1. Abstract

Nutrient leaching, including nitrates (NO_3^-), causes environmental problems in areas with high livestock production. Strategies to reduce nutrient leaching are being investigated, which include the use of binding materials. Biochar was produced from Sitka spruce using a uniquely designed pyrolysis unit named Kon-Tiki kiln. The biochar had a high surface area, porosity and complied with all thresholds for European biochar classification. The aim of the study was to investigate the effectiveness of the biochar as a means to reduce NO_3^- leaching from cow slurry. Soil columns of 40 cm in height and a diameter of 16 cm were prepared. Four treatments were included in the experiment: slurry, slurry treated with biochar, biochar and the control (soil only). The application rate of cow slurry corresponded to the general Irish land spreading limit of 170 kg N ha^{-1} yr^{-1} and the biochar was applied at 10 t ha^{-1} per column. Nitrogen uptake to grass (*Kent indigenous*) and quantification of bacterial and archeal *amoA* genes and *nosZ* genes were carried out to evaluate nitrification and denitrification capabilities. Neither biochar treatments alone nor biochar in combination with slurry had a significant influence on nitrogen uptake to grass or on NO_3^- leaching from the soil columns. With regard to gene abundances an effect of biochar was only evident when applied in combination with slurry. Biochar when amended with slurry reduced archaeal *amoA* abundances significantly at the application zone and increased archaeal *amoA* abundances significantly at lower depth compared to un-amended slurry treatments. Biochar alone showed no effect compared to soil alone, revealing that biochar behaved differently when combined with slurry than alone. Further systematic studies using different application rates of Sitka spruce biochar for several years are needed, to assess its long-term benefits as a soil amendment.

6.2. Introduction

Nutrient leaching, including nitrate (NO_3^-) and phosphate (PO_4^{3-}), causes environmental problems in areas with high livestock production (Spalding and Exner, 1993; Sharpley *et al*., 1994). Livestock manure contains high quantities of nitrogen and phosphorous and these can be lost from agricultural soil when the application rate of manure exceeds the maximum required by the crops and the infiltration capacity of the soil is exceeded. Specifically, contamination of open waters and groundwater are a problem leading to eutrophication, algal bloom and poor water quality in general. Excessive application of manure may also lead to losses of nitrogen in form of ammonia (NH_3) and nitrous oxide (N_2O). This inefficient use of N and P nutrients may result in additional production of artificial fertilisers, which is an energy intense process and may lead to further environmental burdens. (Sørensen and Jensen, 2013a)

Ammonium (NH_4^+) is one form of manure nitrogen, and is readily adsorbed by the soil. When NH_4^+ nitrifies to NO_3^- in aerobic soil, NO_3^- is not adsorbed and stays in solution making it more vulnerable to leaching (Sørensen and Jensen, 2013b). Attempts are made to reduce NO_3^- leaching, including regulating the manure application rate, soil slurry injection, solid-liquid separation as the liquid has better infiltration in soil, and composting to immobilise NH_4^+ (Sørensen and Jensen, 2013a). All member states of the European Union (EU) are limited to the quantity and timing of application of nitrogen to soil, with a livestock manure application limit of 170 kg ha^{-1} $year^{-1}$ (Nitrates Directive (91/676/EEC)). Despite all efforts, other strategies to reduce the risk of nutrient leaching are being investigated, for example the use of binding materials such as chars.

Char is derived from pyrolysis, typically between 300 °C and 700 °C, of a carbonaceous material and possesses properties that have shown to be beneficial for ameliorating soils (Barrow, 2012). Char used for agricultural purposes is now commonly known as biochar. There is evidence that soils amended with biochar have found to cause fundamental changes in soil nutrient cycles and this has resulted in improved crop production and reduction of greenhouse gas (GHG) emissions (Xu *et al*., 2014; Van Zwieten *et al*., 2014). The effect on plant growth is more evident when the soil is acidic or low in soil organic matter, as biochar has liming properties and is

rich in organic carbon (Verheijen *et al*., 2010). Furthermore, the recalcitrant carbon structure suggests its benefits for carbon sequestration (Lehmann and Joseph, 2009).

Interaction of biochar with NO_3^- is influenced by the physico-chemical characteristics of biochar. These include the surface area, pore size distribution, hydrophobicity, rate of biochar addition, cation exchange capacity (CEC), anion exchange capacity (AEC), NO_3^- adsorption, and changes in nitrification rates (Clough *et al*., 2013). According to the review by Clough *et al*., (2013) literature findings have been consistent in that biochars produced at high temperatures (> 600 °C) are able to remove NO_3^- from solution (Yao *et al*., 2012; Mizuta *et al*., 2004; Kameyama *et al*., 2012; Dempster *et al*., 2012). The reason for this might be the development of base functional groups on the chars' surface and not physical adsorption as surface area, micropore volume and particle density did not correlate with NO_3^- adsorption (Kameyama *et al*., 2012). Lawrinenko (2014) found that biochars with different levels of aromatic condensation oxidise differently, for example biochars produced at 500 °C develop hydroxyl and carbonyl groups while biochars produced at 700 °C biochar develop peroxy ether groups. They suggest that the AEC in biochars is primarily due to the oxonium functional groups formed during pyrolysis.

Leaching of NO_3^- from soil has shown to be reduced when the soil was amended with biochar (Yao *et al*., 2012; Dempster *et al*., 2012), however it is unclear how permanent the adsorption of NO_3^- is. Kameyama *et al*. (2012) found that NO_3^- was only weakly adsorbed onto biochar with an increased residence time of NO_3^- presenting a greater opportunity for plant uptake. The results obtained by Prendergast-Miller *et al*. (2011) propose localisation of NO_3^- within the rhizosphere of biochar-amended soils. Another study by Prendergast-Miller *et al*. (2014) suggested that biochar particles retained soil nitrogen in the form of NO_3^- and that the roots of spring barley preferred soil containing biochar particles. Adsorption or immobilisation of nitrogen might also be the cause for reduced foliar nitrogen concentration as previously reported (O'Toole *et al*., 2013; Kammann *et al*., 2011). The difference between sorption experiments at laboratory scale and column leaching experiments at a larger scale is that other loss pathways occur in soil, such as immobilisation and denitrification of NO_3^-. (Clough *et al*., 2013)

The degrees of nitrification and denitrification influence NO_3^- concentrations in soil. The reactions involved in the microbial nitrogen cycle are illustrated in Figure 6-1 (Jetten, 2008). The transformation reactions are catalysed by enzymes produced by aerobic and anaerobic microorganisms. Nitrification and denitrification are often coupled systems as a consequence of both aerobic and anaerobic sites in manure and soil and their reaction rate is dependent on pH, soil type, soil fertilisation, water content, oxygen availability and temperature (Jensen and Sommer, 2013a).

Nitrification occurs when total ammoniacal nitrogen (TAN = NH_4^+ and NH_3) is oxidised into nitrite and then into NO_3^- by autotrophic microorganisms (Jensen and Sommer, 2013a). The enzyme ammonia monooxygenase (Amo) catalyses the oxidation of TAN to nitrite via NH_2OH in an oxic environment. The *amoA* gene of these organisms encodes the active site of Amo. N_2O is a by-product of this reaction. The enzymes are sensitive to pH and are more active at neutral pH rather than low pH (Jensen and Sommer, 2013b) Ammonia oxidising bacteria or archaea can be investigated by quantifying bacterial and archaeal *amoA* genes. Denitrification is the enzymatic conversion of NO_3^- to N_2. The conversion occurs stepwise via NO_2^-, NO, and N_2O (Figure 6-1). Denitrification represents a major source of N_2O, a potent greenhouse gas. The key enzyme for mitigating N_2O emissions is *nosZ*, which catalyses N_2O reduction to N_2.

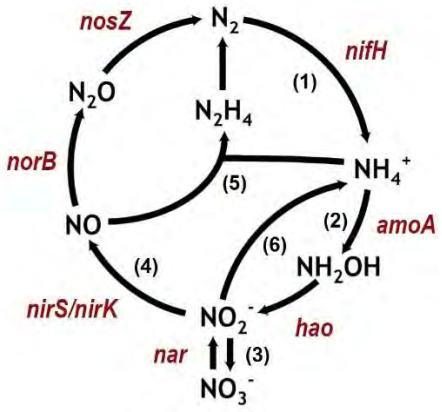

Figure 6-1: Reactions of the microbial nitrogen cycle. (1) Dinitrogen gas fixation, (2) aerobic ammonium oxidation by bacteria and archaea, (3) aerobic nitrite oxidation, (4) denitrification, (5) anaerobic ammonium oxidation, and (6) dissimilatory nitrate and nitrite reduction to ammonium (Jetten, 2008), nifH: nitrogenase reductase gene, amoA: ammonia monooxygenase gene, hao: hydroxylamine oxidase, nar: nitrate reductase, nirS/nirK: nitrite reductase (cytochrome cd1 and copper containing forms), norB: nitric-oxide reductase gene, nosZ: nitrous oxide reductase gene

Schmalenberger and Fox (2016) extensively reviewed the existing literature and found publications with both evidence of increased and decreased nitrification with biochar addition to soil, but also evidence of it having no effect. For example, Prommer *et al*. (2014) found that biochar promoted soil bacterial and archaeal nitrifiers and accelerated gross nitrification rates more than two-fold. Also a study by Song *et al*. (2014) found that biochar application generally enhanced the abundance and altered the composition of ammonia oxidizers. On the other hand, other investigations found that biochar had a negative impact on nitrification or did not find an influence of biochar on nitrification at all (Zhu *et al*., 2015; Martin *et al*., 2015). Some differences in results can be explained by the diversity of feedstocks and soils utilised, the choice of pyrolysis process conditions, such as maximum temperature and residence time, and environmental differences, from incubation experiments at lab scale to field trials, and some experiments include e.g. plant growth (Schmalenberger and Fox, 2016). The neutralising capacity of biochar might benefit nitrification, as under acidic conditions nitrifying prokaryotes might find a habitat in pH neutral biochar pores. Schmalenberger and Fox (2016) also commented that nitrification might be inhibited if the initial concentration of TAN substrate is low; however, the ability of NH_4^+ or NO_3^- to be adsorbed by the biochar might have a short term influence on nitrification and NH_4^+ or NO_3^- uptake by plants. Denitrification rates might be influenced by biochar through changes in pH (Yanai, 2008; Han *et al*., 2013; Wang *et al*., 2013). Even though the majority of scientific publications observed a reduction in N_2O emissions (Chintala *et al*., 2015; Harter *et al*., 2014; Martin *et al*., 2015; Nelissen *et al*., 2014; Rizhiya *et al*., 2015), some studies were not able to find any reduction in N_2O emission (Xiang *et al*., 2015) or even higher abundances of *nosZ* (Dicke *et al*., 2015). Clough *et al*. (2013) commented that *"much of the biochar-soil research to date, with respect to N cycling, is fragmented with results as diverse as the types of biochar used and the biochar-soil combinations tested".*

The objective of this study was to investigate the change of NO_3^- leaching when adding the Sitka spruce biochar at an application rate of 10 t ha^{-1} to cow slurry. Simultaneously, we investigated the N-uptake to grass grown in soil amended with biochar and changes in gene abundances to evaluate nitrification (bacterial and archaeal *amoA*) and denitrification (*nosZ*) capabilities.

6.3. Methodology

6.3.1. Biochar production and characterisation

Methodology and results on production and characterisation of the Sitka spruce biochar can be found in chapter 5 (section 5.3.1).

6.3.2. Slurry and soil

Cow slurry was collected on a farm in Co. Limerick, Ireland, after a storage period of 6 months. The cows were silage fed. Soil was collected in Kilteely in East Limerick, Ireland. It was a medium based status of brown earths, of mostly grit and shale origin with some limestone and sandstone. The soil was dried and sieved to a particle size < 3.15 mm. The slurries and the soil samples were analysed for their moisture (according to BS EN 14774-1), organic matter (OM) (according to I.S. EN 14775:2009), and total carbon (TC) and nitrogen content (TN) using an Elemental Vario EL Cube analyser. The pH of the slurries was measured using a calibrated Orion 420 pH meter. The soil was shaken for 2 hours at 100 rpm in a 0.01 M $CaCl_2$ solution (1 wt.%) before pH measurement. The maximum water holding capacity was measured gravimetrically according to Ahn *et al*. (2009). The properties of the individual components are displayed in Table 6-1.

Table 6-1: Slurry, biochar and soil characteristics on dry basis (db) or as received (ar). The results are expressed as the average of three measurements.

	pH	MC[1] ($wt.\%_{ar}$)	DM[2] ($wt.\%_{ar}$)	Ash ($wt.\%_{db}$)	OM[3] ($wt.\%_{db}$)	TC[4] ($g\ kg^{-1}_{ar}$)	TN[5] ($g\ kg^{-1}_{ar}$)
Slurry	7.7	97.7 ± 0.6	2.3 ± 0.6	9.3 ± 0.2	90.7 ± 0.2	6.6 ± 0.1	0.68 ± 0.03
Biochar	9.2	69.1 ± 0.5	30.9 ± 0.5	5.4 ± 0.3	94.6 ± 0.3	258 ± 1.1	1.2 ± 0.1
S + B[6]	8.0	93.5 ± 0.6	6.5 ± 0.6	9.2 ± 0.2	91.3 ± 0.2	16.9 ± 0.2	0.73 ± 0.02
Soil	7.0	3.7 ± 0.7	96.3 ± 0.7	89.6 ± 0.2	10.4 ± 0.2	36 ± 4.0	1.9 ± 0.4

[1]Moisture content, [2]Dry matter content, [3]Organic matter content, [4]Total carbon content, [5]Total nitrogen content, [6]Slurry/Biochar combined

6.3.3. Preparation of soil columns and leaching

Four treatments were included in the experiment and replicated four times: slurry only (S), slurry with biochar (SB), biochar only (B) and the control with soil only (C). The application rate of S and SB was 500 g_{ar}, which corresponded to the general land spreading limit of 170 kg N ha^{-1} yr^{-1} according to the European Union (Good Agricultural Practice for the Protection of Waters) Regulations S.I. No. 31 of 2014. Biochar was applied at 10 t ha^{-1} (20 g_{ar}) per column. For SB the slurry was mixed with the biochar thoroughly before application to the column. For the control 5.0 kg of soil was added to the PVC columns directly. For the other treatments slurry injection to 10 cm depth was simulated by applying the slurry and biochar mixtures to the top layer of 3.5 kg soil and then covering them with the remaining 1.5 kg of soil. The PVC columns were of 0.4 m length and an internal diameter of 0.16 m and sealed at the bottom with 35 µm nylon monofilament. The soils were saturated with distilled water. Irrigation was simulated twice a week with 200 ml of distilled water, which corresponds to the approximate average annual rainfall in Ireland. The columns were placed on top of an upside down tray with holes and the leachate was collected in a covered tray beneath it. The leachate was analysed for NO_3^- using ion chromatography. A schematic of the experiment is illustrated in Figure 6-2.

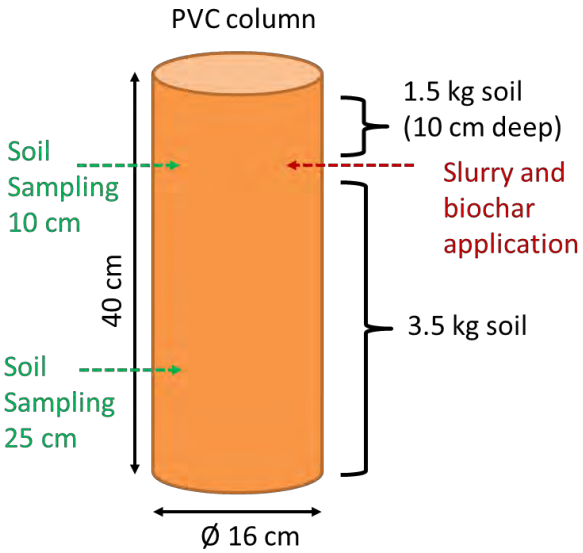

Figure 6-2: Schematic of leaching columns

6.3.4. Grass Growth

Certified grass seeds (200 mg) of the species *Lolium perenne* and variety *Kent indigenous* (Ref.No: 13/CL/243/3377, country of production: UK) were spread on the surface of the soil. After germination the grass was thinned down to 100 seeds per column. The columns were arranged in a completely randomised design in a naturally lighted glasshouse. Artificial light was used during night-time (10 h) and the temperature was set not to go below 16 °C. The grass was harvested the first time after 5 weeks and the second time after 11 weeks. The harvested grass was dried at 40 °C and weighed (± 0.001 g). The samples were milled to fine particle size before analysis of nitrogen as described above for the biochar. The total nutrient accumulation by plants (mg pot^{-1}) was calculated as the product of the nutrient concentration (mg g^{-1}) and the grass yield (g).

6.3.5. Microbial analyses

Quantitative real-time polymerase chain reaction (qPCR) was carried out for archeal and bacterial *amoA* and *nosZ* genes to evaluate the influence of biochar on the potential nitrification and denitrification changes in the soil. Approximately 5 g of soil was sampled at two depths below the soil surface of each column (10 cm and 25 cm) and stored at -20 °C before further use. DNA was extracted from the soils following the protocol of the PowerSoil® DNA Isolation Kit purchased from MO BIO laboratories, USA. DNA recovery was determined spectrophotometrically at 260 nm with an Eon plate reader and diluted with H_2O to a final concentration of 10 ng μl^{-1}. The qPCR was performed using the KAPA SYBR FAST qPCR Kit Master Mix. The bacterial and archeal *amoA* genes were amplified using the primers amoA1F and amoA2R (Rotthauwe *et al*., 1997) and amo19F (Leininger *et al*., 2006) and cren*amoA*616r48x (Schauss *et al*., 2008) respectively. The *nosZ* gene was amplified using the primers nosZ2F and nosZ2R (Henry *et al*., 2006). For bacterial *amoA* gene amplification the total volume of 10 µl contained 5 µl 2X master mix, 2 µl Betaine (5 M), 0.1 µl primers (50 µM), 1.8 µl H_2O and 1 µl template DNA (10 ng μl^{-1}). PCR cycling started with enzyme activation at 95 °C for 3 min, followed by 45 cycles of denaturation at 95 °C for 3 s and annealing at 60 °C for 20 s, and finally extension at 72 °C for 20 s. Archeal *amoA* gene amplification was performed under the same cycling conditions, however with an annealing step at 55 °C for 20 s and 40 cycles. The *nosZ* gene amplification

was also performed under the same cycling conditions as for the bacterial *amoA* gene. PCR amplicons from End-Point PCR were used as external standards. The End-Point PCR was performed for a total volume of 25 µl as follows: 2.5 µl buffer (10 M), 5 µl Betaine (5 M), 0.5 µl dNTP-Mix (10 mM), 0.2 µl primers (50 µM), 16 µl H_2O, 0.1 µl Taq (5 μl^{-1}) and 0.5 µl template. PCR cycling conditions were the same as outlined above. Gel electrophoresis was carried out using an agarose gel (1.5 wt.%) stained with 2 µl SaveView at 80 V for 30 min in the dark in buffer (TAE IX). The gel was examined using a gel image analysis system with a UV transilluminator (G:Box; Syngene, Cambridge, UK). The PCR products were purified using a GeneJET PCR Purification Kit (Thermo Scientific). Quantification of DNA was performed with a Qubit Fluorimeter following the procedure supplied by the manufacturer. The standards were prepared in the calibration range between 10^1 and 10^6 copies per µl. The qPCR was performed in 96-Well Skirted PCR Plates using a Roche LightCycler 480 Real-Time PCR System.

6.3.6. Statistical analysis

Data obtained on the dry grass yield, nitrogen uptake, NO_3^- leaching, and gene abundances were analysed using a one-way ANOVA (IBM SPSS statistics22). A Shapiro-Wilk's test ($p > 0.05$) showed that the results were approximately normally distributed. The results were tested for homoscedasticity using Leven's test. The data violating the model assumption were logarithmically transformed before analysed by ANOVA. Means were partitioned using a Tukey's HSD post-hoc test to assess significant differences ($p < 0.05$) between treatment means.

6.4. Results and Discussion

6.4.1. Grass yield and nitrogen uptake

No significant difference ($p < 0.05$) was observed amongst all treatments for the grass yield (db) or N uptake after the first and second harvest (Figure 6-3). Nevertheless, an increase in the average grass yield by about 12%, 28% and 15% after the second harvest was found for the treated soils S, SB and B respectively compared to the control. Likewise, a significant enhancement of grass growth with biochar amended soil or slurry was not observed; however, when comparing average grass yields SB

improved by 14% compared to S and B improved by about 15% compared to C. The N uptake was influenced by the increase in dry grass yield. Again, all treatments showed enhanced N uptake compared to the control; however it was not statistically significant. Both SB and B enhanced nutrient uptake by about 11% compared to S and C respectively.

The results suggest that biochar might have an impact on grass yield and nitrogen uptake; however, further studies are required using a range of different biochar application rates with the aim of finding the optimal application rate for each soil-biochar system. For example Mia *et al*. (2014) found that biochar applied at a rate of 10 t ha^{-1} led to the highest rate of biological nitrogen fixation in red clover, while a 120 t ha^{-1} significantly decreased biomass production. Rajkovich *et al*. (2011) concluded that a biochar application rate above 2 wt.% (26 t ha^{-1}) either did not improve growth or decreased the growth of corn depending on the original feedstock. In their study, N uptake was highest at an application rate of only 0.2 wt.%.

The effect of biochar on crop yield is the result of changes in soil nutrition, water holding capacity and microbial activity, with results varying due to soil type, as reviewed by Spokas *et al*. (2012). The Sitka spruce biochar had twice the maximum water holding capacity compared to the soil (1.38 ± 0.03 g $g^{-1}_{biochar}$ and 0.68 ± 0.01 g g^{-1}_{soil}), and was assigned to the morphology and surface functionality of the biochar. The contribution of increased water retention to crop growth enhancement and its availability to plants might be more significant in dry regions or in sandy soils following biochar application. The slurry treatments S and SB, despite their nutrient value, did not have a significant impact on grass yield over the growth period and this could be attributed to leaching of some nutrients through the columns. The extent of variance from the mean was high for some replicates, which would have influenced the statistical results. In addition, environmental factors might have played a role, as the ambient temperature during the growth period remained around 16 °C and the optimum day temperatures for *Lolium perenne* lie between 20 °C - 25 °C (Silsbury, 1971).

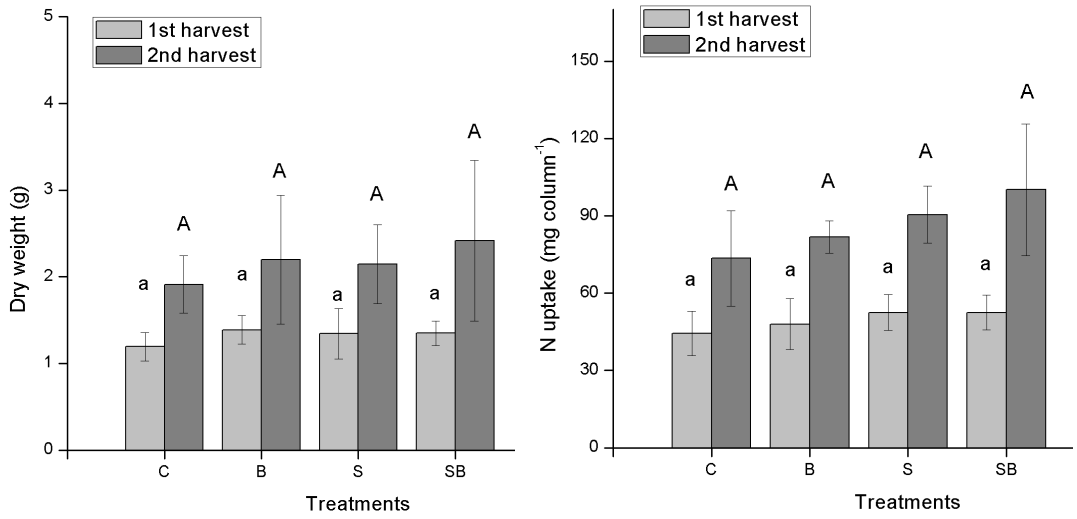

Figure 6-3: Grass yield (left) and nitrogen uptake (right) by grass grown in soil (C), amended with biochar (B), cow slurry (S), and biochar amended slurry (SB). Error bars represent standard error of the means (n=4). Different small letters indicate significant differences ($p < 0.05$) after the 1st harvest and different capital letters indicate significant differences ($p < 0.05$) after the 2nd harvest.

6.4.2. Nitrate leaching

Figure 6-4 illustrates the amount of NO_3^- leached per week over the 11 week leaching period. An initial increase in NO_3^- leaching for all treatments was observed. The amount of NO_3^- leached from treatment B and C decreased gradually after 7 weeks while NO_3^- leaching continued at a similar rate for S and SB. Figure 6-4 shows that SB and S resulted in a significantly higher cumulative amount of NO_3^- eluted from the columns as opposed to B and C over the 11-week period. No significant impact of biochar on reducing NO_3^- leaching from soil was observed, as biochar treated B and SB were not significantly different compared to the un-amended treatments C and S. Nevertheless, when comparing mean values, SB resulted in a reduced cumulative amount of NO_3^- by about 6% compared to S, while B resulted in a reduced cumulative amount of NO_3^- by about 2% compared to C. A possible reduction of NO_3^- either by adsorption to biochar or changes in nitrification or denitrification behaviours in the soil can only be speculated given the small reduction of the average cumulative NO_3^- amounts eluted from the columns.

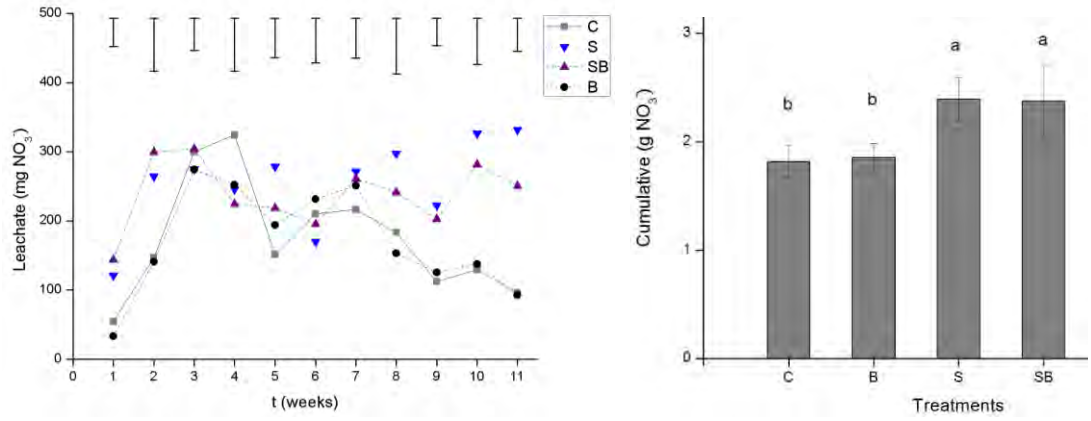

Figure 6-4: Amount of nitrate (left) and cumulative amount of nitrate (right) eluted from the columns packed with soil (C), amended with biochar (B), cow slurry (S), and biochar amended slurry (SB). The biggest error bars are displayed above representing standard errors of the means (n=4).

The effect of biochar on N cycling and subsequently on NO_3^- leaching behaviour in soil are complex in terms of environmental changes and biota. The properties of the Sitka Spruce biochar (section 5.4.1) seem suitable after reviewing the existing literature, which generally agrees that fresh and highly carbonised biochar produced at > 600 ºC has NO_3^- adsorption potential (Yao *et al*., 2012; Mizuta *et al*., 2004; Kameyama *et al*., 2012; Dempster *et al*., 2012, Lawrinenko, 2014). Eykelbosh *et al*. (2015) found that filtercake biochar produced at 575 ºC did not lessen NO_3^- fluxes, but attenuated dissolved organic carbon leaching. This observation suggests that cow slurry organic particles might have blocked the biochar pores reducing the contact with NO_3^- ions. Although this again might depend on interaction of biochar with slurry or other bulk materials, since Iqbal *et al*. (2015) found no significant difference between biochar produced at 650 ºC and co-composted biochar amendments in terms of nutrient leaching, including dissolved organic matter, NO_3^-, and phosphorus.

Biochar combined with manure or slurry has previously been shown to reduce NO_3^- leaching from manure. Results obtained by Laird *et al*. (2010) showed that biochar obtained by slow pyrolysis from mixed hardwood influenced leaching of NO_3^- following application of swine manure to a typical American Midwestern agricultural soil. In their experiment they also included a pre-leaching time of 12 weeks before applying the manure. No-manure biochar treatments of concentrations between 5 and 10 g kg^{-1} did not influence NO_3^- leaching, while 20 g kg^{-1} increased NO_3^- leaching by 26% over a 45-week period. The authors attributed it to enhanced mineralisation of organic N with the high rate of biochar addition. In contrast biochar combined with

manure significantly reduced NO_3^- leaching from the columns between week 23 and 36. The authors speculated that the biochar adsorbed NH_4^+ and soluble organic compounds and hence inhibited nitrification of NH_4^+ and mineralisation of organic N. Troy *et al*. (2014) found the addition of Sitka spruce biochar produced via slow pyrolysis at 600 °C increased soil water, carbon and organic matter contents, while reducing NO_3^- and organic carbon leaching following application of pig manure to a tillage soil. They assumed that biochar impacted on nitrification and denitrification rates in the soil, for example through nitrification inhibitors present in freshly used and un-weathered biochar and the stimulation of denitrification through a higher water-filled pore space and organic carbon content through biochar addition.

6.4.3. Effect of biochar on ammonia oxidizers and nitrous oxide reductase

The abundances of ammonia oxidising bacteria (AOB) and ammonia oxidising archaea (AOA) in the soils after eleven weeks of grass growth were determined by quantifying their respective *amoA* genes (Figure 6-5). Ammonia oxidation is the first and rate limiting step of nitrification (Song *et al*., 2013). In addition, the nitrous oxide reductase encoding *nosZ* gene, indicative for denitrification was determined (Figure 6-6). The soils were collected at two different column depths measured from the soil surface, at around 10 cm where the cow slurry and/or biochar had been applied (a) and at 25 cm closer to the base of the column (b).

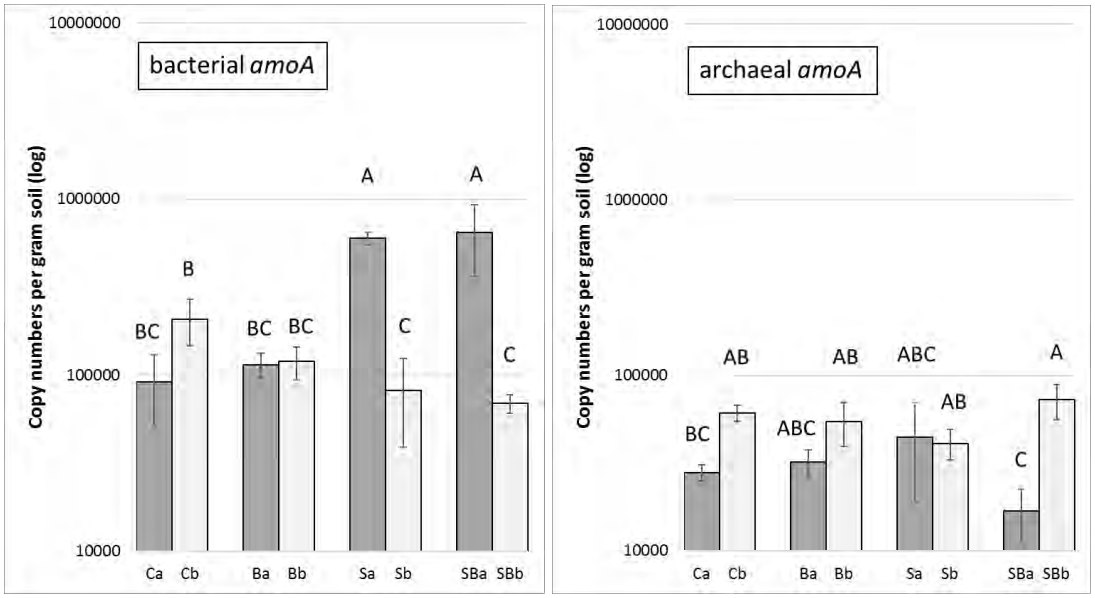

Figure 6-5: Abundances of bacterial (left) and archaeal (right) amoA genes at the slurry and biochar application zone (a) and 25 cm below the soil surface (b). Error bars represent standard error of the means (n = 4). Different letters indicate significant differences (p < 0.05) between treatment means according to Tukey's HSD post-hoc test.

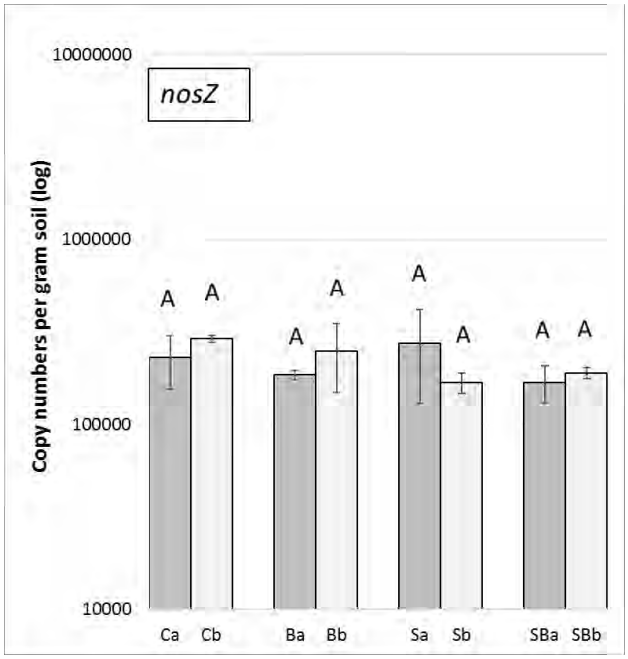

Figure 6-6: Abundances of nosZ genes at the slurry and biochar application zone (a) and 25 cm below the soil surface (b). Error bars represent standard error of the means (n = 4). Different letters indicate significant differences (p < 0.05) between treatment means according to Tukey's HSD post-hoc test.

The slurry treated soils sampled at the application zone (Sa and SBa) held a significantly higher abundance of bacterial *amoA* genes in comparison with Ba and Ca treatments. This would result in higher NO_3^- leaching from these columns, which supports the findings in section 6.4.2 (Figure 6-4), apart from the fact that slurry might contain higher amounts of NO_3^-. Furthermore, Sa and SBa held a significantly higher abundance of bacterial *amoA* genes in comparison with the soils sampled at the lower depth (Sb and SBb). This finding indicates that a significant amount of TAN supplied to the soil with the slurry was still available for the bacteria at the application zone and hadn't been leached to lower depths. The opposite was the case for the non-amended control treatment, where the soil sampled at lower depth (Cb) contained a higher abundance of bacterial *amoA* genes compared to the soil sampled at the application zone (Ca). This might be attributed to leaching of TAN already present in the soil. The abundance of bacterial *amoA* genes was fairly equal in biochar treated soil at both depths (Ba and Bb) and this observation suggests that biochar was able to retain TAN present in the soil at the application zone (a) avoiding or delaying leaching of TAN to lower depth.

Bacterial *amoA* genes outnumbered archaeal *amoA* genes for all treatments except for SBb. Some investigations have shown that AOA predominate among AOB in soils of different origin (Leininger *et al*., 2006; He *et al*., 2007); however, in Song *et al*. (2013) AOB consistently outnumbered AOA. The findings by Nicol *et al*. (2008), suggest that AOA tend to favour low soil pH, while AOB activity increases at a neutral pH, and this would explain our results considering the neutral to alkaline soil pH. In most treatments a strong and sometimes significant increase in abundance of archaeal *amoA* was found at lower depth (b) compared to the application zone (a). Again this might be attributed to gradual leaching of TAN or pH changes. An effect of biochar was only observed when applied in combination with slurry. The abundance of archaeal *amoA* genes for the SBa soil sample was lower than for Sa, however SBb was higher than Sb, suggesting that biochar treated slurry increased TAN leaching in slurry. Again, this might be explained by the biochars affinity to sorb organic carbon present in the slurry, inhibiting contact with other ions and influencing their leaching behaviour (Eykelbosh *et al*., 2015). Another explanation would be decreased mineralisation of organic N in manure with biochar application, reducing the amount of NH_4^+ available for the archaea. Furthermore, as Troy *et al*. (2014) previously commented, nitrification

inhibitors in biochar and the stimulation of denitrification through a higher water-filled pore space and organic carbon content might explain the results. Treatments B and C contained the same abundance of archaeal *amoA* at both depths and suggests that biochar alone had no effect when applied to soil.

In addition to the amount of TAN added to or present in soil, other factors might have affected the abundance of AOA and AOB. These include the soil pH, the presence of nitrification inhibitors, soil oxygenation, and sorption of TAN to biochar making it unavailable to nitrification in the short term. As the optimum pH for soil nitrifiers is known to be slightly acidic to neutral (Jensen and Sommer, 2013b), the abundances of the nitrifiers might alter at different depths along with pH changes with leaching of alkaline metals from the application zone. Ulyett *et al*. (2014) attributed the enhanced soil nitrification with biochar addition to the increase in pH. On the other hand, an excessively alkaline environment could reduce the abundance of nitrifiers, and this might also be a reason for the low abundance of archaeal *amoA* genes in SBa when applying a mixture of two alkaline materials, slurry and biochar. Another explanation might be the presence of nitrification inhibitors. Wang *et al*. (2015) indicated that phenolic compounds remaining in the biochar are likely to reduce AOB abundance and diversity. Deenik *et al*., (2010) investigated the effect of biochar on plant growth and seed germination and found evidence that in particular biochars produced at lower temperatures contain a high amount of toxic substances as part of the labile carbon. Changes in soil water status might also have influenced the abundances of nitrifiers. As already mentioned, the biochar had a higher water holding capacity than the soil, 1.38 ± 0.03 g $g^{-1}_{biochar}$ and 0.68 ± 0.01 g g^{-1}_{soil} respectively. The high porosity might have also influenced soil oxygenation, but as we could not see a significant influence of biochar on neither AOA nor AOB this effect appears to have been negligible.

The abundance of denitrifying bacteria bearing the *nosZ* gene did not vary significantly amongst the different treatments. Treatment B showed very similar results to the control. SBa on the other hand was slightly less abundant in *nosZ* genes compared to Sa and this again suggests an inhibition effect of biochar when combined with slurry. A different behaviour of biochar in combination with slurry as opposed to biochar alone has previously been observed by Troy *et al*. (2013) as the addition of pig slurry to soil columns with biochar increased N_2O emission, but biochar alone

didn't. They assumed that denitrification was increased by higher water filled pore space and organic carbon contents.

A limitation of the present study is that only a single biochar application loading and one soil type were used. Song *et al*. (2013) found that biochar loading affected the rate and dynamics of nitrification. The authors comment that the risk for increased alkalinity and nitrogen leaching of the studied soil was lower with a lower application rate. Applying the Sitka spruce biochar at different application rates and soil conditions might give a better insight into the effectiveness of this unique biochar on soil-N-soil dynamics. Furthermore, most biochar related studies on NO_3^- leaching, plant growth and microbial N transformation were short-term in nature, but long-term and systematic studies are lacking. Clough *et al*. (2013) suggested paying attention to changes of functional groups on the surface of biochar, water retention and hydraulic conductivity, especially as these factors could even enhance NO_3^- leaching.

6.5. Conclusions

The properties of the biochar derived from Sitka Spruce wood produced with the uniquely designed Kon-Tiki kiln suggest that this biochar could be effective in adsorbing anions such as NO_3^- from soil or animal slurry, making these nutrients more plant available and reducing their risk of leaching to lower grounds. These include a high surface area, porous structure and a high degree of carbonisation. However, at an application rate of 10 t ha^{-1} a positive effect of biochar on reducing NO_3^- leaching or on nitrogen uptake by grass was barely noticed. At this application rate biochar applied to soil alone had no effect on the abundances of bacterial or archaeal *amoA* and nitrous oxide reductase encoding *nosZ* genes; however, in combination with slurry biochar did impact on the abundance of archaeal *amoA* genes by decreasing their abundance at the application zone and increasing their abundance at lower depth significantly. Several reasons might explain this phenomenon, such as the biochars affinity to adsorb dissolved organic carbon from the slurry inhibiting contact with other ions, decreased mineralisation of organic N in manure, the presence of nitrification inhibitors in biochar and the stimulation of denitrification through a higher water-filled pore space and organic carbon content. The results of this study reveal that biochar affects soil-N dynamics differently when in combination with a nutrient rich bulk material, such as slurry, than in its un-amended state, at least in the short term.

6.6. Acknowledgement

Financial support for this work is gratefully acknowledged from the People Programme (Marie Curie Actions) of the European Union's Seventh Framework Programme FP7/2007-2013/ under REA grant agreement n° [289887], and from the SEAI under the Energy Research, Development & Demonstration (RD&D) Programme. Furthermore, we would like to thank Dr. Achim Schmalenberger, Israel Ikoyi, and Dr. Paulo Trazzi for their contribution.

6.7. References

Ahn, H.K., Sauer, T.J., Richard, T.L., Glanville, T.D., 2009. Determination of thermal properties of composting bulking materials. Bioresour. Technol. 100, 3974-3981.

Barrow, C.J., 2012. Biochar: Potential for countering land degradation and for improving agriculture. Appl. Geogr. 34, 21–28.

Chintala, R., Owen, R. K., Schumacher, T. E., Spokas, K. A., McDonald, L. M., Kumar, S., Clay, D.E., Malo, D.D., Bleakley, B., 2015. Denitrification kinetics in biomass- and biochar-amended soils of different landscape positions. Environmental Science and Pollution Research. 22, 5152-5163.

Clough, T., Condron, L., Kammann, C., Müller, C., 2013. A Review of Biochar and Soil Nitrogen Dynamics. Agronomy 3, 275–293.

Deenik, J.L., McClellan, T., Uehara, G., Antal, M.J., Campbell, S., 2010. Charcoal Volatile Matter Content Influences Plant Growth and Soil Nitrogen Transformations. Soil Sci. Soc. Am. J. 74, 1259-1270.

Dempster, D.N., Jones, D.L., Murphy, D.M., 2012. Clay and biochar amendments decreased inorganic but not dissolved organic nitrogen leaching in soil. Soil Res., 50, 216–221.

Dicke, C., Andert, J., Ammon, C., Kern, J., Meyer-Aurich, A., Kaupenjohann, M., 2015. Effects of different biochars and digestate on N_2O fluxes under field conditions. Science of the Total Environment. 524-525, 310-318.

Eykelbosh, A.J., Johnson, M.S., Couto, E.G., 2015. Biochar decreases dissolved organic carbon but not nitrate leaching in relation to vinasse application in a Brazilian sugarcane soil. Journal of Environmental Management. 149, 9–16.

Gai, X., Wang, H., Liu, J., Zhai, L., Liu, S., Ren, T., Liu, H., 2014. Effects of feedstock and pyrolysis temperature on biochar adsorption of ammonium and nitrate. PLoS One 9, 1–19.

Han, G., Meng, J., Zhang,W., Chen, W., 2013. Effect of biochar on microorganism's quantity and soil physicochemical property in rhizosphere of spinach (Spinacia oleracea L.). Applied Mechanics and Materials. 295-298, 210-219.

Harter, J., Krause, H. M., Schuettler, S., Ruser, R., Fromme, M., Scholten, T., Kappler, A., Behrens, S., 2014. Linking N_2O emissions from biochar-amended soil to the structure and function of the N-cycling microbial community. ISME Journal. 8, 660-674.

He, J., Shen, J., Zhang, L., Zhu, Y., Zheng, Y., Xu MG, Di H. 2007. Quantitative analyses of the abundance and composition of ammonia-oxidizing bacteria and ammonia- oxidizing archaea of a Chinese upland red soil under long-term fertilization practices. Environmental Microbiology. 9, 2364–2374.

Henry, S., Bru, D., Stres, B., Hallet, S., Philippot, L. 2006. Quantitative detection of the *nosZ* gene, encoding nitrous oxide reductase, and comparison of the abundances of 16S rRNA, *narG*, *nirK*, and *nosZ* genes in soils. Appl Environ Microbiol 72, 5181–5189.

Iqbal, H., Garcia-Perez, M., Flury, M., 2015. Effect of biochar on leaching of organic carbon, nitrogen, and phosphorus from compost in bioretention systems. Science of the Total Environment. 521-522, 37–45.

Jensen, L.S., Sommer, S.G., 2013a. Manure Organic Matter – Characteristics and Microbial Transformation. In Sommer, S.G., Christensen, M.L., Schmidt, T., Jensen, L.S. (Eds.). Animal Manure Recycling - Treatment and Management. John Wiley and Sons Ltd. Chichester, West Sussex, UK. p.83.

Jensen, L.S., Sommer, S.G., 2013b. Manure Organic Matter – Characteristics and Microbial Transformation. In Sommer, S.G., Christensen, M.L., Schmidt, T., Jensen, L.S. (Eds.). Animal Manure Recycling - Treatment and Management. John Wiley and Sons Ltd. Chichester, West Sussex, UK. p.85.

Jetten, M.S.M., 2008. The microbial nitrogen cycle. Environ. Microbiol. 10, 2903–2909.

Joseph, S.D., Camps-Arbestain, M., Lin, Y., Munroe, P., Chia, C.H., Hook, J., van Zwieten, L., Kimber, S., Cowie, A., Singh, B.P., Lehmann, J., Foidl, N., Smernik, R.J., Amonette, J.E., 2010. An investigation into the reactions of biochar in soil. Aust. J. Soil Res. 48, 501-515.

Kameyama, K., Miyamoto, T., Shiono, T., Shinogi, Y., 2012. Influence of sugarcane bagasse-derived biochar application on nitrate leaching in calcaric dark red soil. J. Environ. Qual. 41, 1131–1137.

Kammann, C.I., Linsel, S., Gößling, J.W., Koyro, H-W., 2011. Influence of biochar on drought tolerance of Chenopodium quinoa Willd and on soil-plant relations. Plant Soil. 345, 195–210.

Laird, D., Fleming, P., Wang, B., Horton, R., Karlen, D., 2010. Biochar impact on nutrient leaching from a Midwestern agricultural soil. Geoderma. 158 (3-4), 436–442.

Lawrinenko, M., 2014. Anion exchange capacity of biochar. Graduate Theses and Dissertations. Paper 13685.

Lehmann, J., Joseph, S., 2009. In Lehmann, J., Joseph, S. (Eds.). Biochar for Environmental Management – Science and Technology: An Introduction. Earthscan. London, UK. 1-12.

Leininger, S., Urich, T., Schloter, M., Schwark, L., Qi, J., Nicol, G.W., Prosser, J.I., Schuster, S.C., Schleper, C., 2006. Archaea predominate among ammonia-oxidizing prokaryotes in soils. Nature. 442, 806–809.

Martin, S.L., Clarke, M.L., Othman, M., Ramsden, S.J., West, H.M., 2015. Biochar-mediated reductions in greenhouse gas emissions from soil amended with anaerobic digestates. Biomass and Bioenergy. 79, 39-49.

Mia, S., van Groenigen, J.W., van de Voorde, T.F.J., Oram, N.J., Bezemer, T.M., Mommer, L., Jeffery, S., 2014. Biochar application rate affects biological nitrogen fixation in red clover conditional on potassium availability. Agric. Ecosyst. Environ. 191, 83–91.

Mizuta, K., Matsumoto, T., Hatate, Y., Nishihara, K., Nakanishi, T., 2004. Removal of nitrate-nitrogen from drinking water using bamboo powder charcoal. Bioresour. Technol. 95, 255–257.

Nelissen, V., Saha, B. K., Ruysschaert, G., Boeckx, P., 2014. Effect of different biochar and fertilizer types on N_2O and NO emissions. Soil Biology and Biochemistry. 70, 244-255.

Nicol, G.W., Leininger, S., Schleper, C., Prosser, J.I., 2008. The influence of soil pH on the diversity, abundance and transcriptional activity of ammonia oxidizing archaea and bacteria. Environmental Microbiology. 10, 2966-2978.

O'Toole, A., Knoth de Zarruk, K., Steffens, M., Rasse, D.P., 2013. Characterization, stability, and plant effects of kiln-produced wheat straw biochar. J. Environ. Qual. 42(2), 429-436.

Prendergast-Miller, M.T., Duvall, M., Sohi, S.P., 2011. Localisation of nitrate in the rhizosphere of biochar-amended soils. Soil Biol. Biochem. 43, 2243–2246.

Prendergast-Miller, M.T., Duvall, M., Sohi, S.P., 2014. Biochar-root interactions are mediated by biochar nutrient content and impacts on soil nutrient availability. European Journal of Soil Science, 65(1), 173–185.

Prommer, J., Wanek, W., Hofhansl, F., Trojan, D., Offre, P., Urich, T., Schleper, C., Sassmann, S., Kitzler, B., Soja, G., Hood-Nowotny, R.C., 2014. Biochar decelerates soil organic nitrogen cycling but stimulates soil nitrification in a temperate arable field trial. PLoS ONE, 9(1).

Rajkovich, S., Enders, A., Hanley, K., Hyland, C., Zimmerman, A.R., Lehmann, J. 2012. Corn growth and nitrogen nutrition after additions of biochars with varying properties to a temperate soil. Biol Fertil Soils. 48, 271–284.

Rizhiya, E.Y., Buchkina, N.P., Mukhina, I.M., Belinets, A.S., Balashov, E.V., 2015. Effect of biochar on the properties of loamy sand Spodosol soil samples with different fertility levels: a laboratory experiment. Eurasian Soil Science. 48, 192-200.

Rotthauwe, J.H., Witzel, K.P., Liesack, W. 1997. The ammonia monooxygenase structural gene *amoA* as a functional marker: molecular fine-scale analysis of natural ammonia-oxidizing populations. Appl. Environ. Microbiol. 63, 4704–4712.

Schauss, K., Focks, A., Leininger, S., Kotzerke, A., Heuer, H., Thiele-Bruhn, S., *et al*. 2008. Dynamics and functional relevance of ammonia-oxidizing archaea in agricultural soil. Environ Microbiol. 11(2), 446-456.

Schmalenberger, A., Fox, A., 2016. Bacterial Mobilization of Nutrients from Biochar-Amended Soils. In Sariaslani, S., Gadd, G.M. (Eds.), Advances in Applied Microbiology. 109–159.

Sharpley, A.N., Chapra, S.C., Wedepohl, R., Sims, J.T., Daniel, T.C., Reddy K.R., 1994. Managing Agricultural Phosphorus for Protection of Surface Waters: Issues and Options. J. Environ. Qual. 23, 437-451.

Silsbury, J.H., 1971. The effects of temperature and light energy on dry weight and leaf area changes in seedling plants of Lolium perenne L. Aust. J. agric. Res. 22, 177-187.

Song, Y., Zhang, X., Ma, B., Chang, S. X., Gong, J., 2014. Biochar addition affected the dynamics of ammonia oxidizers and nitrification in microcosms of a coastal alkaline soil. Biology and Fertility of Soils. 50(2), 321–332.

Sørensen, P., Jensen, L.S., 2013a. Nutrient Leaching and Runoff from Land Application of Animal Manure and Measures for Reduction. In Sommer, S.G., Christensen, M.L., Schmidt, T., Jensen, L.S. (Eds.). Animal Manure Recycling - Treatment and Management. John Wiley and Sons Ltd. Chichester, West Sussex, UK. p.203.

Sørensen, P., Jensen, L.S., 2013b. Nutrient Leaching and Runoff from Land Application of Animal Manure and Measures for Reduction. In Sommer, S.G., Christensen, M.L., Schmidt, T., Jensen, L.S. (Eds.). Animal Manure Recycling - Treatment and Management. John Wiley and Sons Ltd. Chichester, West Sussex, UK. p.196.

Spalding, R.F., Exner. M.E., 1993. Occurrence of Nitrate in Groundwater-A Review. J. Environ. Qual. 22, 392-402.

Spokas, K.A., Cantrell, K.B., Novak, J.M., Archer, D.A., Ippolito, J.A., Collins, H.P., Boateng, A.A., Lima, I.M., Lamb, M.C., McAloon, A.J., Lentz, R.D., Nichols, K.A., 2012. Biochar: A synthesis of its agronomic impact beyond carbon sequestration. J. Environ. Qual. 41, 973–989.

Troy, S.M., Lawlor, P.G., O'Flynn, C.J., Healy, M.G., 2014. The impact of biochar addition on nutrient leaching and soil properties from tillage soil amended with pig manure. Water, Air, and Soil Pollution. 225(3).

Troy, S.M., Lawlor, P.G., O'Flynn, C.J., Healy, M.G., 2013. Impact of biochar addition to soil on greenhouse gas emissions following pig manure application. Soil Biology and Biochemistry. 60, 173-181.

Ulyett, J., Sakrabani, R., Kibblewhite, M., Hann, M., 2014. Impact of biochar addition on water retention, nitrification and carbon dioxide evolution from two sandy loam soils. European Journal of Soil Science. 65, 96-104.

Van Zwieten, L., Singh, B.P., Kimber, S.W.L., Murphy, D. V., Macdonald, L.M., Rust, J., Morris, S., 2014. An incubation study investigating the mechanisms that impact N_2O flux from soil following biochar application. Agric. Ecosyst. Environ. 191, 53–62.

Verheijen, F., Jeffery, S., Bastos, A.C., von der Velde, M., Diafas, I., 2010. Biochar Application to Soils - A Critical Scientific Review of Effects on Soil Properties, Processes and Functions. Office for Official Publications of the European Communities. Luxembourg. 1-116.

Wang, Z., Zong, H., Zheng, H., Liu, G., Chen, L., Xing, B., 2015. Reduced nitrification and abundance of ammonia-oxidizing bacteria in acidic soil amended with biochar. Chemosphere. 138(3), 576–583.

Xiang, J., Liu, D., Ding, W., Yuan, J., Lin, Y., 2015. Effects of biochar on nitrous oxide and nitric oxide emissions from paddy field during the wheat growth season. Journal of Cleaner Production. 104, 52-58.

Xu, H., Wang, X., Yao, H., Su, J., Li, H., Zhu, Y.-G., 2014. Biochar impacts soil microbial community composition and nitrogen cycling in an acidified soil. Environ. Sci. Technol. 17, 9391–9399.

Yanai, Y., Hatano, R., Okazaki, M., Toyota, K., 2008. Analysis of the C_2H_2 inhibition-based N_2O production curve to characterize the N_2O-reducing activity of denitrifying communities in soil. Geoderma. 146, 269-276.

Yao, Y., Gao, B., Zhang, M., Inyang, M., Zimmerman, A.R. 2012. Effect of biochar amendment on sorption and leaching of nitrate, ammonium, and phosphate in a sandy soil. Chemosphere. 89, 1467–1471.

Zhu, J., Wei, X., Zhu, P., Yu, H., Shu, L., Xu, Z., Chen. D., 2015. Biochar addition inhibiting nitrification of reclaimed soils in coal-mining subsidence area. Nongye Gongcheng Xuebao/Transactions of the Chinese Society of Agricultural Engineering. 31, 264-271.

7. Conclusions

Thermal treatment of animal waste to improve the environmental performance of the entire manure management chain is gaining importance and is stimulating scientific research. This study investigated the use of substoichiometric thermochemical processes, including updraft gasification and slow pyrolysis, to produce energy and biochar. The research had two primary aims. The first was to investigate the use of different manure feedstocks to produce biochar and recycle nutrients back to agricultural land. The second aim was to investigate the use of a virgin wood biochar derived from Sitka spruce, produced via a uniquely designed Kon-Tiki kiln, to reduce ammonia emissions from stored cow slurry and nitrate leaching from agricultural soil. The main outcomes of the two research sections will be discussed in more detail and then recommendations for future work will be given.

7.1. Main outcomes

The moisture content and alkali metals present in manures pose a hindrance for applying thermal treatment as a waste management tool. Poultry litter (PL) has a relatively low moisture content, and therefore results in a positive energy balance, eliminating the requirement for pre-treatment. Poultry litter was subject to on-farm auto-thermal updraft gasification at sub stoichiometric oxygen conditions. The main aim was to produce a low to medium calorific value product gas to use as an energy carrier to heat the poultry sheds, while obtaining a tar and char residue. The results in chapter 1 show that updraft gasification at temperatures below the ash melting point of PL (639 °C) was indeed robust and reliable, producing a product gas with a low calorific value of 3.39 MJ m^{-3}_N (LHV) and a cold gas efficiency (CGE) of 0.26. The tar was collected as an emulsion containing 87 wt.% water and the extracted organic compounds were identified. The char was rich in nutrients and was subject to further investigation regarding its potential as a crop fertiliser (biochar) in the following chapter.

The biochar obtained from updraft gasification was compared with slow pyrolysis biochars derived from the same PL feedstock and produced at laboratory scale at maximum pyrolysis temperatures of 400 °C and 600 °C. The biochars were subject to detailed analysis regarding their physico-chemical characteristics and nutrient recycling potential. The results revealed that the biochars obtained from pyrolysis were homogenous in nature due to the controlled laboratory scale operation; however, biochar obtained from updraft gasification was less homogeneous, containing small ash particles and incompletely charred PL material as a result of the uneven temperature distribution in the pilot scale gasifier. The gasification biochar had a higher ash content than the pyrolysis biochars as some of the PL feedstock was burned to produce heat for maintaining the bed temperature and driving the endothermic gasification reactions, while at laboratory scale pyrolysis the PL feedstock was exposed to an external heat source.

Cow manure (CM) and swine manure (SM) are only suitable for pyrolysis when pre-treated to separate or evaporate moisture. In our study dehydrated CM was processed to biochar using the same batch pyrolysis unit and process conditions as the PL feedstock. Biochars of an anaerobically pre-treated and dehydrated SM were obtained

from ECN, the Netherlands, treated under the same temperature as PL and CM, however using a continuous pyrolysis unit. The feedstock properties, including bulk density, proximate and ultimate analysis, influenced the pyrolysis process and extent of carbonisation, especially for PL, and therefore process conditions should be considered accordingly. Cow manure and SM showed almost identical physico-chemical properties as revealed by the proximate analysis, solid-state ^{13}C NMR, FTIR and Van Krevelen classification and this suggests that different reactor designs can provide similar results at the same process conditions. The results of the solid-state ^{13}C NMR was broadly in agreement with the Van Krevelen parameter for classifying biochar and may offer a reasonable alternative analytical technique for manure biochar classification. Plant nutrients were recovered to a higher degree in the biochar compared to volatile toxic heavy metals (HM) and this results in an improved biochar quality. However, under the current European guidelines for biochar certification (EBC) manure chars cannot meet the set thresholds unless blended with a low ash biomass or through alterations of the content of nutrients in animal feed.

The results obtained for the plant growth experiment using biochar amended soils (2 wt.%) showed that the increase in dry biomass yield of lettuce (*Lactuca sativa*) was statistically significant for all manure biochars compared to the control soil (no amendment). Nutrient uptake was highest for PL, followed by SM and CM treatments. Biochars produced via slow pyrolysis of PL resulted in a higher nutrient uptake than biochar produced from updraft gasification with the exception of P and K uptake, which were not affected by process type. Biochars obtained at low pyrolysis temperatures (400 °C) showed a better short term crop performance than biochars obtained at high pyrolysis temperatures (600 °C). This was attributed to the inhibited nutrient uptake for highly carbonised biochar processed at high process temperature, possibly due to the formation of insoluble inorganic phases via precipitation as crystals. The high degree of aromatic carbon structure with increased temperature however suggest a high carbon stability and carbon sequestration potential.

Sitka spruce is the most common tree species in the Republic of Ireland and was subject to pyrolysis using a uniquely designed pyrolysis kiln. The process is cheap, simple and robust and results in a clean and smokeless combustion of the volatile gases. The obtained biochar complied with all required threshold values for premium grade European biochar certification, and possessed a high surface area, porous

structure and a high degree of carbonisation. The biochar was used as a cow slurry amendment to reduce NH_3 emissions during a storage period of 49 days, and investigate the impact on CH_4 and H_2S emissions. Sulfuric acid was used as a comparison. Biochar had no or inconsistent impacts on NH_3 and CH_4 emissions, while sulfuric acid and the combined acid and biochar treatment decreased cumulative NH_3 emissions by about 50%. Cumulative CH_4 fluxes decreased for acidified slurry; and to a lesser extent for the combined biochar and sulfuric acid treatment. Acidification however resulted in elevated H_2S emissions, while no H_2S emissions were observed for biochar treated slurry. Biochar changed the physico-chemical characteristics of cow slurry by increasing total carbon, dry matter, and the C:N ratio and evidence of altered aeration properties and microbial activity was observed.

Furthermore, the effect of the Sitka spruce biochar on soil N-dynamics when applied to soil in combination with cow slurry was evaluated, primarily to reduce nitrate (NO_3^-) leaching and enhance crop production. At an application rate of 10 t ha^{-1} no positive effect of the biochar on reducing NO_3^- leaching or on nitrogen uptake by grass was observed. Biochar applied to soil alone had no effect on the abundances of bacterial or archaeal *amoA* and nitrous oxide reductase encoding *nosZ* genes; however, in combination with cow slurry biochar decreased the abundance of archaeal *amoA* genes in the biochar/slurry application zone and increased their abundance at lower soil depths significantly. Results obtained from the abundances of bacterial *amoA* genes provide evidence that biochar was able avoid or delay NH_4^+ leaching to lower soil depth. Biochar affected soil N-dynamics differently when in combination with slurry than in its un-amended state, at least in the short term.

7.2. Recommendations for future work

For future research with regard to PL gasification, we suggest that the focus should be on obtaining a higher quality biochar, since a certified biochar might be easier to market rather than undergoing an expensive upgrading and refining process to improve the tar quality. This should be possible to achieve by management of the overall poultry production chain including amending the poultry feed supplements to exclude Zn and Cu, or alternatively blending of the PL with dry lignocellulosic biomass prior to gasification. Furthermore, by ensuring an even oxygen supply to the gasification reactor resulting in a uniform temperature distribution the charring

process would be improved obtaining a homogenous biochar. Modifications should be undertaken without affecting the gas yield and quality. The tar was collected as an emulsion containing 87 wt.% water and extracted organic compounds, some of them halogenated which might result in harmful emissions during combustion. Therefore, suitable disposal options or post-treatment of the emulsion are required.

One of the main drawbacks of thermal treatment of manure feedstocks is the loss of nitrogen through volatilisation and transformation of ammoniacal nitrogen (NH_3 and NH_4^+) and organic nitrogen to other species during gasification or pyrolysis, which is dependent on the nitrogen speciation within the different manures, which again depends on the animal feed, excreta, digestibility of the crop and storage. The fate of different nitrogen species during thermal treatment would be worth investigating. In addition, as a high content of nitrogen was found in the tar/water emulsions from gasification, it would be worth investigating options for recovering nitrogen from the emulsion.

The effect of maximum pyrolysis temperature on biochar properties and subsequently nutrient availability has been excessively investigated, while plant growth experiments using biochars derived from different process types, including fast pyrolysis, fixed or bubbling fluidised bed gasification are rare and should be subject to investigation in the future. Further research is required on the toxicity of the manure biochars, such as seed germination tests, quantification of PAH, PCBs and dioxins and HM toxicity, e.g. the oxidation state of Cr.

A drawback of this work is that the biochar studies were all short-term; however, long-term studies in biochar research are required, as the physico-chemical properties and effectiveness of biochar is prone to change with changing environment. Long-term investigations on the movement and fate of nutrients and HM of manure biochar when applied to soil should be conducted in the future. Also with regard to biochar as a slurry amendment, a prolonged study throughout the entire storage period (e.g. six months), as well as release of harmful emissions thereafter (e.g. during land application) are important. Acidification of biochar prior to biochar addition to slurry might result in combined advantages of lowering the pH and taking advantage of the unique biochar morphology. Changes in aeration properties, crust formation,

emissions of odour compounds, as well as microbial abundances, e.g. methanogens or methanotrophs should also be subject to further research.

Soil N-dynamics are complex, therefore laboratory scale experiments are required prior to pilot or field scale experiments, including the influence of Sitka spruce biochar on ammonium/ammonia, nitrates and nitrite concentrations and their proportions in soil and slurry. Furthermore, different biochar loadings in soil would show different results to those obtained during this work. In general, research goals should revolve around factors like feedstock availability; available technologies; local energy needs; infrastructure; demand for thermo-chemical co-products; economic cost; but also health issues and practical aspects. For example, CM biochars were more difficult to handle as they were lighter than biochars derived from PL and SM with a lower bulk density.

Appendix I

Table I-1: Mass balance of poultry litter updraft gasification process

	Mass Flow	C	H	N	O	S	Ash
	($kg\ h^{-1}$)						
PL (as received)	40						
PL (dry basis)	27.92	11.42	1.4	1.28	8.16	0.13	5.53
PL (moisture)	12.08		1.34		10.74		
Air	23.82			18.82	5		
Total	63.82	11.42	2.74	20.1	23.9	0.13	5.53
Output							
Char (as received)	10						
Char (dry basis)	9.32	3.09	0.15	0.6	0.31	0.07	5.1
Char (moisture)	0.69		0.08		0.61		
Tar (as received)	13.3						
Tar (dry basis)	1.73	0.69	0.059	0.16	0.72	0.00016	0.097
Tar (moisture)	11.58		1.29		10.29		
Product gas	36.84	5.15	0.24	19.34	12.11		
Total	60.14	8.93	1.82	20.1	24.04	0.07	5.2

Table I-1: Mass balance of poultry litter updraft gasification process

Stoichiometric A/F ratio			
Elemental composition	Mass fraction	Multiplication factor	Stoichiometric oxygen
Carbon	0.41	32/12* = 26	1.09
Hydrogen	0.05	8/1 = 8	0.4
Sulphur	0.005	1/1 = 1	0.005
Oxygen	0.29	-1	-0.29
			1.20 (oxygen)
			5.74 (air)

**For example 1 kg C reacts with 32/12 kg O_2 following 1 mol C + 1 mol $O_2 \rightarrow$ 1 mol CO_2*

Table I-2: The density of product gas species used in the calculations

Component	Density (kg m^{-3})
O_2	1.4285
N_2	1.2493
CH_4	0.717
CO_2	1.9658
CO	1.2501
H_2	0.0899
C_2H_4	1.2586
NH_3	0.769

Green, D., Perry, R., 2007. Perry's Chemical Engineers' Handbook, Eighth Edition, McGraw-Hill Education.

Appendix II

Table II-1: Values presented in the Van Krevelen Diagram

Samples	H	O	$H:C_{molar}$	$O:C_{molar}$
	($wt.\%_{db}$)		Van Krevelen	
BM	5.9 ± 0.1	43.6 ± 0.5	1.51	0.7
PL	5.0 ± 0.2	29.2 ± 0.9	1.47	0.54
PL400	4.2 ± 0.07	13.6 ± 1.4	1.07	0.22
PL600	1.2 ± 0.08	3.6 ± 2.5	0.3	0.06
PLgas	2.1 ± 0.02	8.2 ± 0.4	0.6	0.15
CM	5.5 ± 0.02	36.6 ± 0.4	1.36	0.57
CM400	3.2 ± 0.03	12.0 ± 0.7	0.67	0.16
CM600	1.5 ± 0.05	3.9 ± 0.2	0.27	0.04
SM	ND	ND	ND	ND
SM400	2.6 ± 0.20	8.8 ± 3.5	0.6	0.13
SM600	1.1 ± 0.04	3.5 ± 1.4	0.23	0.05

Abbreviations same as Table 4-1

Table II-2: Hydro-solubility of some micronutrients from feedstocks and biochar samples

	Fe	Mn	Zn	Cu
	($g\ t^{-1}$)			
PL	68	41	25	23
PL400	18	11	10	6
PL600	1	1	0	6
PLgas	7	0	0	1
CM	37	72	6	5
CM400	1	2	7	4
CM600	0	1	0	2
SM	ND	ND	ND	ND
SM400	2	1	0	2
SM600	0	1	0	1

Abbreviations same as Table 4-1

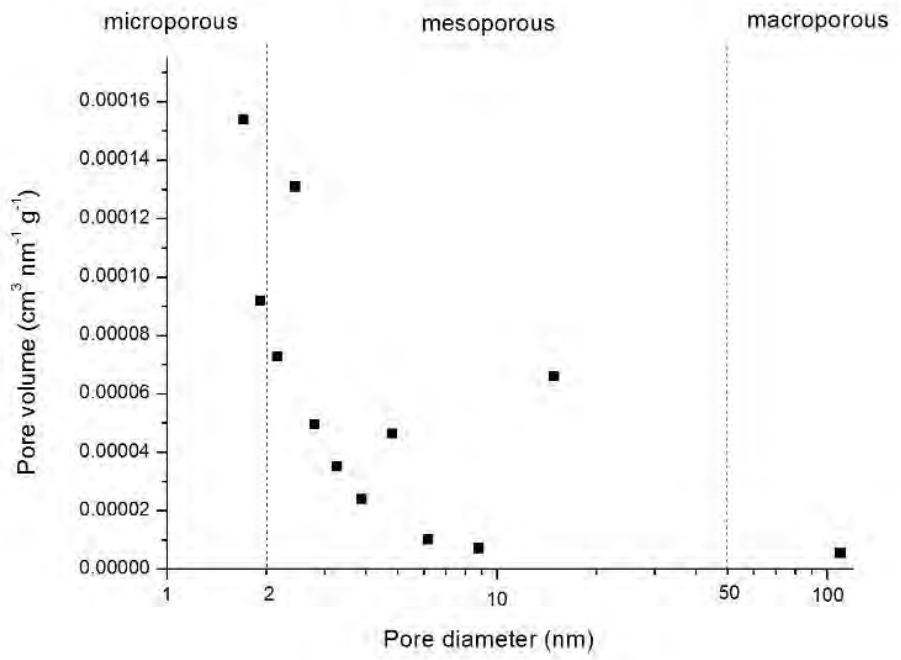

Figure I-1: Pore size distributions of the Sitka spruce biochar